Energy saving for belt conveyors by speed control

He, Daijie

DOI

10.4233/uuid:a315301e-6120-48b2-a07b-cabf81ab3279

Publication date
2017

Document Version
Final published version

Important note
To cite this publication, please use the final published version (if applicable).
Please check the document version above.

Energy Saving for Belt Conveyors by Speed Control

Daijie He

Energy Saving for Belt Conveyors by Speed Control

Proefschrift

ter verkrijging van de graad van doctor

aan de Technische Universiteit Delft,

op gezag van de Rector Magnificus Prof. ir. K.C.A.M. Luyben,

voorzitter van het College voor Promoties,

in het openbaar te verdedigen op woensdag 5 juli 2017 om 12:30 uur

door

Daijie HE

Master of Science in Agricultural Mechanization Engineering, Southwest University, P.R. China

geboren te Jiangyou, Sichuan, P.R. China.

Dit proefschrift is goedgekeurd door de
promotor: Prof. dr. ir. G. Lodewijks
copromotor: Dr. ir. Y. Pang

Samenstelling promotiecommissie:

Rector Magnificus	chairperson
Prof. dr. ir. G. Lodewijks	Delft University of Technology, promotor
Dr. ir. Y. Pang	Delft University of Technology, copromotor
Independent members:	
Prof. dr. ir. W. de Jong	Delft University of Technology
Prof. dr. -Ing. J. Reger	Technische Universität Ilmenau, Germany
Prof. dr. G. Cheng	China University of Mining and Technology, China
Dr. M.W.N. Buxton	Delft University of Technology
Prof. ir. J. Rijsenbrij	Delft University of Technology

Printed in the Netherlands

To my parents, my wife, and my daughter

Preface

The period of my doctoral research and study is a memorable journey at Delft University of Technology in the Netherlands. During my PhD journey, I was supported and encouraged by many people. Herein, I would like express my great appreciation to all of you.

First of all, I would like to thank the Chinese Scholarship Council for providing me the funding to support my daily life in the Netherlands.

Furthermore, I would like to thank my promotor Prof. Gabriel Lodewijks and my daily supervisor Dr. Yusong Pang. Dear Gabriel, please receive my sincere appreciation for all your time and effort. You always took time for me to have a full discussion of my research and to push me into the right direction, in spite of your busy schedules. As a professional expert on belt conveyors, you gave me a lot of critical comments and valuable suggestions on my research. Particularly, it is also you who reminded me to keep curiosity alive. Dear Yusong, please also receive my deep appreciation. You are always so kind and patient on supervising. You are not only an instructor, but also a friend. Thanks for your first lesson on my PhD research, "to be your own manager". This benefited me a lot and it made me an independent and efficient researcher. In addition, I appreciate all your instruction on my research, especially on my manuscripts of the thesis and journal papers. Moreover, I would like to thank you for your encouragement specially when I met troubles in life and study.

To all my colleagues in the Department of Maritime Transport Technology (MTT), thank you for creating such a nice working environment. I would like to thank all secretaries of our department for providing generous supports. A special thank should be given to Dick Mensch for proof checking of the manuscript and translating the Summary into Dutch. In addition, I would like to thank all PhD researchers and postdocs of our department. Special thanks are given to my officemates, Stef, Ebrahim, Xiaojie and QinQin, for their kind accompany during my four-years research.

In addition, I would like to thank all my Chinese friends in Delft. Anqi, Fei, Jie, Long, Peiyao, Xian, Yixiao, Yu,Yueting, Zhijie, etc., thanks for your accompany at the weekend in pubs with Uno; Fan and Runlin, thanks for your exciting comment on UEFA Champions League; Guangming, Jie, Qingsong, Wenbin,Qu, Wenhua, Xiangwei, Xiao, etc., thanks for your accompany

during the traditional Chinese festivals with delicious food; and other Chinese friends, thanks for your accompany in my four-years life in Delft.

Moreover, I would like to thank my parents for their unconditional love and support in the past years. I also would like to thank my wife, Sixin, for her encouragement and support during my PhD research. Thanks for your kind forgiveness for not insisting on being with you when you were pregnant. Thanks for your warm food and drink at mid-light, especially during the days when I was in a hurry to complete my final thesis. Please receive my deepest love and appreciation for you. Last but not least, I would like to thank the coming of my daughter, Jiahuan. You beautiful smile melts my heart.

Daijie He
Delft, June, 2017

Contents

Chapter 1

Introduction

1.1 Background

Belt conveyor systems are typical continuous transport systems that can convey materials without any interruptions (see Figure 1.1). For more than a century, belt conveyors have been an important part of material handling for both in-plant and overland transportation (Hetzel, 1922; Pang, 2010). In the last decades, the technology of belt conveyor systems has been continually improved. Especially after the Second World War, rubber technologies began a period of rapid development and these changes promoted the improvement of conveyor systems. Moreover, belt conveyors in recent decades have become longer and faster, with higher capacity and less environmental impact (Lodewijks, 2002). In addition, belt conveyors have proven themselves to be one of the most cost-effective solutions for handling bulk material mass flows. Furthermore, the belt conveyor systems today are controlled and monitored by computers and the automatically-controlled conveyor systems are used to maximize their performance and flexibility (EagleTechnologies, 2010).

Due to their inherent advantages, such as high capacity and low labor requirements, belt conveyors play a significant role in bulk solids handling and conveying, especially in districts

Figure 1.1: Belt conveyors in Shanghai Port, Luojing Phase II ore terminal. (Courtesy of Shanghai Keda Heavy Industry Group Co., Ltd. (KDHI, 2016))

where infrastructure is underdeveloped or non-existent (Nuttall, 2007). According to Daniel Clénet (2010), there are more than 2.5 million conveyors operating in the world each year. Considering the extensive use of belt conveyors, their operations involve a large amount of electricity. Hiltermann (2008) gives an example, showing that belt conveyors are responsible for 50% to 70% of the total electricity demand in a dry bulk terminal. Furthermore, coal-fired power plants currently fuel 41% of the global electricity (Goto et al., 2013), and coal makes up over 45% of the world's carbon dioxide emissions from fuels (International Energy Agency, 2015). Therefore, taking the relevant economic and social challenges into account, there is a strong demand for lowering the energy consumption of belt conveyors and reducing the carbon footprint.

In the past decades, several different solutions have been designed for reducing the electricity cost of belt conveyors. These different cost saving approaches can be classified into five groups:

- methods applying energy efficient components, such as, low loss conveyor belts (Kropf-Eilers et al., 2009; Gerard van den Hondel, 2010; Lodewijks, 2011), new types of idler sets (Tapp, 2000; Mukhopadhyay et al., 2009) and high efficient driving systems (Emadi, 2004; Dilefeld, 2014);

- methods optimizing the design, especially the conveyor route (Yester, 1997; Alspaugh, 2004);

- methods recovering energy, including recovering the kinetic and the potential energy of the transported material (Michael Prenner and Franz Kessler, 2012; Graaf, 2013);

- methods optimizing the drive operation, as by controlling motor sequences (Dalgleish and Grobler, 2003; Levi, 2008) or adjusting the conveyor speed (Hiltermann, 2008; Jeftenic et al., 2010; Pang and Lodewijks, 2011; Ristic and Jeftenic, 2011);

- and method accounting for the operational philosophy, for example, the time-of-use tariff (Zhang and Xia, 2010, 2011; Luo et al., 2014).

In the case of installing new belt conveyors, the first two methods are effectively and efficiently applied to reduce power consumption. However, in the case of well-working conveyors these methods require large extra investments, since they need to replace existing conveyor components or change the current layout of belt conveyor systems. The third method, which attempts to recover the kinetic and the potential energy of the transported material, is ecologically promising and technically possible. However, as suggested by Graaf (2013), this method may be not economically viable because it costs more money than it generates. The fourth and fifth methods can be applied to the conveyors to be installed, or to the existing conveyors with limited extra investments. However, the fifth method, which reduces the electricity cost via the time-of-use tariff, does not reduce the power consumption in practice. Therefore, the thesis focuses on methods that optimize the drive operation, especially the method of adjusting the conveyor speed.
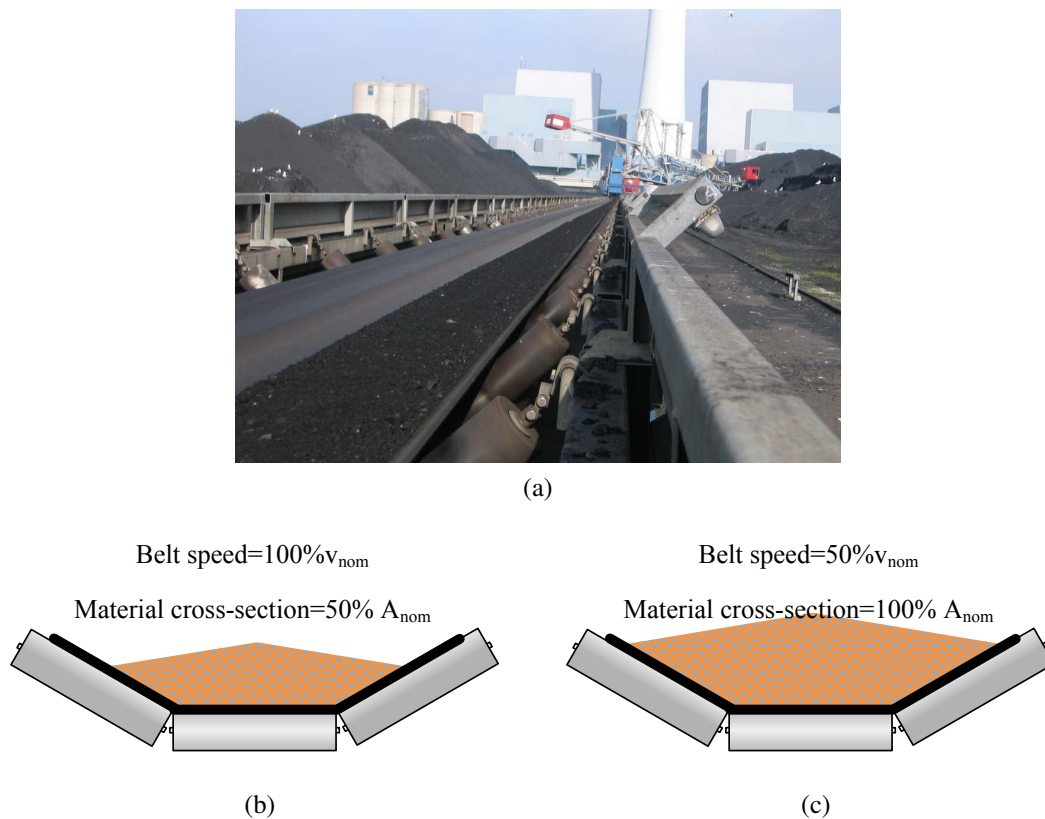
Figure 1.2: Principle of speed control. (a) Low filling ratio of a belt conveyor, courtesy of IWEB-I.com. (b) The belt conveyor is running at nominal speed with partically loaded. (c) The belt conveyor is running at non-nominal speed with fully loaded.

The method of adjusting conveyor speed to reduce energy consumption is called speed control (Hiltermann, 2008). Generally, belt conveyors are running at a designed nominal speed and in most cases they are only partially loaded (see Figures 1.2a and 1.2b). This can result from the variation of bulk material flow discharged onto the belt conveyors, since they can be part of a bulk material handling chain in which the actual material flow is determined by the upper-stream handling process. Taking the bulk material transportation system in a terminal for instance, the material flow varies with the variable-in-time number of available ship unloaders. The peak of the material flow feeding rate can be predicted on the basis of the actual number of available unloaders. In such cases, the conveyor speed can be adjusted to match the material flow, and as a consequence the conveyor's filling ratio is to be significantly improved (see Figure 1.2c). Then, according to the standard DIN 22101 (German Institute for Standardization, 2015), the belt conveyor's energy consumption is expected to be reduced.

The research on speed control can be dated back to the end of the last century (Daus et al., 1998). Over the past few years, several important results have been achieved. Based on the standard DIN 22101, Hiltermann et al. (2011) proposed a method of calculating the energy savings achieved via speed control. Field tests were carried out in which the belt speed was manually adjusted by varying the output frequency of the installed frequency converter. According to the measurement data of a studied belt conveyor, speed control resulted in a 21% decline of the total power consumption at a certain operation condition. Zhang and Xia (2009) put forward a

modified energy calculation model which combined energy calculations in DIN 22101 and ISO 5048 (International Organization for Standardization, 1989). Based on this model, the time-of-use tariff was considered in the relative research (Zhang, 2010; Zhang and Xia, 2011; Luo et al., 2014), and a model-predictive-control method was proposed to optimize the operating efficiency of belt conveyors. As the simulation result showed, both the electrical energy and the payment were considerably reduced by the variable-speed-drive-based optimal control strategy. Considering the dynamics of belt conveyors, Pang and Lodewijks (2011) proposed a fuzzy control method to adjust the conveyor speed in a discrete manner. The experimental result showed that the fuzzy control system could be effectively applied to improve the energy efficiency of bulk material conveying systems. A fuzzy logic controller was built by Ristic et al. (2012) for the purpose of applying speed control to belt conveyors. Measurements over a long period of time were carried out on a system with an installed power of 20 MW. Data for three belt conveyors was collected over eight months. The measurement results affirmed that the fuzzy logic control allowed belt conveyors to save energy.

Besides the promising energy savings, extra benefits are also expected to accrue from the applications of speed control, such as a reduced carbon footprint, and less mechanical and electrical maintenance (Daus et al., 1998).

1.2   Problem statement

The research on belt conveyor speed control has been ongoing for more than 20 years, and some important results have been achieved. However, previous research did not cover some issues for practically applying speed control, such as the potential risks and the dynamic analysis of belt conveyors in transient operations. Traditionally, the operational conditions of belt conveyors can be distinguished into the stationary operation and the transient operation. The stationary operation, defined by Lodewijks and Pang (2013a), includes both the case where the belt is not moving at all and the case where the belt is running at full design speed. Differing from the stationary operation, the transient operation normally includes the normal operational start, the aborted start, the normal operational stop and the emergency stop (Lodewijks and Pang, 2013a). In the thesis, we expand the definition of transient operations into normal acceleration or deceleration operations between neighboring stationary operations. Pang and Lodewijks (2011) state that in transient operations, a large ramp rate of conveyor speed might result in very high tension on the belt, which is the major reason for belts breaking at the splicing area. Besides the risk of belt over-tension, several other risks in transient operations should also be taken into account. These include the risk of belt slippage around the drive pulley, the risk of material spillage away from the belt, the risk of motor over-heating, and the risk of pushing the motor into the regenerative operation.

Besides the potential risks, another important issue is the dynamic analysis of transient operations in speed control. Researchers and engineers have already studied conveyor dynamics for decades. However, these researches mainly focus on the realization of soft start-ups or soft stops. The transient operations for speed control should be given more attention, since the belt conveyors often have a high filling ratio due to the conveyor speed adjustment. Moreover, the

dynamics of belt conveyors in transient operation are more complex, especially in cases where the conveyor speed is frequently adjusted to match a variable material flow.

The energy model, derived from the standard DIN 22101, is widely used in practice for assisting the design of a belt conveyor. The DIN-based energy model uses a constant value of the artificial frictional coefficient f to calculate the main resistances. However, as Spaans (1991) suggests, the coefficient of main resistances varies with different belt conveyors and different operating conditions. This is also confirmed by Song and Zhao (2001) and Hiltermann (2008). Hiltermann (2008) further carried out physical experiments to calculate the f factor value. However, physical experiments in practice are expensive, and they may cause a negative impact on the operational plan. Therefore, another technique is required to calculate the f factor value.

1.3   Research aims and questions

This thesis aims to investigate *the application of speed control to belt conveyors for reducing energy consumption*. The key research questions is

* How well can belt conveyors perform under speed control, taking both the dynamic belt performance and the energy savings into account?

To answer the main research questions, several sub-questions need be examined:

- What is the research status of the belt conveyor speed control?

- How can we determine the permitted maximum acceleration and the demanded minimum acceleration time in transient operations, taking both the potential risks and the dynamic performance of belt conveyors during speed control into account?

- How can we accurately estimate the energy consumption of belt conveyors?

- How should the belt conveyor speed control system be modeled to assess the conveyor performance under speed control?

- To what extent can the energy consumption be reduced by using speed control in different manners?

1.4   Methodologies

Both theoretical and experimental methodologies will be applied in the research. In order to determine the maximum acceleration and the minimum acceleration time in transient operations, a three-step method will be proposed. It can be briefly expressed by Estimation-Calculation-Optimization, and is called ECO in short. The ECO method takes both the potential risks and the conveyor dynamics in transient operations into account. In the Estimation process, an estimator is built on the basis of potential risks to approximate the permitted maximum acceleration.

The Calculation process carries out computational simulations to analyze the performance of belt conveyors in transient operations. Taking the potential risks and the conveyor dynamics into account, further simulations are carried out in the Optimization process to determine the optimum acceleration time. These computational simulations are based on an existing finite-element-method (FEM) belt model which is described in detail by Lodewijks (1996).

The DIN-based energy model is used to calculate the power consumption, and to estimate the power reduction via speed control. In order to accurately estimate the energy consumption of belt conveyors, an analytical calculation method will be proposed to calculate the f factor values for different loads and for different speeds. The method will calculate the sub-resistances of the main resistances by using the calibrated sub-resistances models. These sub-resistances include the indentation resistances of the belt, the flexural resistances of the belt and material, and the rotating resistances of the rollers. Importantly, the impact of the variation of the belt tension will be taken into account to calculate the flexural resistances.

To evaluate the performance of speed control, several speed control models will be built and a series of computational experiments will be carried out with different control algorithms. In the experiments, different loading scenarios will be taken into account. Both the passive speed control and the active speed control will be studied. In addition, in order to evaluate the economical and social benefits, several key performance indicators (KPIs) will be defined and used to analyze the speed control performance.

1.5   Thesis outline

The thesis outline is graphically shown in Figure 1.3.

Chapter 2 introduces the speed control of belt conveyors. It includes the definition, the principle, the classification and the prerequisites of speed control. In addition, after a literature review, the benefits and the challenges of speed control are analyzed in detail.

Chapter 3 presents the speed adjustment operations. Risks in transient operations are analyzed, and the ECO method is introduced to determine the minimum speed adjustment time. In addition, the FEM-based belt model is used to analyze the conveyor's dynamic performance in transient operations.

Chapter 4 analyzes the energy loss of belt conveyors. According to the individual energy losses along the conveyor length, a analytical model is proposed to calculate the artificial frictional coefficient for different loads and speeds. The variable drive system efficiency is also taken into account.

Chapter 5 builds the modeling of belt conveyor speed control systems. The speed adjustment operation discussed in Chapter 3 and the energy model introduced by Chapter 4 are taking into account. According to different loading scenarios, the passive and active speed controllers are built, and several control strategies are taken into account. In addition, several key performance indicators are defined to assess the speed control performance.

Chapter 6 investigates the performance of speed control. Both the passive speed control and the active speed control are performed. The study of the passive speed control carries out both the static calculations and the dynamic simulations. The active speed control accounts for

the fixed time interval strategy and the variable time interval strategy. In terms of the fixed time interval, the impact of different speed sets and of different time intervals are further studied.

Chapter 7 concludes and provides recommendations for further research.
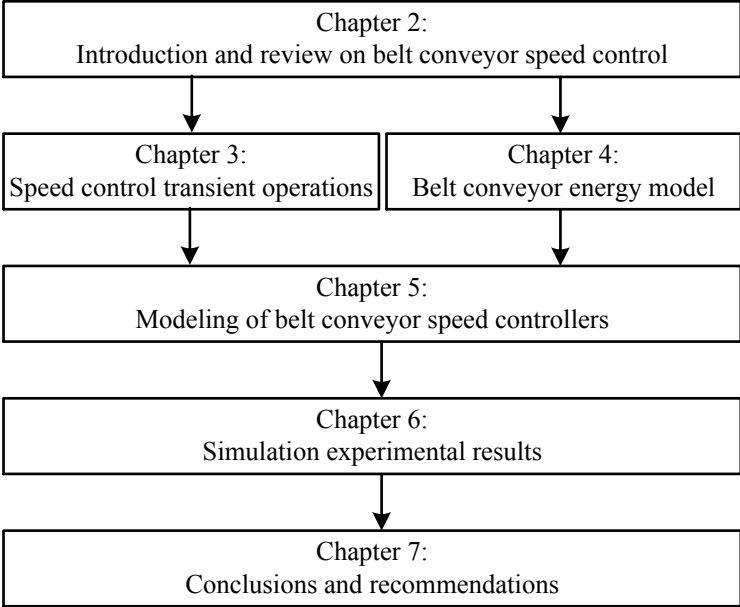
Figure 1.3: Thesis outline

Chapter 2

Belt conveyors and speed control

Belt conveyors have been widely used in the solid material handling and conveying systems. The extensive utilization of belt conveyor results in a large consumption of electricity. Taking the economic and ecological demands into account, several power reduction solutions have been proposed. According to the standard DIN 22101, a certain reduction of power consumption can be achieved by adjusting the conveyor speed to match the material flow. The technique of adjusting the conveyor speed to achieve energy savings of belt conveyors is called speed control. This chapter details speed control and reviews the relative researches. Section 2.1 introduces the basic configuration of belt conveyors in brief. Section 2.2 investigates the solutions of power savings of belt conveyors, and classifies them into four groups: methods of applying energy efficient components, methods of optimizing the design, methods of recovering energy, and methods of optimizing the drive operation. Speed control belongs to the last method, and the conception of speed control is defined in Section 2.3. The conveyor speed has a linear relationship with the conveying capacity, and Section 2.4 discusses the principle of speed control. According to different operational manners, Section 2.5 suggests that speed control can be applied either in a passive or active way. Moreover, the active speed control can be realized by a continuous or discrete way. No matter whether speed control is carried out passively or actively, as discussed in Section 2.6, a speed control system requires at least a speed controller to direct the variable speed drive to match the material flow observed by a material flow sensor. After satisfying these prerequisites, speed control is expected to be applied to reduce the energy consumption of belt conveyors. As reviewed in Section 2.7, speed control has been studied for almost twenty years, and several important research results have been achieved. Besides the power reduction, the implementation of speed control can achieve other additional benefits. In Section 2.8, these benefits are grouped into operational benefits, ecological benefits and economic benefits. Additionally, Section 2.8 gives an analysis of the research challenges. Some conclusions are drawn in the last section.

2.1 Basic configuration of belt conveyors

Figure 2.1 illustrates a typical belt conveyor. The moving belt carries the material towards the head pulley. In order to overcome the motional resistances along the conveying direction, the

conveyor is driven by a head pulley. Generally, the drive pulley is located at the head of the belt conveyor. Belt conveyor lengths are in the range of a few meters to tens of kilometers. In the case of long belt conveyors, intermediate drives are sometimes installed to reduce the required belt tension. Along the conveying route, the belt is supported by a huge number of rotating idler rollers. Between neighboring idler stations, the moving belt has a sag due to its own weight and the material load. To reduce the sag ratio, a large pre-tension is produced by a gravity take-up device. In the application shown in Figure 2.1, the take-up device is tied to the tail pulley. The gravity take-up device, or named tension weight, gives a constant belt tension which is independent of the belt load. Beside the tension weight, the belt tension also can be achieved by a mechanical tensioning system, and normally the belt is pre-tensioned after the drive pulley.
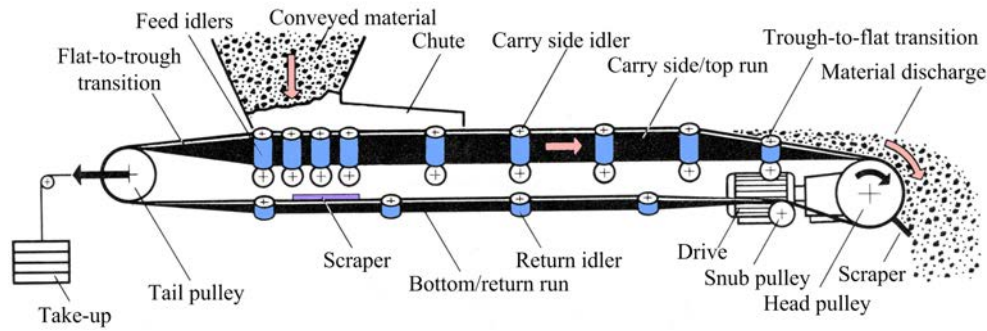
Figure 2.1: Belt conveyor components and assembly (Courtesy of ConveyorBeltGuide.com (ConveyorBeltGuide, 2016))

The research object of this thesis is the trough belt conveyor system.That is the most common belt conveyor system in the industrial applications. As illustrated in Figure 2.2, the idler station at the carrying side consists of three equal-length rollers, and the station of return side is composed of a two-roll "V" idler. As the figure shows, at the carrying side, two wing rolls are mounted in a defined angle λ. Together with the surcharge angle β of dry bulk material, they create a material cross section on the top of the belt. According to the standard DIN 22101 (German Institute for Standardization, 2015), the nominal cross-section area A_{nom} of a troughed belt conveyor is determined by:

$$A_{nom} = \left[l_m + \frac{(b_c - l_m)}{2} cos\lambda \right] \frac{(b_c - l_m)}{2} sin\lambda + \left[l_m + \frac{(b_c - l_m)}{2} cos\lambda \right]^2 \frac{tan\beta}{4} \qquad (2.1)$$

where b_c is the contact length of bulk material. According to DIN 22101, the contact length depends on the belt width:

$$B \leq 2000mm \quad b_c = 0.9B - 50mm \qquad (2.2)$$

$$B > 2000mm \quad b_c = B - 250mm \qquad (2.3)$$

Accordingly, the nominal conveying capacity Q_{nom} is

$$Q_{nom} = 3.6 A_{nom} \rho_s v_{nom} \qquad (2.4)$$

in which

ρ_s density of bulk solid material conveyed

v_{nom} nominal speed of a belt conveyor
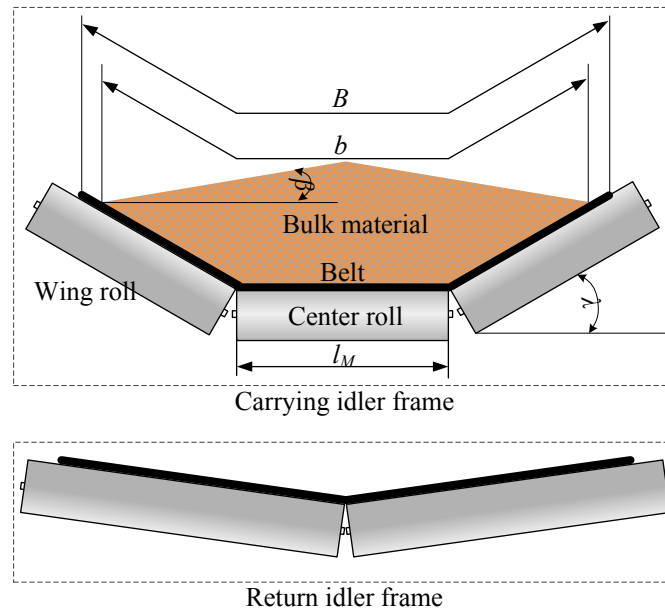
Figure 2.2: Troughed idler sets

2.2   Solutions for reducing energy consumption of belt conveyors

Due to their inherent advantages, such as high capacity and low labor requirement, belt conveyors play a significant role in bulk solids handling and conveying. According to Daniel Clénet (2010), there are more than 2.5 million conveyors operating in the world. Considering their extensive use, the operations of belt conveyors involve a large amount of electricity. For instance, belt conveyors are responsible for 50% to 70% of the total electricity demand in a dry bulk terminal (Hiltermann, 2008) and about 10% of the total maximum demand in South Africa is used by bulk material handling (Marais, 2007). Furthermore, coal-fired power plants currently fuel 41% of the global electricity (Goto et al., 2013) and the coal makes up above 45% of the world's carbon dioxide emissions from fuels (International Energy Agency, 2015). Therefore, taking the economic and ecological challenges associated into account, there is a strong demand for lowering the energy consumption of belt conveyors, and for reducing the carbon footprint.

Over the past decades, several different techniques have been proposed. Based on different objects of the belt conveyor, these different approaches can be classified into four groups:

- methods of applying energy efficient components, such as

    - low loss conveyor belts

        * low loss rubber of bottom cover (Falkenberg and Wennekamp, 2008; Gerard van den Hondel, 2010)

        * low weight belt (Lodewijks and Pang, 2013c)

    - energy-saving idler stations

        * low loss rollers (Mukhopadhyay et al., 2009)

        * new design of idler stations, such as ESIdler (Stephens Adamson, 2014)

    - energy efficient driving systems

        * efficient driving units, such as frequency converters, gearboxes and motors (ABB, 2000)

- methods of optimizing the design, such as

    - optimizing the route of conveyors (Yester, 1997)

    - reducing the number of intermedium transfers (Alspaugh, 2004)

- methods of recovering energy, such as

    - braking based re-generators (Rodriguez et al., 2002)

    - driven-turbine based generators (Michael Prenner and Franz Kessler, 2012; Graaf, 2013)

- and methods of optimizing the drive operation, such as

    - controlling motor sequences (Dalgleish and Grobler, 2003; Levi, 2008)

    - adjusting the conveyor speed (Hiltermann, 2008; Jeftenic et al., 2010; Pang and Lodewijks, 2011; Ristic and Jeftenic, 2011)

In the case of installing new belt conveyors, the first two methods are effectively and efficiently applied to reduce the power consumption. However, in the case of well-working conveyors these methods require large extra investments, since they need to replace existing conveyor components or change the current layout of belt conveyor systems. The third method, which attempts to recover the kinetic and the potential energy of the transported material, is ecologically promising and technically possible. However, as suggested by Graaf (2013), this method may be not economically viable since this solution costs more money than it generates. The fourth method can be applied to the conveyors to be installed or the existing conveyors with limited extra investments. Therefore, the thesis focuses on the method optimizing the drive operation, especially the method adjusting the conveyor speed.

As Equation 2.4 suggests, the belt conveyor's nominal capacity is dependent on the nominal cross-section area of bulk material, the density of the bulk material and the nominal conveyor speed. Normally, the actual material flow is generally lower than the nominal conveying capacity of belt conveyors. Therefore in most cases when the belt conveyor is running at nominal speed, the belt will be partly filled. As proved by Daus et al. (1998); Hiltermann (2008); Lodewijks et al. (2011), lowering belt speed can achieve considerable energy savings of belt conveyors by adjusting the conveyor speed. (Hiltermann, 2008) defined this technique as speed control.

2.3 Conceptions of speed control and transient operations

Speed control is "the intentional change of the drive speed to a value within a predetermined rate under certain conditions for specific purposes" (Anonymity, 2016). Traditionally, speed control is widely applied to achieve soft start-up or stop operations. In terms of star-ups, several techniques, such as variable frequency control, variable fill hydro-kinetic coupling and variable mechanical transmission couple, have been employed to provide acceptable start-up performance under all belt load conditions (Nave, 1996). In addition, the sinusoidal and triangular acceleration profiles, individually commended by Harrison (1983) and Nordell (1987), are commonly applied to provide good dynamic performance of belt conveyors. In terms of soft stop operations, intelligent braking systems have been developed, which use cutting-edge technologies to allow a specified braking time (Al-Sharif, 2007). Moreover, the overshoot and oscillations at the end of the braking sequence can be minimized or eliminated. Differing from the traditional applications of speed control on belt conveyors, speed control in this thesis is applied to adjust the conveyor speed to match the material flow, so that the power reduction of belt conveyors is expected to be realized. Therefore, speed control in the thesis is redefined as: a technique of adjusting the conveyor speed for the purpose of reducing energy consumption of belt conveyors.

The operation of adjusting speed is defined as the transient operation. In Lodewijks and Pang (2013a), the operations of belt conveyors are distinguished into two types: the stationary operation and the transient operation. The stationary operation includes both the case where the belt is not moving at all and the case where the belt is running at full design speed. Differing from the stationary operation, the transient operation normally includes the normal operational start, the aborted start, the normal operational stop and the emergency stop (Lodewijks and Pang, 2013a). In this thesis, the definition of stationary operation is expanded into the operation where the belt is running at a predetermined speed and this speed can be either nominal or non-nominal speed. In addition, the transient operations are expanded into the acceleration or deceleration operations between neighboring stationary operations. This will be further detailed in Chapter 3.

2.4   Principle of Speed control

Belt conveyors are designed to cope with the potential peak of material flow. If it is assumed that the conveying capacity of belt conveyor system equals the demanded maximum, then as suggested by Equation 2.4, the value of the nominal belt speed and the value of nominal cross-section area of bulk material on the belt are responsible for the maximum conveying capacity.

(a) Nominal speed   (b) Non-nominal speed
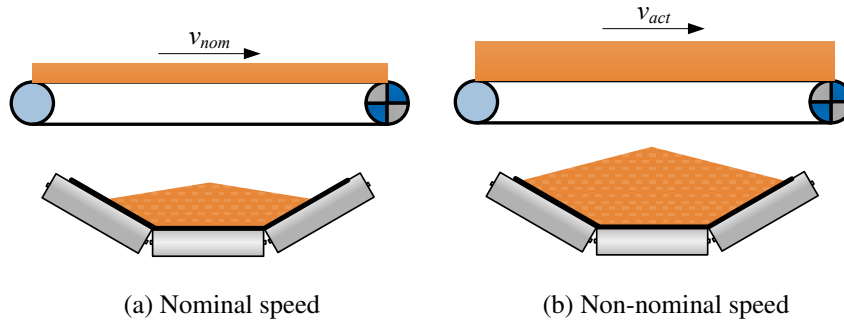
Figure 2.3: Principle of speed control. v_{nom}: nominal speed, v_{act}: actual non-nominal speed.

Figure 2.3 illustrates the principle of speed control. Most often the belt conveyor is running at nominal speed. In a large number of cases, the feeding rate is lower than the nominal conveying capacity . In these cases the belt conveyor is partially filled by the dry bulk material (see Figure 2.3a). In order to reduce the energy consumption, the conveyor speed can be reduced to follow the actual feeding rate. As shown in Figure 2.3b, the belt filling ratio is significantly improved due to speed control. Taking the permitted cross-section area of material on the belt into account, the actual conveyor speed v_{act} should satisfy the following equation

$$v_{act} \geq \frac{Q_{act}}{Q_{nom}} v_{nom} = \frac{A_{act}}{A_{nom}} v_{nom} \qquad (2.5)$$

where

- Q_{act} is the actual feeding rate.

- A_{act} is the cross-section area of material on the belt when the conveyor is running at nominal speed.

Practically the belt speeds are determined slightly higher than the required minimum belt speed, so that the risk of material overload can be prevented (Pang and Lodewijks, 2011). However, Pang and Lodewijks (2011) also suggest that the actual cross-section area of bulk solid material on the belt conveyor is allowed to be 10% larger than the nominal for a short time period. The similar suggestion is also given by Kolonja et al. (2003), since according to DIN 22101 (German Institute for Standardization, 2015), the conveyor capacity is calculated on the basis of 80% of belt cross-section utilization.

2.5   Classifications of speed control

According to Hiltermann (2008), speed control of belt conveyors can be performed in two ways: passively and actively. Accordingly, speed control can be basically classified into two groups: the passive speed control and the active speed control.

In the passive speed control, the belt speed is lowered but fixed. According to the potential peak of material flow in the future minutes or hours, a suitable belt speed is selected prior. Taking the bulk material conveying system in an import terminal for example. At the unloading area of the land side, several ship unloaders are mounted. According to the unloader schedule, the number of available ship unloaders varies in time. Based on the number of operating unloaders in a certain time period, the potential peak of material flow in that time interval can be determined. Then the conveyor speed can be adjusted to match the potential peak of material flow rate, or to match the number of available unloaders. The applications of the passive speed control can be found in (Daus et al., 1998; Lodewijks et al., 2011; Hiltermann et al., 2011), and as suggested by Hiltermann (2008), in the applications of the passive speed control, the selection of the belt speed is significantly responsible for the magnitude of the final energy savings.

In the active speed control, the material flow is monitored in real time. Then, according to the variation of the actual material rate, the conveyor speed is adjusted automatically to ensure the cross-section area of bulk material on the belt to be in the greatest possible degree. According to Lodewijks et al. (2011), the active speed control can be realized in a continuous or discrete manner. However, as suggested by Pang and Lodewijks (2011), the discrete speed control for belt conveyor is more preferred for practical reasons. Firstly, a continuous active speed control needs to adjust the belt speed according to the actual material flow on the belt. When the material flow fluctuates, detrimental vibrations may occur on the belt and conveyor construction at certain belt speeds. The belt speed at which vibration occurs should therefore be avoided. Secondly, when the material flow fluctuates considerably, the demanded acceleration can be larger than the permitted. An unexpected large tension can result in for instance reducing the service life of belt. Therefore, the discrete active speed control is preferred in practice.

The passive speed control employs a fixed speed based on the expected material flow in the future time interval. Under this control, small and/or temporary variations in the material flow do not result in belt speed variations, so that the passive speed control is a semi-optimal method. The active speed control accounts for the variation of material flow. If the variation is considerable, the conveyor speed will be adjusted to reduce the deviation. Therefore, compared to the passive speed control, the belt speed in active speed control is lower on average. Therefore more energy savings are expected to be achieved by the active speed control. However, due to the frequent speed adjustment, the active speed control has not been implemented anywhere to date in practice.

2.6 Prerequisites of speed control system

The speed control has already been proved to be effectively to reduce the energy consumption of belt conveyors. In order to apply speed control, at least two prerequisites must be satisfied: the proper feeding conditions and the speed control systems. According to Pang et al. (2016), the feeding condition or the loading conditions can be classified into different scenarios which will be detailed in Section 5.1. This section mainly discusses the requirement of speed control systems.

Almost any modern control system contains a controller to analyze the data observed from sensors, and to command the actuator to respond for moving or for controlling a mechanism or system. The speed control system is such a modern control system, of which a speed controller directs the variable speed drives to match the material flow observed by a material flow sensor.

2.6.1 Speed controller

Speed controller is the key of a speed control system. It analyzes the potential peak or the real value of the material flow, and then commands the motor to keep or change the belt speed. According to different operating principles, the control system has two types: passive and active speed control systems. In the passive speed control, the selection of conveyor speed determines the magnitude of energy savings of belt conveyors. Moreover, the speed curves generated by the controller are responsible for the conveyor dynamics in transient operations. In transient operations, especially in acceleration operation, the improper speed curves might result in for instance the risk of belt over-tension. Therefore, the passive speed control system requires a precise selection of belt speed and a good speed curve generator. Comparing with the passive speed control, the active speed control is more complex, since in the active speed control, the belt speed might be more frequently adjusted to match the variable material flow. Moreover, differing with the passive speed controller which generally is an open-loop controller, the active speed controller can be either an open-loop or closed-loop controller.

2.6.2 Variable speed drives

Variable speed drives are the actuator of the speed control system, and they are having been widely used for achieving soft start-ups of belt conveyors. Variable speeds can be realized by employing mechanical or electronic devices (see Figure 2.4). According to Conveyor Equipment Manufacturers Association (2005), the common mechanical methods of obtaining variable speeds are: V-belt drives on variable pitch diameter sheaves or pulleys, variable-speed transmission, and variable-speed hydraulic couplings. The electrical variable speed drivers mainly rely on the variable frequency converter, which varies the motor input frequency and voltage to control the alternating-current (AC) motor's speed and torque. Comparing with other variable speed drivers, the variable frequency converter based drivers behave more efficiently, and can drive belt conveyors in specialized patterns to further minimize mechanical and electrical stress. Especially in the active speed control where the conveyor speed is frequently adjusted,

the frequency-controller drive shows a good controllability in speed adjustment operations.
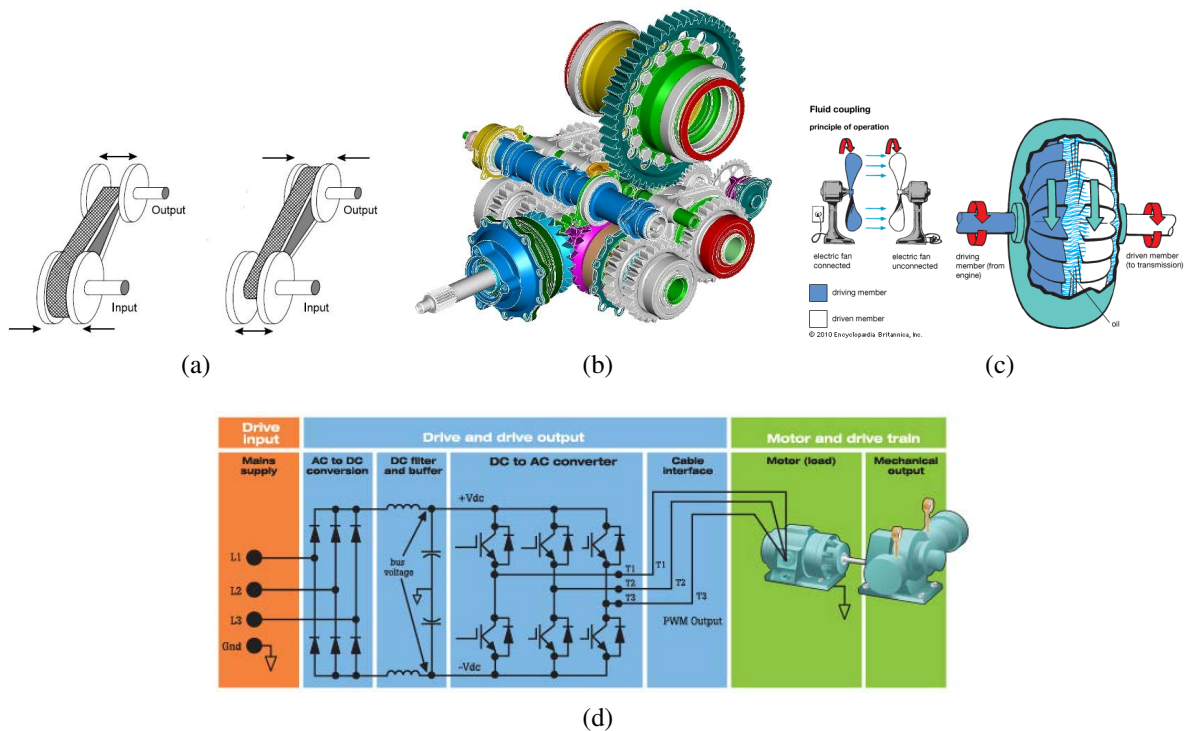
Figure 2.4: Variable speed drivers. (a) V-belt drives, courtesy of Barnes (2003). (b) Variable-speed transmission, courtesy of Ricardo (2010). (c) Variable-speed hydraulic coupling, courtesy of Encyclopedia (2010). (d) Variable frequency drives, courtesy of Fluke Corporation (2016).

Figure 2.5: Material flow sensors. (a) Belt scale, courtesy of FLSmidth Pfister Limited (2017). (b) Laser profilometer, courtesy of SICK B.V. (2017).

2.6.3 Material mass/volume sensor device

The material flow can be detected by a sensor. In the passive speed control, the value of material flow rate is detected to ensure that the material loading rate is no larger than the permitted conveying rate, so that the belt's overburden can be avoided. In the active speed control, the

material feeding rate is monitored in real time, so that the belt speed can be precisely adjusted to match the variable flow rate. In addition, the actual value of material flow can be used to estimate the power consumption of belt conveyors, and to evaluate the power savings by means of speed control. The material flow rate can be measured either by belt weighers or volume flow sensors. According to different principles, the material flow rate can be measured by a belt scale (Figure 2.5a) or by a laser profilometer (Figure 2.5b).

2.6.4   Others

Besides above discussed components, some other accessories also contributes to improve the performance of speed control. For example, extra cooling fans are recommended to improve the cooling effect of shaft-mounted radial fan on the AC motor, especially when operating speeds are reduced more than 50%. In addition, variable geometry discharge chutes are required to avoid severe wear of the chute, since varying the belt speed changes the material discharge parabola at the discharge points.

2.7   Review on academic research and industrial applications

Previous sections briefly described the belt conveyor speed control. This section will review its academic researches, including the industrial applications. Researches on belt conveyor speed control can be distinguished into three aspects. The first aspect is characterized by the viability analysis of speed control for the purpose of energy savings. Subsequently, the development is continued by exploiting different control algorithms of speed control and investigating the efficacy of different forms of speed control.

2.7.1   Aspect I- Analyzing the viability of speed control

The research of viability analysis of speed control can be dated back to a report by Daus et al. (1998), in which a new conveying and loading system was installed to replace the old one. A load-dependent belt-speed adjustment system was developed in order to achieve energy savings of the new conveyor system. According to the standard DIN 22101 (German Institute for Standardization, 2015), the kinetic resistance F could be approximated by

$$F = CfL \left(m'_{roll} + \left(2m'_{belt} + m'_{bulk} \right) cos\delta \right) g + Hm'_{bulk}g \tag{2.6}$$

in which

$\quad$ C $\qquad$ the coefficient of secondary resistances

$\quad$ f $\qquad$ the artificial coefficient of frictional resistances

$\quad$ L $\qquad$ the conveying length of conveyor

$\quad$ m'_{roll} $\quad$ the mass of idler rolls in unit length

m'_{belt} the linear density of belt

m'_{bulk} the linear density of bulk material

δ the inclination angle of a belt conveyor

g gravity acceleration

H the height difference between the loading and unloading areas of a belt conveyor

Then taking the conveyor speed v and the efficiency η_{sys} of the driving system into account, the required electrical power was

$$
\begin{aligned}
P_e &= \frac{Fv}{\eta_{sys}} = \frac{1}{\eta_{sys}} \left[CfL \left(m'_{roll} + 2m'_{belt} \right) gv + (CfLg + Hg) \left(m'_{bulk}v \right) \right] \\
&= \frac{1}{\eta_{sys}} \left[CfL \left(m'_{roll} + 2m'_{belt} cos\delta \right) gv + (CfLgcos\delta + Hg) \frac{Q_{act}}{3.6} \right] \quad (2.7)
\end{aligned}
$$

If it was assumed that the values of f and η_{sys} were constant at different temperatures and speeds, then Equation 2.7 yielded that the energy consumption was lowered over a reduction of belt speed. Accordingly, the theoretical viability of speed control was determined. Moreover, from Equation 2.7 it can be learned that, the principle behind power savings by means of speed control is to reduce the movement of idler rolls and the belt.

The viability of belt conveyor speed control was also determined by physical experiments. Hiltermann (2008) performed measurements at a dry bulk terminal. Both the material loading rate and the conveyor speed were manually altered. Power consumption was measured by using a digital clam meter to detect the input power of a frequency converter. Figure 2.6 illustrates the experimental result. The data clearly shows that the operation running at a higher belt speeds had consumed more power as compared to that running at a lower speed. Accordingly, speed control had successfully allowed the power reduction of the concerned belt conveyor.

2.7.2   Aspect II- Developing speed control algorithms

In order to improve the energy efficiency of belt conveyors, several speed control algorithms have been developed. Daus et al. (1998) introduced an algorithm in which the conveyor speed was determined by the number of excavators in use. This algorithm is simple and can be detailed by the following equation:

$$
\text{actual belt speed} = \begin{cases}
50\% \text{ nominal belt speed} & \text{1 excavator} \\
75\% \text{ nominal belt speed} & \text{2 excavators} \\
100\% \text{ nominal belt speed} & \text{3-4 excavators}
\end{cases} \quad (2.8)
$$

This algorithm can be applied in the passive speed control, in which the deviation of material flow rate in a certain time period can be ignored.
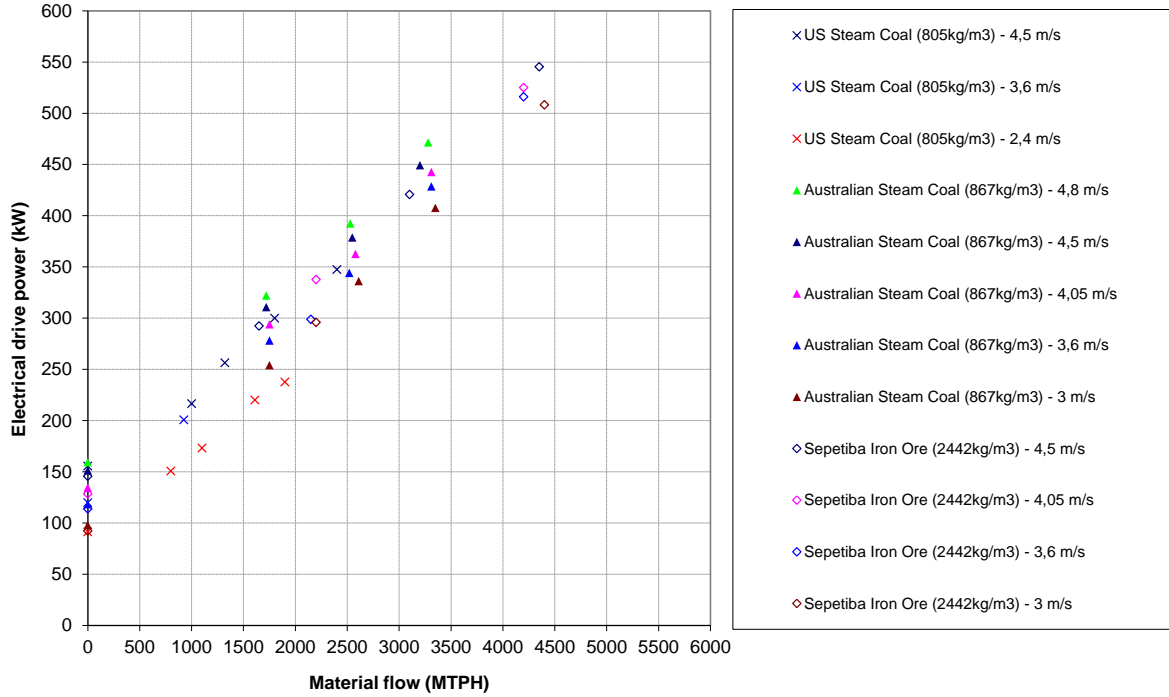
Figure 2.6: Measured electrical power of the studied belt conveyor. Courtesy of Hiltermann (2008).

As suggested by Hiltermann (2008), the passive speed control normally results in less energy savings than active speed control, especially in cases where the material flow has a considerable deviation. However, the active speed control might result in continuous high belt tension. Therefore, rather that in a continuous speed manner, the active speed control in practice prefers to work in a discrete manner. Pang and Lodewijks (2011) proposed fuzzy control, as one control method based on fuzzy logic to provide discrete control strategy, to discretize the operations of speed control. Pang and Lodewijks (2011) defined a finite number of fuzzy boundaries $b_n(n = 1, 2, ..., n)$ in the percentage of nominal conveying capacity. If a value x was in the range $[b_i, b_{i+1})$, the fuzzy membership function was constructed as

$$f_{b_{i+1}}(x) = \frac{b_{i+1} - x}{b_{i+1} - b_i} \tag{2.9}$$

$$f_{b_i}(x) = \frac{x - b_i}{b_{i+1} - b_i} \tag{2.10}$$

where

$$f_{b_i}(x) + f_{b_{i+1}}(x) = 1 \tag{2.11}$$

As shown in Figure 2.7a, the fuzzy values, derived from Equations 2.9 and 2.10, shows the position of a determined material loading rate within its range. Pang and Lodewijks (2011) further suggested that the adjustment of belt speed was determined based on the comparison of the fuzzy values of $f_{b_i}(x)$ and $f_{b_{i+1}}(x)$. Taking the case shown in Figure 2.7b for example, the conveyor was running at speed v_{i+1} in the case of the scenario $f_{b_{i+1}}(x) > f_{b_i}(x)$. When the
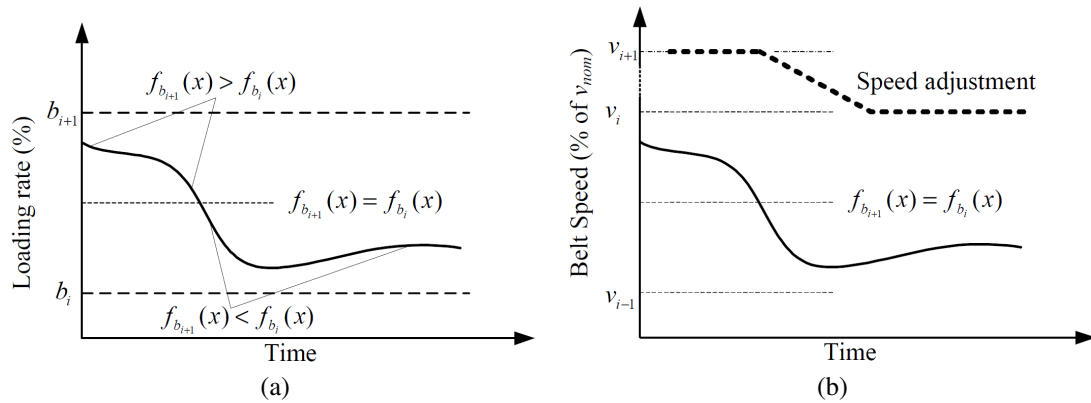
Figure 2.7: Fuzzy speed control. (a) Fuzzy values of loading rate in one fuzzy range. (b) Speed adjustment. Courtesy of Pang and Lodewijks (2011).

loading rate reached the midpoint of the range it fall, the fuzzy values $f_{b_i}(x)$ and $f_{b_{i+1}}(x)$ were equal, and then the speed adjustment with targeted speed v_i was triggered. Accordingly, speed control was discretized and the unnecessary continuous high belt tension could be avoided by the fuzzy control algorithm.

However, it is important to note that Pang and Lodewijks (2011) failed to take a special condition into account where the loading rate is fluctuating around a certain level, like $(b_i + b_{i+1})/2$ in Figure 2.8. In such cases, as the green line in Figure 2.8 shows, the speed adjustments are frequently triggered to match the variation of the loading rate. Taking the time required by the speed adjustment into account, the algorithm in (Pang and Lodewijks, 2011) may fail to be applied in that special condition. Therefore, before the implementation of fuzzy control, researches should be undertaken prior to analyze the material feeding conditions and to improve the control algorithm to avoid the frequent speed adjustment.
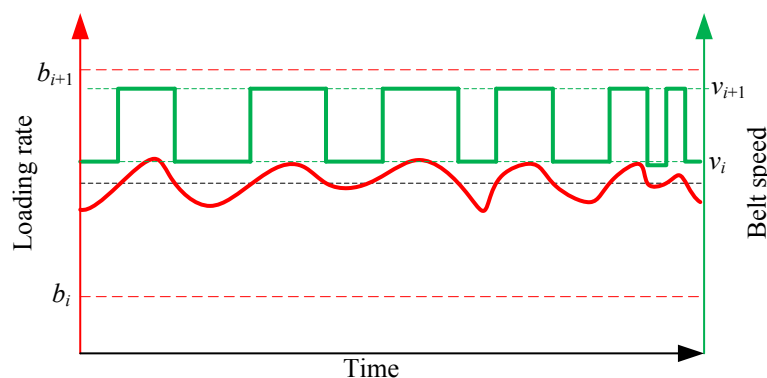
Figure 2.8: Loading rate is fluctuating around a certain level.

Differing from the fuzzy algorithm proposed by Pang and Lodewijks (2011), Ristic et al. (2012) used fuzzy logic to control the conveyor in a continuous way. The fuzzy logic controller built by Ristic et al. (2012) has three variables: two inputs (the drive torque Te and the speed error $DWref$) and one output ($N(DWref)$). The output $N(DWref)$ is the ramp rate of the belt speed. Ristic et al. (2012) gave the fuzzy rules as shown in Table 2.1. For the input

variable Te, if the driving torque is close to zero, narrow fuzzy sets are required to improve the control sensitivity and to avoid the braking operation donated by the fuzzy element "N". For any positive value of the Te, if the input variable $DWref$ is positive, then the fuzzy controller gave the output a big value $N(DWref)$ so that the conveyor could have a dramatic increase to avoid material spillage away from the belt. For the value of $DWref$, if the speed deviation is limited, the system had no sudden change of $N(DWref)$ so that the continuous high belt tension could be avoided.

Table 2.1: Fuzzy rules. The output is $N(DWref)$. N: negative; NS: negative small; NM: negative medium; NB: negative big; ZE: zero; PS: positive small; PM: positive medium; PB: positive big. Courtesy of Ristic et al. (2012).

Te DWref	N	ZE	PS	PM	PB
NB	ZE	NS	NM	NB	NB
NM	ZE	ZE	NS	NM	NB
ZE	ZE	ZE	ZE	ZE	ZE
PM	ZE	PB	PB	PB	PB
PB	ZE	PB	PB	PB	PB

To test the performance of the algorithm, Ristic et al. (2012) carried out a series of simulations. The experimental results showed that in the case of sudden decrease of incoming material flow, the control algorithm provided maximum deceleration but without braking. In addition, during the instantaneous and short-term increase of the incoming material flow, the algorithms provided maximum acceleration to follow the variable material flow. In the simulations, the spillage of material over the belt was avoided. As explained by Ristic et al. (2012), the transport could still be conducted without spillage, even when the actual cross-section area reached 116% of the theoretical value. However, the authors did not provide more information about the method of determining the value of the maximum acceleration in transient operations.

2.7.3   Aspect III- Investigating speed control efficiency

Based on the energy model shown in Section 2.7.1, Daus et al. (1998) computed the power saving potential for variable material feeding rates and for different belt speeds. The authors assumed that the minimum conveyor speed is 0.5 times of the nominal speed. The computational results were as shown in Figure 2.9, which suggests that lowering belt speed effectively and efficiently reduces the energy consumption. For instance, it can be learned from Figure 2.9 that if the material feeding rate is half of the nominal conveying capacity, lowering the conveyor speed to half of the nominal speed could reduce over 25% of that consumed by a nominal speed operation. Besides the computational experiment, Daus et al. (1998) implemented a long-term field test of a belt conveyor system at an opencast mine. The average loading rate was below 50%, and the average belt speed was 0.68 times of the nominal speed. After a long-term field test, Daus et al. (1998) yielded that the power consumption had been reduced by up to 16%.
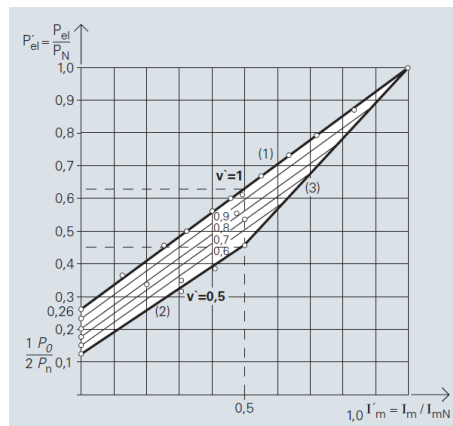
Figure 2.9: Power savings of belt conveyors by means of speed control. Courtesy of Daus et al. (1998)

Hiltermann (2008) implemented speed control of belt conveyors at a dry bulk terminal. In the field test, the material feeding rate was controlled and the belt speed was manually altered. The power consumption for different loads and for different speeds were shown in Figure 2.6. The data clearly shows that the power reduction varied with different loads and speeds.

Hiltermann et al. (2011) further suggested that, the power savings by means of speed control are dependent on the configuration of belt conveyors, the magnitude of experienced material flow and the selected belt speeds. To illustrate the dependency, Hiltermann et al. (2011) evaluated speed control efficiency on three different belt conveyors. The conveyors' characteristics were as illustrated in Table 2.2. These conveyors had the same trough configuration, and were operated under similar conditions on the same terminal. It was further assumed that these conveyors had the same f factor value. The experimental results were illustrated in Table 2.2. The data showed that in the defined feeding scenario, the potential power savings were varying from 8% to 21% over different belt conveyors. In addition, Hiltermann et al. (2011) further suggested that the inclination angle of belt conveyors could have a considerable impact on the relative power savings.

Zhang and Xia (2010) studied a coal conveying system in a coal-fired power plant. In the experiments, both the material feeding rate and the conveyor speed were controlled, so that the cross section of material onto the belt was kept near the maximum value. Two important experiments were carried out with different upper limitations of feeding rate: 1500 $MPTH$ and 750 $MTPH$, and 5.38% and 15.35% of the energy savings were achieved, respectively.

Ristic and Jeftenic (2011) implemented an active speed control on a belt conveyor system in an open-pit mine. During the experiment, the system operation alternated between the speed control mode and the constant speed mode, each for several hours. Twenty series of experimental data for three belt conveyors were collected. The average power in the individual series of measurements were as shown in Figure 2.10. The data indicated that the average consumption was reduced by the range from 3% to 19% by means of speed control.

Table 2.2: Belt conveyor characteristics and speed control savings. Courtesy of Hiltermann et al. (2011).

Parameters	Case 1	Case 2	Case 3
Length (m)	660	1,410	95
Material lifting height (m)	46.1	5.8	9.0
width (mm)	1,800	1,800	1,800
Trough angle (°)	40	40	40
Nominal speed (m/s)	4.5	4.5	4.5
Nominal capacity ($MPTH$)	6,000	6,000	6,000
$P_e(6,000\ MPTH)\ (kW)$	722	657	261
$P_e(3,250\ MPTH,\ 4.5\ m/s)\ (kW)$	449	471	156
$P_e(3,250\ MPTH,\ 2,75\ m/s)\ (kW)$	400	373	144
$P_{e,savings}(kW)$	49	98	12
$P_{e,savings}(\%)$	11	21	8
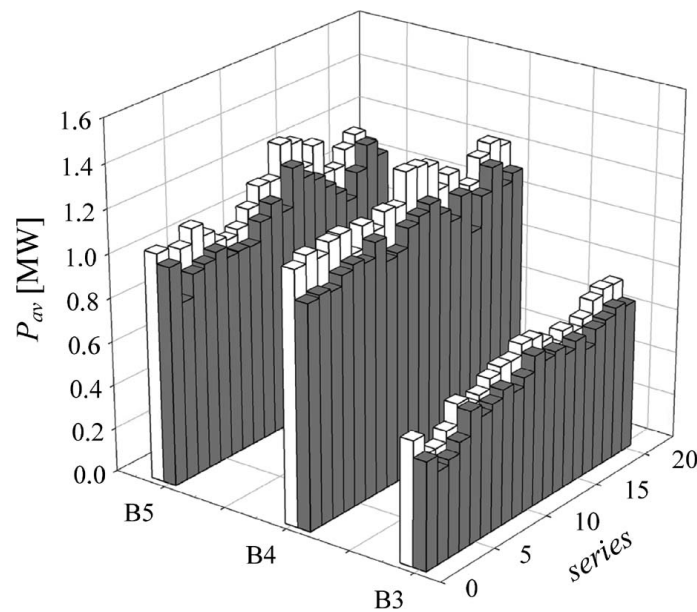
Figure 2.10: Average power consumption of belt drives on the third, fourth, and fifth belt conveyor stations (B3, B4, and B5): white bars—constant speed operation, gray bars—variable speed operation with fuzzy logic control. Courtesy of Ristic and Jeftenic (2011).

2.8   Benefits and challenges of speed control

According to the experimental results shown in Section 2.7, a certain amount of power reduction of belt conveyors can be achieved by speed control. Besides energy savings, the implementation of speed control can achieve other additional benefits, including operational benefits, ecological benefits and economic benefits. In terms of the operational benefits, speed control results in a considerable reduction in the wear rate of the system (Hiltermann, 2008; A.P. Wiid et al., 2009; Lodewijks et al., 2011). Taking the belt for instance, since material has to be accelerated less in the loading and accelerating areas, less wear will behave on the top rubber of belt. In addition, the variable speed operation presents a benefit in the expected pulley performance on basis of dynamic life expectancy. Therefore, speed control results in operational benefits of belt conveyors.

In terms of ecological benefits, due to lower average belt speed and reduced surface area per transported unit of material, less dust will be produced. Then dust emissions can be significantly reduced (Hiltermann, 2008). Moreover, the emissions of pollutants and greenhouse gases from fossil-based electricity generations can be lowered as a consequence, due to less electrical power consumption.

In terms of economic benefits, less power consumption of belt conveyors leads a reduction of electricity cost. In addition, if we take the social cost into account, a great reduction of social costs of environmental pollution can be achieved by speed control. Moreover, due to the longer service life time of conveyor components, such as pulleys, a reduction of maintenance costs can be achieved by speed control. This is also suggested by Daus et al. (1998) and (Hiltermann, 2008).

However, according to the literature survey, implementations of speed control that can be found in practice to reduce energy consumption are rare. Some problems of previous researches on speed control have not been handled. These major problems can be classified into two aspects. From the control aspect, previous research does not cover some issues, like the potential risks and the dynamic analysis of belt conveyors in transient operations. In previous researches, both Pang and Lodewijks (2011) and Ristic and Jeftenic (2011) suggested that the maximum acceleration should be limited to avoid unhealthy conveyor dynamics. However, these researches did not provide any general method of determining the permitted maximum acceleration of belt conveyors. From the energy saving aspect, the current power calculations use the constant f factor value, derived from DIN 22101, to estimate the power savings by means of speed control. However, more researches show that the f factor value varies with loads and speeds. Therefore, it is highly suggested to use the variable f factor values to improve the evaluation, instead of the constant f factor value.

This thesis aims to investigate the application of speed control on a belt conveyor, especially on improving the performance of a belt conveyor in terms of dynamics and economics. Based on the above mentioned research problems, this research is striving to overcome the following challenges:

(i) Providing a method to determine the permitted maximum acceleration and the requested minimum acceleration time.

(ii) Seeking an a method of calculating the DIN f factor values for different loads and for speeds.

2.9   Conclusion

This chapter described the belt conveyor speed control, and reviewed the academic researches and the industrial applications. From the literature, it can be concluded that speed control is a promising approach of reducing power consumption of belt conveyors. The literature research further suggests that previous researches did not cover some issues like potential risks and the dynamic performance of belt conveyors in transient operations. Moreover, the literature review indicates that the current research on speed control faces two major challenges: providing a method to determine the requested minimum speed adjustment time to ensure healthy dynamics of a belt conveyor during transient operations, and seeking an accurate energy model to assess the belt conveyor speed control. Taking these challenges into account, Chapter 3 will study the transient operations, and the belt conveyor energy model will be studied in Chapter 4.

Chapter 3

Speed control transient operations

Chapter 2 presented an overview of the academic researches of belt conveyor speed control. As the previous chapter concluded, the speed control of a belt conveyor lacks applicability, since the previous researches rarely took the conveyor dynamics in transient operations into account. This chapter is going to investigate the transient operations of belt conveyors. To improve the conveyor dynamic performance, a new method will be proposed to determine the minimum speed adjustment time in transient operations.

This chapter is based on (He et al., 2016a,b,c).

3.1 Introduction

When considering the operational conditions, Lodewijks and Pang (2013a) defined the operations of belt conveyors, and distinguished these operations into two groups: the stationary operation and the transient operation. The stationary operations include two cases: the case where the belt is totally stopped, and the case where the belt is running at a steady state speed. Conventially, belt conveyors are running at nominal speed. Due to speed control, the belt conveyor however is often running at non-nominal speed to match the actual material feeding rate. Therefore, as shown in Figure 3.1, the applications of stationary operations in this thesis are extended into three cases. If we do not take into account other issues, such as the efficiency of the driving system, the non-nominal speed can be any value between zero and the nominal speed.

Besides the stationary operation, Lodewijks and Pang (2013a) further defined the transient operation which normally includes the following situations:

- *Normal operational start.* A normal operational start is a start where the belt conveyor is started as planned. In a conventional normal operational start, a motor can be started simply by a direct online starter which directly connects the motor terminals to the power supply. This however only works for belt conveyors with motor power up till about 15 *kW*. Nowadays, variable speed drives are widely applied to control the conveyor speed in the starting procedure to realize a soft start-up.

- *Aborted start.* An aborted start is an abnormal operational start in which the start-up is

27
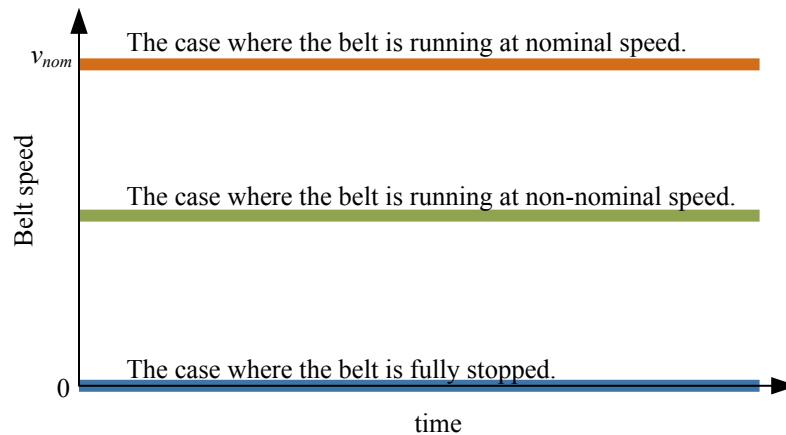
Figure 3.1: Cases of stationary operations.

accidentally terminated before the conveyor reaches the full designed speed. This can be caused by the thermal overload of the drives, serious deviation between the planned and the actual belt speed profiles, serious misalignment of the belt triggering a misalignment switch, a power outage or an operator manually switching the power supply off.

- *Normal operational stop*. A normal operational stop is a stop where the belt is stopped in a planned manner. Similar to the normal operational start, the normal operation stop can be realized either in a non-controlled or controlled manner. In a non-controlled stop, the power supply of motor is switched off and then the conveyor belt drifts to rest. In a controlled normal stop, the drive torque or the velocity is controlled. In the cases where the drive torque is controlled the drive forces are kept constant but less than the motional resistances. In another case where the velocity is controlled, the velocity is monitored in real time and the variable drive torque ensures the velocity decreasing as the designed rules (such as a sinusoidal deceleration profile). In such cases, the stop time can be independent of the bulk material mass loaded on the belt, as long as it is longer than the belt drift time.

- *Emergency stop*. When an emergency event occurs, for example the belt is slipping around the drive pulley, an emergency stop is carried out so that the belt can be stopped in a short period of time. During an emergency stop a brake may be applied.

Similarly, the applications of transient operations can be further expanded in this thesis. In the case of belt conveyors under speed control for the purpose of power reduction, the belt conveyor is often running at a defined speed. If the material feeding rate has a considerable change, the belt conveyor should speed up or slow down to match the actual material flow rate. Here, the operation between adjacent stationary operations is defined as the transient operation. As shown in Figure 3.2, the transient operations include both the accelerating and decelerating processes.

    A healthy transient operation is an important prerequisite of belt conveyor speed control. The performance of transient operations has a significant impact on the service life of conveyor components. High ramp rate of adjusting the belt speed causes very high tensions in the belt,
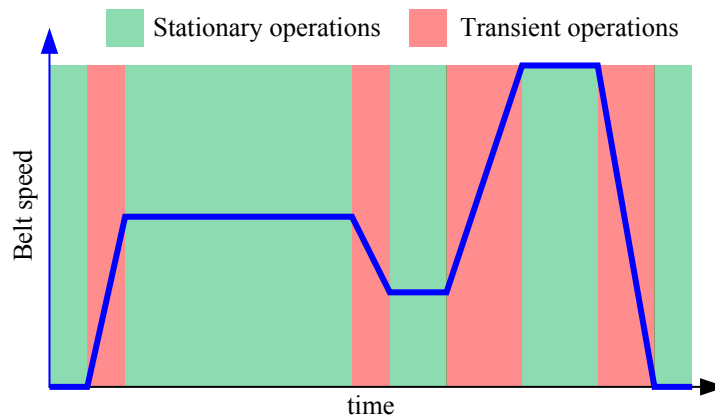
Figure 3.2: Stationary operations and transient operations.

and will be detrimental to the belt conveyor structure (Pang and Lodewijks, 2011). Besides the risk of belt over-tension, the improper transient operations can also cause, for instance, the risk of belt slippage and the risk of material spillage. In transient operations, such risks must be prevented.

This chapter will study the conveyor dynamic performance in transient operations under speed control. In Section 3.2, the potential risks caused by improper transient operations will be discussed in detail. In order to avoid these risks, Section 3.3 will propose a method to determine the minimum speed adjustment. This method consists of three steps. Each step will be individually detailed from Sections 3.4 to 3.6. To show how the method works, a long horizontal belt conveyor will be studied in Section 3.7, including the acceleration and deceleration operations. The last section is the conclusion.

3.2 Risks in transient operations

In stationary operations, belt conveyors are normally running at full speed. In the case of well designed belt conveyors, the belt tension varies smoothly over the conveying route and the driving forces exerted on the drive pulley are limited. In transient operations, the motor speed or torque is controlled so that the conveyor speed can follow a planned speed profile. However, as Pang and Lodewijks (2011) suggested, during improper transient operations, a large acceleration might result in a very high tension in the belt. Over-tensioning is the major reason of belt breaking at the splicing area. Therefore, the value of acceleration must be considered with more attention when we design the speed profile of transient operations, so that risks caused by improper transient operations can be avoided.

In transient operations, besides the risk of belt over-tension, several other risks also should be accounted. These risks mainly include (He et al., 2016b,c):

- the risk of belt slippage around the drive or brake pulley,

- the risk of material spilling away from the belt,

- the risk of motor over-heating,

• and the risk of pushing the motor into the regenerative operation.

3.2.1   Belt breaking at the splicing area

Figure 3.3: Belt breaking at the splicing area. Courtesy of BMG (2016).

The belt strength is mainly determined by the strength of its carcass. For a certain conveyor belt, the belt tension rating is a given and thus constant. However, as Nordell (1998) stated, "the chain is only as strong as its weakest link. In conveyor belts,... the weak link is the splice". Figure 3.3 illustrates an example of belt breaking at the splicing area. As the standard DIN 22101 (German Institute for Standardization, 2015) suggests, the maximum safe working tension is far less than the belt rating due to issues such as splice fatigue and degradation. In DIN 22101, the ratio between the working tension and the actual breaking tension is referred to as the service factor or safety factor (SF). Accordingly, the ratio between the maximum safe working tension and the breaking tension is referred to as the minimum safety factor:

$$S_{A,min} = \frac{T_{max,A}}{k_N} \tag{3.1}$$

$$S_{B,min} = \frac{T_{max,B}}{k_N} \tag{3.2}$$

where

$S_{A,min}$ minimum safety factor in the steady operating condition

$S_{B,min}$ minimum safety factor in transient operations

$T_{max,A}$ maximum safe working tension in the steady operating condition in kN

$T_{max,B}$ maximum safe working tension in transient operations in kN

k_N belt tension rating, minimum breaking strength in kN

DIN 22101 suggests that the requested minimum safety factor is determined by three important factors:

- the dynamic fatigue strength behaviors of the belt splice

- the influence of additional belt elongations resulted from the belt deflections on pulleys, the commencement and termination of troughing, change of the direction and transition curves

- and the peak belt loading which only occurs temporarily, such as during start-up or stop operations

As DIN 22101 further suggests, the value of minimum safety factors can be calculated by

$$S_{A,min} = \frac{1}{1-(r_0+r_1)} \tag{3.3}$$

$$S_{B,min} = \frac{1}{1-(r_0+r_1+r_2)} \tag{3.4}$$

where

r_0 a basic reduction which takes the dynamic fatigue strength of the belt splice into account

r_1 the reduction factor taking the belt elongation into account

r_2 a reduction taking the peak belt loading in transient operations into account

Table 3.1 illustrates the minimum values of safety factors and of reductions related to the belt joint. According to the data in Table 3.1, the belt conveyor should be designed with belt rating larger than 8.0 times of maximum belt tension in stationary operations under normal operating conditions. Moreover, in transient operations under normal operating conditions, the maximum belt tension should be no larger than 1/5.4 times of the belt rating. Otherwise, it increases the risk of belt over-tension.

Table 3.1: Minimum value of the safety factor S and of the reductions r related to the belt joint. Courtesy of DIN 22101 (German Institute for Standardization, 2015).

Belt type	Operating conditions	r_0	r_1	r_2	$S_{A,min}$	$S_{B,min}$
	Favorable	≥0.691	≥0.100	≥0.060	4.8	6.7
Fabrics	Normal	≥0.715	≥0.100	≥0.060	5.4	8.0
	Unfavarble	≥0.734	≥0.100	≥0.060	6.0	9.5
	Favorable	≥0.641	≥0.150	≥0.060	4.8	6.7
Steel cord	Normal	≥0.665	≥0.150	≥0.060	5.4	8.0
	Unfavarble	≥0.684	≥0.150	≥0.060	6.0	9.5

In transient operations, an excessive speed ramp rate is an important reason of belt over-tensioning. Taking the case in Figure 3.4 for instance. In the stationary operations, the belt tension T_1 before the drive pulley equals the belt tension T_2 after the drive pulley plus the driving forces F_d: $T_1 = T_2 + F_d$. However, extra driving forces are required to overcome the inertia F_{ac}

in acceleration operations, and the belt tension T_1 arises subsequently: $T_{1,a} = T_2 + F_d + F_{ac}$. If the value of acceleration is large, then the value of T_1 may exceed the maximum safe working tension. That leads to belt over-tension which may cause breakage of the belt splice. In addition, the belt over-tension can also reduce the life of pulleys. Therefore, the belt tension must be limited to a safe level in transient operations.
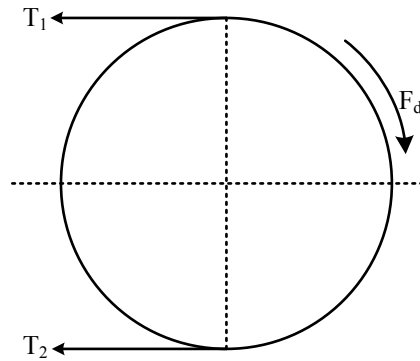
Figure 3.4: Forces around the drive pulley.

3.2.2 Belt slippage around the drive pulley

The rationale of power transmission between the drive pulley and the conveyor belt is the frictional connection between the drive pulley and the belt. However, as suggested by Euler (1762) and Entelwein (1832), the friction between the drive pulley and the belt is limited, and that belt slippage occurs whenever the driving force attempts to exceed the available friction. Attaway (1999) and Nel and Shortt (1999) detail the calculation of the maximum available frictional forces.
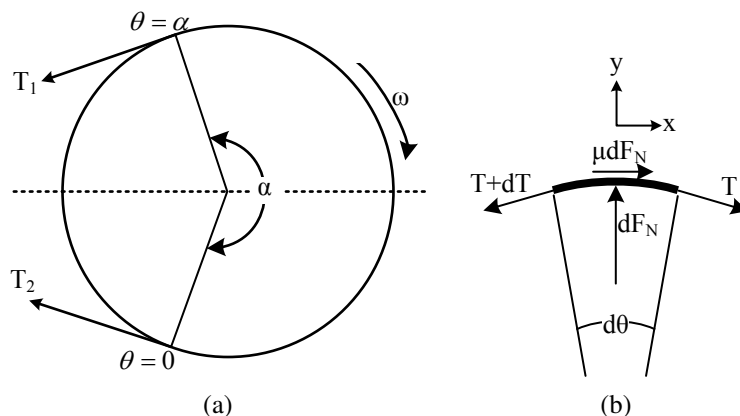
Figure 3.5: Principle of the friction drive of the belt conveyor. Courtesy of Attaway (1999).

The basic of the calculation is the integration of the frictional forces around the drive pulley. Taking the case in Figure 3.5 for instance where the pulley drives the belt clockwise. Figure 3.5b illustrates a belt in a finite length bending over a small segment of the driving pulley in an angle $d\theta$. As the diagram shows, the tension in the belt increases from T to $T + dT$. Assuming that

the normal force is dF_N. If it is further assumed that frictional coefficient between the belt and the drive pulley is μ, then the maximum frictional force is μdF_N without belt slippage. Taking the forces distributed on the belt into account, the forces in the x direction can be equated by

$$\sum F_x = 0 \qquad (3.5)$$

$$T\cos\frac{d\theta}{2} + \mu(dF_N) - (T + dT)\cos\frac{d\theta}{2} = 0 \qquad (3.6)$$

Since the angle of $d\theta$ is very small and $\cos\frac{d\theta}{2} \approx 1$, Equation 3.6 can be reduced to

$$\mu dF_N = dT \qquad (3.7)$$

Similarly, the forces in the y direction can be equated by

$$\sum F_y = 0 \qquad (3.8)$$

$$dF_N - (T + dT)\sin\frac{d\theta}{2} - T\sin\frac{d\theta}{2} = 0 \qquad (3.9)$$

which reduces to

$$dF_N = T\,d\theta \qquad (3.10)$$

since $\sin\frac{d\theta}{2} \approx 0$. Then substituting Equation 3.10 into 3.7 yields

$$\frac{dT}{T} = \mu d\theta \qquad (3.11)$$

Then the integration over the total contact angle α gives :

$$\int_{T_2}^{T_{1,max}} \frac{dT}{T} = \int_0^\alpha u\,d\theta \qquad (3.12)$$

which yields the maximum belt tension without slippage:

$$T_{1,max} = T_2 e^{\mu\alpha} \qquad (3.13)$$

Accordingly, the maximum value of the available frictional forces is

$$F_{f,max} = F_{d,max} = T_{1,max} - T_2 = T_2\left(e^{\mu\alpha} - 1\right) \qquad (3.14)$$

and the belt is slipping around the drive pulley whenever the driving forces exceed the maximum available frictional forces between the belt and the drive pulley.

   If belt slippage occurs then the drive fails to drive the belt as planned, since the available driving force is less than the required. If the belt slippage continues to the extent that it slows down the conveyor, then blockage of the belt's feeder chute or material spillage may occur. Moreover, the relative movement wears out the bottom cover of the belt and the surface cover

Figure 3.6: Pieces of a head pulley's rubber lagging were frequently torn loose due to the belt slippage around the drive pulley. Courtesy of Belzona (2016).

of the drive pulley. A slipping pulley wears more rapidly by the heat generated as it slips (see Figure 3.6). Besides the wear of covers, the accumulative heat may cause the damage to the carcass and the splice. Moreover, there is an increased danger of fire if the slippage continues for a long period of time, especially in an environment with coal dust. Nel and Shortt (1999) mentioned a case where the belt slippage set the conveyor on fire and the fire totally destroyed the conveyor. Unscheduled stops lead to a negative financial impact caused by lots of revenue. Therefore, the driving forces in transient operations must be restricted to avoid the risk of belt slippage and to keep the operation uninterrupted.

3.2.3 Material spillage away from the belt

Even though a belt conveyor is carefully designed, spillage from the carrying side of the belt may occur at the loading point and elsewhere along the belt conveyor. There are many reasons that cause the spillage, such as the material off-center loading at the transfer points and the belt mistracking along the conveying route. Here, the focus is on the unnecessary spillage caused by improper transient operations.

In the case of belt conveyors with large speed fluctuations, the instantaneous conveying capacity can be less than the actual loading rate, so that the belt at the loading area may be overloaded. This can lead to the escape of bulk materials from the belt. Both the excessively low and the excessively high belt tension can result in the material spillage. In transient operations, the belt tension is varying along the conveying route and fluctuating over time. On one hand, if the improper transient operation results in excessively low belt tension, the belt may drop significantly between neighboring idler stations. According to Conveyor Equipment Manufacturers Association (2005), material may spill over the edges of the belt when the conveyor belt sags more than 3 percent of the span between idlers, see Figure 3.7a. On the other hand, in the case of dipping belt conveyors, the large belt tension can lead to the lift of the belt from the idler stations, see Figure 3.7b. The lift also can cause the material spillage away from the belt.

If the material escapes from the carrying belt, it may land on the return side of the belt.
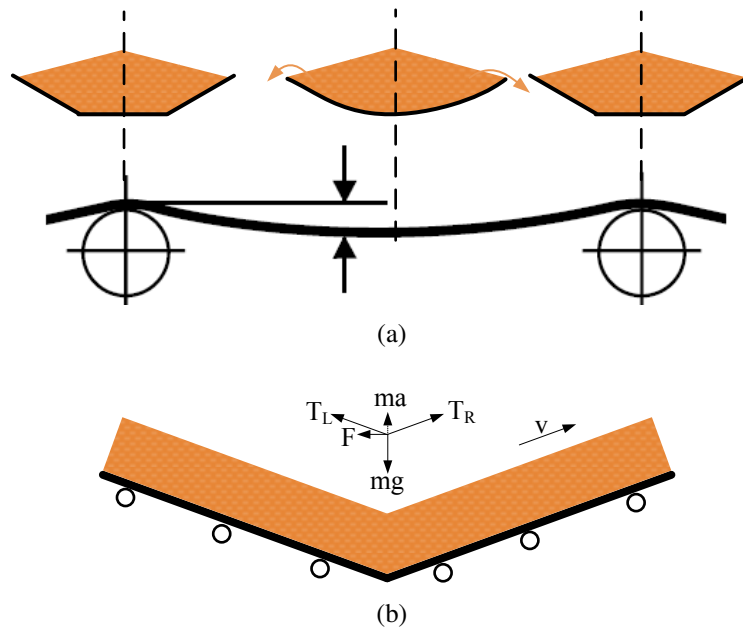
Figure 3.7: Material spillage. (a) Caused by low tension. (b) Caused by high tension. Courtesy of Lodewijks and Pang (2013b).

When it moves to the tail pulley, the escaped material can cause the overstretching of the belt's carcass and the cover damage of the pulley. Consequently, the maintenance costs increase. Moreover, if the bulk material conveyed is sticky, the escaped material can be accumulated around the idler rolls. This can cause not only the wear of conveyor components, but also the loss of belt alignment. In return, the misalignment of the belt increases the spillage. Besides the maintenance cost, the spillage also increases the cleaning cost if it falls on the floor. Moreover, the spilled material can pose threats to personal safety if it falls from a height. Therefore, taking all these negative impact into account, the unnecessary material spilling from the belt must be prevented in transient operations.

3.2.4 Motor overheating

As a motor operates, it converts electrical energy to mechanical energy. In this conversion, part of the energy is lost due to motor losses. The motor temperature rises due to the heat generated from the motor losses during operation. If the winding's temperature is above the rated temperature, the motor is overheated. Overheating occurs due to a number of factors, one of which can be the unhealthy transient operation with a rapid acceleration. Normally, motors can provide larger shaft torque than the nominal for a short period of time without overheating. However, if the overload continues for a long time period or the load exceeds the permitted load greatly, it increases the risk of overheating. Especially in the cases where a motor is operated at a low frequency and the cooling fan is mounted on the rotor shaft, the reduced cooling efficiency increases the risk of motor overheating.

Overheating is a serious problem in a motor, and can cause a number of performance problems. For instance, the winding's insulation life is cut in half for every $10\,°C$ rise above the rated temperature (Wiedenbrug, 2003). For example, in the case of a motor with a service life

20 years and with the rated temperature 40 °C, the life of the motor is cut to about 2.5 years if it runs at 80 °C. Moreover, as suggested by Umair Mirza (2013), more than 55% of the insulating failures are caused by overheating. Despite the fact that modern insulating materials are more durable, temperature rises still drastically shorten their service lives. Therefore, the transient operations should not increase the risk of overloading the driving machine.

3.2.5   Pushing the motor into the regenerative operation
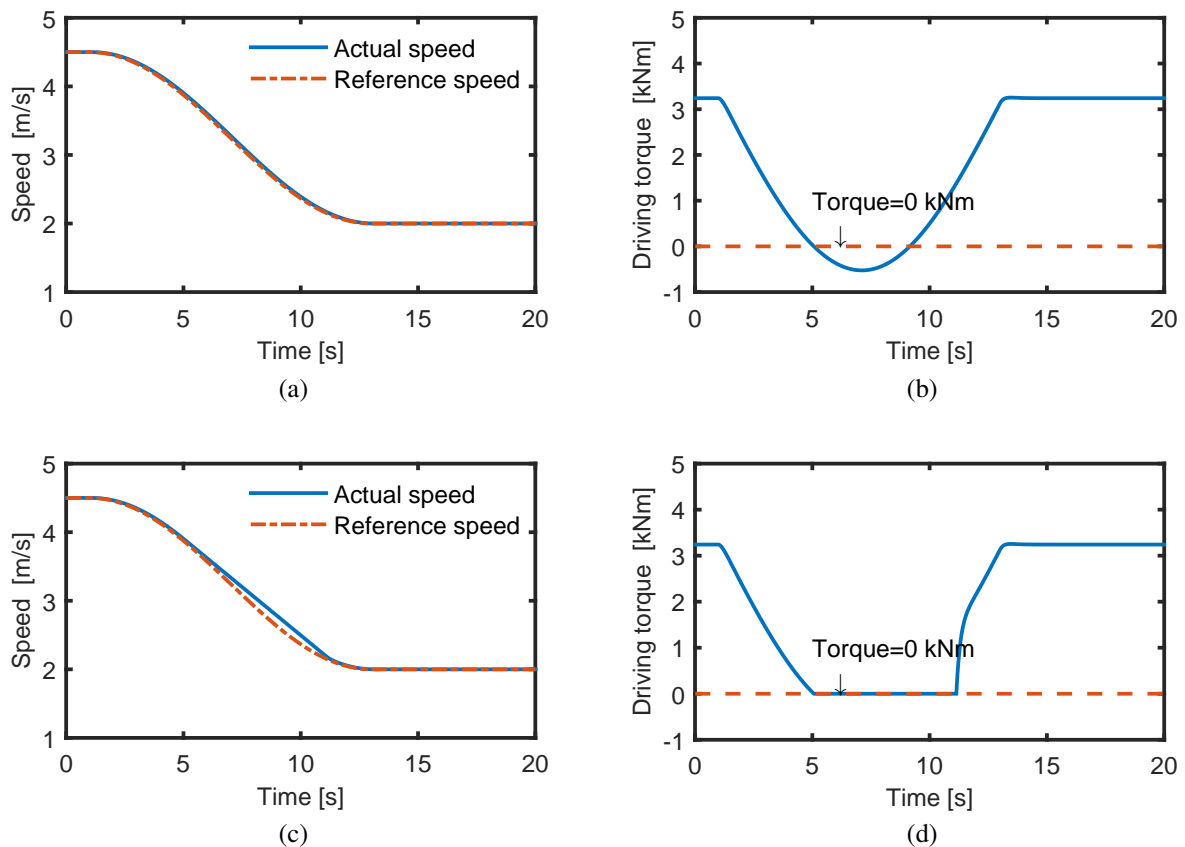
Figure 3.8: Deceleration operations over different operating conditions. (a-b) Condition 1: Driving system provides negative driving torque. The conveyor speed follows the reference speed profile. (c-d) Condition 2: Driving system does not provide negative driving torque. The conveyor fails to follow the reference speed.

The risk of pushing the driving motor into the regenerative operation can be caused by the improper deceleration operation. Taking the case in Figure 3.8 for in instance. In order to follow a planned speed profile, negative driving forces or braking forces sometimes are required, as shown in Figure 3.8b. The negative driving forces can be provided by a brake system or by pushing the driving motor into the regenerative operation. However, in the case of a conveyor system without neither the braking system nor the function of regenerating, the driving system fails to produce a negative torque. In such cases, the driving torque suddenly is lost, and the belt fails to run as planned, as shown in Figure 3.8c. Therefore, in cases where the driving

system can not produce generative driving torque, the risk of pushing motor into the regenerative operation should be paid more attention, especially in the deceleration operations.

3.3 Determination of the minimum acceleration time

3.3.1 Introduction

In the design of belt conveyors, existing standards, such as DIN 22101 (German Institute for Standardization, 2015), CEMA (Conveyor Equipment Manufacturers Association, 2005) and ISO5048 (International Organization for Standardization, 1989), are usually applied to calculate the required driving forces on the driving pulleys, to select the components of belt conveyors, to define the space of neighboring idler stations, and even to deal with the vertical curves along the conveyor length. In addition, the safety factor and the maximum acceleration can be approximated by applying these standards (Nuttall, 2007). It is important to note that in the calculation of these standards, the conveyor belt is assumed to be a rigid body and the belt elastic-visco properties are not taken into account. In the case of low capacity and small belt conveyor systems, this may lead to an acceptable design and acceptable operational behavior of the belt (Lodewijks, 2002). However, Lodewijks (2002) further suggests that in the case of belt conveyor systems with high capacity or long distance, the ignorance of belt dynamics can cause operational problems, such as the premature collapse of the belt and the damage of drive systems. This suggestion can also be found in (Pang and Lodewijks, 2011). Therefore, a method is required to determine the permitted acceleration, taking both the potential risks and the conveyor dynamics into account.

3.3.2 Existing methods for determining the acceleration time

Determining the acceleration time is significantly important to avoid for instance the risk of belt over-tension caused by an improper transient operation. In current research, several methods have been proposed to estimate the acceleration time of belt conveyors, and some of them have already been applied in practice. The applications mainly are on start-up operations. These methods can be summarized into three types of approximations. The first approximation suggests that the time length of start-up procedure is no less than five times the time it takes for a longitudinal wave to travel from the head to the tail of the conveyor. An example can be found in (Singh, 1994). This rule is based on the findings of (Funke, 1973) and can be mathematically expressed by:

$$t_a \geq 5\frac{L}{c_1} \tag{3.15}$$

where t_a is the acceleration time, L is the conveyor length from head to tail, and c_1 is the propagation speed of longitudinal stress waves. However, this start-up time is only valid if it is used for torque controlled start-ups, and the drive torque is increased from zero to the required start-up torque during the starting operation (Funke, 1973; Lodewijks, 1997). Moreover, the

applications of Equation 3.15 may result in a steep acceleration ramp and a high peak tension during starting (Singh, 1994; Lodewijks, 1997).

To reduce the risk of belt over-tension during starting, Singh (1994) introduced a rule of thumb to approximate the acceleration time. The rule is "one minute per km of conveyor length". According to Singh (1994), this rule generally yields satisfactory results. However, if the rule applies to the conveyor whose length exceeds 2 to 3 km, the time length of starting procedure may be unnecessarily long, so that the belt dynamic analysis is suggested to be carried out to determine an acceptable start-up time (Lodewijks, 1997).

Lodewijks (1997) proposed a more accurate method estimating the start-up time. In this approximation, it is assumed that the conveyor speed is controlled by a static power converter, and that the speed increases linearly. So the acceleration of the belt on the drive pulley is constant. Then based on Euler-Eytelwein formula (see Equation 3.13), the maximum belt force of the considered conveyor during stationary operation can be expressed as:

$$T_{1,max} = \left(\frac{e^{\mu\alpha}}{e^{\mu\alpha} - 1} \right) F_d \tag{3.16}$$

In the case of a long horizontal belt conveyor, the driving force F_d can be calculated by

$$F_d = CfgL \left(m'_{roll} + 2m'_{belt} + m'_{bulk} \right) \tag{3.17}$$

Then substituting Equation 3.17 into 3.16 yields

$$T_{1,max} = \left(\frac{e^{\mu\alpha}}{e^{\mu\alpha} - 1} \right) CfgL \left(m'_{roll} + 2m'_{belt} + m'_{bulk} \right) \tag{3.18}$$

In order to accelerate the lump mass of belt, bulk material and idler rolls, an extra force F_{ac} is required which can be estimated by

$$F_{ac} = \left(m'_{roll} + 2m'_{belt} + m'_{bulk} \right) La \tag{3.19}$$

where a is the value of acceleration. The extra drive force yields an extra belt tension T_{1ac} which approximates to

$$T_{1ac} = \left(\frac{e^{\mu\alpha}}{e^{\mu\alpha} - 1} \right) F_{ac} \tag{3.20}$$

Then taking the risk of belt over-tension into account yields the actual minimum safety factor:

$$S_{A,min} = S_{B,min} \left(\frac{T_1}{T_1 + T_{1ac}} \right) \tag{3.21}$$

The substitution of Equations 3.18 and 3.20 into 3.21 gives:

$$S_{A,min} = S_{B,min} \left(1 + \frac{a}{Cfg} \right)^{-1} \tag{3.22}$$

In the case of a belt conveyor with a linear increase of the speed, the belt acceleration is

$$a = \frac{v_b}{t_a} \qquad (3.23)$$

Finally, the combination of Equations 3.23 and 3.22 obtains the acceleration time:

$$t_a = \frac{v_b}{Cfg} \left(\frac{S_{A,min}}{S_{B,min} - S_{A,min}} \right) \qquad (3.24)$$

Equation 3.24 has been successfully applied to estimate the start-up time of belt conveyors, especially in the cases of horizontal belt conveyors. The applications can be found in (Lodewijks, 1997; Nuttall and Lodewijks, 2007). However, it is important to note that, the value resulted by Equation 3.24 normally is larger than the minimum required strat-up time. The deviation might be caused by the over-estimation of the belt tension. As shown in Figure 3.4, the belt tension T_1 before the drive pulley equals the tension T_2 after the drive pulley adding the driving forces. In addition, the increase of belt tension T_{1ac} equals the extra driving force F_{ac}. Therefore, the extra belt tension can be overestimated by Equation 3.20. In addition, Equation 3.21 is lack of accuracy since the actual belt rating in practice may be far larger than that calculated by Equation 3.2. Therefore, Equation 3.24 results in a large but safe start-up time. Due to the overestimation, Equation 3.24 can be applied to calculate the start-up time of conveyors with a limited inclination angle. This is confirmed by He et al. (2016a).

From the above description on these three methods, it is clear that these methods can not be directly applied to determine the minimum acceleration time of the transient operations. However, the method proposed by Lodewijks (1997) provides an inspiration for the proposal of the Estimation-Calculation-Optimization (ECO) method.

3.3.3   ECO Method

The ECO method derives from the approach proposed by Lodewijks (1997). It is based on simulations and accounts for the dynamic performance of belt conveyors in transient operations under speed control. The ECO method consists of three steps: Estimation, Calculation and Optimization. In the Estimation step, an estimator is built to compute the permitted maximum acceleration and initialize the acceleration time. Taking the potential risks caused by improper transient operations into account, the estimator considers the belt as a rigid element, and computes the permitted maximum acceleration in transient operations statically. Then accounting for the acceleration profiles, the demanded minimum speed adjustment time can be rough estimated. Section 3.4 describes the estimation in detail.

The purpose of the Calculation step is to detect whether the potential risks occur in transient operations with the estimated acceleration time. This step accounts for the effect of belt dynamics and hysteresis. The dynamic behavior in transient operations is analyzed by simulations. The simulations are based on an existing finite element model, which has been widely applied in practice. Section 3.5 gives a detailed description of the dynamic analysis.

With respect to belt viscous-elastic properties, belt performance in transient operations is

complex. The transient operation with the estimated acceleration time may result in, for instance, the risk of belt over-tension. In such cases, optimizations are required to improve the dynamic performance and to achieve the minimum acceleration time, which results in healthy transient operations. Section 3.6 details the optimization.

3.4   Estimation- static computation

Taking the potential risks in transient operations into account, an estimator is built in this step to compute the permitted maximum acceleration. In order to describe the estimator clearly, a case as shown in Figure 3.9 is exampled. The belt conveyor is installed with an inclined angle δ and driven by a head pulley. In order to provide a pre-tension, a single sheave gravity take-up device with mass M_T is mounted at the return side after the head pulley. In the following, both the permitted maximum acceleration and the permitted maximum deceleration are computed.
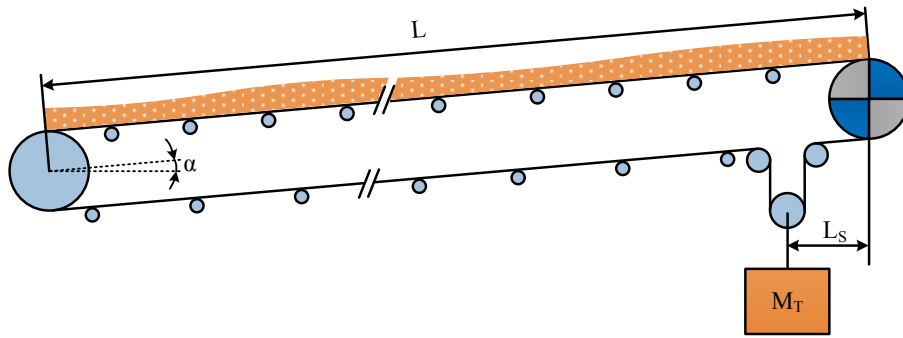
Figure 3.9: An inclined belt conveyor with a single sheaved gravity take-up.

3.4.1   Maximum acceleration

With respect to the risk of belt breaking at the splice caused by over-tension, the belt tension along the conveying route must be maintained in a safe level. In cases as shown in Figure 3.9, the maximum belt tension generally occurs right before the drive pulley. The tension T_1 in steady state before the drive pulley can be approximated by

$$T_1 = T_2 + F_d \tag{3.25}$$

where F_d is the driving force and T_2 is the belt tension after the drive pulley. As shown in Figure 3.9 where the conveyor is tensioned by a single sheave gravity take-up device, if the distance between the gravity take-up and the drive pulley is small, the belt tension T_2 after the drive pulley can be approximated by

$$T_2 = \frac{1}{2}M_T g \tag{3.26}$$

According to Equation 3.1, the permitted belt tension before the drive pulley can be estimated by

$$T_{1,max} = \frac{k_N B}{S_{A,min}} \tag{3.27}$$

where B is the belt width. Then the combination of Equations 3.25 to 3.27 yields the maximum permitted driving force

$$F_{d,max,tensioin} = \frac{k_N B}{S_{A,min}} - \frac{1}{2} M g \tag{3.28}$$

with respect to the belt over-tension risk.

Belt slippage is another major risk in the acceleration operations. As stated by Euler (1762) and Entelwein (1832), if the driving force exerted on the drive pulley attempts to exceed the available frictional forces, the belt will slip around the drive pulley. Then according to Equation 3.14, the maximum driving force is

$$F_{d,max,slip} = F_{f,max} = T_2 \left(e^{\mu\alpha} - 1 \right) \tag{3.29}$$

with respect to the belt slippage risk.

The rated motor torque is the maximum continuous torque available at the design speed that allows the motor to do work without overheating. In the practical acceleration operations, the maximum service torque is allowed to be slightly larger than the rated torque $T_{motor,nom}$ for few seconds. The ratio of the maximum service torque and the rated torque is defined as service factor (i_{sf}). For example, the standard service factor for an open drip-proof motor is 1.15 in (Emadi, 2004). Then in the acceleration operation, the permitted motor service torque $T_{motor,max}$ is

$$T_{motor,max} = i_{sf} T_{motor,nom} \tag{3.30}$$

and the maximum driving force $F_{d,max,heat}$ onto the drive pulley is

$$F_{d,max,heat} = i_{rf} \frac{T_{motor,max}}{R_d} = \frac{i_{rf} i_{sf} T_{motor,nom}}{R_d} \tag{3.31}$$

in which i_{rf} is the gearbox reduction ratio and R_d is the drive pulley's radium.

Then taking these three risks in acceleration operations into account, the permitted maximum driving force $F_{d,max}$ in transient operations is

$$F_{d,max} = min \left(F_{d,max,tension}, F_{d,max,slip}, F_{d,max,heat} \right) \tag{3.32}$$

As described by Newton's Second Law, the acceleration is the net result of any and all forces acting on belt conveyors. Then in acceleration operations, the permitted acceleration is

$$a_{ac,max} = \frac{F_{d,max} - F_f}{m} \tag{3.33}$$

where F_f is the total motional resistances, and m is the total lump mass of the belt, rollers and the bulk material on the belt. According to the standard DIN 22101, the motional resistance along the conveying route can be estimated by

$$F_f = C f g L \left(m'_{roll} + \left(2m'_{belt} + m'_{bulk} \right) \cos\theta \right) + m'_{bulk} g H \tag{3.34}$$

and the total mass is

$$m = L \left(m'_{roll} + 2m'_{belt} + m'_{bulk} \right) \tag{3.35}$$

Finally, the maximum permitted acceleration can be estimated by substituting Equations 3.34 and 3.35 into Equation 3.33.

3.4.2   Maximum deceleration

In a soft deceleration operation, the driving force exerted on drive pulleys decreases gradually and the conveyor speed is reduced smoothly. Differing from the acceleration operation, the deceleration operation mainly considers the risk of pushing the motor into the regenerative operation. In the case of belt conveyors which can not provide the negative driving forces, the maximum deceleration can be estimated by:

$$a_{de,max} = \frac{-F_f}{m} \tag{3.36}$$

3.4.3   Speed adjustment time
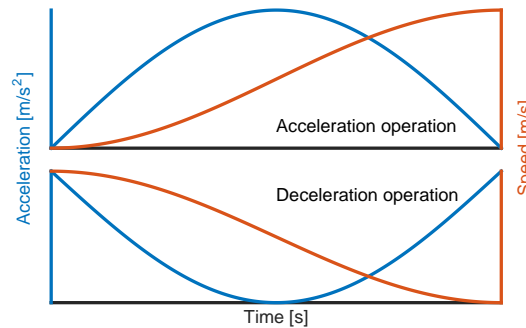
Figure 3.10: Acceleration profiles and speed curves in the transient operation

The speed adjustment time is the time required in acceleration or deceleration operations, and its value is dependent on the planned acceleration profile. Conventionally, the linear acceleration was widely applied in start-up operations. However, due to the sudden change of the acceleration at the beginning and the ending of transient operations, the linear acceleration operations result in a large mechanical jerk. In order to reduce the mechanical jerk and to enable a soft-start operation, Harrison (1983) recommended a sinusoidal acceleration profile as shown in Figure 3.10. The figure includes the curves of an acceleration operation and of a deceleration operation. Mathematically, the acceleration and the speed can be expressed:

$$a(t) \quad = \quad \frac{\pi}{2} \frac{\Delta v}{t_a} \sin \frac{\pi t}{t_a} \tag{3.37}$$

$$v(t) = v_0 + \frac{\Delta v}{2} \left(1 - cos \frac{\pi t}{t_a} \right) \tag{3.38}$$

where Δv is the speed adjustment range, t_a is the speed adjustment time, t is the instantaneous time ($0 \leq t \leq t_a$), and v_0 is the original speed before the transient operation. According to Equation 3.37, the maximum acceleration occurs at $t = t_a/2$ and

$$a_{max} = a \left(\frac{t_a}{2} \right) = \frac{\pi}{2} \frac{\Delta v}{t_a} \tag{3.39}$$

Then in transient operations with sinusoidal acceleration profiles, the required minimum speed adjustment time is

$$t_{ac,min} = \frac{\pi}{2} \frac{\Delta v}{a_{ac,max}} \tag{3.40}$$

$$t_{de,min} = \frac{\pi}{2} \frac{\Delta v}{a_{de,max}} \tag{3.41}$$

where the subscripts ac and de represent the operations of the acceleration and deceleration, respectively.

3.5   Calculation- dynamic analysis

In the Estimation step, an estimator is used to approximate the permitted acceleration and the demanded adjustment time. The estimator views the belt as a rigid element, and assumes that all masses are accelerated or decelerated at the same time with the same rate. However, Lodewijks (2002) suggests that the neglect of belt elasticity in high capacity and/or long distance conveyors may lead to operational problems, for instance premature collapse of the belt and the destruction of pulleys. Moreover, the estimator fails to account for the risk of material spillage caused by the low speed or by the low belt tension. Therefore, the dynamic analyses play an important role when detecting whether the potential risks are prevented in transient operations.

Historically, finite element models of belt conveyor systems have been developed to calculate the conveyor dynamic behavior, especially during staring and stopping. Although these models only determine the longitudinal response of the belt by mainly using truss like elements, they have been successful in predicting the elastic response of the belt during starting and stopping. An important case study is given by Lodewijks and Kruse (1998) in which both the field measurements and the finite-element-model-based simulations are carried out. The experimental results show that the deviation between the measured results and the calculated results could be restricted within 5%, which falls within the accuracy of the field measurements. Therefore, the finite element model, accounting for the belt elasticity, is capable of analyzing the conveyor dynamics in transient operations.

The finite element model of (Lodewijks and Kruse, 1998) is derived from Lodewijks (1996). In the finite element approach, the distributed mass of the belt, the idler rolls and the bulk material is divided into finite number of elements. In Figure 3.11, these elements are presented

by nodes and numbered in sequence. In addition, due to the belt viscosity-elasticity, the adjacent nodes are coupled by a spring-damping connector, presented by a spring element in Figure 3.11.
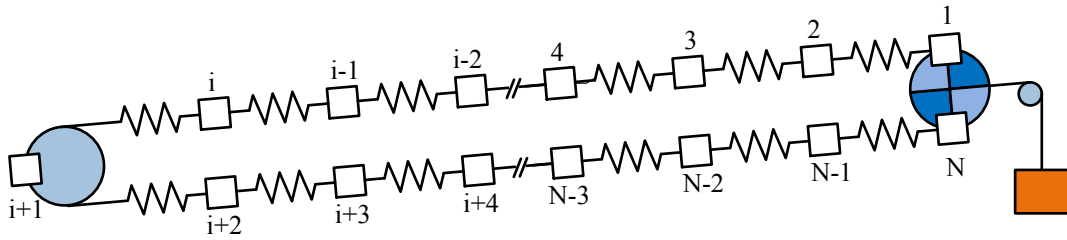
Figure 3.11: Lump-mass spring-dampened finite element method
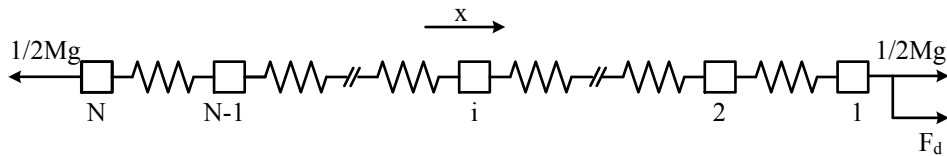
Figure 3.12: One dimensional model of belt conveyor system.

As Lodewijks (1996) suggests, it is reasonable to suppose that the belt is laid in a horizontal direction and moves towards one direction. Figure 3.12 illustrates the one dimensional model of a single drive belt conveyor system. In this model, the driving force F_d is placed on the 1st node and the pre-tension is placed on both the 1st and N^{th} nodes. The displacement of all nodes can be expressed relative to the displacement of Nth node. Then according to Newton's Second Law, the motion of a belt conveyor can be described as

$$\mathbf{M}\ddot{\mathbf{x}} + \mathbf{C}\dot{\mathbf{x}} + \mathbf{K}\mathbf{x} = \mathbf{F} \tag{3.42}$$

where

    M   mass matrix, size $N \times N$

    C   matrix of damping factors, size $N \times N$

    K   matrix of spring factors, size $N \times N$

    x   vector of nodal displacement, size $N \times 1$

    $\dot{\mathbf{x}}$ vector of nodal velocity, size $N \times 1$

    $\ddot{\mathbf{x}}$ vector of nodal acceleration, size $N \times 1$

    F   vector of force, size $N \times 1$

3.6   Optimization- dynamics improvement

With respect to the belt elasticity-viscosity, the dynamic performance of the belt conveyor is complex. Due to the fact that the estimator views the belt as a rigid object, the conveyor transient

operation in the Calculation step might result in, for instance, the risk of belt slippage. If so, further studies must be carried out to improve the conveyor dynamic performance in transient operations (He et al., 2016b). Table 3.2 summarizes some solutions, including replacing a new belt with higher tension rating, optimizing the mass of the take-up device, applying a softer deceleration profile and increasing the speed adjustment time. With respect to the fact that changing the construction or components of an existing conveyor is not practical to some extent, the general method of improvement is to extend the speed adjustment time. Then the third step, Optimization, is carried out to find the minimum speed adjustment time.

Table 3.2: Potential risks in transient operations and their solutions

Potential risks	Suggested solutions
Belt over-tension at the splicing area	Replace a new belt with higher tension rating
	Extend the speed adjustment time or apply a softer acceleration profile
	Decrease the mass of take-up devices
Belt slippage around the drive pulley	Increase the mass of take-up device
	Increase the wrap angle or replace a new pulley with a higher friction resistance coefficient
	Extend the speed adjustment time and reduce the driving force
Motor overheat	Extend the speed adjustment time and reduce the driving force
	Reduce the frequency of speed regulation process
	Replace a new motor with higher torque rating
	Install a cooling device
Material spillage away from belt	Reduce the mechanical jerk by extending speed adjustment time or applying a softer deceleration profile
Pushing motor into the regenerative operation	Apply a softer acceleration profile or extend speed adjustment time

The optimization is realized by using finite-element-model-based simulations. The optimizing procedure can be viewed as a process of root finding. Taking the risk of belt slippage for instance. The maximum available frictional resistances between the belt and the drive pulley is $F_{f,bd}$. It is assumed that during the transient operations, the driving force can exceed the maximum available friction $F_{f,bd}$. It is further assumed that $F_d(t)$ represents the maximum driving force over different acceleration time t. For instance $F_d(30)$ represents the maximum driving force during a specific transient operation within the acceleration time 30s. Then with respect to the risk of belt slippage, the minimum acceleration time can be approached by finding the root of function

$$f(t) = F_d(t) - F_{f,bd} = 0 \qquad (3.43)$$

In spited of the fact that the computer nowadays is very powerful and can quickly complete the calculations, iteration methods are highly suggested to find the solutions more quickly. These

methods mainly include the bisection method, the false position method, the Newton-Raphson method and the secant method. Because the research of iteration methods is beyond the scope of this thesis, the iteration methods will not be further discussed here. More details of the iteration methods can be found in (Press et al., 1987; Phillips and Taylor, 1996; Pal, 2009).

3.7   Case study: a long horizontal belt conveyor

In order to show how the ECO method is used to determine the minimum acceleration/deceleration time, this section studies a long horizontal belt conveyor. The belt conveyor is designed by Lodewijks (1996). The designed capacity is 2500t/h for conveying coal with density $850kg/m^3$, and the conveying distance is $1000m$. A fabric belt, with Young's modulus of $370MPa$ and tension rating of $500kNm$, is selected. The linear density of the belt is $14.28kg/m$. The carrying part of the belt is supported by three-roll idler stations with average mass per unit length $14.87kg/m$. The return part is supported by one-roll idler stations with average mass per unit length $7.72kg/m$. The conveyor is driven by a $250kW$ motor with torque rating $1592Nm$. More parameters of the belt conveyor system are illustrated in Table 3.3. As examples of the case study, an acceleration operation from $2m/s$ to $4m/s$ and a deceleration operation from $4m/s$ to $2m/s$ are studied in sub-sections 3.7.1 and 3.7.2, respectively.

3.7.1   Acceleration operation from $2m/s$ to $4m/s$

3.7.1.1   Step 1: Estimation

On the basis of data in Table 3.3, Equation 3.28 suggests that the permitted driving force is

$$F_{d,max,tension} = \frac{k_N B}{S_{A,min}} - \frac{1}{2}Mg = 86.3kN \tag{3.44}$$

with respect to the risk of belt over-tension. Taking the risk of belt slippage around the drive pulley into account, Equation 3.29 yields the permitted driving force

$$F_{d,max,slip} = \frac{1}{2}Mg\left(e^{\mu\alpha} - 1\right) = 49.6kN \tag{3.45}$$

In addition, with respect to the risk of motor over-heating, the maximum driving force is approximated by Equation 3.31:

$$F_{d,max,heat} = \frac{i_{rf}i_{sf}T_{motor,nom}}{R_d} = 54.9kN \tag{3.46}$$

Then taking these three risks into account, the permitted maximum driving force is

$$F_{d,max} = min\left(F_{d,max,tension}, F_{d,max,slip}, F_{d,max,heat}\right) = 49.6kN \tag{3.47}$$

The result in Equation 3.47 suggests that in acceleration operations of this specific belt conveyor system, the highest risk is the belt slippage around the drive pulley. Moreover, it further suggests that due to the phenomenon of belt slippage, both the risk of belt over-tension

Table 3.3: Parameters of a coal conveying system with a textile belt. Courtesy of Lodewijks (1996).

Parameters (symbol, unit)	value	Parameters (symbol, unit)	value
Conveyor length (L, m)	1000	Mass of bulk material on the belt per unit length (m'_{bulk}, kg/m)	133.54
Nominal capacity (Q_{nom}, $MTPH$)	2500	Mass of gravity take-up device (m_T, kg)	5060
Nominal speed (v_{nom}, m/s)	5.2	Friction coefficient between drive pulley and conveyor belt (μ, $-$)	0.35
Belt width (B, m)	1.200	Wrap angle of the belt on the drive pulley (α, °)	180
Young's modulus of belt (E_b, N/mm^2)	340	Motor torque rating ($T_{nom,motor}$, Nm)	1592
Damping factor (D_f, $-$)	0.35	Motor service factor (i_{sf}, $-$)	1.15
Cross section area of belt (A_{belt}, m^2)	0.01236	Reduction factor of gearbox (i_{rf}, $-$)	18
Nominal rupture force of belt per unit width (k_N, kN/m)	500	Minimal safety factor in steady state operation ($S_{B,min}$, $-$)	8.0
Mass of belt per unit length (m'_{belt}, kg/m)	14.28	Minimal safety factor in transient operation ($S_{A,min}$, $-$)	5.4
Mass of idler per unit length on the carrying side ($m'_{roll,c}$, kg/m)	14.87	Coefficient of secondary resistances (C, $-$)	1.09
Mass of idler per unit length on the return side ($m'_{roll,r}$, kg/m)	7.72	Artificial friction coefficient (f, $-$)	0.018
Total mass of idler per unit length (m'_{roll}, kg/m)	22.59		

and the risk of motor over-heating are prevented. Then taking the motional resistances along the conveying route into account, Equation 3.33 yields the permitted acceleration in acceleration operations

$$a_{ac,max} = \frac{F_{d,max} - CfgL\left(m'_{roll} + 2m'_{belt} + m'_{bulk}\right)}{L\left(m'_{roll} + 2m'_{belt} + m'_{bulk}\right)} = 0.076 m/s^2 \tag{3.48}$$

Accordingly, the minimum acceleration time is initialized as

$$t_{ac,min} = \frac{\pi}{2}\frac{\Delta V}{a_{ac,max}} = 41s \tag{3.49}$$

to complete the acceleration operation from $2m/s$ to $4m/s$ with a sinusoidal acceleration profile.

3.7.1.2   Step 2: Calculation

In this step, simulations are carried out to examine the conveyor dynamic behavior in the acceleration operation from $2m/s$ to $4m/s$ within 41 seconds. Simulations are based on the following suppositions:

- The conveyor belt is fully loaded over the simulations.

- Whenever the driving force attempts to exceed the available frictional resistances, the belt is slipping around the drive pulley, and the forces exerted on the drive pulley equals the available frictions between the belt and the drive pulley.

In addition, another important assumptions are given that the maximum permitted belt sag ratio is 3% and that the permitted speed deviation is 15%. Therefore, with respect to the risk of material spillage caused by the excessive low belt tension, the belt tension along the carrying side should be no less than

$$T_{min} \geq \frac{g(m'_{belt} + m'_{bulk})L_c}{8h_{rel}} = 9.05kN \tag{3.50}$$

where L_c is the distance between the idler centers in the carrying side, and h_{rel} is the maximum permitted belt sag ratio. With respect to the risk of material spillage caused by the excessive low belt speed, the belt speed at the tail pulley should be no less than 3.4m/s after the deceleration operation.

Figure 3.13 illustrates the conveyor dynamics in the acceleration operation. The acceleration
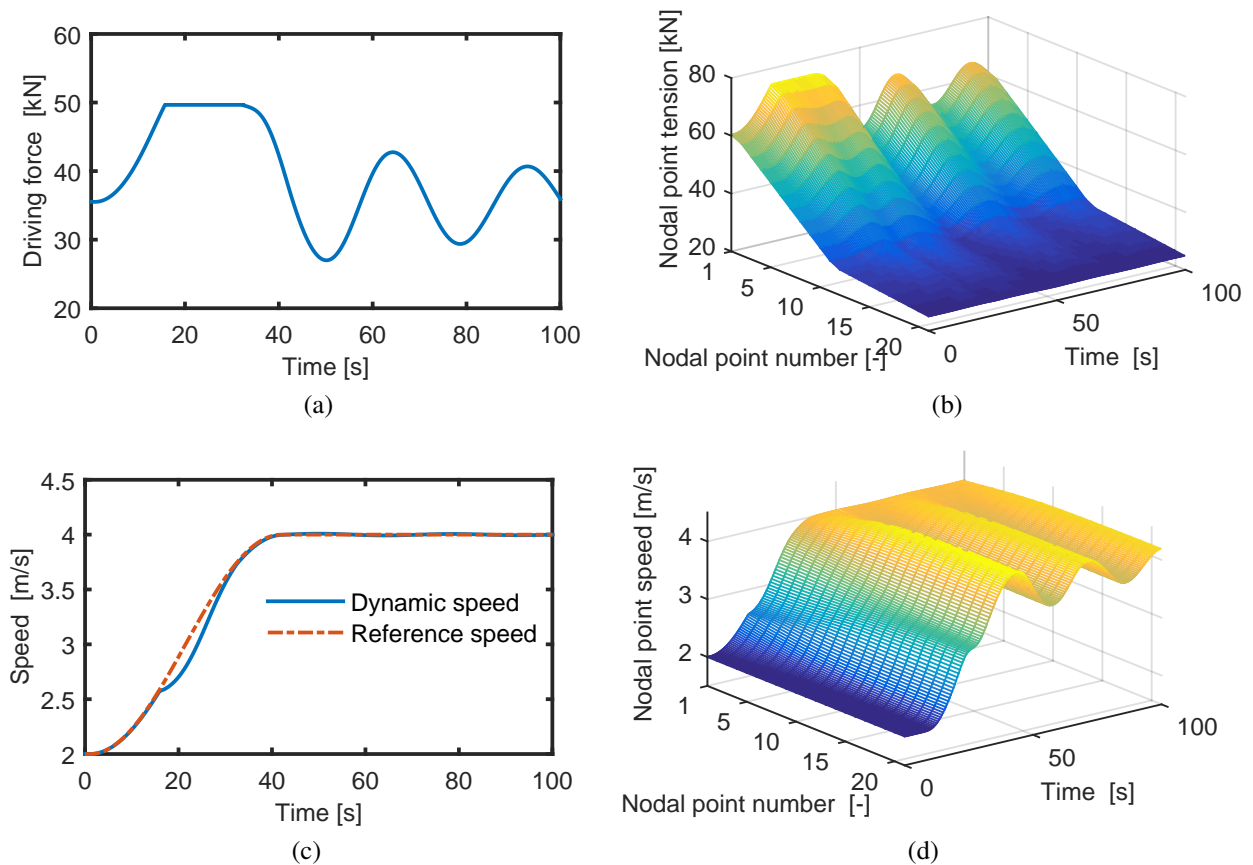
Figure 3.13: Belt conveyor dynamic performance in the acceleration operation with $\Delta V = 2m/s$ and $t_{ac} = 41s$. (a) Driving forces exerted on the drive pulley. (b) Belt tension at each nodal point. (c) Belt speed at the drive pulley. (d) Belt speed at each nodal point along the conveying route.

starts from the time point 1 second. The diagram of Figure 3.13a illustrates the driving force exerted on the drive pulley. It shows that at the beginning of acceleration, the driving force increases gradually. Around the time point 16 second, the driving force reaches to the limit 49.6 kN. Due to the fact that the drive pulley cannot provide more frictional resistances to couple the exceeding driving forces, the belt is then slipping around the drive pulley and the driving force remains at 49.6 kN. The belt slippage continues for 16 seconds, and after that the driving force decreases. Due to the belt elasticity, the driving force fluctuates around a certain level after the acceleration operation. Meanwhile, due to the belt viscosity, the fluctuation amplitude is decreasing over time.

Figure 3.13b presents the belt tension at each nodal point. Overall, the diagram shows along the carrying side, the minimum belt tension is over 20 kN during and after the acceleration operation. That means in this acceleration, the risk of material spillage caused by the excessive low belt tension is avoided. However, the diagram further shows when the belt is slipping around the drive pulley, an uncontrolled belt tension wave travels from the head pulley to the tail. After that, the belt tension oscillates with dampened amplitudes.

Figure 3.13c shows the dynamic speed curve of the belt around the drive pulley, and the reference speed over time. As the figure shows, the belt speed at the drive pulley gently increases and follows the reference speed at the beginning of acceleration. However, due to the phenomenon of belt slippage, the belt speed at the drive pulley suddenly shocks at the time point 16 second. Moreover, due to the fact that the drive pulley can not provide sufficient driving forces during the period of belt slippages, the dynamic speed is lower than the reference speed until the disappearance of belt slippage. After that, the belt speed at the drive pulley successfully catches up the reference speed. At the time point 42 second, it finally reaches the desired speed 4 m/s. Similar to the driving force, the dynamic speed is fluctuating around the desired speed with a limited deviation after the acceleration operation.

Figure 3.13d illustrates the belt speed at each node over time. During the acceleration, the belt speed at each node increases successively. Similar to the belt speed around the drive pulley, the speed curves of other nodes are not thus smooth due to the uncontrolled acceleration waves caused by belt slippage. In addition, the belt speed is fluctuating with a dampened amplitude for a certain period in response to the belt viscosity-elasticity. Moreover, as is shown the amplitude of fluctuation of belt speed at the carrying side is less than that at the return side. However, it clear shows that after accelerating, the minimum speed of belt at the tail pulley is larger than 3.4 m/s. Therefore, the risk of material spillage caused by exceeding speed deviation is avoided.

Overall, taking the conveyor dynamics shown in Figures 3.13 into account, the acceleration operation from 2 m/s to 4 m/s within 41 seconds is not acceptable. Optimizations are given in the next section to find the minimum acceleration time.

3.7.1.3   Step 3: Optimization

The excitation of uncontrolled belt tension waves and of uncontrolled acceleration waves are caused by the phenomenon of belt slippage. In order to improve the conveyor dynamics, the risk of belt slippage should be avoided. Taking the belt slippage into account, the problem of

optimizing acceleration time is defined as a problem of finding root of function $f(t)$:

$$f(t) = F_{d,max}(t) - 49.6 = 0 \tag{3.51}$$

where an important assumption is given that the driving force can exceed the maximum available friction resistances between the belt and the drive pulley.

In order to reduce the computational time, the secant method is applied. Compared to the bisection method and the false position method, the secant method generally can find the root faster. In addition, the secant method is more applicable than the Newton-Raphson, due to the fact that the derivative of the maximum driving force over time is hardly expressed in a mathematical way. In the implementation of the secant method, the two initial time points are $t_0 = 41s$ and $t_1 = 71s$. The stopping criterion is the function value $f(t)$ less than 0.1.

Table 3.4: Root finding function of $f(t) = F_{d,max}(t) - 49.6 = 0$ with the secant method. The stop criteria is $|\epsilon| < 0.1$.

	t_1	t_2	t_3	$f(t_1)$	$f(t_2)$	$f(t_3)$
1	41	71	55,01	5,0930	-5,8101	-1,6228
2	71	55,01	48,81	-5,8101	-1,6228	0,8562
3	55,01	48,81	50,95	-1,6228	0,8562	-0,0732

The experimental results are shown in Table 3.4. As the data shows the secant method costs only three iterations for finding the minimum acceleration time. The data suggests the optimum acceleration time approaches to 51 seconds. Figure 3.14 presents the examination results of the conveyor dynamics during the execution of the 51 seconds acceleration profile. The diagram of Figure 3.14a clearly shows during the acceleration, the maximum driving force is 49.5 kN. It suggests that the risk of belt slippage is successfully avoided. The diagrams of Figures 3.14b to 3.14d also show that in the acceleration, both the tensile force and the speed vary smoothly over time. From the presented results it can be concluded that the conveyor dynamic behavior in this acceleration operation is acceptable. The operation accelerating the studied conveyor from 2 m/s to 4 m/s requires at least 51 seconds.

Figure 3.14: Belt conveyor dynamics in the acceleration operation from 2 m/s to 4m/s within 51 seconds. (a) Driving forces exerted on the drive pulley. (b) Belt tension at each nodal point. (c) Belt speed at the drive pulley. (d) Belt speed at each nodal point along the conveying route.

3.7.2 Deceleration operation from 4 m/s to 2 m/s

3.7.2.1 Step 1: Estimation

Pushing the motor into the regenerative operations is the major risk during the deceleration operation. With respect to this risk, the driving torque of the drive pulley should be non-negative. Accordingly, the maximum deceleration is

$$a_{de,max} = -Cfg = -0.19m/s^2 \tag{3.52}$$

Then based on the formula 3.41, the estimated deceleration time is

$$t_{de,min} = \frac{\pi}{2} \frac{\Delta V}{a_{de,max}} = 16.5s \approx 17s \tag{3.53}$$

With respect to the risk of material spillage caused by the excessive low belt speed, the belt speed at the tail pulley should remain over 1.7 m/s after the deceleration operation.

3.7.2.2 Step 2: Calculation

Figure 3.15 illustrates the examination results of the deceleration operation from 4 m/s to 2 m/s within 17 seconds. Figure 3.15a presents the driving forces exerted on the drive pulley. The diagram shows at the start of the decelerating procedure, the driving force decreases gradually over time. Meanwhile, both the belt tension and the belt speed change smoothly, see Figures 3.15b and 3.15d respectively. However, the diagram in Figure 3.15a shows at the time point 11 second, the driving force reduces to the bottom 0kN, and then the driving forces are lost. This phenomenon continues for about 8 seconds. As Figures 3.15b to 3.15c show, the belt tension and speed along the conveyor are uncontrollable during this period. The diagram in Figure 3.15c clearly shows the belt speed at the drive pulley fails to follow the reference speed. Therefore, the deceleration from 4 m/s to 2 m/s within 17 seconds is unacceptable.

Besides the sudden loss of driving force, this deceleration also results in the belt slippage around the drive pulley. As the diagram in Figure 3.15a shows, at the time point 26 second, the driving force reaches its traction limit, and then the slippage occurs. The slippage causes an uncontrollable acceleration wave, see Figures 3.15d and 3.15c. As the diagram in Figure 3.15c shows, the slippage results in an unexpected speed deviation. The deviation lasts for around 10 seconds.

The diagram in Figure 3.15d also shows a large speed deviation during and after the deceleration. The largest deviation between the drive and tail pulley can be over 1m/s. The figure further shows at the time point 24 second, the tail pulley speed drops to 0.9 m/s, less than half of the required speed. This phenomenon increases the risk of material spillage away from the belt at the loading area. Therefore, special attention should be paid to this phenomenon during the deceleration operation.

From the presented results in Figure 3.15, it can be concluded that the deceleration activity from 4 m/s to 2 m/s within 17 seconds will result in the risk belt slippage, the risk of pushing the motor into the regenerative operation, and the risk of material spillage. Therefore, the
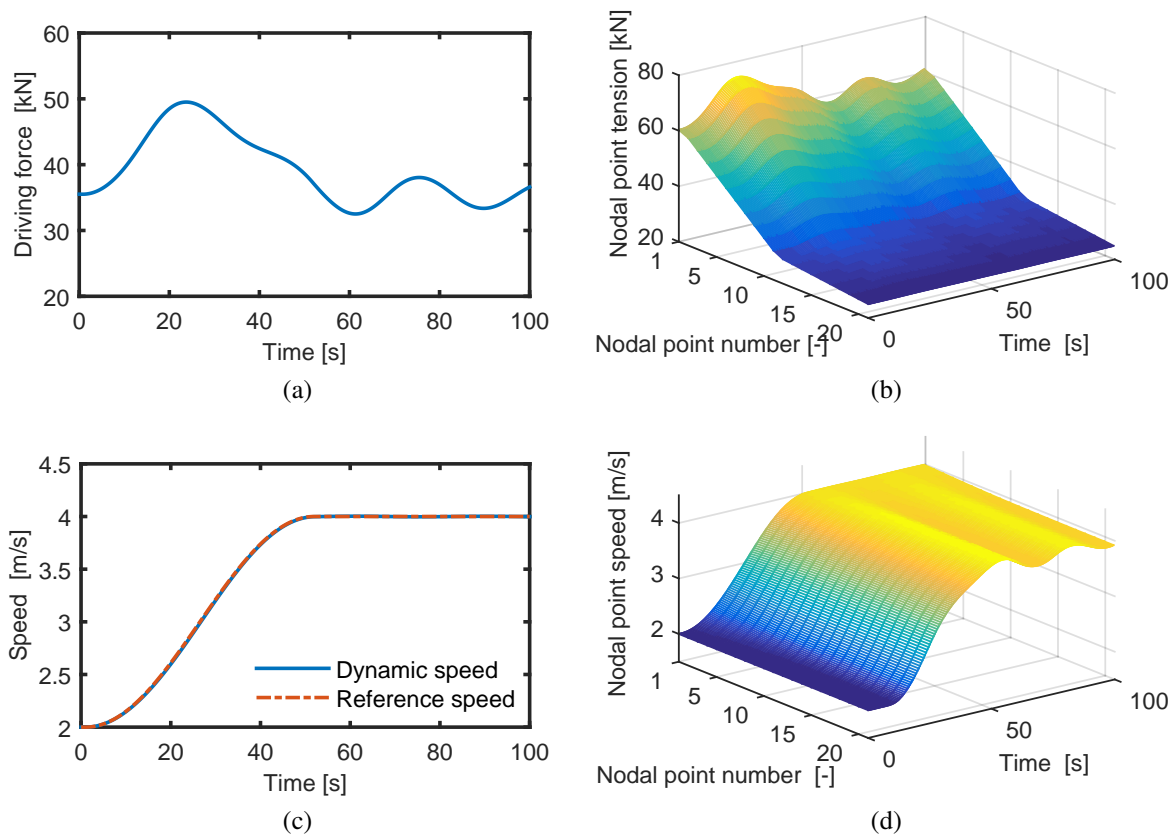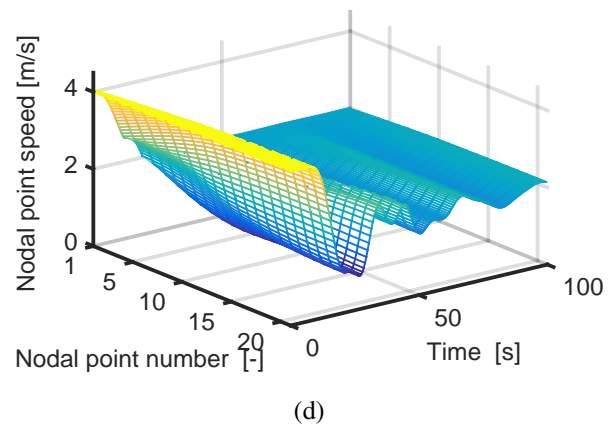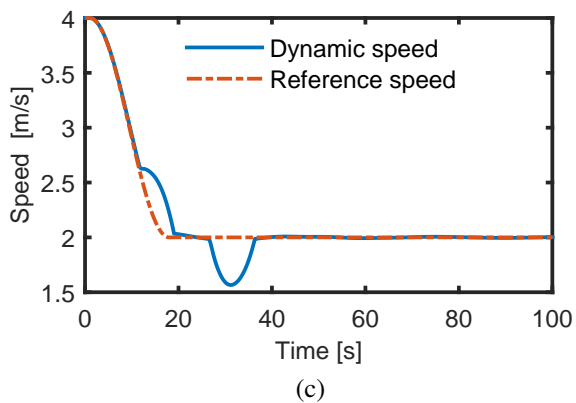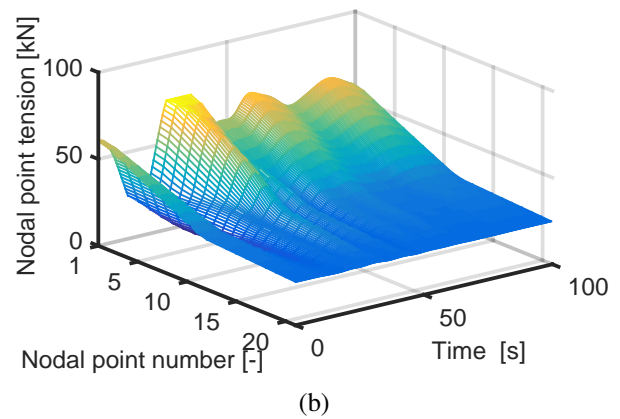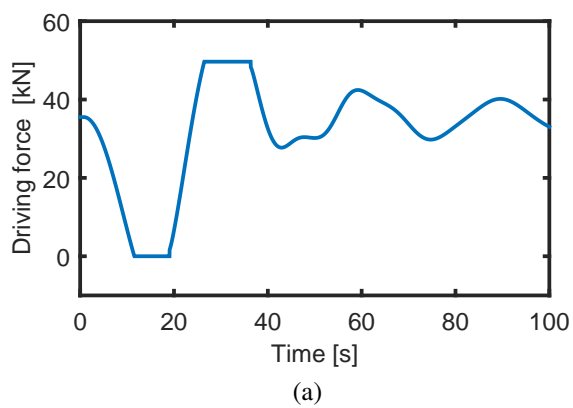
Figure 3.15: Belt conveyor dynamic behaviors in the deceleration from 4 m/s to 2 m/s within 17 seconds. (a) Driving forces exerted on the drive pulley. (b) Belt tension at each nodal point. (c) Belt speed at the drive pulley. (d) Belt speed at each nodal point along the conveying route.

deceleration operation with estimated deceleration time is not acceptable. Taking these risks into account, the next step will carry out further simulations to improve the conveyor dynamics and to find the minimum deceleration time.

3.7.2.3   Step 3: Optimization

The examination results in Figure 3.15 illustrate the existence of the risk of pushing motor into the generative operation, of the risk of belt slippage and of the risk of material spillage. Taking the risks into account, the problem of optimizing deceleration time can be defined as:

$$t^* = max(t_f^*, t_g^*, t_h^*) \tag{3.54}$$

in which

t_f^* the root of function $f(t) = F_{dA,max}(t) - 49.6 = 0$ with respect to the risk of belt slippage

t_g^* the root of function $g(t) = F_{dA,min}(t) = 0$ with respect to the risk of pushing motor into the regenerative operation

t_h^* the root of function $h(t) = v_{min}(t) - 1.7 = 0$ with respect to the risk of material spillage caused by the excessive low belt speed.

Similar to the optimization step in the acceleration operation, the secant method is applied here for finding the roots for functions $f(t)$, $g(t)$ and $h(t)$. Then comparing these roots yields the minimum deceleration time for deceleration operation from 4 m/s to 2 m/s with acceptable dynamic performance. It is important note that in order to implement the secant method, the value of the driving force can be either over 49.5 kN or below 0 kN.

Finding the root of function $f(t)$ first. The initial points are 17 and 47, and the stop criteria is $|\epsilon| < 0.1$. Table 3.5 presents the root finding result. The root is approached after four times of iterations. The data in Table 3.5 suggests that with respect to the risk of belt slippage, the minimum deceleration time is 30.37 second.

The data in Table 3.5 also includes the function values of $g(t)$ and $h(t)$ at point t_3. The data implies that the activity of finding root of $g(t)$ can be canceled since when the deceleration time equals 30.37 seconds, the minimum driving force is far larger than 0kN. However, there still exists the risk of material spillage when $t_3 = 30.37s$. But the data in the second row clearly shows the root of function $h(t)$ should near 35.2. Table 3.6 illustrates the root finding result of function $h(t)$ with initial points 35.2 and 47. The root 35.44 is found after three times of iterations.

Finally, the optimum deceleration time for the deceleration operation from 4 m/s to 2 m/s is obtained, and equals 35.44 seconds. If we continue round the root to the nearest integer which is no less than the root, the minimum deceleration time of this deceleration operation is 36 seconds. Figure 3.16 presents the dynamic performance of the belt conveyor during the deceleration operation from 4 m/s to 2 m/s within 36 seconds. The figure shows during and after the execution of the 36 seconds deceleration operation, the driving forces value always stay

Table 3.5: Root finding function of $f(t) = F_{d,max}(t) - 49.6 = 0$ with the secant method. The stop criteria is $|\epsilon| < 0.1$. The function values $g(t_3)$ and $h(t_3)$ are also given.

	t_1	t_2	t_3	$f(t_3)$	$g(t_3)$	$h(t_3)$
1	17	47	35,2	-6,4518	12,0559	-0,0109
2	47	35,2	25,23	8,0495	1,5833	-0,6066
3	35,2	25,23	30,76	-0,6148	7,9286	-0,2487
4	25,23	30,76	30,37	-0,0479	7,5258	-0,2719

Table 3.6: Root finding function of $h(t) = v_{min}(t) - 1.7 = 0$ with the secant method. The stop criteria is $|\epsilon| < 0.01$. The function values $f(t_3)$ and $g(t_3)$ are also given.

|	t_1	t_2	t_3	$f(t_3)$	$g(t_3)$	$h(t_3)$
1	35,2	47	35,78	-7,1217	12,5364	0,0163
2	47	35,78	34,83	-6,0124	11,7427	-0,0288
3	35,78	34,83	35,44	-6,7318	12,2563	0,0005
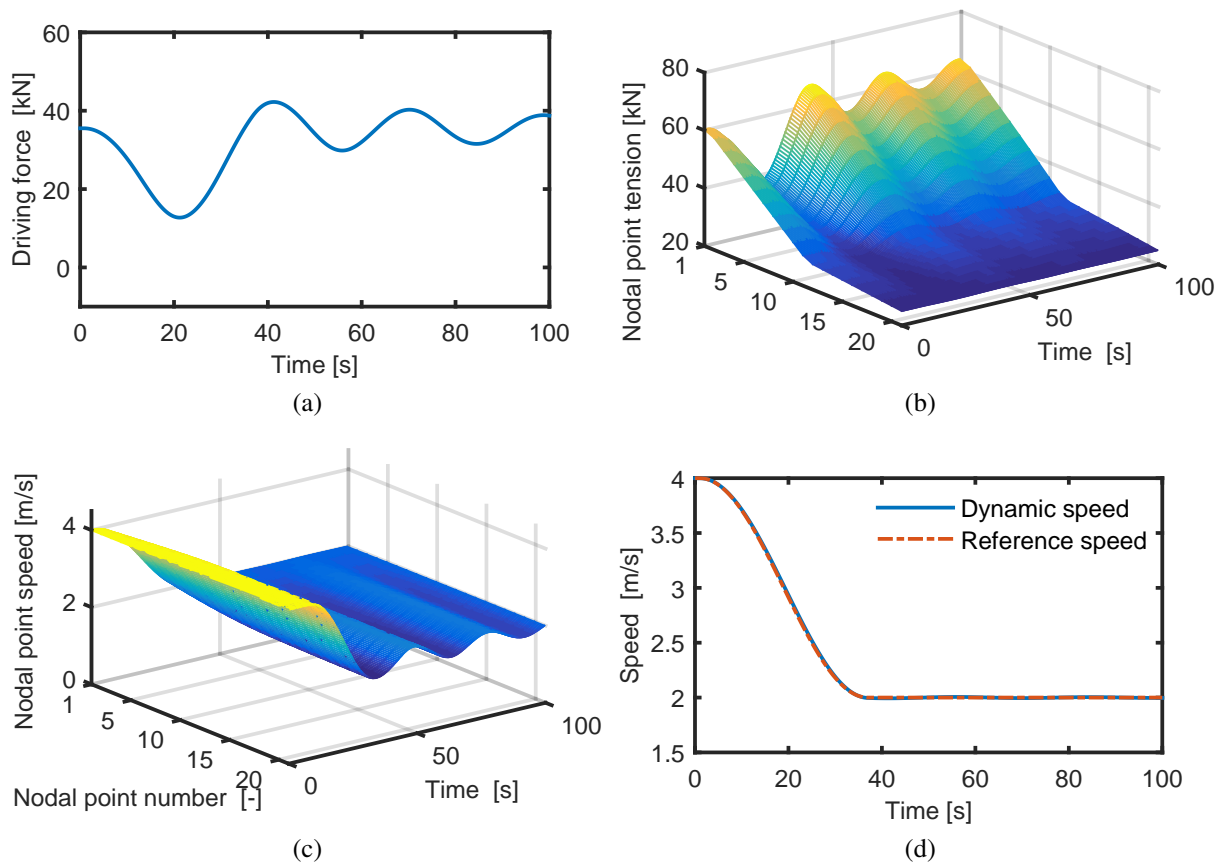
Figure 3.16: Belt conveyor dynamics in the deceleration operation from $4m/s$ to $2m/s$ within 36 seconds. (a) Driving forces exerted on the drive pulley. (b) Belt tension at each nodal point. (c) Belt speed at each nodal point along the conveying route. (d) Belt speed at the drive pulley.

positive but below the friction limit. Meanwhile, both the belt tension and the belt speed along the conveying route are varying smoothly. Apparently, this deceleration operation is acceptable.

In the case of belt conveyors with variable material feeding rate, the belt speed is expected to be regulated accurately to match the varying mass flow. In order to prevent continuous high stress, the conveyor speed is regulated discretely with several specific speeds. For the studied belt conveyor, it is assumed that the selected speeds are $2\ m/s$, $2.5\ m/s$, $3\ m/s$, $3.5\ m/s$, $4\ m/s$, $4.5\ m/s$, $5\ m/s$ and $5.2\ m/s$. Using the ECO method, more research is carried out, and Figure 3.17 gives the minimum speed adjustment time, both in acceleration and deceleration operations.

(a)

(b)
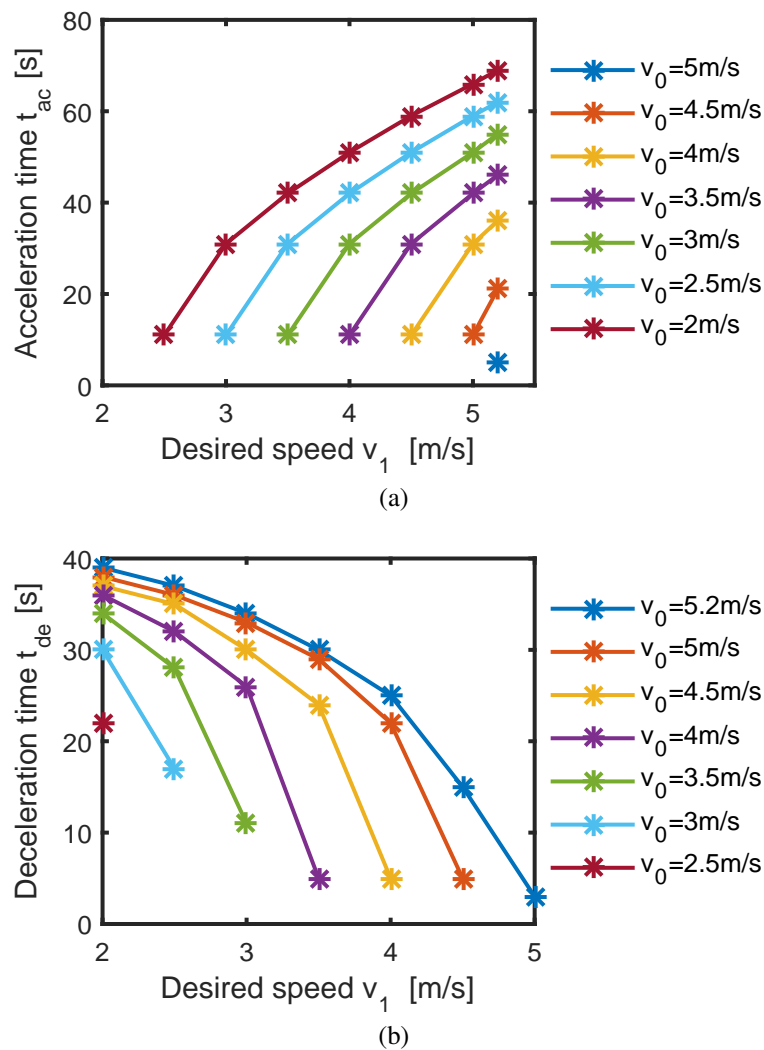
Figure 3.17: Minimum speed adjustment time for different speed adjustment ranges. (a) Minimum acceleration time. (b) Minimum deceleration time.

3.8   Conclusion

This chapter answered the second key research question raised in Chapter 1: *How to determine the permitted maximum acceleration and the demanded minimum acceleration time in transient*

operations? It proposed the ECO method and a long horizontal belt conveyor was studied. According to the experimental data, an overall conclusion can be drawn: the ECO method is applicable to determine the minimum speed adjustment time, both in acceleration and deceleration operations. In addition, the following sub-conclusions can also be drawn based on the experimental results:

- The finite element method can be used to examine the conveyor dynamic performance in transient operations.

- The transient operations with the initialized acceleration time may result in the risks.

- These risks can be successfully prevented if the optimized speed adjustment time is used.

Chapter 4

Belt conveyor energy model

Chapter 3 discussed the transient operations of a belt conveyor under speed control, and proposed the ECO method for determining the minimum speed adjustment time. That improved the applicability of belt conveyor speed control. In order to evaluate the economic performance of speed control, it is worth building a parametric energy model for belt conveyors. This chapter discusses the energy model of belt conveyors. Standard DIN 22101 (German Institute for Standardization, 2015) is widely used in practice for estimating the power consumption of belt conveyors. DIN-based energy model is detailed in Section 4.1 in which the artificial frictional coefficient f is used to calculate the main resistances of a belt conveyor. Section 4.2 proposes two ways to achieve the f factor value: physical experiment and analytical calculation. However, physical experiments are expensive in practice and they may have a negative impact on the production plan. Therefore, the thesis uses the analytical method for determining the f factor value. The analytical method divides the main resistances into four types of individual resistances and calculates these resistances by using the individual calibrated resistance models. Section 4.3 details the modeling of the sub-resistances and a case is studied in Section 4.4 to show the analytical calculation. Taking the power losses of the driving units into account, Section 4.5 discusses the driving system efficiency. Some conclusion remarks of this chapter is given in Section4.6.

4.1   DIN-based belt conveyor energy model

In last decades, several energy models have been developed to estimate the power consumption of belt conveyors. Most of energy models are based on belt conveyor design standards, such as DIN 22101 (German Institute for Standardization, 2015) and ISO 5048 (International Organization for Standardization, 1989). The thesis uses the DIN-based energy model for estimating the power consumption of belt conveyors and so that to assess the performance of belt conveyors under speed control.

Standard DIN 22101 is proposed by German Institute for Standardization (2015) for calculating and dimensioning belt conveyor components. This standard is widely used in practice for assisting in designing belt conveyors. This section gives a detail of the calculations. German Institute for Standardization (2015) suggests that the required mechanical power P_m is determined

by the driving forces F_d exerted on the driving pulley(s) and the conveyor belt speed v

$$P_m = F_d v \tag{4.1}$$

Then taking the power losses in the driving system into account, the demanded electrical power P_e is

$$P_e = \frac{P_m}{\eta_{sys}} = \frac{F_d v}{\eta_{sys}} \tag{4.2}$$

in the cases of non-generating belt conveyors. In the steady operating conditions, the driving forces equal to the total motional resistances F_f along the conveying route

$$F_d = F_f \tag{4.3}$$

DIN 22101 divides the total motional resistances into four groups: main resistance F_H, secondary resistances F_N, gradient resistances F_{St} and special resistances F_S:

$$F_f = F_H + F_N + F_{St} + F_S \tag{4.4}$$

These resistances are individually described below.

4.1.1 Main resistances F_H

The main resistances F_H, also called primary resistances, are resistances occurring along the whole length of the conveyor. These resistances consist of belt indentation resistances, belt and bulk material flexural resistances, and rotating resistances of rollers. German Institute for Standardization (2015) indicates that the main resistances can be responsible for up to 90% of the total resistances. In order to estimate the main resistances, German Institute for Standardization (2015) further introduces an index of artificial frictional coefficient f, and approximates the main resistances by

$$F_H = f g L \left[m'_{roll} + \left(2m'_{belt} + m'_{bulk} \right) cos\delta \right] \tag{4.5}$$

where

    L the conveyor length, m

    m'_{roll} the mass of idler rolls per unit length, kg/m

    m'_{belt} the mass of belt per unit length, kg/m

    m'_{bulk} the mass of bulk solid material on the belt per unit length, kg/m

    δ inclination angle of a belt conveyor system, °. In the case of declined belt conveyor systems, the value of δ is negative.

As German Institute for Standardization (2015) emphasizes, the selection of the artificial frictional coefficient is significantly important in the design process of belt conveyors. For the

cases satisfying the following limiting conditions, German Institute for Standardization (2015) suggests the standard value for the f factor shown in Table 4.1 for estimating the total main resistances of belt conveyors:

- 3 roller fixed idler sets in the top run

- carrying idlers with anti-friction bearings and labyrinth seals

- values of belt sag ratio less than 1%

- filling ratio within a range from 70% to 110%

Table 4.1: Standard values for the artificial friction coefficient f for estimating the total primary resistance. Courtesy of the standard DIN 22101 German Institute for Standardization (2015).

Characteristic	Values for characteristic		
Internal friction of the bulk material	medium	low	high
Belt conveyor alignment	medium	good	bad
Belt tension	medium	high	low
Operating conditions (dusty, sticky)	medium	good	bad
Idler diameter	108 to 159	> 159	< 108
Spacing of upper strand idlers in m	1.0 to 1.5	< 1.0	> 1.5
Spacing of lower strand idlers in m	2.5 to 3.5	< 2.5	> 3.5
Belt speed in m/s	4 to 6	< 4	> 6
Troughing angle in °	25 to 35	< 25	> 35
Ambient temperature in °C	15 to 25	> 25	< 15
Artificial frictional coefficient f	standard value≈0.020	0.010~0.020	0.020~0.040

4.1.2   Secondary resistances F_N

Differing from the main resistances existing along the whole conveying route, the secondary resistances F_N only occur at the head and tail of the systems. German Institute for Standardization (2015) suggests, the secondary resistances are mainly composed of fives parts:

- the inertia resistance of material conveyed and the friction resistance between material conveyed and the belt in the feeding zone, F_{Auf};

- the friction resistance between conveyor belt and lateral chutes in the acceleration zone of a feeding point, F_{Schb};

- the friction resistance caused by belt cleaners, F_{Gr};

- the bending resistance of the conveyor belt where it runs over a pulley, F_{Gb};

- and the resistance of the bearings of non-driven pulleys, F_{Tr}.

In the case of belt conveyors where secondary resistances occupy a small proportion in the total resistance, German Institute for Standardization (2015) introduces the secondary coefficient C to approximate the total secondary resistances

$$F_N = (C - 1) F_H \tag{4.6}$$

German Institute for Standardization (2015) further suggests that, the C factor is dependent on the conveyor length. If the belt filling ratio is in the range from 70% to 110%, Table 4.2 illustrates the value of coefficient C over different conveyor lengths.

Table 4.2: Standard values of coefficient C for belt conveyor installations with filling ratios in the range from 70% to 110%. Courtesy of the standard DIN 22101 (German Institute for Standardization, 2015).

$L(m)$	80	100	150	200	300	400	500
C	1.92	1.78	1.58	1.45	1.31	1.25	1.2
$L(m)$	600	700	800	900	1000	1500	≥ 2000
C	1.17	1.14	1.12	1.1	1.09	1.06	1.05

4.1.3 Gradient resistances F_{St}

When the belt and bulk solid travel uphill or downhill with a slope of δ, the weight of belt and bulk solid can be divided into two components: one perpendicular to the conveying direction which is the major reason of the main resistance F_H, and the other along the conveying direction which generates the gradient resistance F_{St}. In the case of inclined or declined belt conveyors, the gradient resistance can be relatively larger than other resistances. German Institute for Standardization (2015) suggests, the gradient resistance can be up to 65% of the total motional resistances in the case of a belt conveyor with 5% inclination. Differing from the main resistances and the secondary resistances, the gradient resistance can be precisely determined by

$$F_{St} = L m'_{bulk} g \sin\delta = H m'_{bulk} g \tag{4.7}$$

where H is the height difference of the belt conveyor.

4.1.4 Special resistances F_S

Special resistances F_S generally occur only on specially designed belt conveyor systems. As German Institute for Standardization (2015) and Phoenix Conveyor Belt Systems GMBH (2004) suggest, the special resistances can be caused by

- tilted idler position, which arises the tilting resistance F_{Rst} at side carrying idlers

- chutes outside the feeding points, which arise extra chute frictional resistances F_{Sch}

- devices for lateral bulk material discharge along the conveying length, which arise scraper resistances F_{Ga}

The total special resistances F_S of a conveyor are the sum of the mentioned individual resistances. Note again, these individual special resistances do not occur on all belt conveyors. Then taking the total sum of special resistances F_S into account, the total motional resistances of belt conveyors running at steady state can be approximated by substituting Equations 4.5 to 4.7 into Equation 4.4:

$$F_f = CLfg\left[m'_{roll} + \left(2m'_{belt} + m'_{bulk}\right)cos\delta\right] + Hgm'_{bulk} + F_S \tag{4.8}$$

Finally, the required electrical power in steady state amounts to

$$P_e = \frac{CLfg\left[m'_{roll} + \left(2m'_{belt} + m'_{bulk}\right)cos\delta\right] + Hgm'_{bulk} + F_S}{\eta_{sys}}v \tag{4.9}$$

4.2   Calculation of the DIN f factor value

Equation 4.9 has been widely used to determine the magnitude of motor power in the design of belt conveyors. In the design of a new through belt conveyor, standard values for the artificial friction coefficient f can be selected from Table 4.1 to help calculate the required dimensions and ratings of belt conveyor components. However, it is important to note that the values of the f factor in Table 4.1 are only for the purpose of estimating the ratings of belt conveyors. Generally, the suggested standard value often overestimates the power consumption to avoid the overload of the drive system for safety reasons. In addition, the research results of such as (Lodewijks, 2011) show that the frictional coefficient f varies with different conveyor parameters, such as the cover material of a belt. Moreover, Alles (1994) and Hiltermann et al. (2011) suggests that the f factor value will change with both belt load and belt speed of a given belt conveyor. Therefore, the calculation of the f factor value is required before the DIN-based energy model is used for calculating the power consumption of a belt conveyor. Calculations of the f factor value can be performed either by field experiments or by theoretical analyses. The experimental method is illustrated in Section 4.2.1 and Section 4.2.2 details the the analytical method.

4.2.1   Experimental method

Hiltermann et al. (2011) proposed an experimental method for calculating the f factor of an existing belt conveyor. This calculation was done by implementing simple measurements on power consumption of the concerned belt conveyor. Hiltermann et al. (2011) supposed that the efficiency of the driving system is constant and that the special resistances F_S are negligible. Then on the basis of Equation 4.9, the frictional coefficient can be calculated by

$$f = \frac{\frac{P_e\eta_{sys}}{v} - m'_{bulk}gH}{CLg\left[m'_{roll} + \left(2m'_{belt} + m'_{bulk}\right)cos\delta\right]} \tag{4.10}$$

The paper (Hiltermann et al., 2011) does not give the detail of the measurement, but the thesis of (Hiltermann, 2008) does. The studied belt conveyor is frequency-controlled, so that

it is possible to manually alter the conveyor speed by changing the output frequency of the installed frequency converter. The belt conveyor is driven by three motors. Two motors drive the main drive pulley and the third drives a secondary drive pulley which nears the main drive pulley. Hiltermann (2008) assumed that the load of these motors is always more or less equal. The input power of the frequency converter of the first motor is recorded by a power clam meter, so that the total power consumption can be obtained by assuming that all motors deliver the same power.

The material flows deposited onto the belt conveyor is controlled by means of a hopper with speed-controlled apron feeder. Prior to the measurement, the speed of the hopper conveyor is fixed for a specific material feeding rate. The actual material flow is monitored by a belt weighing system with a high accuracy. Belt speeds of the studied conveyor can be varied during operations. Once the belt speed has reached the desired speed and the belt conveyor has acquired a constant material load over the entire belt length, the data of the actual electrical power consumption can be collected and recorded.

Measurements were performed at various steady material flows with different belt speeds. Figure 4.1 illustrates the experimental results. Figure 4.1a shows the measured electric drive power. As the data shows, the power is relatively linearly correlated with the material flow. Moreover, it clearly shows that lower belt speed requires a lower electric drive power at the same material flow.

Figure 4.1b gives the derived values of the f factor over different material feeding rates and belt speeds. From the diagram, it can be seen that the average value for the f factor is about 0.022. With the derived average value, Equation 4.9 was used in (Hiltermann, 2008; Hiltermann et al., 2011) to predict the actual power consumption of the belt conveyor under different operational conditions.

However, it is important to note that Figure 4.1b also indicates that the frictional coefficient varies with different speeds and loads. Using the average value for the f factor may result in errors of energy savings by means of speed control. Moreover, this experimental calculation itself is not that accurate. The reasons are twofold. First, Hiltermann (2008) assumed that the driving system efficiency is constant so that he only measured the electric power, instead of the mechanical power. However, experimental results in (ABB, 2000) shows that that the driving system efficiency varies over loads and speeds. Another reason is that, Hiltermann (2008) assumed that the three motors of the concerned conveyor could equally share the driving power, so that he only detected the electric power of one of the three motors, instead of the total electric power of these three motors. However, Hiltermann (2008) did not proof that the three motors provide the same amount of power. The uneven distribution of the driving torque among the three motors can result in the error of the calculation. Hereby, taking these two reasons into account, the experimental calculation is suggested to be improved by measuring the driving torque by strain gauges, instead of measuring the electric power. Then the f factor can be calculated by:

$$f = \frac{P_m - m'_{bulk}gH}{CLg\left[m'_{roll} + \left(2m'_{belt} + m'_{bulk}\right)cos\delta\right]} = \frac{\sum_{k=1}^{n} T_{shaft,k}\omega_{shaft,k} - m'_{bulk}gH}{CLg\left[m'_{roll} + \left(2m'_{belt} + m'_{bulk}\right)cos\delta\right]} \tag{4.11}$$
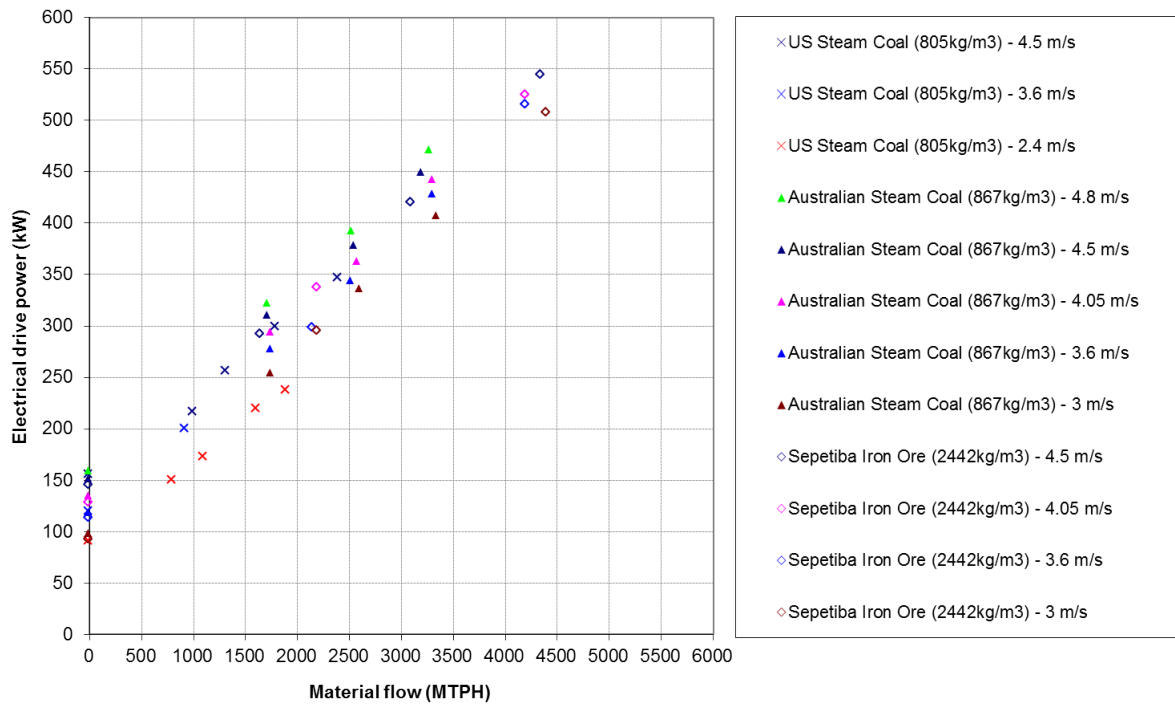
(a)
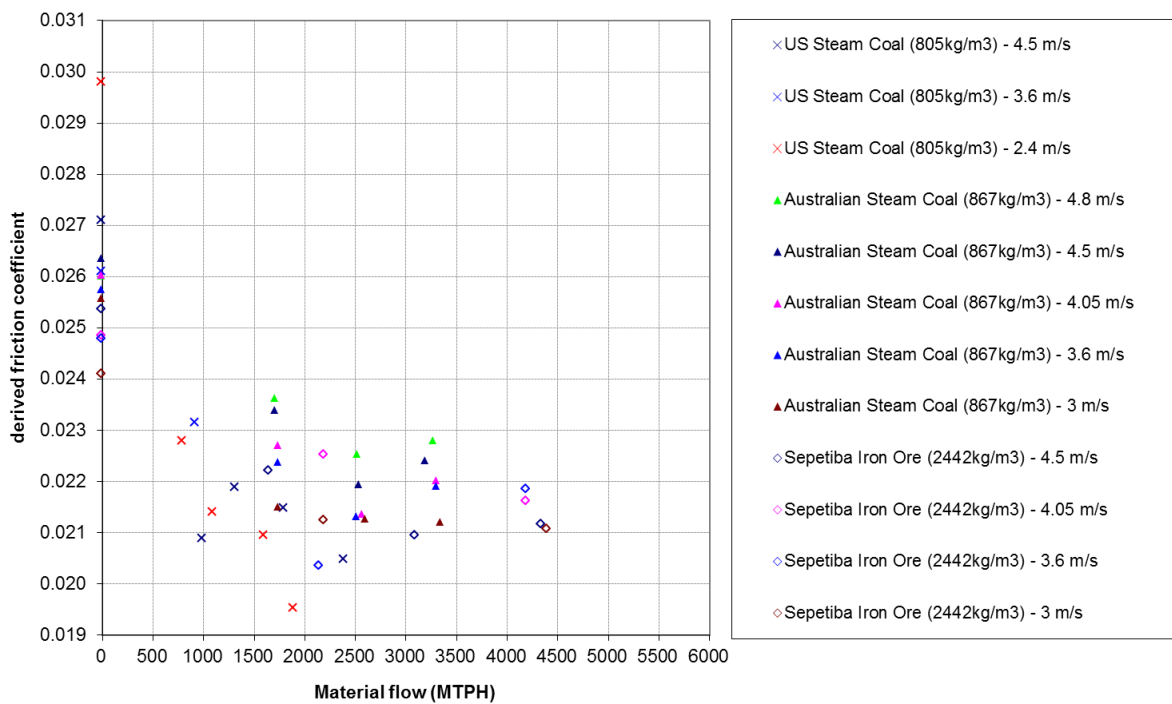
(b)

Figure 4.1: Experimental results. (a) Measured electrical power. (b) Derived friction coefficient. Courtesy of Hiltermann et al. (2011).

where n is the total number of the driving pulleys, and $T_{shaft,k}$ and $\omega_{shaft,k}$ represent the driving torque and the angular speed of the kth driving pulley, respectively.

4.2.2 Analytical method

Equations 4.11 illustrates the improved formula of calculating the f factor by filed experiments. However, the physical experiments are expensive in practice, and the control of material feeding rate may have a negative impact on the production plan. Theoretical analysis provides another important technique of calculating the f factor value. The theoretical analysis is based on the proved resistance models. As German Institute for Standardization (2015) indicates, the main resistances of belt conveyors occur along the entire length of the conveyor between head and tail. German Institute for Standardization (2015) further suggests that the friction coefficient f is defined mainly by the belt indentation resistances F_i, the flexural resistances F_{fb} of belt , the flexural resistances F_{fs} of the bulk solid material, and the rotation resistance F_r of rollers. Then based on the definition, the f factor can be calculated by

$$f = \frac{F_H}{Lg\left[m'_{roll} + \left(2m'_{belt} + m'_{bulk}\right)cos\delta\right]} = \frac{\sum F_I + \sum F_{fb} + \sum F_{fs} + \sum F_r}{Lg\left[m'_{roll} + \left(2m'_{belt} + m'_{bulk}\right)cos\delta\right]} \qquad (4.12)$$
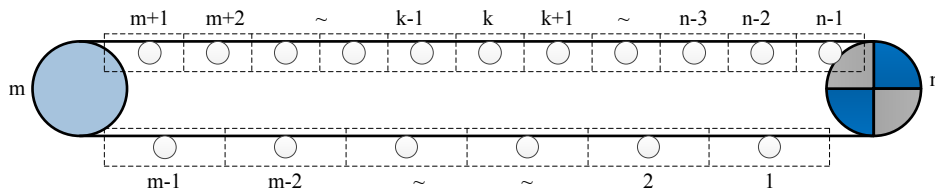
Figure 4.2: Interpretation of finite element method

Herein, a finite-element-method (FEM) based model is proposed to calculate the sum of these individual resistances along the conveyor route. Figure 4.2 illustrates the basic idea where the belt conveyor is virtually divided into a finite number of elements. The boundary of each element is the center of neighboring idler stations. At the carrying side, the frictional resistances F_k of the kth element equals

$$F_k = F_i^k + F_{fb}^k + F_{fs}^k + F_r^k \qquad \text{if } m+1 \le k \le n-1 \qquad (4.13)$$

where the superscript ^{k} stands for the element number. Similarly, the frictional resistance of elements at the return side can be calculated by

$$F_k = F_i^k + F_{fb}^k + F_r^k \qquad \text{if } 1 \le k \le m-1 \qquad (4.14)$$

Then accordingly, the total main resistances are

$$F_H \quad = \quad \sum_{k=1}^{m-1} F_k + \sum_{k=m+1}^{n-1} F_k = \sum_{k=1}^{m-1} \left(F_i^k + F_{fb}^k + F_{fs}^k + F_r^k \right) + \sum_{k=m+1}^{n-1} \left(F_i^k + F_{fb}^k + F_r^k \right) \quad (4.15)$$

Finally, the f factor can be calculated by

$$f = \frac{\sum_{k=1}^{m-1} \left(F_i^k + F_{fb}^k + F_{fs}^k + F_r^k \right) + \sum_{k=m+1}^{n-1} \left(F_i^k + F_{fb}^k + F_r^k \right)}{Lg \left[m'_{roll} + \left(2m'_{belt} + m'_{bulk} \right) cos\delta \right]} \quad (4.16)$$

According to Equation 4.16, the key-point of the analytical approach is to calculate the individual resistances along the conveyor route. This can be achieved by using proved sub-resistance models from literature. The next section will detail the calculation models of these resistances.

4.3   Modeling of sub-resistances

4.3.1   Indentation resistance of belt

The belt indentation resistance model is based on May et al. (1959), Spaans (1991) and Lodewijks (1995).

When the belt moves over a roller station, the contact region of the belt bottom cover is indented by the hard roll(s) due to the belt and load weight. Figure 4.3 illustrates the deformation of the belt where a and b represent the front and rear part of the contact length between belt and roller. Due to the belt elasticity-viscosity, the material requires more time to relax to the original pattern so that the rear contact region length b is smaller than the front contact length a. The asymmetrical deformation results in the asymmetrical pressure distribution, shown as Figure 4.3. In such a way, the indentation rolling resistance is generated.

Based on the phenomenon of the asymmetrical pressure distribution, May et al. (1959) provides an indentation resistance model, accounting for the rubber elasticity-viscosity. May et al. (1959) assumes that the conveyor belt is lying on the ground and that a hard roller is rolling over the belt bottom cover, see Figure 4.4. May et al. (1959) further assumes that the belt carcass is a rigid base, and that the cover rubber is a linear visco-elastic material. When the roller is moving over the cover rubber, the material in front of the cylinder is compressed, and the original shape is recovered behind the roller. The rubber elasticity-viscosity results in an asymmetrical contact shape between the belt and the roller. May et al. (1959) describes the cover material by using a Winkler foundation model (see Figure 4.4) to approximate the stress pattern. The Winkler model is composed of an infinite number of independent three-parameter Maxwell models. These Maxwell models can be compressed without affecting their neighbors. May et al. (1959) suggests that the stress distribution between roll and the cover rubber can be calculated by
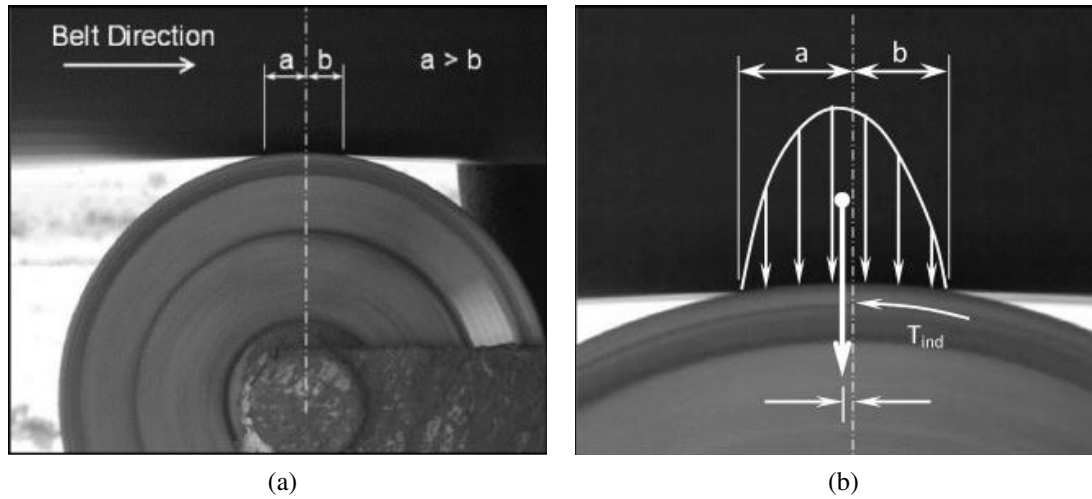
Figure 4.3: Indentation rolling resistance. (a) Cyclic compression and recovery. (b) Asymmetric pressure distribution. Courtesy of (Munzenberger and Wheeler, 2016).
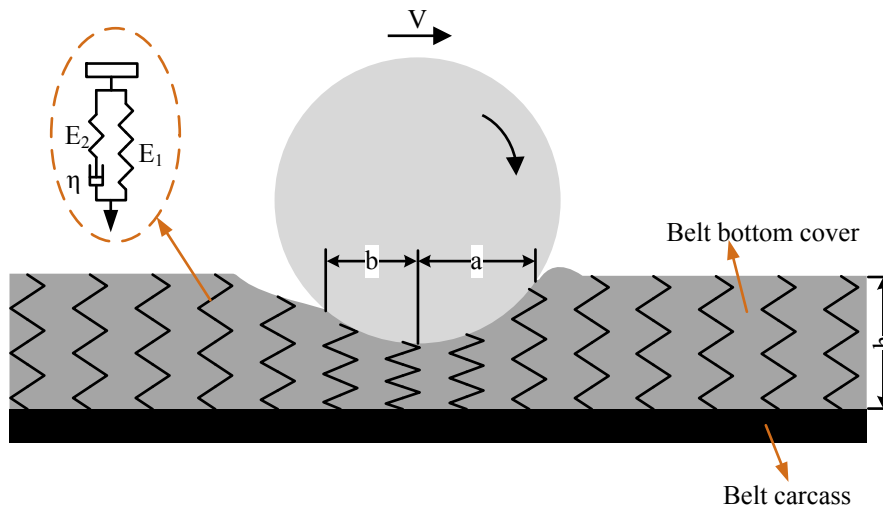
Figure 4.4: A cylinder rolling over a conveyor belt.

$$\sigma(x) = a^2 \left\{ \frac{E_1}{2Rh} \left(\frac{a-x}{a} \right) \left(\frac{a+x}{a} \right) + \frac{E_2 k}{Rh} \left[(1+k) \left(1 - e^{\left(-\frac{1}{k} \frac{(a-x)}{a} \right)} \right) - \left(\frac{a-x}{a} \right) \right] \right\} \qquad (4.17)$$

where

a front part of contact length between belt and idler, m

E Young's modulus (E_1 and E_2), N/m^2

R roll radius, m

h thickness of belt bottom cover, m

x distance to the center line of the roll, m

> k Deborah number, defined by $v\tau/a$, where v is the belt speed and τ is the relaxation time ($\tau = \eta/E_2$)

If the belt moves at a constant speed v, then the distributed vertical force can be calculated by

$$
\begin{aligned}
F_v' &= \int_{-b}^{a} \sigma(x)\,dx \\
&= \frac{E_1 a^3}{6Rh}\left[2 - \left(\frac{b}{a}\right)^3 + 3\left(\frac{b}{a}\right)\right] + \frac{2E_2 k a^3}{Rh}\left[1 - \left(\frac{b}{a}\right)^2\right]
\end{aligned}
\tag{4.18}
$$

where b is the rear part of contact length between belt and idler in m, see Figure 4.4. Derived from Equation 4.18, the contact length a can be calculated by

$$
a = \frac{F_v'^{1/3}}{\left[\frac{E_1}{6Rh}\left(2 - \left(\frac{b}{a}\right)^3 + 3\left(\frac{b}{a}\right)\right) + \frac{2E_2 k}{Rh}\left(1 - \left(\frac{b}{a}\right)^2\right)\right]^{1/3}}
\tag{4.19}
$$

Similarly, the total moment M about the center is

$$
M = \int_{-b}^{a} \sigma(x)\,x\,dx
\tag{4.20}
$$

Then the total distributed frictional force per unit length is

$$
\begin{aligned}
F_{im}' &= \frac{M}{R} = \frac{E_1 a^4}{8R^2 h}\left[1 - 2\left(\frac{b}{a}\right)^2 + \left(\frac{b}{a}\right)^4\right] + \frac{E_1 a^4 k}{R^2 h} \\
&\quad \left[k^3 - \frac{k}{2}\left(1 + \left(\frac{b}{a}\right)^2\right) + \frac{1}{3}\left(1 + \left(\frac{b}{a}\right)^3\right) - k(1+k)\left(k + \frac{b}{a}\right)e^{\frac{-1}{k}\left(\frac{a+b}{a}\right)}\right]
\end{aligned}
\tag{4.21}
$$

Calculation result in Equation 4.21 normally underestimates the indentation resistances. As Lodewijks (1995) indicates, May et al. (1959) only considered the normal stress in the material, and ignored the shear stresses between adjacent rubber materials, as well as the inertia of the material. To improve the accuracy of the indentation resistance model, Lodewijks (1995) proposes a correction factor derived from Hunter (1961):

$$
f_s = \frac{f_{ih}^*}{f_{im}^*}
\tag{4.22}
$$

where

> f_s the correction factor defined by Lodewijks (1995)

> f_{ih}^* the indentation resistance factors derived from the Hunter (1961)

> f_{im}^* the indentation resistance factors derived from the modified May et al. (1959) model

The calculations of these two indentation resistance factors f_{ih}^* and f_{im}^* are detailed in (Lodewijks, 1995), and the improved estimation is given by

$$F_i' = f_s F_{im}'$$ (4.23)

As suggested by Limberg (1988), the indentation rolling resistance could be written as a function of the vertical force and the conveyor speed. Hereby, the indentation resistance can be presented by

$$F_i' = \bar{f}\left(F_v', v\right)$$ (4.24)

where $\bar{f}$ is the function. It is important to note that the result in Equation 4.23 stands for the indentation resistance for unit belt width. To approximate the indentation resistances of a belt over an idler station, it requires to consider the normal force distribution over idler stations. If it is assumed that the normal force at a distance x in width to one of belt edges is $F_v'(x)$, then the total indentation resistance over the idler station can be calculated by

$$F_i = \int_0^B F_i'(x) = \int_0^B \bar{f}\left(F_v'(x), v\right)$$ (4.25)

In the case of through belt convectors, Spaans (1991) hypothesizes that with respect to the weight of bulk material, the surface pressure on the center roll is evenly distributed and that the surface pressure on the covered wing roll section will increase linearly. To calculate the normal forces acting on the side idler roll of a three-roll idler set, Krause and Hettler (1974) applies a modified version of Coulomb's earth pressure theory. Krause and Hettler (1974) further suggests that in the coming part of the belt approaching an idler, there is a passive state of stress in the bulk material. After traveling over the idler, the belt is opening and the stress in the material is in an active state. Then taking both the active and passive stress states into account, Krause and Hettler (1974) approximates the normal force on the wing roll by

$$F_{Nw} = \frac{1}{4}l\rho_s g l_1^2 \left(K_a + K_p\right) cos\phi_w$$ (4.26)

where

    ρ_s density of solid material, kg/m^3

    l the space of adjacent idler stations, m

    l_1 width of the belt section on the wing roll, covered by bulk solid materials, m

    ϕ_w wall friction angle between the belt and the bulk material

    K_a the active pressure factor derived from Krause and Hettler (1974)

    K_p the passive pressure factor derived from Krause and Hettler (1974)

On the basis of the Coulomb's earth pressure theory, Krause and Hettler (1974) gives the values of pressure factors by

$$K_a = \left[\frac{sin(\lambda + \phi_i)}{\sqrt{sin(\lambda - \phi_w)} + \sqrt{\frac{sin(\phi_i + \phi_w)sin(\phi_i - \beta)}{sin(\lambda + \beta)}}} \right]^2 \quad (4.27)$$

$$K_p = \left[\frac{sin(\lambda - \phi_i)}{\sqrt{sin(\lambda + \phi_w)} + \sqrt{\frac{sin(\phi_i + \phi_w)sin(\phi_i + \beta)}{sin(\lambda + \beta)}}} \right]^2 \quad (4.28)$$

where

λ trough angle of the wing roll

ϕ_i angle of internal friction of bulk solid material

β angle of repose of bulk solid material

Then taking the total masses of solid materials exerted on a idler set into account, the normal force on the center roll due to the bulk solid is

$$F_{Nc} = m'_{bulk}gl - \frac{1}{2}\rho_s gal_1^2 \left[K_a cos(\lambda - \phi_w) + K_p cos(\lambda + \phi_w) \right] \quad (4.29)$$

Taking both the belt and load weight into account, Figure 4.5 illustrates the surface pressure onto conveyor belt at the carrying side. Diagram in Figure 4.5a virtually divides the belt into five sections: two uncovered wing sections (A1 and A5), two covered wing sections (A2 and A4), and one center section (A3). As the diagram in Figure 4.5b shows, the normal forces distributed on wing rolls at sections A1 and A5 are even. The normal force per width unit on these two sections is:

$$F_v'(x) = \rho_b l d_b g cos\lambda \quad 0 \le x \le B_1 \ or \ B_4 \le x \le B_5 \quad (4.30)$$

where

ρ_b the belt density, kg/m^3

d_b the belt thickness, m

x the distance in the width direction to the left belt wedge in Figure 4.5b, m

If it is assumed that the normal force along covered wing section increases linearly, then the normal force on area A2 per width unit is

$$F_v'(x) = \frac{2(x - B_1)F_{Nw}}{B_{A2}} + \rho_b l d_b g cos\lambda \quad B_1 \le x \le B_2 \quad (4.31)$$

As the forces on two wing rolls are symmetric, the normal force on area A4 per width unit can be calculated by

$$F_v'(x) = \frac{2(B_4 - x)F_{Nw}}{B_{A4}} + \rho_b l d_b g cos\lambda \quad B_3 \le x \le B_4 \quad (4.32)$$
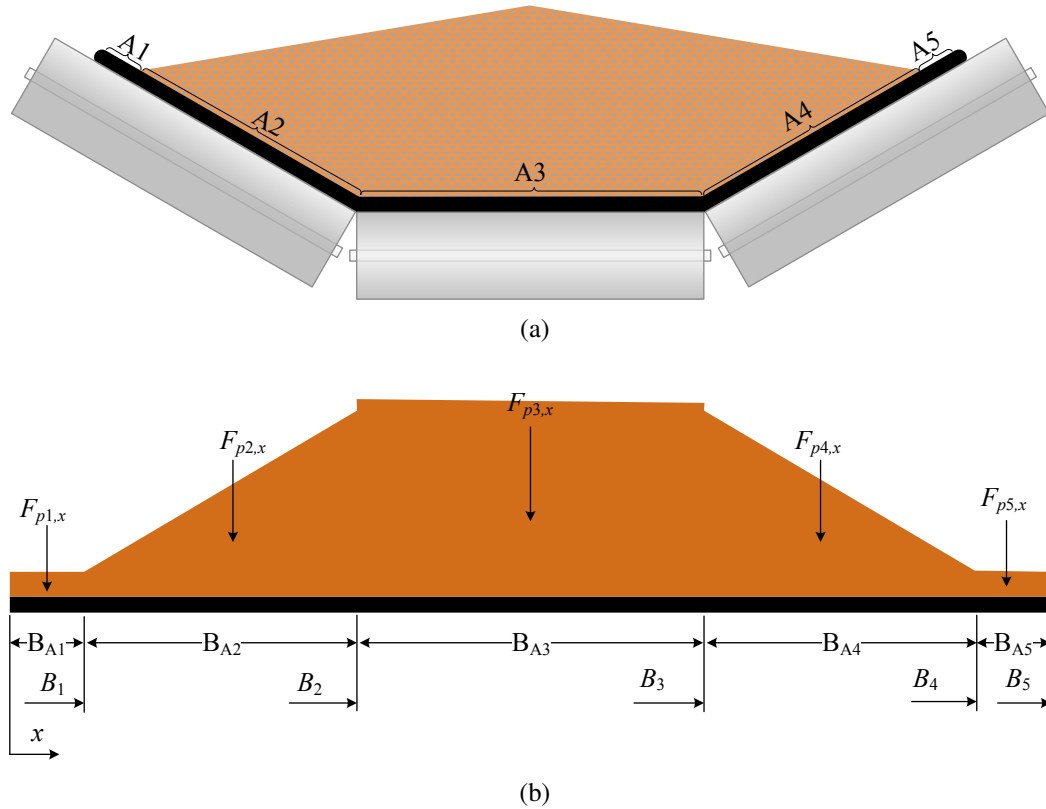
Figure 4.5: Surface pressure on a conveyor belt with respect to the weight of bulk solid material and the weight of the belt. (a) Dividing a belt into five sections. (b) Surface pressure distribution. B_1-B_5, the distance to the left belt wedge. B_{A1}-B_{A5}, the width of individual belt section.

The surface pressure on the center roll is assumed to be uniform, and then the normal force on the center roll per width unit is

$$F_v'(x) = \frac{F_{Nc}}{B_{A3}} + \rho_b l d_b g \quad B_2 \leq x \leq B_3 \tag{4.33}$$

Then the Combination of Equations 4.30 to 4.33 gives the weight distribution of belt and the bulk:

$$F_v'(x) = \begin{cases} \rho_b l d_b g cos\lambda & 0 \leq x \leq B_1 \\ \frac{2(x-B_1)F_{Nw}}{B_{A2}} + \rho_b l d_b g cos\lambda & B_1 \leq x \leq B_2 \\ \frac{F_{Nc}}{B_{A3}} + \rho_b l d_b g & B_2 \leq x \leq B_3 \\ \frac{2(B_4-x)F_{Nw}}{B_{A4}} + \rho_b l d_b g cos\lambda & B_3 \leq x \leq B_4 \\ \rho_b l d_b g cos\lambda & B_4 \leq x \leq B_5 \end{cases} \tag{4.34}$$

Finally, the substitution of Equation 4.34 into Equation 4.25 gives the belt indentation resistance over a three-roll idler station.

4.3.2   Flexural resistances of belt

The modeling of the flexural resistance of belt is based on the calibrated model of Spaans (1991).

As Spaans (1991) suggested, flexural resistances of belt are caused by the hysteresis losses of belt under cyclic bendings. Spaans (1991) further suggests that the coefficient of energy loss due to the belt flexure can be approximated by:

$$\Psi_b = \Delta M / M \tag{4.35}$$

where

Ψ_b energy loss factor due to indentation

M moment, Nm

ΔM loss of moment , Nm
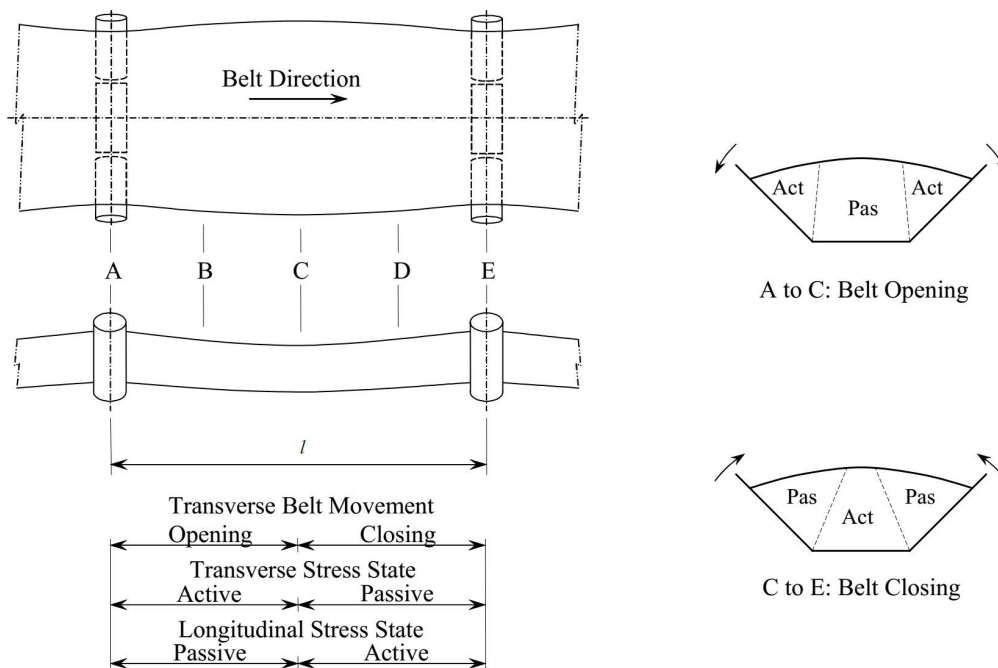
Figure 4.6: Transverse and longitudinal stress states. Courtesy of Wheeler (2003).

Considering a piece of belt supported by two rolls, see Figure 4.6. It is assumed that the conveyor belt is evenly loaded and that the load distribution is q with N/m. It is further assumed that there are two bending curves: one whose center of curvature is at the one directly above the roll, and another one whose center of curvature is at the point of maximum sag. Then according to Spaans (1991), the radius of curvatures can be calculated by:

$$\frac{1}{R_1} = \frac{F_v}{2\omega E_I} - \frac{q}{T} \tag{4.36}$$

$$\frac{1}{R_2} = \frac{-q}{T} \tag{4.37}$$

where

R_1 the radius of curvature over the idler roll, m

R_2 the radius of curvature at the point of maximum sag, m

F_v the vertical force due to the weight of the belt and bulk solid refereed to an idler station, N

E_I the flexural rigidity of the belt, Nm^2

q the homogeneous load distribution with respect to the total of the belt and the bulk material, N/m

T the belt tension, N

ω a factor defined by $\omega = \sqrt{T/E_I}$

In (Spaans, 1991), the bending moments are approximated by:

$$M_1 = \frac{E_I}{R_1} \tag{4.38}$$

$$M_2 = \frac{E_I}{R_2} \tag{4.39}$$

M_1 the bending moments occurring within the belt at the point directly above the idler roll, Nm

M_2 the bending moments occurring within the belt at the point of maximum sag, Nm

Then the belt's flexural resistances can be calculated by:

$$F_{fb} = \Psi_b \left(\frac{M_1}{R_1} + \frac{M_2}{R_2} \right) = \Psi_b E_I \left(\frac{1}{R_1^2 + R_2^2} \right)$$

$$= \Psi_b E_I \left[\left(\frac{F_v}{2\omega E_I} - \frac{q}{T} \right)^2 + \left(\frac{-q}{T} \right)^2 \right] \tag{4.40}$$

Spaans (1991) further suggests that, if the conveyor belt is with high tension, Equation 4.40 can be further reduced to

$$F_{fb} = \frac{\Psi_b F_v^2}{4T} \tag{4.41}$$

4.3.3   Flexural resistances of solid materials

The modeling of flxural resistances of bulk solid material is based on the calibrated model of Spaans (1991).

Due to the internal friction of the bulk solid and friction at the belt and bulk solid interface, the flexural resistance of the bulk solid material occurs as a consequence of the belt sag. Spaans (1991) provides an analytical model for calculating the flexural resistance of the bulk solid material due to the longitudinal deformation. As suggested by Spaans (1991), the coefficient of energy loss is a result of the difference between the passive and active stress state when the volume flow deforms. Spaans (1991) further suggests, if the deformation of the belt is slight, the flexural resistance of the bulk solid material over spacing l can be estimated by

$$F_{fs,l} = \frac{F_{vs}F_v}{\sqrt{TE_I}}\left(K_{pv}-K_{av}\right)\frac{d^2}{12l}e^{-\omega\chi} \tag{4.42}$$

where

$F_{fs,l}$ flexural resistance of bulk material due to longitudinal deformation

F_{vs} normal force due to the weight of the material, N

K_{av} active stress coefficient in a vertical plane

K_{pv} passive stress coefficient in a vertical plane

χ a horizontal distance from the smallest radius of curvature to the nearest idler, m. The magnitude of the distance depends on the size of trough angle, the belt width, the belt tension and the modulus of elasticity of the carcass.

On the basis of Coulomb's earth pressure theory, the stress coefficients in a vertical plane are calculated by:

$$K_{av} \quad = \quad \frac{1-sin\phi_i}{1+sin\phi_i} \tag{4.43}$$

$$K_{pv} \quad = \quad \frac{1+sin\phi_i}{1-sin\phi_i} \tag{4.44}$$

Equation 4.42 can be reduced to

$$F_{fs,l} = \frac{F_{vs}F_v}{\sqrt{TE_I}}\frac{4sin\phi_i}{cos^2_{\phi_i}}\frac{d^2}{12l}e^{-\omega\chi} \tag{4.45}$$

Figure 4.7 illustrates the transverse volume deformation of the bulk material. When the through belt opens under the gravity action, the relax of bulk solid forms an active stress state transversely. Reversely, the closing of the through belt generates a passive stress state. The transformation of the stress states also can be found in Figure 4.6. The opening and closing action occurs over individual half of the idler spacing. It is further assumed that the trough
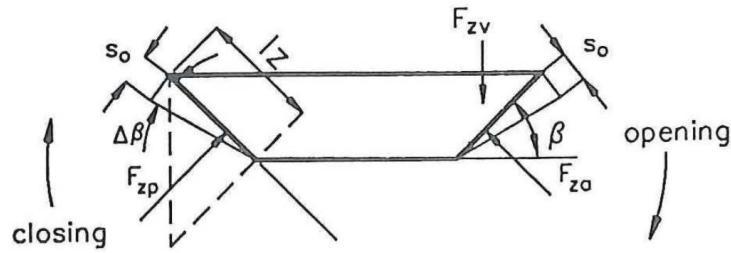
Figure 4.7: Model of the opening and closing of the trough shape. Courtesy of Spaans (1991).

sides turn over an angle $\Delta\beta$ when the trough shape opens and closes. Then taking the transverse deformation of the trough shape into account, Spaans (1991) provides an analytical model for approximating flexural resistance $F_{fs,t}$ of bulk solid material due to the transverse deformation:

$$F_{fs,t} = \frac{1}{6}\Delta\beta\rho_s g B_{A2}^3 \left(K_p - K_a\right)cos\phi_w \tag{4.46}$$

However, as Spaans (1991) further suggests, the flexural resistance caused by the opening and closing of the belt is considerably small, compared to the flexural resistance due to the lengthwise deformation of the volume flow. Therefore, it is eligible to ignore the influence of the transverse deformation in the final calculation of the flexural resistance of bulk solid. Accordingly, the final flexural resistance F_{fs} of bulk solid material can be approximated by

$$F_{fs} \approx F_{fs,l} \tag{4.47}$$

4.3.4   Rotating resistances of rollers

The modeling of the rotating resistances of rollers is based on the calibrated models of Lodewijks (1995), Wheeler (2003, 2016) and SKF (2016).
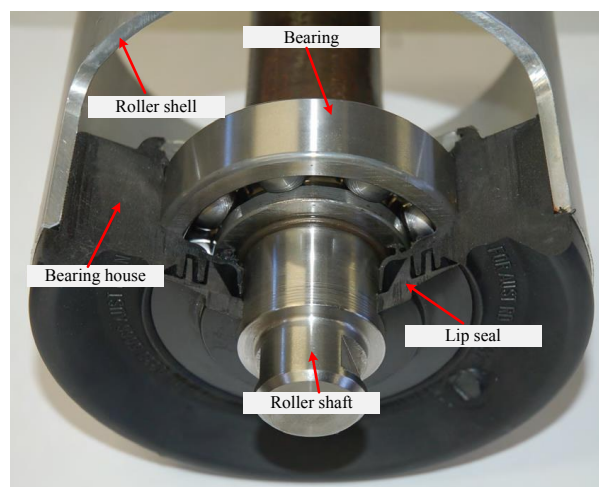
Figure 4.8: Roller construction. Courtesy of JLV Industries Pty Ltd (2009).

Figure 4.8 illustrates the major components of a typical roller. A bearing house is amounted

at each side of the tubing shell. A bearing is assembled into the bearing house to connect a shaft. The bearing house is covered by lip seals to protect the bearing from environmental pollutants and to keep the bearing house clean. The bearing unit typically is composed of rolling components, lubricant and seals. When the idler rolls are rotating, the rolling elements in the bearings cause frictional resistances. Meanwhile, the grease results in energy losses due to the viscous drag of the lubricant. In addition, the relative rotation between lip seals and the bearing house causes energy losses. According to the definition in SKF (2016), the rotating resistances F_r of idler rolls can be approximated by

$$F_r = 2\frac{M_0 + M_1 + M_s}{R} \qquad (4.48)$$

where M_0, M_1, M_s are the friction moments due to the viscous drag of the lubricant, the rolling elements of the bearing and the contact lip seal, respectively.

Lubricants are substances that help to reduce the friction of bearings and to allow smooth movement. In the case of a grease lubricated bearing, the lubricant frictional moment M_0 occurs due to the lubricant's viscosity property. The lubricant frictional moment is independent of the vertical load but is a function of speed. Moreover, the operating viscosity of the lubricant considerably affects the frictional moment M_0. In addition, the mean bearing diameter and the width of the rolling contact areas also have an effect on M_0. In accordance with the experimental results, Lodewijks (1995) and Wheeler (2003) approximate the load-independent moment M_0 by

$$M_0 = 10^{-1} f_0 (\nu n)^{2/3} d_{be}^3 \qquad (4.49)$$

where

f_0 a factor depending on the bearing type and lubrication, in the case of single row deep groove ball bearings, $f_0 = 1.5 - 2.0$

ν the viscosity of lubrication oil, $m^2 s$

n the number of rotations per second, s^{-1}

d_{be} the average bearing diameter, m

The load-dependent friction moment M_1 is caused by the sliding resistance and the hysteresis resistance of the bearing elements. Besides the exerted force, the frictional moment M_1 also depends on the bearing type and the bearing's mean diameter:

$$M_1 = f_1 P_1 d_{be} \qquad (4.50)$$

where

f_1 a load-dependent friction factor

P_1 a decisive load for frictional torque, N

Wheeler (2016) indicates that the axial load is considered negligible during operating conditions in the case of general idler rolls. Therefore the load P_1 determining the friction moment can virtually equal the radial load F_r on the bearing. In addition, Wheeler (2016) suggests that the load-dependent friction factor f_1 is considerably varied by the types of bearings. In the case of 62 series deep groove ball bearings, the factor is given by

$$f_1 = 0.0008 \left(\frac{P_0}{C_0} \right)^{0.55} \tag{4.51}$$

while for 63 series deep groove ball bearings

$$f_1 = 0.0009 \left(\frac{P_0}{C_0} \right)^{0.55} \tag{4.52}$$

where C_0 is the static load rating of the bearing given by the bearing manufacturer, and P_0 is the equivalent static bearing load given by

$$P_0 = X_0 F_r \tag{4.53}$$

where X_0 is the radial factor depending on the bearing design. In the case of sing row deep grove ball bearings, $X_0 = 0.6$.

Seals are used to to retain the lubricant in the bearing, and to form the closure of bearings to prevent contaminants from reaching the critical surface inside the bearing. Wheeler (2003) defines these seals as inner seals. Wheeler (2003) further indicates that, the design of the inner lip seal (if present) varies significantly between manufacturers. Different to inner seals, the outer lip seals are used to form the primary boundary of the bearing house to prevent the eternal contaminants. Wheeler (2003) indicates that the outer lip seals are typically fixed to the shaft, and that the frictional moment of lip seals for idler is approached by

$$M_s = \frac{0.15 e^{25 d_{1s}}}{2 \pi R^2} \tag{4.54}$$

where d_{1s} is the contact diameter of lip seals in m. If grease filled labyrinth seals are required to crucially prevent the dust and water into the rolling elements of the bearing, the viscous drag of the grease generates extra frictional moments. The calculation of the frictional moments of labyrinth seals can be found in (Wheeler, 2003, 2016).

This section has discussed the analytical calculations of the individual resistances along the conveying route. All these calculations are based on the calibrated models from literature. To show how the f factor value is achieved by the analytical approach, a fictive long horizontal belt conveyor will be studied in the next section. The impact of different loads and speeds on the f factor value also will be discussed.

Table 4.3: Parameters of the studied belt conveyor.

Parameter description	Value	Parameter description	Value
Conveyor parameters		Diameter of carrying rolls (D_c in m)	0.133
Conveying capacity (Q_{nom} in $MTPH$)	2000	Diameter of return rolls (D_r in m)	0.108
Nominal speed (v in m/s)	5	Roll mass per length unit (m'_{roll} in kg/m)	27.1
Conveying length (L in m)	1000	Internal diameter of bearing (D_{in} in m)	0.025
Gradient angle (δ in °)	0	External diameter of bearing (D_{ex} in m)	0.062
Belt paramters		Trough angle of idler station (λ in °)	30
Belt thickness in (d_b in m)	0.0135	Lubricant factor ($1.5 \cdot 10^4 f_0 v^{2/3}$ in $Nm^{-2}s^{2/3}$)	40
Rubber thickness of bottom cover (h in m)	0.004	**Solid material parameters**	
Desity of belt (ρ_b in kg/m^3)	1420	Density of the bulk material (ρ_b in kg/m^3)	750
Young's modulus (E_1 in N/m^2)	$5.6 \cdot 10^6$	Internal friction angle of material (φ_i in °)	32
Young's modulus (E_2 in N/m^2)	$6.0 \cdot 10^6$	Wall friction angle between belt and material (φ_w in °)	15
Damping coefficient (η in Ns/m^2)	1500	Angle of repose of material (β in °)	15
Belt width (B in m)	1.2	**Other parameters**	
Damping factor of energy loss due to indentation (Ψ_i)	0.5	Diameter of drive pulley (D_p in m)	1
Damping factor of energy loss due to bending (Ψ_b)	0.6	Friction coefficient between solid material and lateral chutes (μ_2)	0.6
Flexure rigidity of the belt (E_I in N/m^2)	20	Friction coefficient between belt and belt cleaner (μ_4)	0.6
Belt mass per length unit (m'_{belt} in kg/m)	23	Vertical force on belt due to cleaner ($p_{Gr}A_{Gr}$ in N)	105.6
Idler station parameters		Length of skirt boards outside feeder station (l_b in m)	4.5
Spacing of carrying idler stations (l_c in m)	1.2	Interval of the skirt boards (d in m)	0.8
Spacing of return idler stations (l_r in m)	3	Pre-tension right after the drive pulley (T_2 in kN)	30

4.4   Case study of the f factor calculation

4.4.1   Setup

This section performs simulation experiments to show the analytical calculation of the f factor value. A long horizontal belt conveyor is studied. Table 4.3 lists the parameters of the concerned conveyor. To simplify the experiments, it is assumed that

- At the carrying side, the conveyor belt is supported by three-roll idler sets with the same trough angle. The idler sets are evenly distributed along the conveying route. The conveyor belt is visually divided into L/l_c pieces where l_c is the idler spacing of the carrying side. The three-roll idler station is in the lengthwise middle of the belt piece.

- At the return side, the conveyor belt is supported by one-roll idler sets and these sets are with constant pitch. The conveyor belt is evenly divided into L/l_r pieces where l_r is the idler spacing of the return side. The one-roll idler station is in the lengthwise middle of the belt piece.

The case will be studied in which the belt conveyor is running at nominal speed with nominal loading rate. Due to the fact that the belt tension has a significant impact on the flexural resistances, the secondary resistances at the tail pulley are taken into account to improve the accuracy of the calculation. The separate calculations of the individual secondary resistances are detailed in DIN 22101 (German Institute for Standardization, 2015).The next section gives the computational results.

4.4.2   Experimental results

4.4.2.1   Belt indentation resistances

The calculation results of the belt indentation resistances are illustrated in Table 4.4. As the data shows, at the return side where the belt is empty, the belt indentation resistances over an idler station is 4.87 N. Taking all the idler stations of the return side into account, the total belt indentation resistances are 1.62 kN. At the carrying side, due to the weight of belt and bulk, it requires 13.88 N to overcome the indentation resistances on a three-roller idler set. The total indentation resistances of the carrying side are more than 11 kN. Totally, the belt indentation resistances over the whole conveyor are 13.25 kN.

Table 4.4: Belt indentation resistances

	Parameter	Value	Unit
Return side	Indentation resistance on an one-roller idler station	4.87	N
	Total belt indentation resistances of the return side	1.62	kN
Carrying side	Indentation resistances at a three-rollers idler station	13.88	N
	Total indentation resistances of the carrying side	11.63	kN
Total ($\sum F_I$)		13.25	kN

4.4.2.2   Flexural resistances

The flexural resistances includes two parts: the bending losses of the belt and of the bulk solid material. Equation 4.41 suggests that the belt flexural resistances are dependent on the load and the belt tension. However, due to the fact that the tension difference along the return side is limited, the difference of belt flexural resistance at the return side is small, see Table 4.5. Differently, the belt tension of the carrying side increases considerably from the tail to the head of the conveyor. Therefore, as the data in Table 4.5 indicates, the belt flexural resistances at the carrying side are quite different. As the data in Table 4.5 further shows, the total flexural resistances of belt are around 6.8 kN taking the belt of both the return and carrying sides into account.

Table 4.5: Flexural resistances of belt

Parameter		Value	Unit
(Belt tension right after the drive pulley)		30	kN
(Belt tension right before the tail pulley)		34	kN
Flexural resistance between neighboring stations of the return side	minimum	2.02	N
	maximum	2.29	N
Total of the return side		0.71	kN
(Belt tension right after the tail pulley)		37	kN
(Belt tension right before the drive pulley)		67	kN
Flexural resistance between neighboring stations of the carrying side	minimum	5.60	N
	maximum	10.10	N
Total of the carrying side		6.10	kN
Total ($\sum F_{fb}$)		6.81	kN

Table 4.6 illustrates the flexural resistances of the bulk solid material. These resistances only exist at the carrying side. From the tail to the head of the conveyor, the load flexural resistance reduces along the conveying route caused by the increase of the belt tension. As the data in Table 4.6 indicates, the maximum of the load's flexural resistance between neighboring idler stations can be over 11 N but the minimum is lower to below 7 N. Taking the load distributed along the whole carrying side into account, the data of Table 4.6 further shows the load's total flexural resistances, 7.21 kN .

Table 4.6: Flexural resistances of the bulk solid material

Parameter		Value	Unit
(Belt tension right after the tail pulley)		37	kN
(Belt tension right before the drive pulley)		67	kN
Fexural resistance between neighboring stations of the carrying side, F_{fs}	minimum	6.96	N
	maximum	11.17	N
Total ($\sum F_{fs}$)		7.21	kN

Table 4.7: Rotating resistance of idler rolls.

Parameter			Value	Unit
Return side	bottom roll	lubricant friction	0.73	N
		bearing rolling friction	0.11	N
		lip seal friction	1.65	N
		total of the bottom roll	2.50	N
	total of the one-roll idler stations		0.83	kN
Carrying side	wing roll	lubricant friction	0.52	N
		bearing rolling friction	0.03	N
		lip seal friction	1.34	N
		total of the wing roll	1.89	N
	center roll	lubricant friction	0.52	N
		bearing rolling friction	0.16	N
		lip seal friction	1.34	N
		total of the center roll	2.02	N
	total of a three-roll idler station		5.80	N
	total of carrying side		4.83	kN
Total ($\sum F_r$)			5.66	kN

4.4.2.3 Rotation resistances

Due to the fact that the belt pre-tension is large, the belt sag has a limited impact on the rotation resistances of idlers. Therefore, it is eligible to study one three-roll idler station of the carrying side and one one-roll idler station of the return side, instead of the whole idler stations. Table 4.7 illustrates the individual resistances of the rollers, including the lubricant friction, the bearing rolling friction and the lip seal friction. At the return side, the total rotation resistance of the roller is 2.50 N where the lip seal friction occupies up to 1.65 N. Therefore, the lip seal frictions make a major contribution to the rotating resistances of rollers of the return side. Similar phenomenon also occurs at the rollers of the carrying side. The idler station of the carrying side has three rollers, and the total rotation resistances of a three-roller station are 5.80 N, see Table 4.7. Taking all idler stations of the whole conveyor into account, the total rotating resistances of rollers are 5.66 kN.

4.4.2.4 Final Results

Taking all individual resistances into account, Table 4.8 illustrates the total of main resistances, near 33 kN. Accordingly, the value of the artificial friction coefficient f is calculated by using Equation 4.12. As the data in Table 4.8 shows, the value of the f factor in this case is 0.0187, which is in the range from 0.01 to 0.02 suggested by DIN 22101 (German Institute for Standardization, 2015).

Table 4.8: Total of main resistances in kN and the derived value of the f factor.

Parameter	Value	Unit
Total indentation resistances ($\sum F_I$)	13.25	kN
Total flexural resistances of belt($\sum F_{fb}$)	6.81	kN
Total flexural resistances of bulk solid ($\sum F_{fs}$)	7.21	kN
Total rotation resistances of rollers($\sum F_r$)	5.66	kN
Total of main resistances (F_H)	32.93	kN
The DIN f factor	0.0187	

4.4.3 Further discussion

4.4.3.1 Different speeds and loads

The main resistances are dependent on the belt speed and the load on the conveyor. The experimental results in (Hiltermann, 2008; Hiltermann et al., 2011) show that the value of the f factor varies over different speeds and loads. To reduce belt conveyor power consumption, the conveyor speed is adjusted to the match the variable material flow. To analyze the power consumption and to evaluate the power savings by means of speed control, the DIN-based energy model will be used in the following chapters. In order to improve the accuracy of the calculation, variable values of the f factor are taken into account. Taking the same concerned belt conveyor for instance. If it is assumed that the minimal conveyor speed is 40% of the nominal speed, then Table 4.9 illustrates the derived values of the f factor for different filling levels and for different conveyor speeds. In Table 4.9, the filling ratio φ_f is the percentage comparison between the actual load and the nominal load on the belt. From the data in Table 4.9, it indicates that the f factor varies over loads and speeds. Moreover, it also clearly shows that when the conveyor speed is lowered while the loading rate keeps the same, the f factor normally has an increase. Taking the case where the loading rate is 50% of the nominal for instance. If the conveyor is running at nominal speed, the filling ratio is 50% and the f factor value is 0.0143. However, when the conveyor is running at optimum speed 2.5 m/s, the filling ratio is 100% and the f factor value increases to 0.0173, see Table 4.9.

4.4.3.2 Non-uniform distribution

In the above experiments, it is assumed that the bulk material on the belt is evenly distributed along the carrying side. However, in most practical cases, the material feeding rates are varying over time. Therefore, the lengthwise material distribution normally is non-uniform along the conveyor. In addition, because the relationship between the indentation resistance and the mass on the belt is non-linear, the value of the f factor varies with different material flow distributions.

The condition where the conveyor is non-uniform loaded is further studied. Taking the case where conveyor is running at nominal speed and the average filling ratio equals 50% for instance. A number of simulation experiments are performed. In the experiments, the conveyor is load by a random ratio along the conveying route but the average keeps around 50%. The

Table 4.9: The calculated values of the f factor for different speeds and for different loads.

V \ U	0	10%	20%	30%	40%	50%	60%	70%	80%	90%	100%
2	0.0122	0.0118	0.0116	0.0117	0.0119	0.0124	0.0129	0.0137	0.0146	0.0155	0.0166
2.25	0.0125	0.0120	0.0119	0.0120	0.0122	0.0127	0.0133	0.0140	0.0149	0.0159	0.0170
2.5	0.0127	0.0122	0.0121	0.0122	0.0125	0.0130	0.0136	0.0143	0.0152	0.0162	0.0173
2.75	0.0129	0.0124	0.0123	0.0125	0.0128	0.0132	0.0139	0.0146	0.0155	0.0165	0.0175
3	0.0130	0.0126	0.0125	0.0126	0.0130	0.0134	0.0141	0.0148	0.0157	0.0167	0.0178
3.25	0.0131	0.0127	0.0127	0.0128	0.0131	0.0136	0.0143	0.0150	0.0159	0.0169	0.0180
3.5	0.0132	0.0128	0.0128	0.0129	0.0133	0.0138	0.0144	0.0152	0.0161	0.0171	0.0182
3.75	0.0133	0.0129	0.0129	0.0130	0.0134	0.0139	0.0146	0.0153	0.0162	0.0172	0.0183
4	0.0134	0.0130	0.0130	0.0131	0.0135	0.0140	0.0147	0.0155	0.0164	0.0174	0.0184
4.25	0.0135	0.0131	0.0130	0.0132	0.0136	0.0141	0.0148	0.0155	0.0165	0.0175	0.0185
4.5	0.0135	0.0131	0.0131	0.0133	0.0136	0.0142	0.0148	0.0156	0.0165	0.0175	0.0186
4.75	0.0136	0.0132	0.0131	0.0133	0.0137	0.0142	0.0149	0.0157	0.0166	0.0176	0.0187
5	0.0136	0.0132	0.0132	0.0134	0.0137	0.0143	0.0149	0.0157	0.0166	0.0176	0.0187

experimental results are illustrate in Figure 4.9. The bubbles of the diagram represent the cal-
culated f factor values. As the diagram shows, the material distribution of a belt conveyor has
an influence to the f factor. The data in Figure 4.9 shows that the calculated f factor values
are in the range from 0.0133 to 0.0154. The black line of the diagram stands for the average of
the calculated f factor values. As it shows, the average f factor value is 0.0143, which exactly
matches the data of Table 4.9. Therefore, it is relatively accurate to use the data in Table 4.9 to
calculate the power consumption of the concerned belt conveyor.
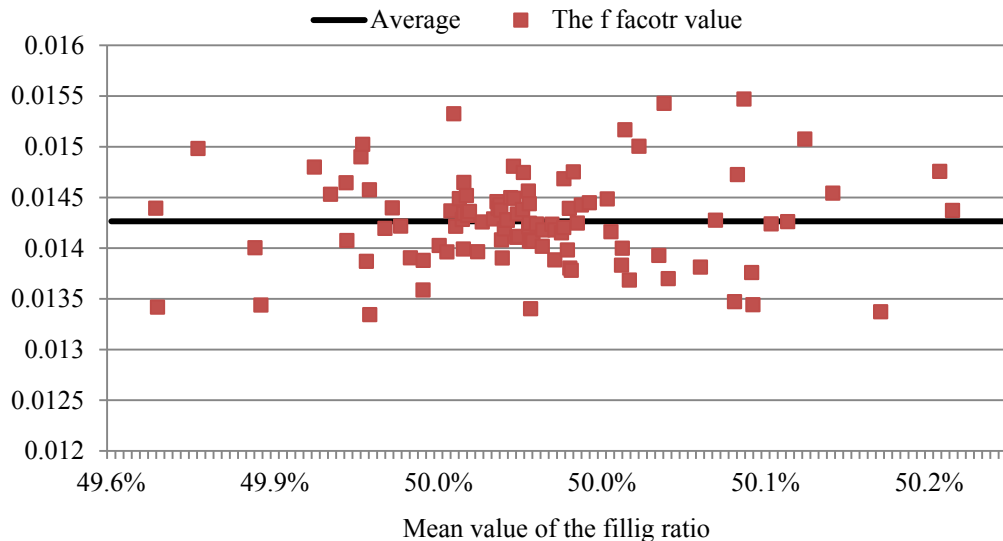
Figure 4.9: Derived values of the f factor in the cases of belt conveyors with non-uniform
material distribution.

4.5   Drive system efficiency

In Section 4.1, Equation 4.2 calculates the electric power consumption P_e of belt conveyors by
dividing the total mechanical power P_m exerted on the driving pulley with the driving system
efficiency η_{sys}. Sections 4.1 to 4.4 showed the mechanical power calculation by using the
DIN-based energy model. This section discusses the power losses along the drive system and
describes the system efficiency.
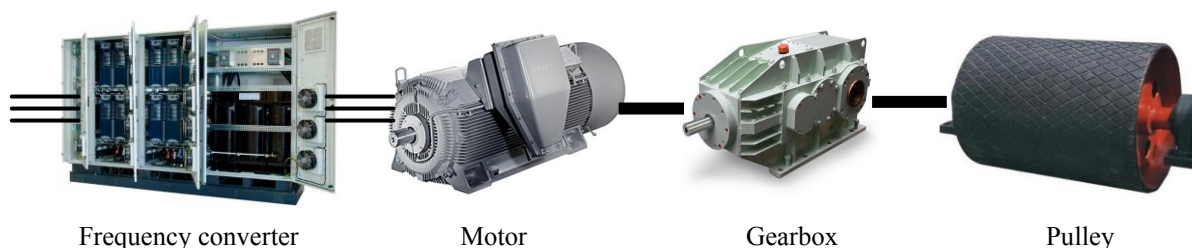
Figure 4.10: Drive system components. The pictures of the components are courtesy of the
Internet.

Figure 4.10 illustrates a typical modern drive system of belt conveyors. The drive pulley of a belt conveyor is driven through a gearbox by an electric motor. The motor is powered by a frequency converter, and the frequency converter can precisely control the speed and the torque of the motor. During the power conversion in the motor and the power transmission in the frequency converter and the gearbox, the driving units are not free of energy losses. In the cases of belt conveyors with a drive system as shown in Figure 4.10, the system efficiency η_{sys} can be calculated by

$$\eta_{sys} = \eta_{freq}\eta_{motor}\eta_{gear} \tag{4.55}$$

where

$\quad\eta_{freq}\quad$ the efficiency of the frequency converter

$\quad\eta_{motor}\quad$ the efficiency of the electric motor

$\quad\eta_{gear}\quad$ the efficiency of the gearbox

In the following of this section, the power losses and the efficiency of the driving units will be briefly discussed.

4.5.1 Frequency converter power losses
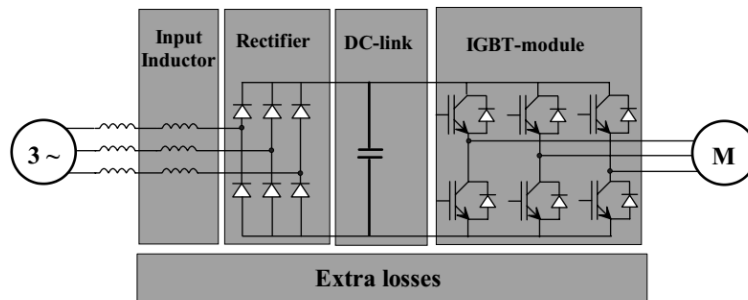
Figure 4.11: Source of the frequency converter losses. Courtesy of Aarniovuori et al. (2007).

Figure 4.11 illustrates the sources of the frequency converter losses. As the diagram shows, the losses in the frequency converters are built up from the input choke losses, the rectifier's conduction losses (diode rectifier), the direct current (DC) link losses, the switching losses of the transistors (the IGBT-module in Figure 4.11), and extra losses. The extra losses include the power consumption of the cooling fan and of the control system. The calculation of these individual energy losses can be found in (Aarniovuori et al., 2007) and (Tsoumas et al., 2014). Aarniovuori et al. (2007) further suggests that the transistors are the major source of the frequency converter losses. Taking all the losses in the converter into account, the efficiency of the converter can be calculated by

$$\eta_{freq} = \frac{P_{out}}{P_{in}} = \frac{P_{in} - \sum loss_{freq}}{P_{in}} \tag{4.56}$$

where

P_{in} the input power of a frequency converter, equalling electric power consumption P_e consumed by a belt conveyor

P_{out} the output power of a frequency converter

$\sum loss_{freq}$ total power loss of a frequency converter

4.5.2   Motor power losses

An electric motor is a machine that converts electric power into mechanical power (Dilshad et al., 2016). The motor input virtually equals the output power of the frequency converter, and it is always larger than the output mechanical power of the motor. The difference between the input electric power and the output mechanical power is the losses during energy transformation inside the machine. The literature, like (Boglietli et al., 2003) and (Kärkkäinen, 2015), subdivides the motor losses into four groups: copper losses, iron losses, mechanical losses and stray losses. Taking all these individual power losses into account, the motor efficiency can be approximated by

$$\eta_{motor} = \frac{P_{mech}}{P_{elec}} = \frac{P_{elec} - \sum loss_{motor}}{P_{elec}} \tag{4.57}$$

where

P_{mech} the output mechanical power provided by a motor

P_{elec} the input electric power of a motor, equal to the output power P_{out} of the frequency converter

$\sum loss_{freq}$ total power losses of a motor

4.5.3   Gearbox power losses

In most industrial applications, the gearbox provides gear reduction and torque increase, and then the output of the gearbox rotates slower but with a higher torque. Michaelis et al. (2011) suggests that the power losses in a gearbox consist of gear, bearing, seal and auxiliary losses (see Figure 4.12). The brief description of the bearing and seal losses can be found in Section 4.3.4. Similar to bearing losses, gear losses can be further separated into load-dependent losses and no-load losses. Fernandes et al. (2015) detail the power losses in gears. Then taking all individual resistances of the gearbox into account, the gearbox efficiency can be calculated by

$$\eta_{gear} = \frac{P_{mech,out}}{P_{mech,in}} = \frac{P_{mech,in} - \sum loss_{gear}}{P_{mech,in}} \tag{4.58}$$

where

$P_{mech,out}$ the output mechanical power of the gearbox, equal to the total mechanical power P_m exerted on the drive pulley

$P_{mech,in}$ the input mechanical power of the gearbox, equal to the output mechanical power of the motor in Figure 4.10

$\sum loss_{gear}$ total power losses of the gearbox, equal to P_V in Figure 4.12
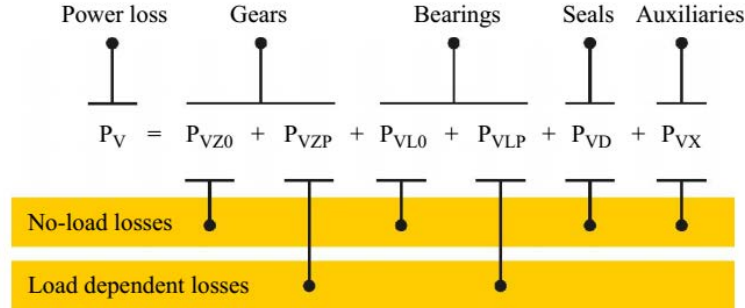
Figure 4.12: Composition of gearbox power loss. Courtesy of Michaelis et al. (2011).

4.5.4   Discussion: calculation of the drive system efficiency

Sections 4.5.1 to 4.5.3 briefly discussed the power losses of the driving units and the relative efficiency. However, the efficiency of the drive units is more used in practice to calculate the final electric power consumption. The efficiency of the driving units can be achieved by measurements or by consultancy from the drive unit component manufactures. If these driving units are connected in a series as shown in Figure 4.10, the final system efficiency can be derived from Equation 4.55.

In order to the simplify the calculation, Hiltermann et al. (2011) and Zhang and Xia (2011) assume that the efficiency of the drive system is constant. However, more experimental results show that the system efficiency is variable over different loads and speeds. Taking frequency converters, motors and gearboxes into account, ABB (2000) gives the efficiency of the whole system, see Table 4.10. Based on these data, an empirical model can be given that allows the calculation of the drive system efficiency as a function of the speed ans load ratios:

$$\eta_{sys}(\varphi_v, \varphi_T) = 0.7878 + 0.1953\varphi_v + 0.05067\varphi_T - 0.1147\varphi_v^2 + 0.048\varphi_v\varphi_T - 0.042267\varphi_T^2 \quad (4.59)$$

where φ_v and φ_T are the ratio of motor speed and torque, respectively.

Table 4.10: Efficiency of the whole drive system (including the frequency converter, the motor and the gearbox). Courtesy of ABB (2000).

Speed ratio φ_v Load ratio φ_τ	50%	75%	100%
50%	0.884	0.903	0.906
75%	0.887	0.911	0.920
100%	0.890	0.913	0.924

4.6   Conclusion

This chapter described the DIN-based energy model for calculating the power consumption of belt conveyors. The experimental results showed that the artificial frictional coefficient f was 0.0187 if the concerned belt conveyor was running at nominal speed with fully loaded. Further simulation results showed that the f factor varied considerably over loads and speeds. Moreover, the experimental data clearly showed that when the conveyor speed was lowered while the loading rate kept the same, the f factor had a noticeable increase. Overall, it is suggested to consider the variable value of the f factor to calculate the power consumption of a belt conveyor for different loads and for different speeds.

Based on the DIN-based energy model, the next chapter will describe the modeling of belt conveyor speed controllers. Both the active and passive speed strategies will be described .

Chapter 5

Modeling of speed control systems

As discussed in the previous chapters, researchers and engineers have already studied the belt conveyor speed control for many years. However, these studies mainly focus on the passive speed control and rarely investigate the active speed control. The performance of speed control can be assessed by field tests or computational simulations. However, field tests are considerably more expensive than computational simulations. Therefore, this chapter describes a simulation model of belt conveyor speed control systems for the purpose of analyzing the performance of speed control, both the active and passive speed control. Before discussing the modeling of speed controllers, this chapter firstly analyzes the applicability of speed control since not all belt conveyor systems can use speed control to reduce power consumption. Section 5.2 briefly introduces the scheme of the simulation model which includes two subsystem, the operational system and the control system. The modeling of the operational system is detailed in Section 5.3, including the process of verification. Section 5.4 discusses the control system and introduces several different control strategies. The passive and active control strategies are introduced individually. In addition, the active speed control strategy is further classified into two groups: the fixed time interval strategy and the variable time interval strategy. To assess the performance of speed control, Section 5.5 defines several key performance indicators (KPIs), including the belt conveyor utilization and the power consumption. Lastly, the conclusion of this chapter is given in Section 5.6.

5.1 Applicability of belt conveyor speed control

The academic review in Section 2.7 indicated that speed control can reduce the power consumption of belt conveyors. Section 2.6 also suggested that a speed control system requires at least a speed controller, a variable speed drive system and a material flow sensor. However, it is important to note that not all belt conveyor systems can use speed control for the purpose of energy savings, even though these systems are equipped with all above mentioned physical devices. Taking a belt conveyor system with a single conveyor for instance. The material feeding rate in a certain period must be predicted, either by acknowledging the upstream process of bulk solid handling system or by knowing the maximum feeding rate of the conveyor feeder. Otherwise, speed control can not be applied, even though the actual material flow onto the belt

can be detected in real time. Therefore, the applicability of speed control should be discussed before the modeling of belt conveyor speed controller.

The applicability of speed control on the belt conveyor system with a single belt conveyor has been discussed above. A general rule can be summarized as: the material feeding rate must be predictable. This rule also can be used on the belt conveyor system with multiple conveyors. Besides the method acknowledging the upstream handling process or the feeder feeding condition, the prediction can also be realized by measurement. In the cases of multiple belt conveyors in a series, a material flow sensor can be used to detect the material volume/mass flow of the upstream belt conveyor in real time. Then taking the speed of the upstream conveyor into account, the material feeding rate onto the downstream belt conveyor(s) can be predicted. Based on the information of the incoming material flow stream, the speed of the downstream belt conveyor(s) can be adjusted.

Additionally, the applicability of speed control is also constrained by the actual loading condition. Taking the belt conveyor system in different application sites into account, the loading scenarios can be categorized into four types and the applicability is analyzed as below:

- Scenario 1: constant loading degree in long term operations. In such a scenario, the bulk solid material is loaded onto the belt conveyor with a roughly constant flow during a long term operation. The material loading degree only changes when one operation is finished or restarted. Such a scenario can be found for instance at an open pit mine where a skilled operator operates an excavator to continuously load a belt conveyor. This scenario can be further categorized into two sub-scenarios as shown in Figure 5.1a. The solid line presents the condition in which the feeding rate nears the nominal conveying capacity. In these cases, the implementation of speed control will not help in achieving a considerable amount of power reduction, even though we take the active speed control into account where the conveyor speed can perfectly match the material flow. The costs of relevant sensors and the controller will be much higher as compared to savings that can be achieved in that specific condition. The dashed line in Figure 5.1a presents anther condition in which the feeding rate is considerably lower than the nominal conveying capacity. In such cases, the passive speed control is strongly suggested. The belt conveyor is running at a pre-defined non-nominal speed so that the conveyor is virtually fully loaded.

- Scenario 2: moderately varying loading degree in between long term operations. This scenario can be found at a dry bulk terminal where multiple cranes feed a belt conveyor. Each crane produces roughly the same mass flow onto the belt conveyor. In cases where not all cranes operate at the same time during different long term operations, the material loading degree to the same conveyor varies in between two operations. In such cases, the conveyor speed can be reduced to match the number of available cranes.

- Scenario 3: moderately varying loading degree in between short term operations. Compared to Scenario 2, some loading scenarios contain roughly constant material flow in between operations but the operations vary relatively on short term. For example, the material loading patterns of the conveyors in underground long wall mining follow such

scenario. In such cases, active speed control is suggested so that the conveyor speed can match the actual material loading rate.

- Scenario 4: excessively varying loading degree in all operations. In this scenario the feeding rate changes excessively. This scenario can be considered to be the completely random loading scenario. Although it can be a rare scenario where the nature of the feed flow is absolutely random, similar loading scenarios can be found in underground iron or copper mines. If the conveyor system has only a single belt conveyor, then the material feeding rate is totally unpredictable. In such cases, speed control is inapplicable for reducing the power consumption of the single belt conveyor. On the other hand, if the conveyor system has multi-conveyors, speed control potentially has the opportunities of energy savings of the downstream belt conveyor(s). However, the frequent speed adjustment may result in considerable stress cycles which may be harmful to the conveyor system and components. Therefore, in such loading scenarios, speed control is less applicable.
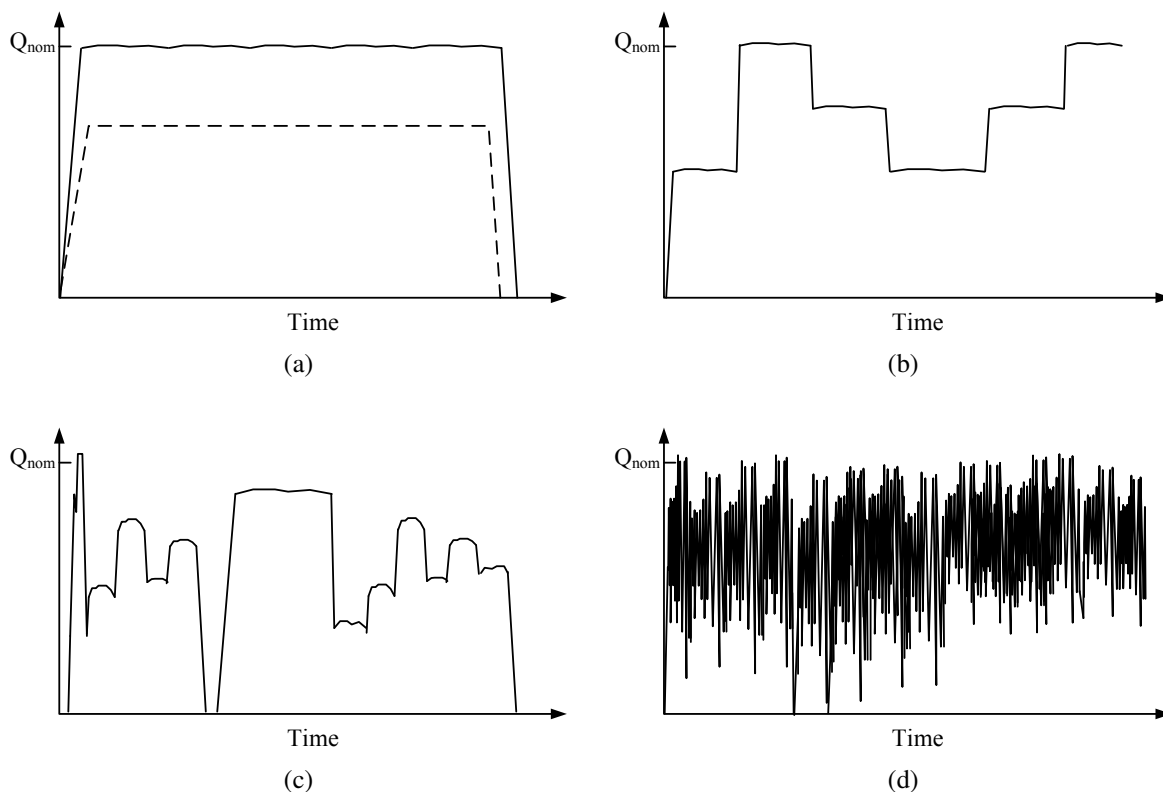

Figure 5.1: Types of material loading scenarios. (a) Scenario 1: constant loading degree in long term operations. (b) Scenario 2: moderately varying loading degree in between long term operations. (c) Scenario 3: moderately varying loading degree in between short term operations. (d) Scenario 4: excessively varying loading degree in all operations.

5.2 Simulation model of belt conveyor speed control systems

A belt conveyor system is a continuous transport system which continuously transports bulk solid materials through the conveying route. Based on the Delft Systems Approach (Veeke et al., 2008), the simulation model of belt conveyor speed control systems can be illustrated as a black box. Figure 5.2 illustrates the scheme of the simulation model which consists of two functional subsystems: the operational system and the control system.
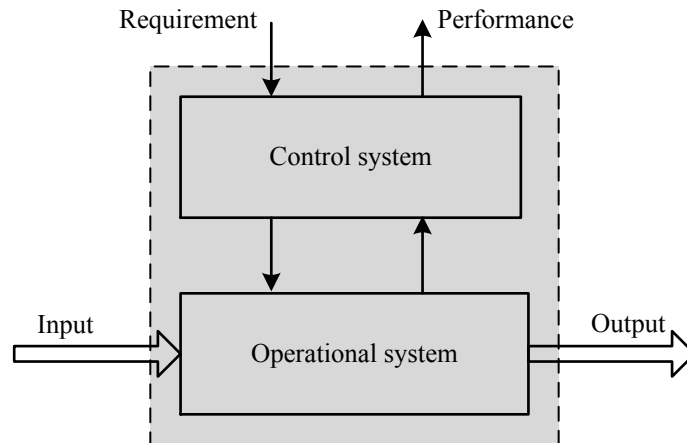
Figure 5.2: A belt conveyor system based on the Delft Systems Approach (Veeke et al., 2008).

The operational system transforms the input into the required output. In a belt conveyor speed control system, the input is the materials loaded onto the conveyor and the output is the materials discharged from the belt. Taking the activities of material into account, Section 5.3 details the modeling of the operational system.

The control system monitors the operational system and translates the requirements to the system into control actions to meet the objective. The objective of the belt conveyor speed control is to achieve maximum potential load which leads to energy savings. Section 5.4 describes the types of speed control and introduces relevant control strategies. The performance shows the outputs of the evaluation indicators. Several key performance indicators (KPIs) of speed control are defined in Section 5.5.

5.3 Modeling of operational system

Figure 5.3 illustrates the modeling of the operational system. It is assumed that the conveyor system has a number of belt conveyors connected in series. Then as the diagram in Figure 5.3a shows, the operational system is divided into several sub-operational systems. Each sub-operational system represents a belt conveyor. Figure 5.3b illustrates the modeling of the sub-operational system, taking the activity of bulk material into account. As the figure shows, the material activities mainly includes the process of being loading onto the conveyor, the process of being conveyed along the conveying route and the process of being discharged or unloaded from the conveyor. In addition, the activity of being transferred in the transfer chute should be

taken into account. In the following of this section, the modeling of bulk material activities are given individually.
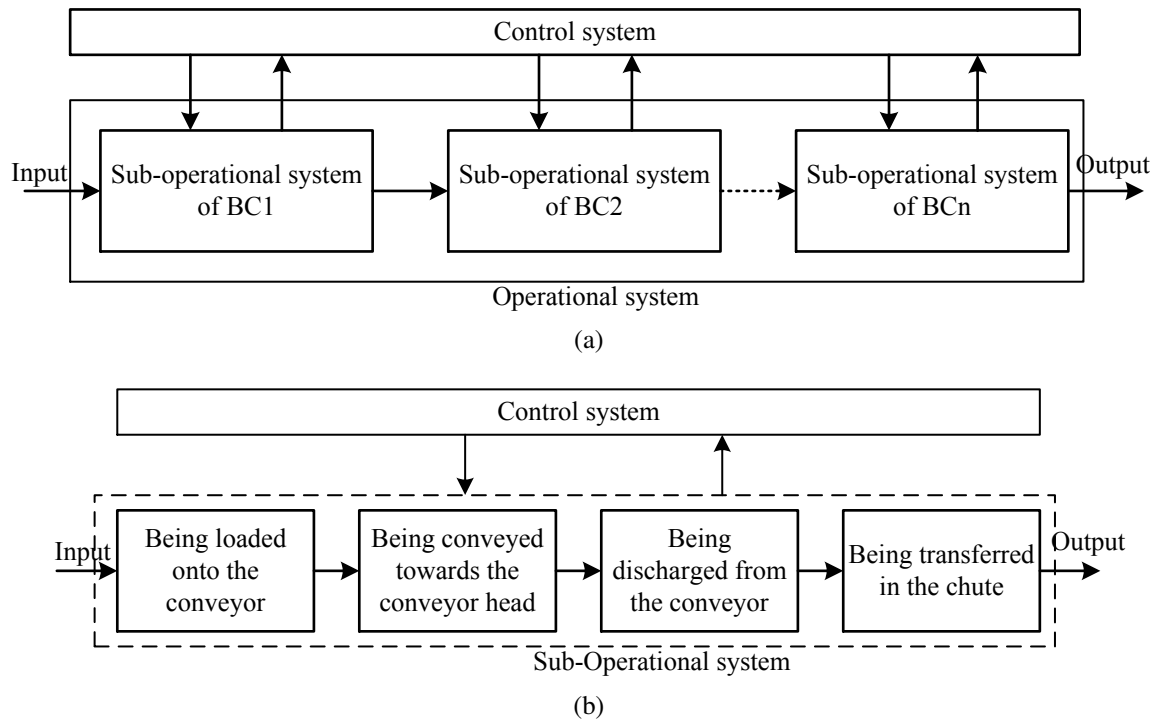
Figure 5.3: Modeling of the operational system. (a) Overview of the operational system. It is assumed that the belt conveyor system has *n* belt conveyors connected in series. (b) Sub-operational system of each belt conveyor.

5.3.1   Modeling of loading process

If a material flow sensor is installed nearby the loading area, the detected value of material flow rate can be viewed as the real material loading rate in the case of a long belt conveyor. Generally, the data acquisition of the sensor is discrete. If the time interval between adjacent detecting operations is small, it is acceptable to represent the continuous material loading activity by a discrete tool.

Figure 5.4 illustrates the discretization of a continuous material loading flow onto a belt conveyor. The diagram in Figure 5.4a shows the real system where the bulk material is continuously loaded. The height of the line represents the actual material loading rate of the conveyor. If it is assumed that the conveyor is running at a constant speed and that the sample time is constant, then the continuous material stream is evenly divided into a finite number of blocks as shown in Figure 5.4b.

The actual material loading rate can vary over time, while a discrete sample is a value at a specific point in time. Therefore, the real material flow rate between adjacent sampling points is unknown. This causes a discretization error whose value depends on the sample rate of the flow sensor. Figure 5.5 illustrates the discretization of the loading rate onto the belt with different cycle times. The comparison indicates that if the cycle time is small enough, the
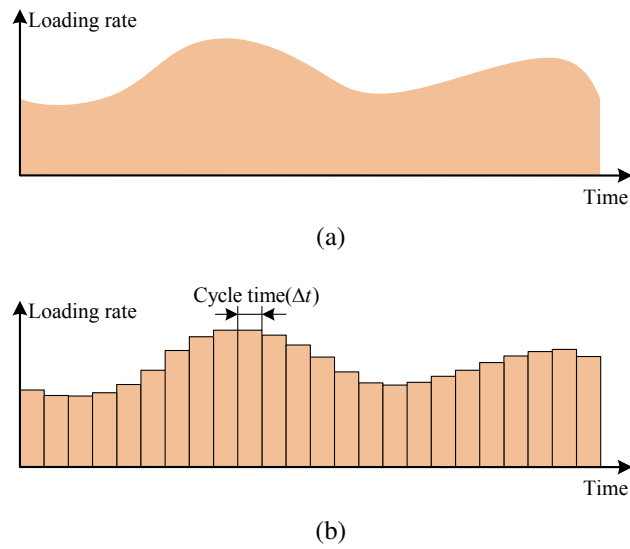
Figure 5.4: Discretization of a continuous material loading flow onto a belt conveyor. (a) Continuous representation of the material loading flow. (b) Discrete representation of the material loading flow.
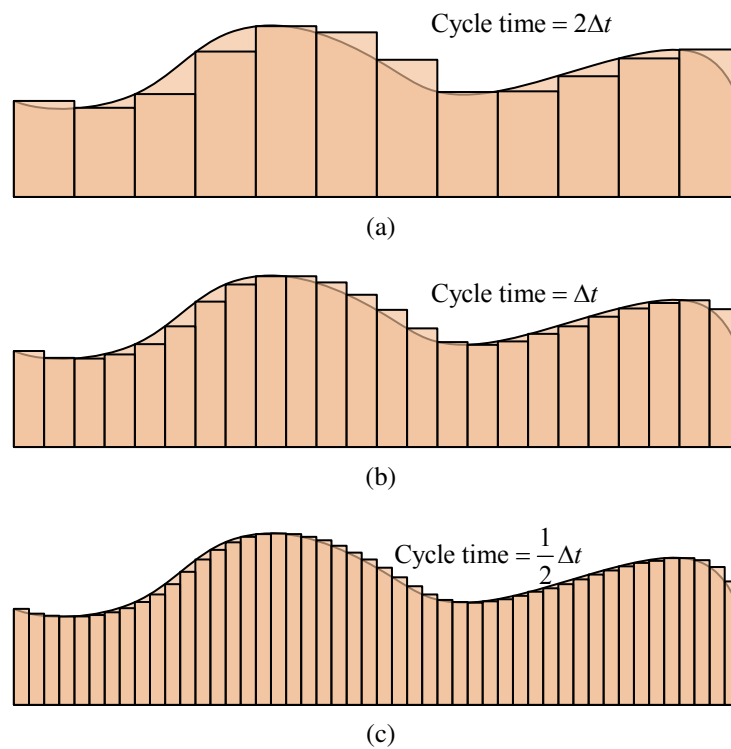
Figure 5.5: Comparison between the continuous and discrete representations. (a) Cycle time $=2\Delta t$. (b) Cycle time $=\Delta t$. (c) Cycle time $=\frac{1}{2}\Delta t$.

discrete representation will be very close to the real continuous system. However, it requires a lot of computational resources. Therefore, selecting a suitable cycle time is important to the modeling of the material loading flow.

5.3.2 Modeling of conveying process

Drive pulley(s) is continuously rotating to drive the belt conveyor. Due to the friction, it is assumed that bulk material is staying still on the belt so that the material is moving toward the head of the conveyor with the conveyor speed. Taking the black block in Figure 5.6 for instance. At the time point t_0, the distance between the mass block and the conveyor tail is $x(t_0)$, see Figure 5.6a. If it is assumed that the belt speed is $v(t_0)$ and then at the time point $t_1 = t_0 + \Delta t$, the traveling distance of the black block in Figure 5.6b can be approximated by

$$x(t_1) = x(t_0) + v(t_0)\Delta t \tag{5.1}$$

Generally, the belt conveyor system can be treated as a first-in-first-out buffer. Therefore, in terms of other mass blocks as shown in Figure 5.6, the conveying activity can be calculated separately.

5.3.3 Modeling of unloading process

It is assumed that the distance between the center lines of the head and the tail pulley is L. Once the total traveling distance of a block exceeds the conveyor length, the block is being discharged
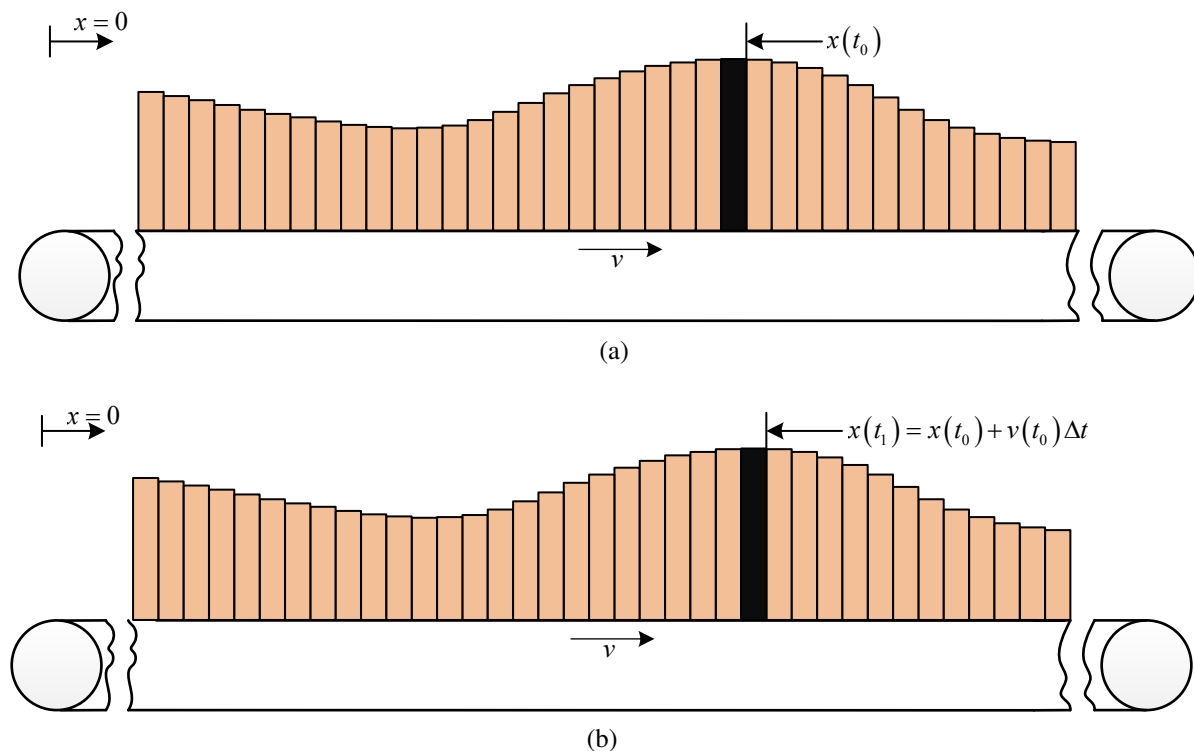
Figure 5.6: Modeling of conveying process. (a) At the time point t_0. (b) At the time point t_1.
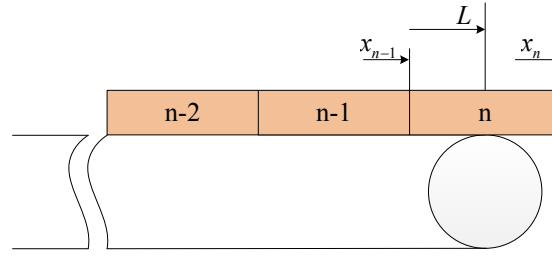
Figure 5.7: Modeling of unloading activity of mass block.

from the belt. If the traveling distance x_n of the nth block exceeds the conveying length L while the distance x_{n-1} of the $(n-1)^{th}$ block is less than L, the nth block is partially discharged from the concerned belt, see Figure 5.7. In such cases, the discharged mass $m_{block,n,dis}$ of the nth block is

$$m_{block,n,dis} = m_{block,n} \left(\frac{x_n - L}{x_n - x_{n-1}} \right) \tag{5.2}$$

and the mass of the nth block should be updated by

$$m_{block,n} = m_{block,n} \left(\frac{L - x_{n-1}}{x_n - x_{n-1}} \right) \tag{5.3}$$

5.3.4   Modeling of transferring process

After being discharged from the conveyor, the material enters into a discharge chute or a transfer chute. Herein, we only discuss the activity of material in the transfer chute. Since the dynamic analysis on behaviors of bulk materials is out of the research scope, we herein assume that the blocks filled by bulk materials move through the transfer chute in a series, see Figure 5.8a. Then the transfer chute also can be simplified as a first-in-first-out buffer, see 5.8b.

After being discharged from the transfer chute, the bulk material is loaded on the downstream conveyor. To reduce the power consumption of belt conveyors, the speed of the downstream conveyor is variable. It is assumed that the upstream conveyor is running at a constant speed v_1, that the original cross section of the block is A_1 and that the cover length is $L_{block,1}$. If it is further assumed that at the time point t_0, the speed of the downstream conveyor is $v_2(t_0)$, then at the loading area of the downstream conveyor, the concerned block is reshaped with the cross section A_2

$$A_2 = \frac{A_1 v_1}{v_2(t_0)} \tag{5.4}$$

5.3.5   Verification of the operational system model

To prove the simulation of the operational system model performs as intended, it is necessary to verify the outputs of the simulation model. The material flow stream on a single belt conveyor
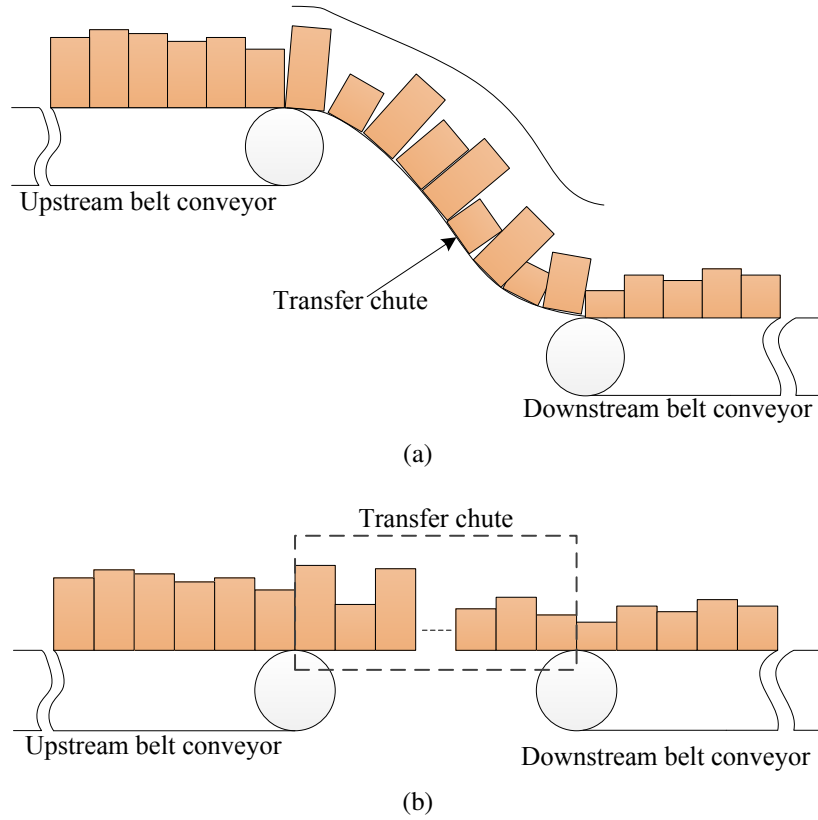
Figure 5.8: Material block in a transfer chute. The transfer chute is treated as a first-in-first-out buffer.

is studied. The verifying method used here is to compare the model output with theoretical values.

The nominal conveying capacity of the conveyor is Q_{nom} in $MTPH$ at nominal speed v_{nom} in m/s. The conveyor length is L in m and then it requires time

$$t_l = L/v_{nom} \tag{5.5}$$

to move the material from the loading location to the discharge area. It is assumed that a material flow sensor is installed at right after the loading area so that the instantaneous material loading rate can be detected. If it is further assumed that the loading rate is fluctuating periodically with a sinusoidal profile, then the material loading rate can be mathematically represented by

$$Q_{in}(t) = Q_1 sin\left(\frac{2\pi}{p}t\right) + Q_2 \tag{5.6}$$

where p is the cycle time. If the belt conveyor is empty at the time point $t = 0$, then at the conveyor discharge area, the unloading rate is

$$Q_{out}(t) = \begin{cases} 0 & t \leq t_l \\ Q_1 sin\left(\frac{2\pi}{p}(t - t_l)\right) + Q_2 & t > t_l \end{cases} \tag{5.7}$$

Correspondingly, if $t \leq t_l$ the total mass M in kg of material on the belt is

$$M_{tot}(t) = \left\{ \int \frac{Q_{in}(t)}{3.6} dt = \frac{Q_2}{3.6}t - \frac{pQ_1}{7.2\pi}\left(cos\left(\frac{2\pi}{p}t\right) - 1\right) \quad t < t_l \right. \tag{5.8}$$

At the time point $t = t_l$, the total material mass is

$$M_{tot}(t_l) = \frac{Q_2}{3.6}t_l - \frac{pQ_1}{7.2\pi}\left(cos\left(\frac{2\pi}{p}t_l\right) - 1\right) \tag{5.9}$$

When $t > t_l$, the total material mass on the belt is

$$M_{tot}(t) = \int_{t_l}^{\infty} \left(\frac{Q_{in}(t) - Q_{out}(t)}{3.6}\right) dt + M_{tot}(t_l) \tag{5.10}$$

$$= \frac{pQ_1}{3.6\pi} sin\left(\frac{\pi}{p}t_l\right)\left[sin\left(\frac{2\pi}{p}t - \frac{\pi}{p}t_l\right)\right] + \frac{Q_2}{3.6}t_l \tag{5.11}$$

The verification is done by comparing the simulation results and the theoretical calculation results. It is assumed that $Q_1 = 200 \; MTPH$, $Q_2 = 1000 \; MTPH$ and $p = 10 \; min$. If it is further assumed that $L = 1000 \; m$ and $v_{nom} = 5 \; m/s$, then

- Equation 5.5 suggests it requires $t_l = 3.33 \; min$ to convey the material through the conveyor. This is proved by the results in Figure 5.9a.

- The comparison between Equations 5.6 and 5.7 suggests that the unloading rate equals the loading rate with a time delay $t_l = 3.33 \; min$. This matches the diagram in Figure 5.9a.

- Equation 5.9 indicates that the total mass on the belt is $63,580 \; kg$ at the time point $t = t_l = 3.33 \; min$, as shown in Figure 5.9b.

- After the time point $t = 3.33 \; min$, the total material mass is fluctuating over time with the average $\frac{Q_2}{3.6}t_l = 55,560 \; kg$ and with the amplitude $\frac{pQ_1}{3.6\pi} sin\left(\frac{\pi T_l}{p}\right) = 9,190 \; kg$, see Figure 5.9b.

Overall, the simulation results in Figure 5.9 match all above mentioned theoretical calculation results. Correspondingly, the simulation model of operational system is verified.

5.4 Modeling of control system

The control system is the core of a belt conveyor speed controller. The control strategies vary over different types of speed control. Taking both the passive and the active speed control into account, this section discusses the modeling of control system.

5.4.1 Passive speed control

In the case of belt conveyors with feeding Scenarios 1 and 2 of Section 5.1, the passive speed control is highly suggested. In a certain period of time, the conveyor speed is fixed in spite of
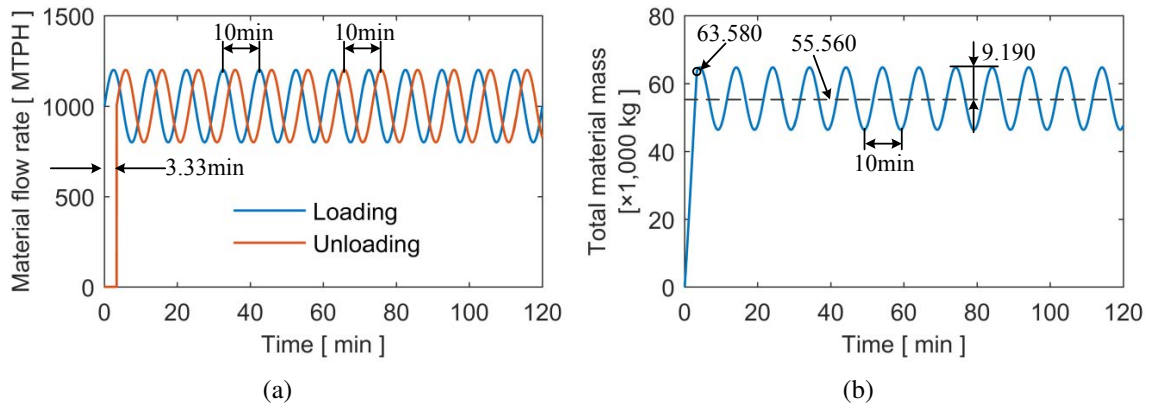
Figure 5.9: Verification of the material flow model. (a) Material loading and unloading rates of the concerned belt conveyor. (b) Total mass of material on the belt over time.
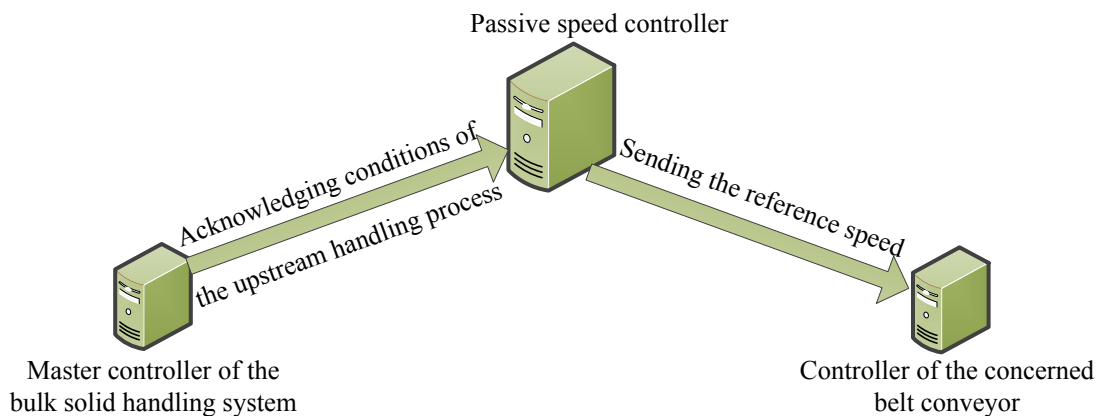
Figure 5.10: Information flow of the passive speed control system.

small and/or temporary variations in the material flow. The conveyor speed is defined prior to a pecific loading condition. Under the passive speed control, the belt load and speed are semi-optimized, and the magnitude of energy savings is primarily determined by the selection of the conveyor speed. Therefore, the keys to passive speed control are to make a precise prediction of the potential maximum material loading rate and to select an appropriate conveyor speed.

Figure 5.10 illustrates the information flow of the passive speed control system. Generally, the passive speed controller does not require a feedback of the actual conveyor speed and the conveyor speed is controlled with an open-loop. However, the passive speed controller needs to be acknowledged with the information of the working condition of the upstream handling process so that the speed controller can predict the potential maximum material loading rate. Based on the level of the loading rate, the speed controller suggests a reference speed to the motor controller of the concerned belt conveyor(s).

In terms of passive speed controllers, the "high-medium-low" strategy is often used to calculate the reference speed if the reference speeds are defined by several different levels. Taking the example of (Daus et al., 1998) for instance. In the described open pit mine, the concerned belt conveyor system is fed by four excavators in a parallel. Based on the number of operating excavators, Daus et al. (1998) suggests the reference speed of the conveyor system with a simple

but effective strategy:

$$
\text{reference speed} =
\begin{cases}
50\% \text{ nominal belt speed} & 1 \text{ excavator} \\
75\% \text{ nominal belt speed} & 2 \text{ excavators} \\
100\% \text{ nominal belt speed} & 3-4 \text{ excavators}
\end{cases}
\tag{5.12}
$$

Figure 5.11 illustrates an application of the "high-medium-low" strategy defined by Equation 5.12. In the diagram of Figure 5.11a, the number of operating excavators is represented by different colored blocks. The solid line represents the actual material loading rate, and the dashed lines illustrate the potential values of the maximum material loading rates in certain periods of time. Based on the number of the operating excavators, the colored line in Figure 5.11b illustrates the suggested speed of the concerned belt conveyor.
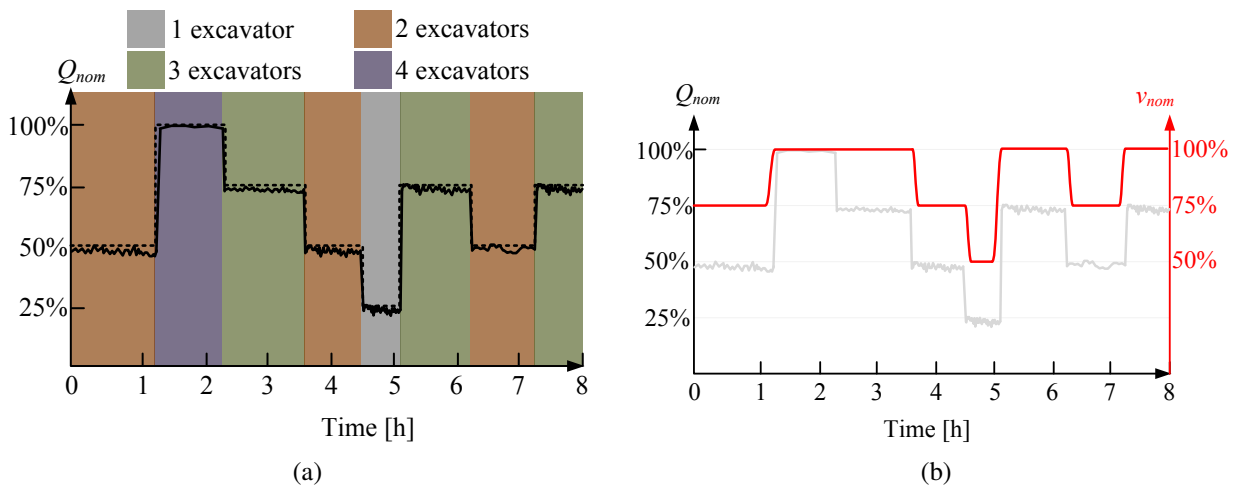
Figure 5.11: Material loading rate and the corresponding conveyor speed under the "high-medium-low" control strategy. (a) The potential material loading rate (dotted lines) and the actual rate (solid lines). The colored blocks represent the number of operating cranes. (b) Suggested conveyor speed based on the algorithm of (Daus et al., 1998). The suggested speed takes the acceleration/deceleration time into account.

Overall, the basic strategy of passive speed control is that the conveyor is running at a specific fixed speed in a long or moderate period until it is acknowledged with the change of the loading levels. It is important to note that the speed suggestion must take the required acceleration/deceleration time into account. In addition, the acceleration operation must be completed before the arrival of the larger material stream, see Figure 5.11b. It is also suggested that the deceleration operation starts after the arrival of the lower material stream, also see Figure 5.11b.

5.4.2   Active speed control

Different to the passive speed control, the active speed control takes the variation of material flow over time into account. The active speed control is widely used on the belt conveyor

systems composed of multiple conveyors. In such cases, the material flow on the upstream belt conveyor is detected in real time, and the speed of the downstream conveyor(s) is adjusted to match the actual upcoming material flow.

Active speed control can be performed either in a continuous or discrete way. If the material feeding rate is varying slightly over time, active speed control can continuously adjust the belt speed without high belt tension and without material spillage. If the variation is considerably large, like Scenario 3 in Section 5.1, the discrete control is suggested so that the belt speed can be adjusted in a soft way.

5.4.2.1   Continuous control

The material flow sensor generally is installed at the upstream conveyor. It is assumed that the material requires time t_{dealy} to travel from the installing location of the sensor to the loading area of the downstream conveyor. Then the instantaneous material feeding rate Q_{in} of the downstream conveyor can be approximated by

$$Q_{in}(t) = Q_{detect}(t - t_{dealy}) \qquad (5.13)$$

where $Q_{detect}(t - t_{dealy})$ represents the material flow detected by the flow sensor at time point $(t - t_{dealy})$. Accordingly, the theoretical instantaneous belt speed $v_{th}(t)$ can be calculated by

$$v_{th}(t) = \frac{Q_{in}(t)v_{nom}}{Q_{nom}} = \frac{Q_{detect}(t - t_{dealy})}{Q_{nom}}v_{nom} \qquad (5.14)$$

If the theoretical belt speed can be strictly followed, then the cross section of the bulk material onto the downstream belt conveyor is kept constant at the design value. Such control is the continuous active speed control.

Lodewijks et al. (2011) provide a case study of the continuous speed control. In the case study, the material flow is smoothly fluctuating in a sine wave with the cycle time 15 minutes. The belt speed fluctuates to accommodate the fluctuating material feed in a strict manner. Simulation-based experimental results of (Lodewijks et al., 2011) show that the continuous speed control can achieve considerable power savings in the studied condition.

However, matching the actual material flow in a strict way is not thus applicable in practice, since the actual material flow in most practical cases changes frequently to some extent. As Chapter 3 suggests, the fast and frequent transient operations can cause, for instance, the risk of belt over-tension and the risk of motor over-heating. Therefore, the continuous active speed control generally is not recommended in practical operations.

5.4.2.2   Discrete control

For practical reasons, discrete speed control for belt conveyors is preferred above continuous control, especially in the cases of the material flow with frequent and large variations. Pang and Lodewijks (2011) suggest that by means of discrete control, the belt speed can be adjusted in a soft way, and that the continuous acceleration operations with high belt tension can be

prevented. In terms of the discrete control, there are two basic strategies: the fixed time interval and the variable time interval.

Strategy 1: Fixed time interval　The material flow sensor is installed at the tail of the upstream conveyor. The incoming material flow of the downstream conveyor in a certain future period can be predicted. Then based on the prediction of the material loading rate, the future speed of the downstream conveyor can be determined. If the decision is made periodically, then the control is dicretized with a fixed time interval.
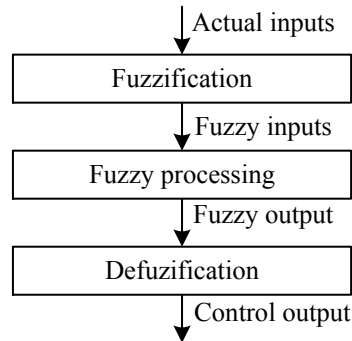
Figure 5.12: The structure and operation of a fuzzy controller. Courtesy of Reznik Leonid (1997).

Fuzzy logic control is a common control method for providing discrete control strategy. Reznik Leonid (1997) details the theory of fuzzy control, and Figure 5.12 illustrates the simplified structure and operation of a fuzzy controller. This controller mainly involves three processes: the fuzzification in which the actual material loading rate is fuzzified and the fuzzy inputs are obtained; the fuzzy processing in which fuzzy inputs are processed and the fuzzy outputs are produced according to the rules set; and the defuzzification in which a real value is produced according to the fuzzy output.

In the determination of the conveyor speed, the input of fuzzy controller is the predicted material feeding rate in a time interval t_s and the actual inputs are fuzzified by the following membership function:

$$f(x) = \begin{cases} b_0, & max\left(X^{t_0}_{t_0-t_s}\right) = r_0 = 0 \\ b_1, & 0 < max\left(X^{t_0}_{t_0-t_s}\right) \leq r_1 \\ b_2, & r_1 < max\left(X^{t_0}_{t_0-t_s}\right) \leq r_2 \\ ..., & ... \\ b_n, & r_{n-1} < max\left(X^{t_0}_{t_0-t_s}\right) \leq r_n \end{cases} \tag{5.15}$$

where $X^{t_0}_{t_0-t_s}$ illustrates the series of the predicted material feeding rates from $t_0 - t_s$ to t_0, r_n (n=0,1,2,...,n) are the fuzzy boundaries and $b_n(n = 0, 1, 2, ..., n)$ are the fuzzy inputs. Due to the linear relationship between material feeding rate and the corresponding speed, the fuzzy processing can be represented as "if the input is b_i, then the output is b_i". In the defuzzication

process, due to the linear relationship between the nominal speed and the nominal conveyor capacity, the reference speed v_{ref} can defuzzified by

$$v_{ref} = b_i v_{nom} \qquad (5.16)$$

Figure 5.13 illustrates the algorithm of the fixed time interval strategy. Taking the example shown in Figure 5.14 for instance. The black solid curve is the predicted material loading rate of the downstream conveyor during the time interval $[t_0, t_6]$. The difference between adjacent points t_i (i=0,1,2,...,6) equals the fixed time interval t_s. In the time period $[t_0, t_1]$, the peak of material loading rate is larger than r_{i-1} but less than r_i, and as a consequence the fuzzy input is b_i. Correspondingly, the suggested speed in the time interval $[t_0, t_1]$ is v_i. However, the predicted material loading rate in the time period $[t_1, t_2]$ is in the range between r_{i-1} and r_{i+1} so that the corresponding speed during the period $[t_1, t_2]$ is v_{i+1}, see the dashed line of Figure 5.14. Therefore, an acceleration operation is required at the time point t_1. However, the belt conveyor system in practice does not allow the sudden speed changes. In addition, in order to prevent the material overloading onto the belt and to avoid the material spillage, the acceleration operation completes before the larger material flow arrives. That means the acceleration operation should be carried out earlier to compensate the time required by the acceleration operation. Then taking the speed adjustment time into account, the colored dotted line in Figure 5.14 illustrates the improved belt speed curve with sinusoidal ac/deceleration profiles. Similarly, the suggested speed between $[t_2, t_6]$ is as the dotted curves in Figure 5.14.
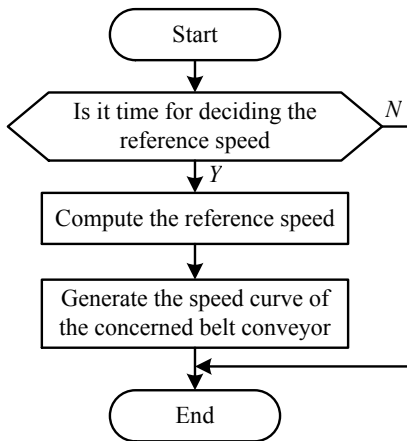
Figure 5.13: Algorithm flowchart of the fixed time interval strategy.
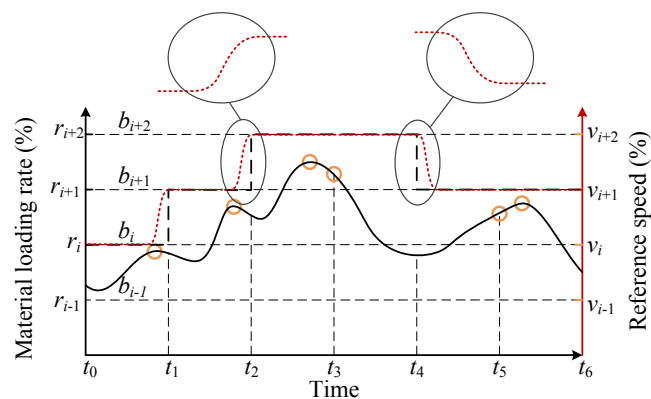
Figure 5.14: Material flow and corresponding reference speed under the fixed time interval strategy.

Strategy 2: Variable time interval   Another strategy for discretizing the active speed control is based on variable time intervals. If the material loading rate is out of a specified boundary, an acceleration/deceleration operation is triggered, and a new reference speed is generated. Due to the fact that the time interval between adjacent transient operations generally is uneven, this event-triggered method is called the variable time interval strategy.
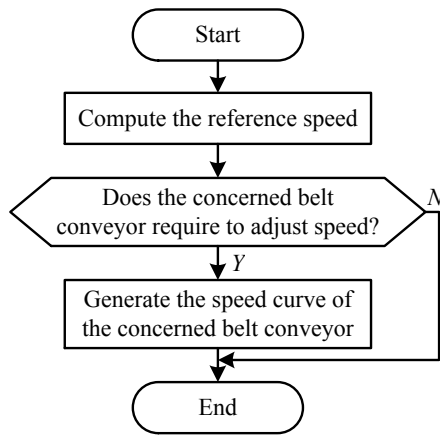
Figure 5.15: Algorithm flowchart of the variable time interval strategy.
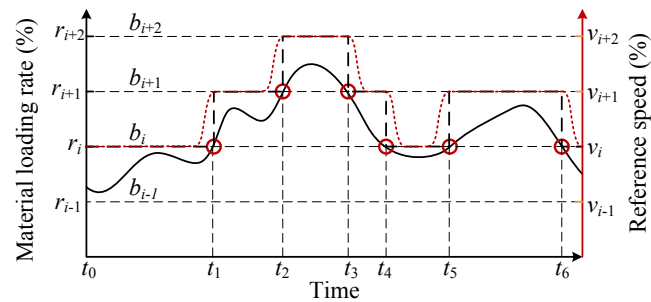
Figure 5.16: Material flow and corresponding reference speed under the variable time interval strategy.

Figure 5.15 represents the flowchart of algorithm of the variable time interval strategy. Different to the algorithm of the fixed time interval strategy, this algorithm requires to compute the reference speed in each computational cycle. Figure 5.16 shows an application of the variable time interval strategy, in which the profile of the predicted material loading rate onto the downstream conveyor equals to that in Figure 5.14. In Figure 5.16, several certain threshold values for feeding rate are defined. As the diagram shows, the material loading rate is in the range $(r_{i-1}, r_i]$ in the time period $[t_0, t_1)$. During this period, the conveyor is running at speed v_i. At the time point t_1, the material loading rate jumps out of the interval $(r_{i-1}, r_i]$ and enters into the interval $(r_i, r_{i+1}]$. Then a new reference speed v_{i+1} is generated, and an acceleration activity is triggered. Similarly, the acceleration or deceleration activities are triggered at time points t_2, t_3, t_4, t_5 and t_6 in Figure 5.16. Correspondingly, the black dashed lines in Figure 5.16 illustrates the suggested speed under the variable time interval strategy. Then taking the speed adjustment time into account, the colored dotted line shows the improved belt speed with sinusoidal ac/deceleration profiles.

Conflicts and solutions To prevent being overloaded, the concerned belt conveyor should complete the acceleration operation before the arrival of the larger quantity material flow and it is suggested to start the deceleration after the arrival of the smaller quantity material flow. However, if the material feeding rate is varying frequently, there may exist a conflict between neighboring transient operations. Conflicts occur both in the fixed time interval strategy and the variable time interval strategy. Taking the conditions in Figure 5.17 for instance where the variable time interval strategy is used. The diagram of Figure 5.17a illustrates the conflict between neighbored deceleration and acceleration operations. At the time point t_1, the material feeding rate drops under r_{i-1}. Based on the control strategy, the conveyor starts to lower speed from v_i to v_{i-1} with the deceleration time t_{de}. At the time point t_2, the material feeding rate exceeds r_i. To avoid the material spillage, the conveyor should start the acceleration from the time point $(t_2 - t_{ac})$. If the sum of time t_{de} and time t_{ac} is larger than the time interval $(t_2 - t_1)$,
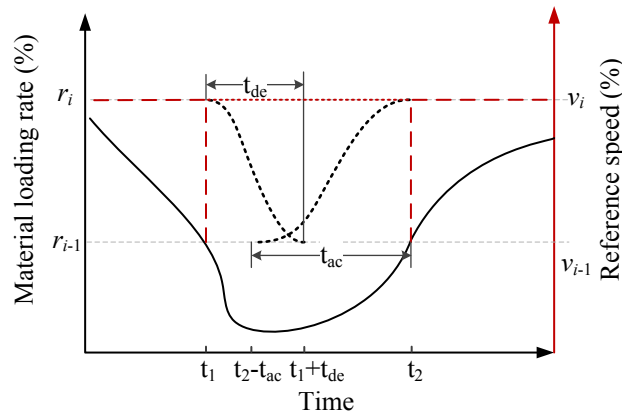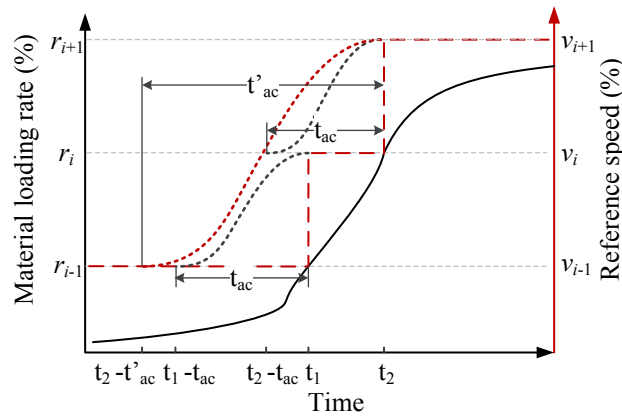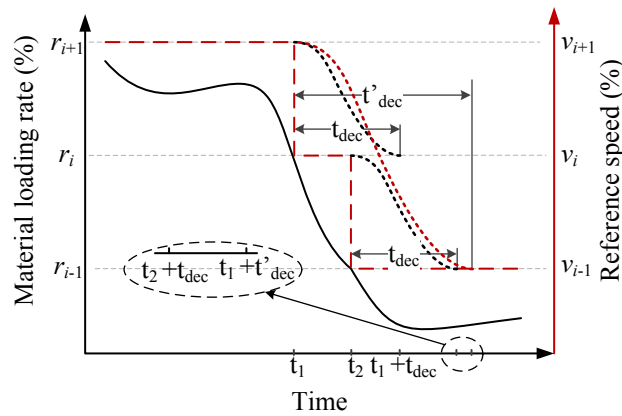
Figure 5.17: Conflicts in discrete speed control. (a) Overlap between neighboring deceleration and acceleration operations. (b) Overlap between neighboring acceleration operations. (c) Overlap between neighboring deceleration operations.

then the conflict occurs as the black dotted lines illustrate in Figure 5.17a. In such cases, both the deceleration and acceleration operations should be canceled, and a new speed curve is suggested which is colored and dotted in Figure 5.17a.

The conflict also occurs in the cases where the material flow has a sudden and large variation. Taking the condition shown in Figure 5.17b for instance. At the time point t_1, the material loading rate exceeds r_{i-1}. As planned, the conveyor should speed up from v_{i-1} to v_i. It is assumed that this acceleration operation has no time conflicts with former transient operations, and then the acceleration operation can be performed in the time interval $[t_1 - t_{ac}, t_1]$. At the time point t_2, the material loading rate increases to above r_{i+1} so that another acceleration operation is expected to be carried out to increase the conveyor speed to v_{i+1}. Taking the conveyor dynamics into account, the second acceleration operation should start from the time point $t_2 - t_{ac}$. If the time point $t_2 - t_{ac}$ is prior to the time point t_1, then the second acceleration overlaps with the first acceleration, see Figure 5.17b. In such cases, the two acceleration operations should be combined into one which is represented by the colored dotted line in Figure 5.17b. Similarly, the overlap between neighboring deceleration operations also can result in conflicts, as shown in Figure 5.17c. The solution is also given by the colored dotted line in Figure 5.17c.

Finally, taking the potential conflicts into account, Figure 5.18 gives the improved algorithm flowcharts of the discrete active speed control strategies.
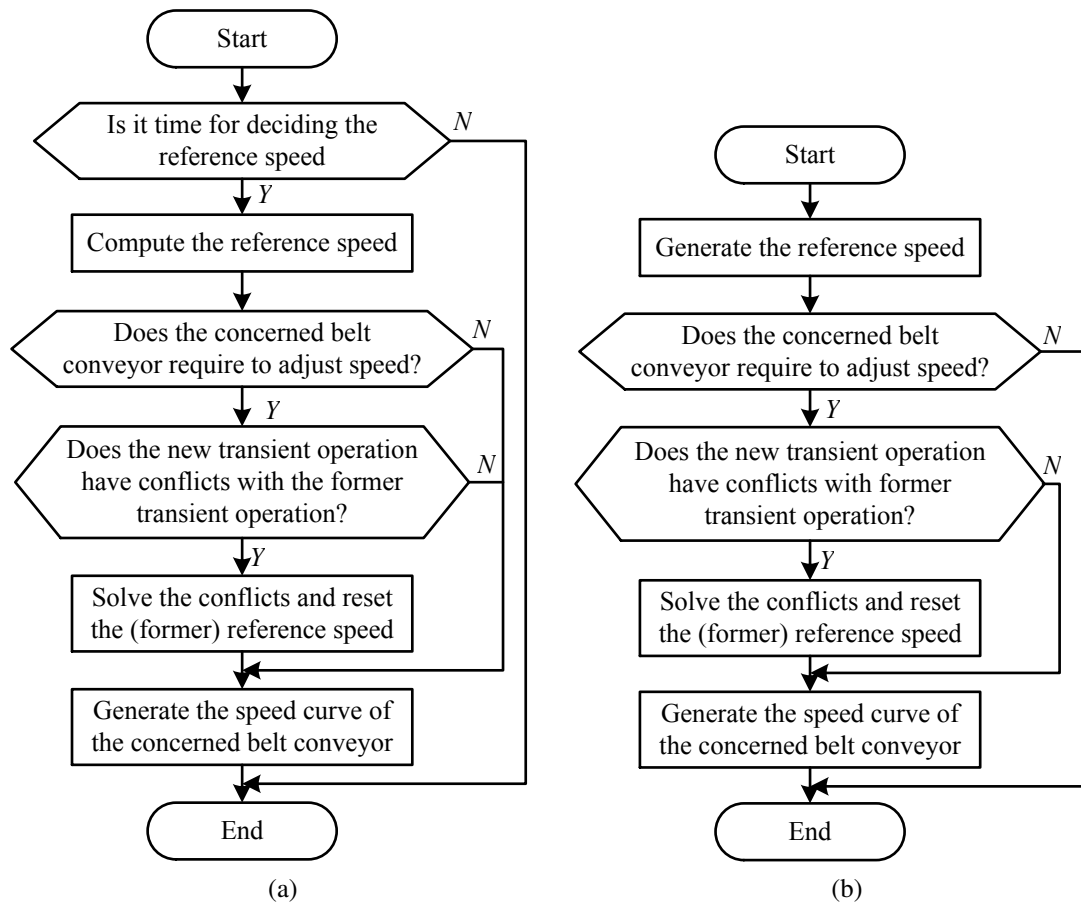
Figure 5.18: Improved algorithm flowcharts of the discrete active speed control strategy. (a) Fixed time interval strategy. (b) Variable time interval strategy.

5.4.3   Verification

Verification of the control system model is realized by using the dynamic simulations. Due to the fact that the the passive speed control algorithm is very sample as compared to the active speed control algorithm, herein we only discuss the verification of the active speed control system. The black curves in Figure 5.19 illustrates the predicted material loading rate onto the concerned belt conveyor over 60 minutes. It is assumed that the reference speed set is defined as {40%,50%,60%,70%,80%,90%,100%} of nominal speed. It is further assumed that the permitted maximum acceleration is 0.1 m/s^2 and that in terms of the fixed time interval strategy, the time interval is 30 seconds. The colored lines of Figure 5.19a illustrates the suggested speed under the fixed time interval strategy taking the acceleration/deceleration operations into account. The colored lines of Figure 5.19b shows the simulation results of the variable time interval strategy. As these two diagrams show, the suggested speed curves are generated as plans, and the conflicts discussed above are successfully solved.

(a)

(b)
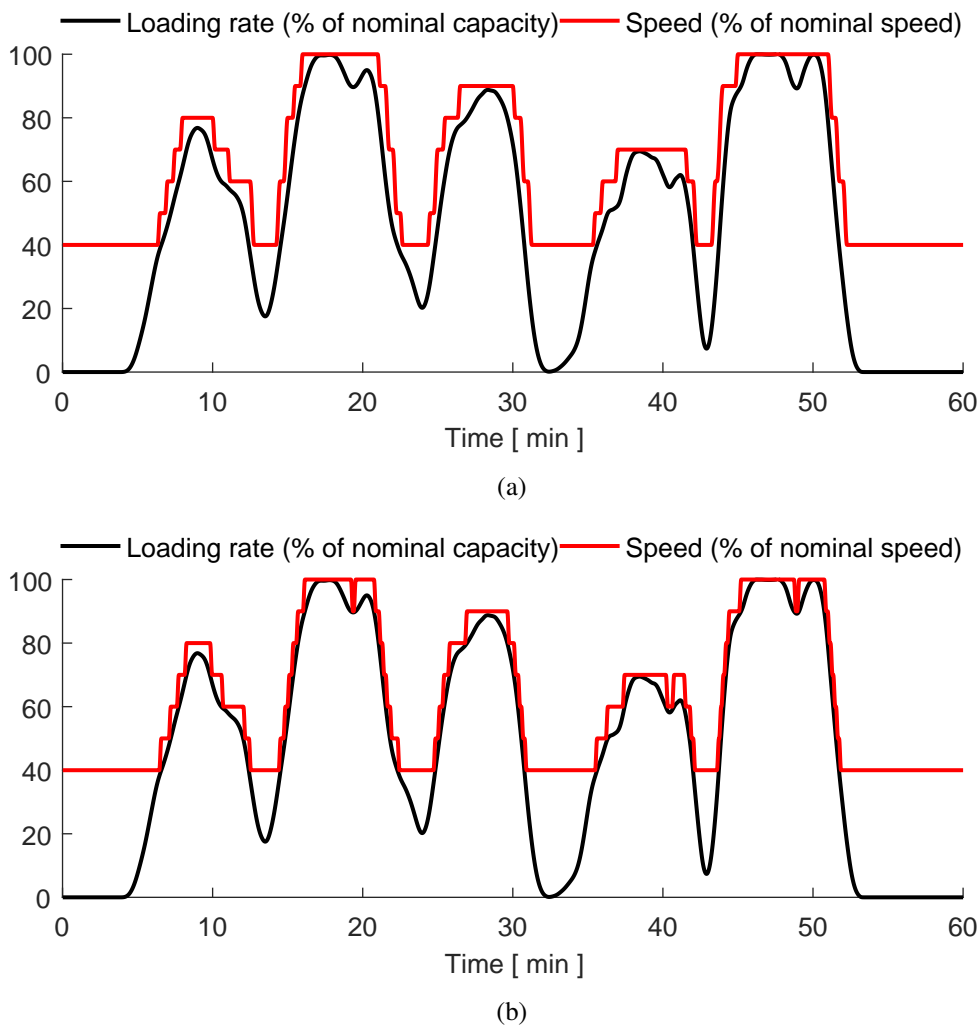
Figure 5.19: Verification of the model of the control system. (a) Fixed time interval strategy. (b) Variable time interval strategy.

5.5 Performances-Key Performance Indicators

The last section introduced several control strategies to build the simulation model of belt conveyor speed control systems. This section defines several key performance indicators (KPIs) to evaluate the performance of speed control. Based on the importance of the indicators, the KPIs are classified into two groups: primary indicators and secondary indicators.

5.5.1 Primary KPIs

In terms of belt conveyor speed control, the primary KPIs majorly consist of the belt utilization rate U, the power consumption P and the power saving ΔP. These indicators are the basic indicators which can be directly used for evaluating the performance of belt conveyors under different control strategies. In the following of this section, these primary indicators will discussed in detail.

Belt utilization rate U Belt utilization rate U is a percental difference between the actual and the nominal cross sections of material on the belt. In the evaluation of speed control, the belt utilization rate is an important indicator. On the one hand, the actual value of the utilization rate suggests the power saving potential by means of speed control. On the other hand, the difference of the utilization rates between the nominal operation and the variable speed operation implies the performance of speed control. Taking the non-uniform distribution of material into account, the utilization rate can be calculated by

$$U = \frac{\text{Average cross section of material on the belt}}{\text{Nominal cross section of material on the belt}} \times 100\% \qquad (5.17)$$

Due to the linear relationship between the mass and the cross section of material, the utilization rate can also be computed by

$$U = \frac{\text{Total mass of material distributed on the belt}}{\text{Nominal total material mass on the belt}} \times 100\% \qquad (5.18)$$

Power consumption P **and power saving** ΔP Power consumption P in kW is another important indicator for evaluating speed control. The power consumption has two terms: one is the mechanical power consumption P_m and another is the electric power consumption P_e. In this and following chapters, the power consumption P refers to the electric power consumption P_e if there is no special notation. The calculation method of the power consumption can be found in Chapter 4. If it is assumed that in the nominal speed operation, the power consumption is P_{con} while P_{non} represents for conditions with non-nominal speed, then the power saving ΔP by means of speed control can be calculated by

$$\Delta P = P_{con} - P_{non} \qquad (5.19)$$

If the saving is represented by a percentage, then the calculation of the power saving can be expressed by

$$\Delta P = \left(1 - \frac{P_{non}}{P_{con}}\right) \times 100\% \tag{5.20}$$

5.5.2 Secondary KPIs

Secondary KPIs are the additional indicators of evaluating the performance of speed control. The values of these indicators are originated from the power consumption P. The secondary KPIs mainly include the total energy consumption W, the electricity cost $Cost_{ele}$, the carbon dioxide (CO2) emissions $Emission_{CO2}$, the social cost of carbon SCC and the total cost $Cost_{tot}$.

Total power consumption W and energy saving ΔW   Total power consumption W in kWh is the amount of work done by belt conveyors and can be calculated by accumulating the instantaneous power consumption over time

$$W = \frac{\int P(t) d(t)}{3600} = \frac{\sum P(t) t_{sample}}{3600} \tag{5.21}$$

where t_{sample} is the sampling cycle time in s of the instantaneous power. Energy saving ΔW is the difference of the energy consumption between the nominal speed operation and the variable speed operation:

$$\Delta W = W_{con} - W_{non} \tag{5.22}$$

where the subscribes $_{con}$ and $_{non}$ represent the operations with the constant-and-nominal speed and with the non-nominal-and variable speed, respectively.

Electricity cost $Cost_{ele}$ Electricity cost is the payment for consuming electricity during the material transportation, which takes the price of electricity into account. The price of electricity varies widely from country to country and also may vary from time to time. Herein, the price of electricity in the Netherlands is used to evaluate the electricity cost and it is assumed that the price is constant over time. According to the latest data from Eurostat (Eurostat, 2016), the price of electricity in the Netherlands averaged 0.1037€per kWh for industrial consumers during the first half of 2016.

Carbon dioxide (CO2) emissions $Emission_{CO2}$ and their social cost SCC   Air pollution, a by-product of electricity, can be extra considered in the evaluation of speed control. Carbon dioxide (CO_2), as a major source of greenhouse gases, is often used to describe the negative impacts of the electricity consumption. As United States Environmental Protection Agency (2015) suggested, the CO2 emissions also cause changes in net productivity, human health, property damages from increased flood risk, and changes in energy system costs. The value of carbon dioxide emission is variable over different activities, and the concept of emission factor $EF_{CO2}$is widely used to calculate the total carbon emissions:

$$Emission_{CO2} = EF_{CO2}W \tag{5.23}$$

The emission factor EF_{CO2} depends on sources of electrical power. The Intergovernmental Panel on Climate Change (IPCC) (Edenhofer et al., 2011) suggests that the CO_2 emission ranges from 4 g/kWh for the hydro-power based electricity generation to 1001 g/kWh for the coal based electricity generation. In addition, the data of (Brander et al., 2011) shows that the CO_2 emission factor varies considerably from country to country due to different compounds of types of electricity generation. As Brander et al. (2011) further suggests, the average CO_2 emission factor nears 410 g/kWh in the Netherlands.

The social cost of carbon SCC, commonly referred to as the carbon price, is widely used to estimate the climate change impacts of the CO_2 emission and to estimate the economic damages associated with a small increase in CO2 emissions. There are many researchers of institutions or of agencies developing models for estimating the SCC. Due to the fact that the research of the SCC is out of the scope of the thesis, these models will not be further discussed. The thesis uses the result of (van den Bijgaart et al., 2016) which suggests a mean value 31 €/tCO_2 to the SCC in the Netherlands for year 2015.

Total cost $Cost_{tot}$ **and total savings** $Saving_{tot}$ The indicator of the total cost takes both the electricity cost and the social cost of carbon into account. The difference of the total cost between the nominal speed and the non-nominal speed shows the total savings $Saving_{tot}$ by means of speed control.

5.6   Conclusion

This chapter answered the fourth key research question presented in Chapter 1, and modeled the belt conveyor speed control system. The system is built up two sub-systems: the operational system and the control system. In terms of the operational system, the comparison between the simulation result and the calculation result show that the operational system was successfully modeled by a discrete tool. In terms of the control system, the experimental results show that the conflicts between neighboring transient operations were prevented by an improved control algorithm.

Additionally, this chapter defined several key performance indicators (KPIs) to evaluate the conveyor performance under speed control. The evaluation will be carried out in the next chapter.

Chapter 6

Simulation experimental results

Chapter 5 presented the modeling of the belt conveyor speed control system, in which the conveyor system was viewed as a first-in-first-out buffer and a discrete tool was used to represent the continuous transport system. A series of computational simulations will be carried out in this chapter to assess the performance of both the passive speed control and the active speed control. In the assessment, the variable DIN f factor values will be used to calculate the power consumption of a belt conveyor. In addition, the acceleration and deceleration time also will be taken into account to ensure healthy dynamics of belt conveyors under speed control.

6.1 Introduction

Chapter 5 classified the bulk material loading scenarios into four groups and introduced several different types of belt conveyor speed control systems. In Scenario 1, the loading rate keeps constant for a long term operation. If the loading rate is non-nominal, the passive speed control is suggested and the conveyor is running at a fixed non-nominal speed. The passive speed control also can be applied in Scenario 2 where the loading degree moderately varies in between long term operations. In such cases, the conveyor speed is fixed until there is a considerable change of the loading rate. If the loading degree is varying moderately in between short term operations, see Scenarios 3 of Section 5.1, the passive speed control is not applicable any more. In such cases, the active speed control is highly suggested. Under the active speed control, the conveyor speed is frequently adjusted, as compared to the passive speed control, to match the actual loading rate. So that the concerned belt conveyor is expected to be running with a high utilization rate. However, if the actual loading varies excessively in all operations as in Scenario 4, the belt conveyor speed control is not suggested since the excessively frequent speed adjustment can result in unhealthy conveyor dynamics.

The objective of this chapter is to study the performance of the speed control. Section 6.2 will study a fictive belt conveyor system of an import bulk terminal to show performance of the passive speed control. Firstly, the assessment of the steady state performance of the passive speed control will be carried out. In the steady state operation, the loading rate is constant and the conveyor is running at a fixed speed. Three kinds of bulk material will be used in the assessment. In addition, the variable value of the f factor defined by DIN 22101 (German

Institute for Standardization, 2015) will be taken into account to improve the accuracy of the assessment. Besides the static analysis, the dynamic performance of the passive speed control also will be studied where the loading rate is varying in between long term operations. Section 6.3 studies another fictive belt conveyor system for assessing the active speed control. In the assessment, both the fixed time interval strategy and the variable time interval strategy will be studied. In addition, in terms of the fixed time interval strategy, the influence of the speed set and of the time interval will be studied. Finally, conclusions are presented in Section 6.4.

6.2   Passive speed control

6.2.1   Setup

A fictive long horizontal belt conveyor in a fictive import dry bulk terminal is studied in this section. The terminal is yearly operating for 360 days at 24 hours per day. Figure 6.1 shows the simplified layout of the terminal and BC1-BC2-BC3 is one of the belt conveyor transport chains. The primary function of this terminal is as follows. The material in ships can be unloaded by four cranes in parallel and discharged onto the BC1 belt. Then the material flow on the BC1 belt is in turn deposited onto the BC2 and BC3 belt conveyors, successively. Finally, the material is discharged from the BC3 belt and stored at a stockyard by stackers.
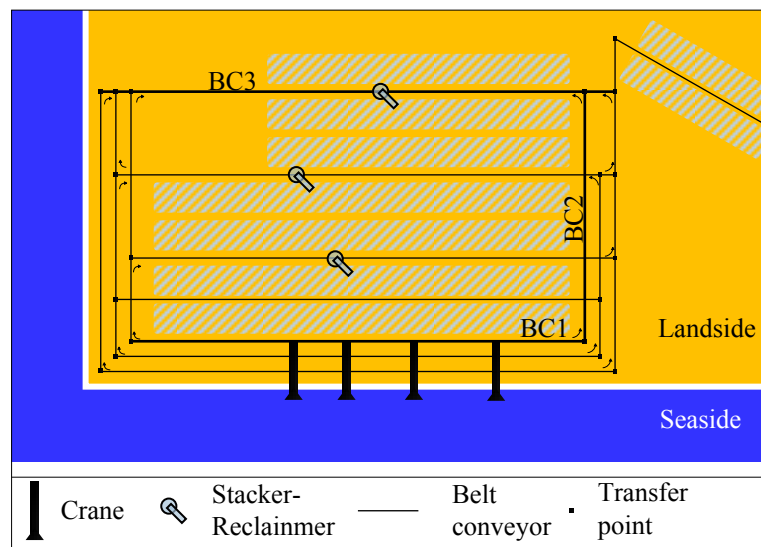
Figure 6.1: The layout of a fictive import terminal in which the BC2 belt conveyor is the studied belt conveyor.

The import terminal handles several types of dry bulk materials, including coal, limestone and iron ore. Table 6.1 illustrates the parameters of these three kinds of bulk materials. Nominally, the conveying capacity of the conveyor system is 2,000 $MTPH$, 3,500 $MTPH$ and 6,000 $MTPH$, in terms of coal, limestone and iron ore, respectively. However, with respect to the crane-scheduling problem in practice, the number of operating cranes is variable-in-time during ship unloading. As a consequence, the material flow on the BC1-BC2-BC3 chain can be considerably lower than the design capacity. Based on the number of simultaneously operating

cranes in a time interval, the ship unloading capacity during this time period however can be determined and the peak of the material feeding rate onto the belt conveyors can be approximated. Accordingly, the conveyor speed can be reduced to match the number of operating cranes and then the utilization of belt conveyors is improved.

Table 6.1: Three sets of bulk material parameters. Courtesy of Spaans (1991).

Bulk material type	Coal	Limestone	Iron ore
Density (kg/m^3)	740	1,580	2,765
Angle of internal friction (°)	32	45	35
Frictional angle between belt and material (°)	15	15	15
Angle of repose (°)	15	15	15

Table 6.2: Basic parameters of the BC2 conveyor.

Parameters	Value	Parameters	Value
Nominal conveying capacity ($MTPH$)	6,000	Belt type	ST 1600
Nominal speed (m/s)	5	Idler spacing (m) (top)	1.2
Conveyor length in (m)	1000	(bottom)	3
Conveyor height in (m)	0	Linear idlers weight (kg/m)	42.8
Troughing angle (°)	30	Linear belt weight (kg/m)	39.4
Special resistances (N)	0	Belt width (m)	1.2

As an example, the BC2 belt conveyor is studied, which has the largest useful conveying length in the BC1-BC2-BC3 chain. The studied belt conveyor is occupied for 40% of the total operation time of the terminal. Table 6.2 illustrates the parameters of the concerned belt conveyor. Taking the drive system efficiency into account, the permitted minimum conveyor speed is defined as 2 m/s. Based on the linear relationship between the conveyor speed and the conveying capacity, the reference speed is classified into four levels:

$$\text{Belt speed=}\begin{cases} 2 \ m/s & 0-1 \text{ crane} \\ 2.5 \ m/s & 2 \text{ cranes} \\ 3.8 \ m/s & 3 \text{ cranes} \\ 5 \ m/s & 4 \text{ cranes} \end{cases} \tag{6.1}$$

6.2.2   Experiment plan

Several steady-state calculations and a dynamic simulation will be performed. Firstly, steady-state calculations are carried out to analyze the power savings, taking three kinds of bulk materials into account. Table 6.1 lists the parameters of the bulk materials. In the static analyses, it is assumed that there always are 2 cranes operating simultaneously. Then it is further assumed that the material loading rate is constant and equals half of the nominal conveying capacity. To

achieve various results and to compare the differences, calculation runs {1,3,5} in Table 6.3 apply the nominal speed 5 m/s while runs {2,4,6} use a non-nominal speed, 2.5 m/s. Section 6.2.3 details the steady-state calculations.

Table 6.3: Plan of Steady-state calculations.

Calculation run	1	2	3	4	5	6
Bulk material	Coal		Limestone		Iron ore	
Loading rate	1000 $MTPH$		1750 $MTPH$		3000 $MTPH$	
Loading distribution	Uniform	Uniform	Uniform	Uniform	Uniform	Uniform
Speed	5 m/s	2.5 m/s	5 m/s	2.5 m/s	5m/s	2.5 m/s

However, due to a possible problem of crane schedules, the number of operating cranes varies over time. As a consequence, the material flow onto the concerned conveyor is variable-in-time. In addition, the actual material flow through the conveyor generally is non-uniform. To analyze the performance of passive speed control, a dynamic simulation is carried out. It is assumed that the number of operating cranes is varying from zero to four. The handling of coal is studied for instance and the actual material loading rate varies from zero to 2,000 $MTPH$. Section 6.2.4 discusses the dynamic simulation and illustrates the experimental results.

6.2.3 Steady-state calculation

Firstly, the variable values of the DIN f factor are achieved by the theoretical calculation method which was discussed in Chapter 4. Table 6.4 shows the calculation results of the f factor over different loads and speeds. Taking the calculation run set {1,2} for instance where the bulk material conveyed is coal. The loading rate is half of the nominal conveying capacity. In Run 1, the conveyor is running at nominal speed and the conveyor belt is half loaded, while in Run 2 the conveyor speed is lowered to ensure that the conveyor belt is fully loaded. Due to the considerable increase of the bulk and belt flexural resistances, the f factor value shows a large increase when the conveyor is fully filled, see Table 6.4. As the data shows, the value of the f factor in Run 2 is 0.0143 as compared to 0.0131 in Run 1. The considerable change of the f factor value can also be found in the run set {3,4,5,6}. The operation in Runs 3 and 4 conveys limestone and the operation of Runs 5 and 6 handles iron ore. Similar to Runs 1 and 2, the conveyors in these runs are loaded with half of the nominal conveying capacity. Runs 3 and 5 uses the nominal speed and Runs 4 and 6 use a lower speed. As illustrated in Table 6.4, when the conveyor is running at a lower speed and the conveyor has a higher utilization, the DIN f factor value has a considerable increase.

Taking the variable f factor values and different conveyor speeds into account, Table 6.5 illustrates the power consumption of belt conveyors in different runs. All the static analyses show positive results in the possibility to save power if the speed controlled operation is used instead of the nominal speed operation. Taking Runs 1 and 2 for instance. In Run 1, the power consumption is 137 kW. Due to the passive speed control, the power consumption in Run 2 is reduced by 36.8 kW, 27% of that in Run 1. This indicates that the passive speed control enables

Table 6.4: Variable values of the artificial frictional coefficient f of the BC2 belt conveyor. The data is achieved by using the theoretical calculation method discussed in Chapter 4.

Calculation run	1	2	3	4	5	6
Bulk material	Coal		Limestone		Iron ore	
Belt utilization rate U (%)	50	100	50	100	50	100
Artificial frictional coefficient f	0.0131	0.0143	0.0148	0.0190	0.0162	0.0188

Table 6.5: Results of the steady-state calculation.

Estimation run	1	2	3	4	5	6
Key performance indicators						
Belt utilization rate U (%)	50	100	50	100	50	100
Power consumption P (kW)	136.61	99.78	189.48	178.96	271.00	256.14
Power savings ΔP (kW)		36.83		10.52		14.86
Electricity consumption W in 24 hours (kWh)	3,279	2,395	4,548	4,295	6,504	6,147
Electricity saving ΔW in 24 hours (kWh)		884		253		357
Electricity cost $Cost_{ele}$ in 24 hours (€)	340	248	472	445	674	637
Carbon dioxide emission $Emission_{CO2}$ in 24 hours (kg)	1344	982	1865	1761	2667	2520
Social cost of carbon SCC in 24 hours (€)	42	30	58	55	83	78
Total cost in 24 hours (€)	382	279	529	500	757	715
Total savings in 24 hours (€)		103		29		42
Yearly prediction						
Predicted annual energy consumption (MWh/yr)	472	345	655	618	937	885
Predicted annual electrical cost (€/yr)	48,960	35,760	67,910	64,140	97,120	91,800
Predicted annual electrical cost savings (€/yr)		13,200		3,770		5,330
Predicted annual CO_2 reduction ($Tons/yr$)		52		15		21
Predicted annual reduction of SCC (€/yr)		1,620		460		650
Predicted total annual savings (€/yr)		14,820		4,230		5,980

a considerable amount of power savings, although the f factor value in Run 2 is larger than that in Run 1. The power saving can also be found in Runs 4 and 6 of Table 6.5.

Derived from the data of Table 6.5, Figure 6.2 illustrates and compares the power saving rates of the steady-state analyses. Taking the variation of the f factor into account, the savings are between 5% and 27%. According to the data, the various saving rate highly depends on the types of bulk materials. As the data in Figure 6.2 suggests, there is a negative correlation between the density of bulk materials and the saving rate. This suggestion can also be applied to the cases where the f factor value is assumed to be fixed. The data in Figure 6.2 considers the condition where the f factor is constant over loads and speeds. As the data shows, in terms of coal, the power saving can be up to 32% while in terms of iron ore, the saving ratio is reduced to 19%. In addition, the data of Figure 6.2 further suggests that compared to the condition with variable f factor values, the condition with a constant f factor over-estimates the power savings, especially in the runs conveying limestone and iron ore. Therefore, it is important to consider the variable values of the f factor to improve the accuracy of the assessment.
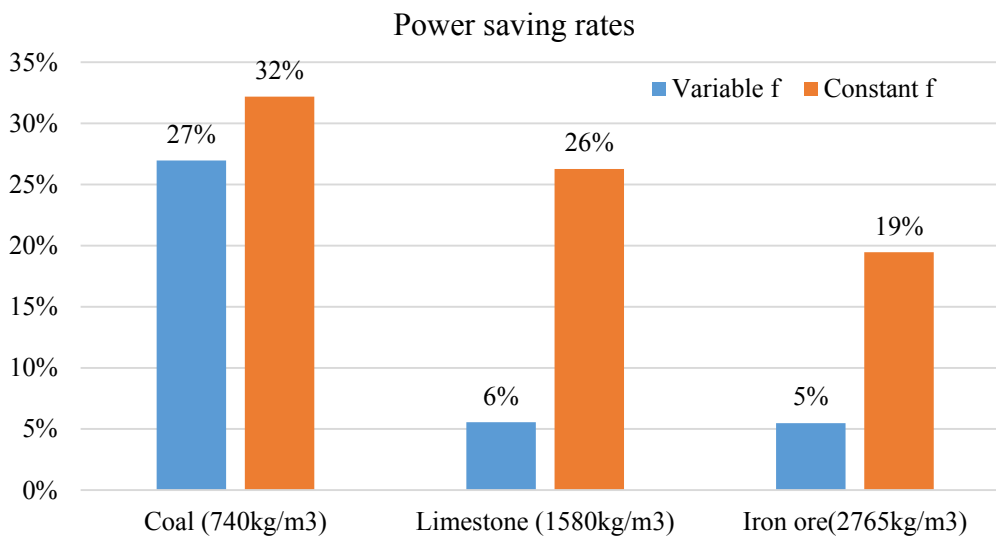
Figure 6.2: Comparison of steady-state estimations.

The data of Table 6.5 also includes the value of other key performance indicators. For example, the results of yearly predictions are given. As the data shows, a large amount of electricity cost and carbon emission can be saved by speed control. Taking the transportation of coal for instance. Due to the passive speed control, the electricity cost yearly can be reduced by €13,200 with 52 tons of carbon emission. If the social cost of carbon is taken into account, the total annual savings can be up to €14,820.

Further calculation and discussion The data in Table 6.4 shows that the DIN f factor value varies with loads and speeds. It further shows that when the conveyor speed is reduced, the DIN f factor increases considerably due to the increase of the load. Therefore, taking the variable DIN f values into account, it is important to find the optimum conveyor speed for maximum power reduction before the application of speed control. Further steady-state calculations are

Table 6.6: Values of the DIN f factor over different loads and speeds. The conveyor is loaded by coal with density 740 kg/m^3. The load is represented by the conveyor utilization U, varying from 10% to 100%. The conveyor speed V is in the range from 2 m/s to 5 m/s.

U \ V	10%	20%	30%	40%	50%	60%	70%	80%	90%	100%
2	0.0099	0.0099	0.0100	0.0102	0.0105	0.0109	0.0114	0.0120	0.0127	0.0135
2.25	0.0102	0.0102	0.0104	0.0106	0.0109	0.0113	0.0118	0.0124	0.0131	0.0139
2.5	0.0105	0.0105	0.0107	0.0109	0.0113	0.0117	0.0122	0.0128	0.0135	0.0143
2.75	0.0107	0.0108	0.0110	0.0112	0.0116	0.0120	0.0125	0.0131	0.0138	0.0146
3	0.0110	0.0110	0.0112	0.0115	0.0118	0.0123	0.0128	0.0134	0.0141	0.0149
3.25	0.0111	0.0112	0.0114	0.0117	0.0121	0.0125	0.0131	0.0137	0.0144	0.0152
3.5	0.0113	0.0114	0.0116	0.0119	0.0123	0.0127	0.0133	0.0139	0.0146	0.0154
3.75	0.0114	0.0116	0.0118	0.0121	0.0125	0.0129	0.0135	0.0141	0.0148	0.0156
4	0.0115	0.0117	0.0119	0.0122	0.0126	0.0131	0.0137	0.0143	0.0150	0.0158
4.25	0.0116	0.0118	0.0120	0.0124	0.0128	0.0132	0.0138	0.0145	0.0152	0.0160
4.5	0.0117	0.0119	0.0121	0.0125	0.0129	0.0134	0.0139	0.0146	0.0153	0.0161
4.75	0.0118	0.0120	0.0122	0.0125	0.0130	0.0135	0.0140	0.0147	0.0154	0.0162
5	0.0118	0.0120	0.0123	0.0126	0.0131	0.0136	0.0141	0.0148	0.0155	0.0163
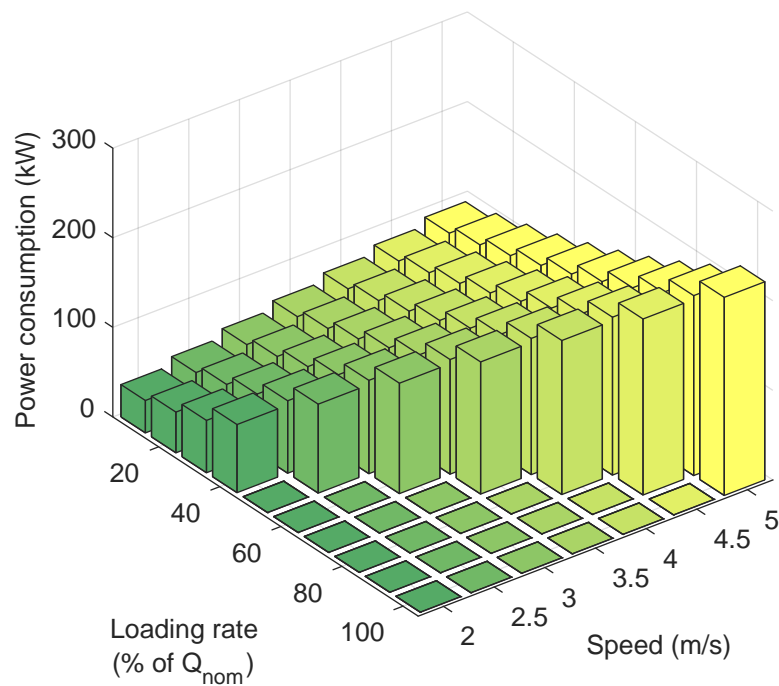
(a)
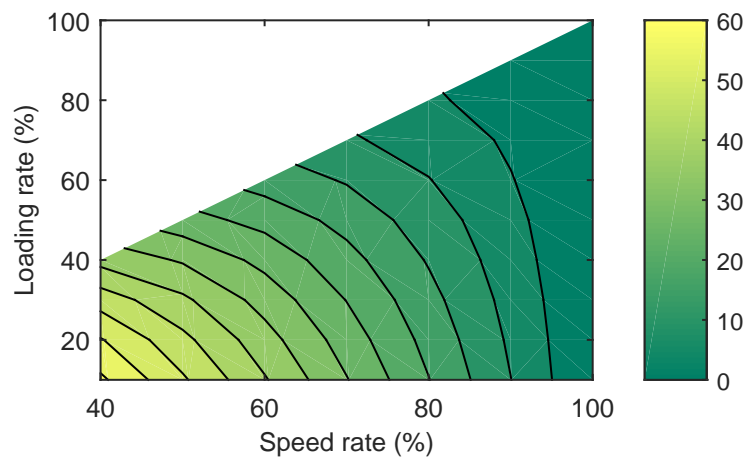
(b)

Figure 6.3: Calculation results. The loading rate varies from 10% to 100% of the nominal conveying capacity. The conveyor speed varies from 2 m/s to 5 m/s. The speed ratio is no less than the loading ratio to avoid the material spilling from the belt. (a) Power consumption for different loading rates and for different speeds. (b) Power saving ratio for different loading rates and for different speeds.

carried out in which coal is conveyed. Table 6.6 illustrates the DIN f factor value for different loads and speeds. It clearly shows that the speeds and loads have a large impact on the f factor value. From the data in Table 6.6, a conclusion can be given for the studied belt conveyor: in the cases where the material loading rates are the same, it results in a larger DIN f value if the belt conveyor is running at a lower speed.

Further calculation results are given in Figure 6.3. The diagram of Figure 6.3a illustrates the power consumption for different loads and speeds. As the diagram shows, due to the reduction of the conveyor speed, the conveyor with a lower speed in the same loading rate consumes less power. Similar phenomenon can also be found in Figure 6.3b which illustrates the power reduction rate by means of speed control. Therefore, according to the data in Figure 6.3, it can be concluded that for this defined belt conveyor, the optimum conveyor speed is that enables 100% conveyor utilization rate if the loading rate is larger than the permitted speed ratio.

(a)

(b)
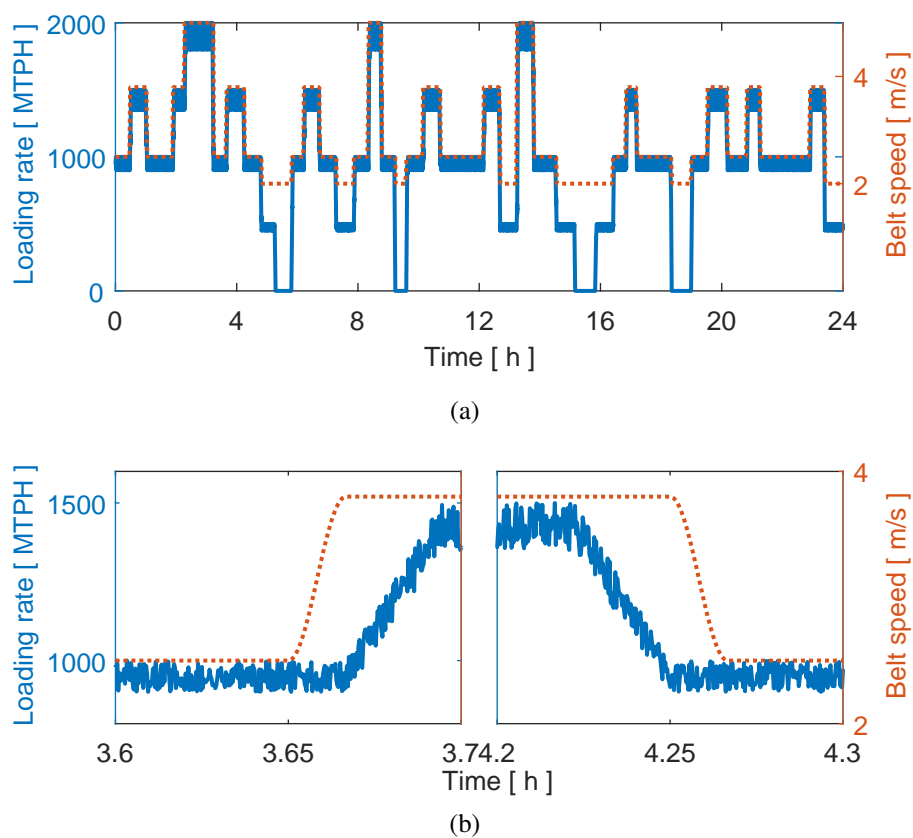
Figure 6.4: Material feeding rate and the corresponding speed of the studied belt conveyor. (a) Feeding rate in 24 hours. (b) Feeding rate in certain periods. The left diagram shows an increasing trend and the right diagram shows a decreasing trend.

6.2.4   Dynamic simulation

The bulk material handling operation in 24 hours is studied. Taking the bulk material coal for instance. The solid line in Figure 6.4 illustrates the material feeding rate onto the BC2 belt over 24 hours. The corresponding speed is represented by the dotted lines. As shown in Figure 6.4a, the feeding rate is varying over time and the conveyor speed is adjusted in accordance

with the peak of material feeding rate. The ECO method is used to decide the permitted acceleration/deceleration value and to ensure soft acceleration/deceleration operations. Furthermore, in order to reduce the risk of material spillage away from the belt caused by overloading, the conveyor speed should reach the desired speed before the arriving of the larger level of material feeding flow, see Figure 6.4b. On the contrary, the event of deceleration operation is triggered after the arriving of the lower level of material feeding flow, also see Figure 6.4b.

The experimental results of simulations are given in Figure 6.5. Overall, the operation running at nominal speed consumes more energy than that running at variable speeds. Figure 6.5a presents and compares the filling ratio of the BC2 conveyor over 24 hours. As the figure shows in the case of the BC2 belt conveyor running at nominal speed, the profile of the filling ratio is similar with the shape of the material feeding rate shown in Figure 6.4. Furthermore, the comparison of the two curves in Figure 6.5a yields that the conveyor's filling ratio is improved to 79.3% from 47.8% on average, due to the variable speed drives.

Figure 6.5b demonstrates the instantaneous power consumption with the consideration of the variable f factor and the variable system efficiency. The figure shows that in the traditional mode with constant speed drives, the average power consumption is 124 kW with the maximum of 168 kW. However, due to the strategy of speed control, the power consumption is reduced to 88 kW on average, although the maximum increases to 197 kW caused by the acceleration.

Figure 6.5c compares the accumulative power consumption of the studied conveyor in the 24 hours' operation. The figure shows the total energy consumption is up to 2,985 kWh in the nominal speed operation. The comparison however illustrates that due to the decrease of the conveyor speed, the electricity consumption is reduced by the amount of 880 kWh.

Table 6.7 summarizes the experimental results, including the yearly predictions. From the data it can be learned that in the given example, the belt conveyor speed control yearly can result in over 130 MWh electrical savings and around 52 $tons$ of CO_2 reduction. According

Table 6.7: Calculation results of speed control of the BC2 belt conveyor.

	Constant speed	Variable speed
Average material feeding rate ($MTPH$)	957	957
Average conveyor utilization rate (%)	47.8	79.3
Average power consumption (kW)	124.3	87.7
Average power reduction (kW)		36.6
Average power reduction (%)		29.4
Total power consumption in 24 hours (kWh)	2,985	2,105
Yearly predictions		
Predicted annual electrical consumption (MWh/yr)	430,000	303,000
Predicted annual electrical cost (€$/yr$)	44,600	31,400
Predicted annual electrical cost savings (€$/yr$)		13,200
Predicted annual CO_2 emission ($Tons/yr$)	176	124
Predicted annual CO_2 emission reduction ($Tons/yr$)		52
Predicted annual reduction of the social cost of CO_2 (€$/yr$)		1,600
Total annual savings (€$/yr$)		14,800
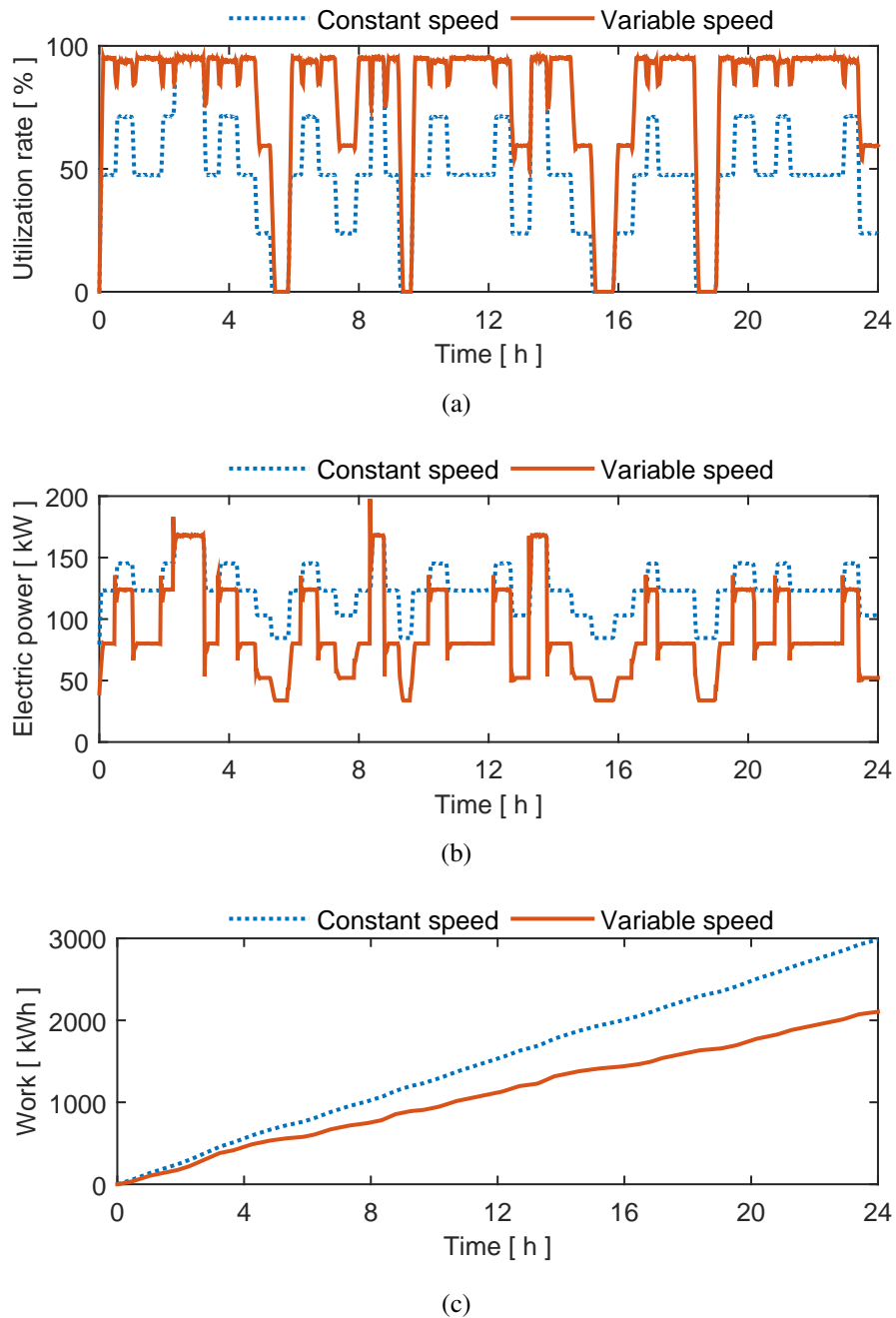
Figure 6.5: Experimental results of passive speed control. (a) Conveyor belt filling ratio. (b) Instantaneous electric power consumption. (c) Accumulating power consumption in 24 hours.

to the latest data from Eurostat (Eurostat, 2016), the Netherlands electricity price for industrial consumers during the first half of 2016 averaged 0.1037 €/kWh. That implies for the concerned belt conveyor working in the given condition, speed control can reduce the operational cost by €13,200 yearly. Furthermore, if the social cost of CO_2 is taken into account, more than €1,600 cost can be reduced annually. In total, speed control on the BC2 belt conveyor realizes over €14,800 cost savings in a year.

6.3   Active speed control

6.3.1   Setup

This section analyzes the performance of the active speed control where another fictive belt conveyor system is studied. As shown in Figure 6.6, the conveying system consists of two belt conveyors connected in series. The upstream conveyor is running at nominal speed. The material loading rate onto the upstream conveyor is moderately varying in between short term operations, whose profile is similar with the Scenario 3 of Section 5.1. As Figure 6.6 shows, a material flow sensor is installed nearby the loading area of the upstream conveyor, and it detects the actual material flow in real time. Based on the data of the flow sensor, the active speed controller predicts the material loading rate of the downstream conveyor and generates the reference speed of the downstream conveyor.
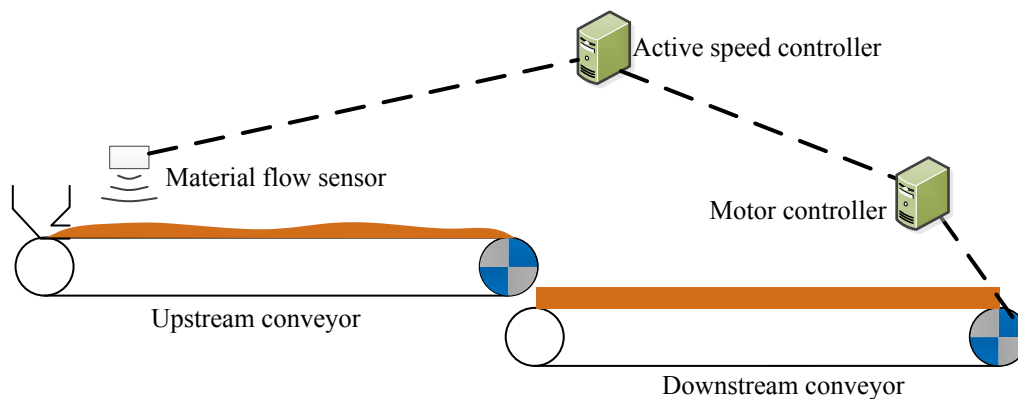
Figure 6.6: Fictive belt conveyor system for active speed control.

Table 6.8 lists the basic parameters of the concerned belt conveyor system. In terms of the downstream conveyor, the variable values of the f factor over different speeds and loads are given in Table 6.9.

6.3.2   Experiment plan

The operation of the system over eight hours is studied. Figure 6.7 illustrates the material loading rate onto the upstream conveyor. As the figure shows, the loading rate varies over time. On an average, the material loading rate is around 870 $MTPH$. Simulations are carried out to show the conveyor performance under the active speed control. Table 6.10 defines different

Table 6.8: Parameters of the belt conveyors.

Parameters	Value	Parameters	Value
Nominal conveying capacity ($MTPH$)	2,000	Belt type	ST 800
Nominal speed (m/s)	5	Ilder spacing (m) (top)	1.2
Conveyor length (m) Upstream	300	(bottom)	3
Downstream	1000	Linear idlers weight (kg/m)	27.1
Conveyor height (m)	0	Linear belt weight (kg/m)	23
Troughing angle (°)	30	Belt width (m)	1.2
Density of bulk material (Coal) (kg/m^3)	740	Special resistances (N)	0
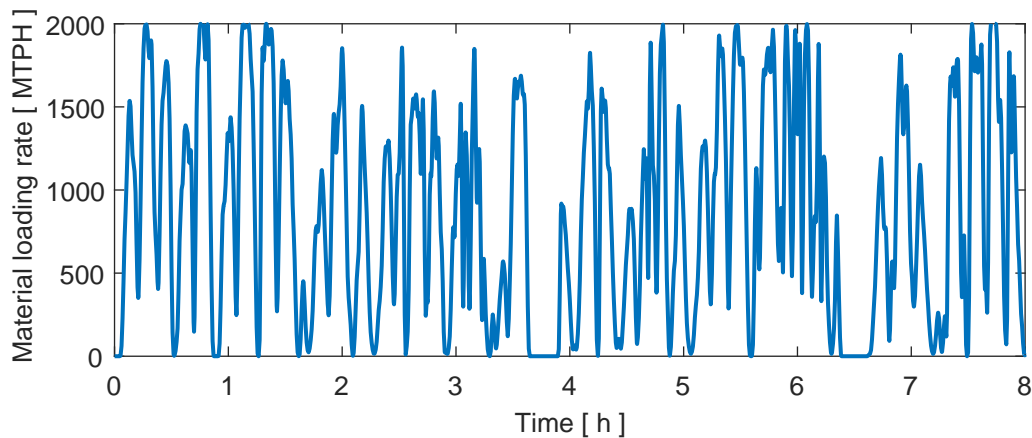
Figure 6.7: Material loading rate onto the upstream conveyor.

simulation runs in order to produce various results. Run 1 is the operation running at nominal speed, and the experimental result of Run 1 is the benchmark of the active speed control. In terms of the fixed time interval strategy, the run set {2,3,4,5} considers different speed sets which are determined by the adjacent speed difference. In Run 2, for instance, the speed set is {2,2.25,2.5,...,4.5,4.75,5} in m/s and the adjacent speed difference is 0.25 m/s. The run set {3,6,7} studies the behaviors of the controller under different time intervals. The run set {3,8} compares the difference between the fixed time interval strategy and the variable time interval strategy.

Table 6.9: Values of the DIN f factor over different loads and speeds. The conveyor is loaded by coal with density 740 kg/m^3. The load is represented by the conveyor utilization U, varying from 0 to 100%. The conveyor speed V is in the range from 2 m/s to 5 m/s with a discrete interval 0.25 m/s. The conveyor is pre-tensioned with 30 kN.

V \ U	0	10%	20%	30%	40%	50%	60%	70%	80%	90%	100%
2	0.0122	0.0118	0.0116	0.0117	0.0119	0.0124	0.0129	0.0137	0.0146	0.0155	0.0166
2.25	0.0125	0.0120	0.0119	0.0120	0.0122	0.0127	0.0133	0.0140	0.0149	0.0159	0.0170
2.5	0.0127	0.0122	0.0121	0.0122	0.0125	0.0130	0.0136	0.0143	0.0152	0.0162	0.0173
2.75	0.0129	0.0124	0.0123	0.0125	0.0128	0.0132	0.0139	0.0146	0.0155	0.0165	0.0175
3	0.0130	0.0126	0.0125	0.0126	0.0130	0.0134	0.0141	0.0148	0.0157	0.0167	0.0178
3.25	0.0131	0.0127	0.0127	0.0128	0.0131	0.0136	0.0143	0.0150	0.0159	0.0169	0.0180
3.5	0.0132	0.0128	0.0128	0.0129	0.0133	0.0138	0.0144	0.0152	0.0161	0.0171	0.0182
3.75	0.0133	0.0129	0.0129	0.0130	0.0134	0.0139	0.0146	0.0153	0.0162	0.0172	0.0183
4	0.0134	0.0130	0.0130	0.0131	0.0135	0.0140	0.0147	0.0155	0.0164	0.0174	0.0184
4.25	0.0135	0.0131	0.0130	0.0132	0.0136	0.0141	0.0148	0.0155	0.0165	0.0175	0.0185
4.5	0.0135	0.0131	0.0131	0.0133	0.0136	0.0142	0.0148	0.0156	0.0165	0.0175	0.0186
4.75	0.0136	0.0132	0.0131	0.0133	0.0137	0.0142	0.0149	0.0157	0.0166	0.0176	0.0187
5	0.0136	0.0132	0.0132	0.0134	0.0137	0.0143	0.0149	0.0157	0.0166	0.0176	0.0187

Table 6.10: Experiment plan of the active speed control.

Simulation run	1	2	3	4
Control strategy	Nominal speed	Fixed time interval		
Time interval	-	30 seconds		
Speed set (m/s)	{5}	{2,2.25,2.5,...,4.5,4.75,5}	{2,2.5,3...,4.5,5}	{2,3,4,5}

Simulation run	5	6	7	8
Control strategy	Fixed time interval		Variable time interval	
Time interval	30s	20 seconds	10 seconds	Variable
Speed set (m/s)	{2,3.5,5}		{2,2.5,3...,4.5,5}	Variable

6.3.3 Results and Discussion

Table 6.11 shows the experimental results of simulation runs. Due to the fact that the upstream conveyor consistently is running at nominal speed in these eight simulation runs, the simulation results of the upstream conveyor are excluded. As the data in Table 6.11 shows, all the simulation runs achieve power savings if the concerned belt conveyor is actively controlled.

Table 6.11: Experimental results of the downstream conveyor under active speed control over 8 hours.

Simulation run	1	2	3	4	5	6	7	8
Total conveying in eight hours ($tons$)	6,900							
Average loading rate $Q(MTPH)$	866							
Average speed $v(m/s)$	5	3.02	3.09	3.23	3.39	3.04	2.99	2.95
Average conveyor utilization $U(\%)$	43.4	67.0	65.5	62.2	59.2	66.5	67.8	68.8
Average power consumption $P(kW)$	97.4	70.0	70.8	72.5	75.3	70.2	69.6	68.9
Power saving ΔP (kW)	-	27.4	26.6	25.0	22.1	27.2	27.8	28.5
($\%$)	-	28	27	26	23	28	29	29
Electricity consumption $W(kWh)$	779	560	566	580	602	562	557	551
Consumption saving $\Delta W(kWh)$	-	219	213	200	177	218	223	228

Figure 6.8 shows the influence of speed sets under the fixed time interval strategy. In Run 2, the minimum speed increment is 0.25 m/s and the speed set has 13 elements. However, in Runs 3 to 5, the minimum increment is defined as 0.5 m/s, 1 m/s and 1.5 m/s, respectively. Accordingly, the number of elements is reduced to 7, 4 and 3, respectively. Generally, the smaller the minimum increment is, the more sensitive the speed controller is and the more power you can save. This is proved by the comparison in Figure 6.8. The diagram of Figure 6.8a illustrates the average conveyor utilization in each hour and Figure 6.8b shows the average power consumption. As the data shows, Run 2 consistently results in the highest utilization rate. By way of contrast, the result of Run 5 shows the lowest average utilization rate. This is also proved by the data in Table 6.11. Over the eight hours' operation, the utilization in Run 2 reaches up to 67% as compared to 29% in Run 5. Correspondingly, Run 2 uses the least number of electricity and Run 5 consumes the most, see Table 6.11 and Figure 6.8b.

The simulation run sets {3,6,7} studies different time intervals of the fixed time interval strategy. In Run 3, the time interval is set to 30 seconds, while the value in Runs 6 and 7 is 20 and 10 seconds, respectively. The experimental results are illustrated in Figure 6.9. The data of Figure 6.9a shows that the high utilization rate can be achieved when a small time interval is used. As a consequence, Runs 6 and 7 consume less power compared to Run 3, see Figure 6.9b. In addition, the comparison between Figures 6.8 and 6.9 suggests that the definition of the speed set has a larger impact on the energy savings than the selection of the time interval.

Figure 6.10 compares the fixed and variable time interval strategies. Run 3 uses the fixed time interval strategy and Run 8 employs the variable time interval strategy. The definitions of the speed set in Runs 3 and 8 are the same, {2,2.5,3,..,4,4.5,5} in m/s. The diagram of Figure 6.10a compares the conveyor utilization over time. As the diagram indicates, the utilization

rate in Run 8 is higher than that in Run 3. In addition, due to the high conveyor utilization, the operation in Run 8 consumes less power than that in Run 3, see Figure 6.10b. Due to the fact that the variable time interval strategy can be viewed as the fixed time interval strategy with a time interval equaling the sampling period of the material flow sensor, it is safe to conclude that the variable time interval strategy can improve the conveyor utilization and can enable more power reduction of belt conveyors, if the variable interval strategy uses the same speed set of the fixed time interval strategy.

Figures 6.11 to 6.18 detail the experimental results of simulation runs.

(a)

(b)
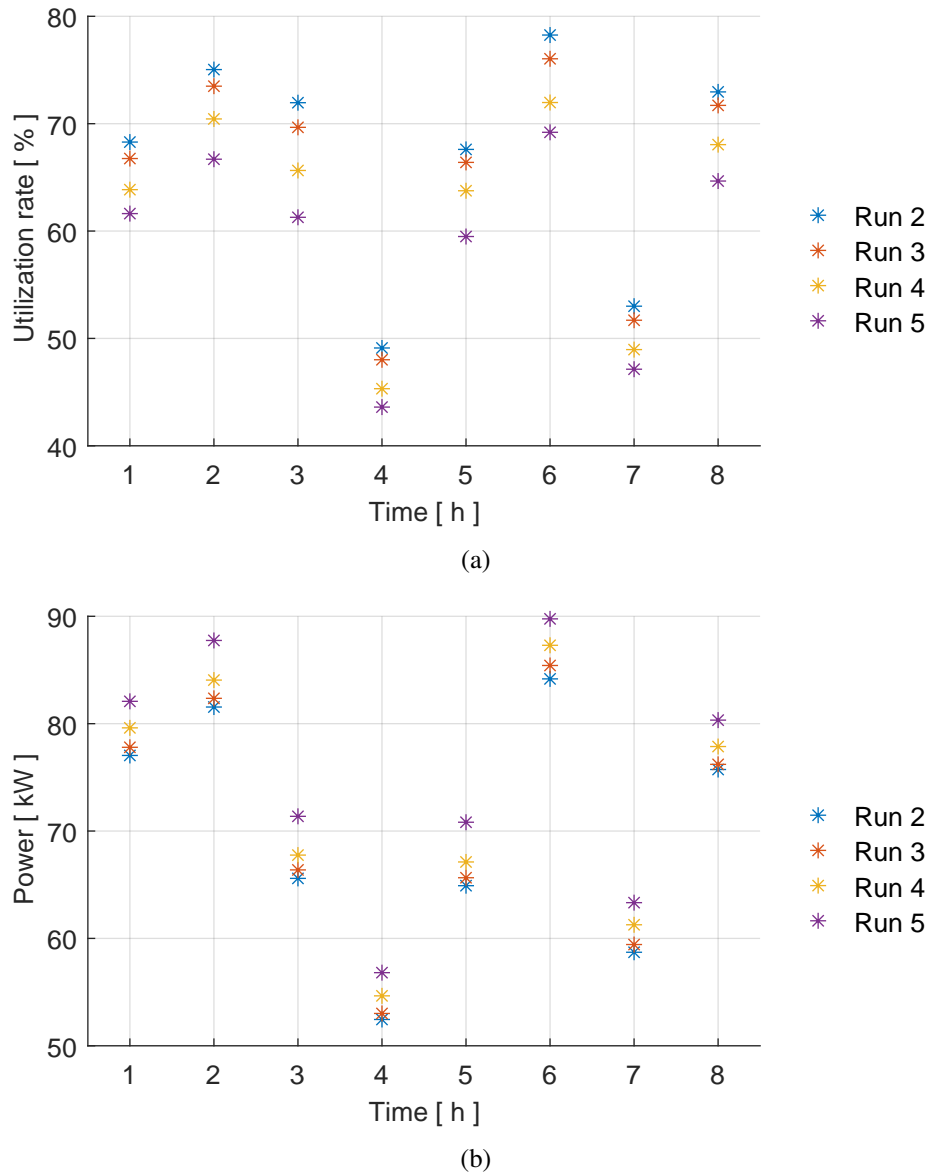
Figure 6.8: Influence of the speed sets to the final values of the main performance indicators.
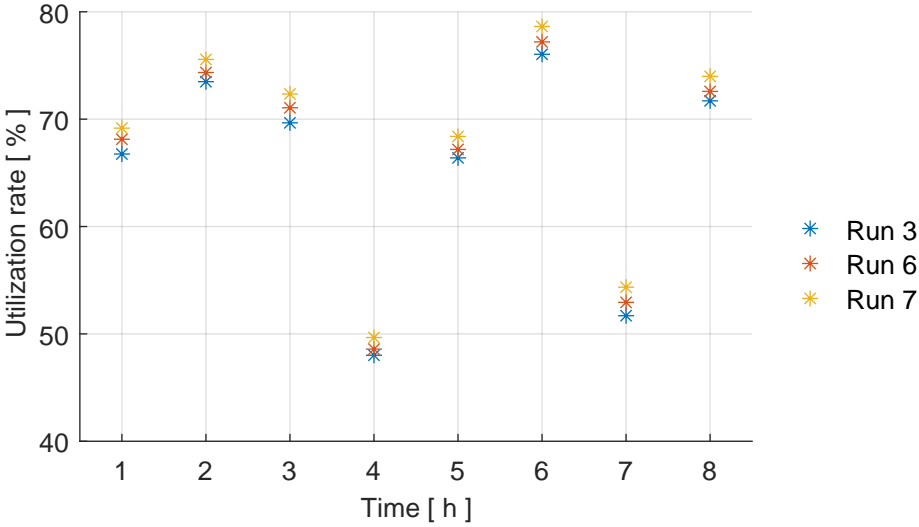
(a)
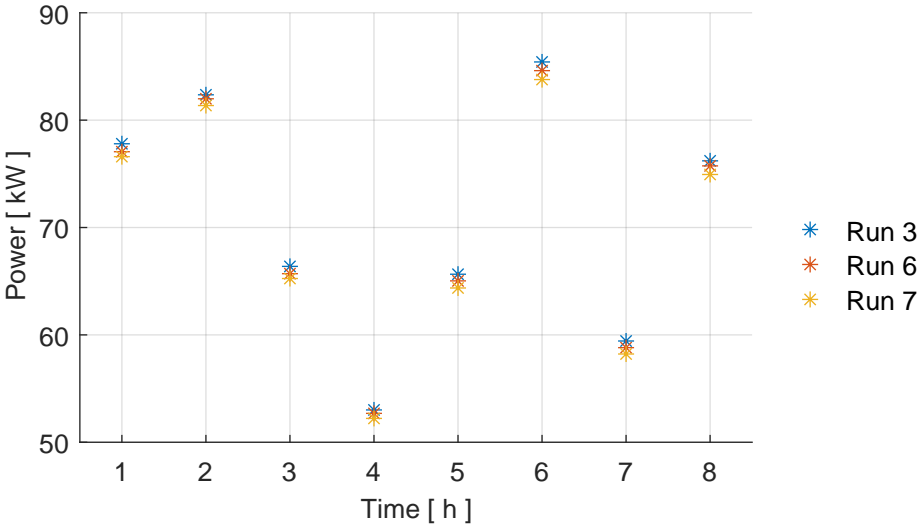
(b)

Figure 6.9: Influence of the time intervals to the final values of the main performance indicators.

(a)

(b)
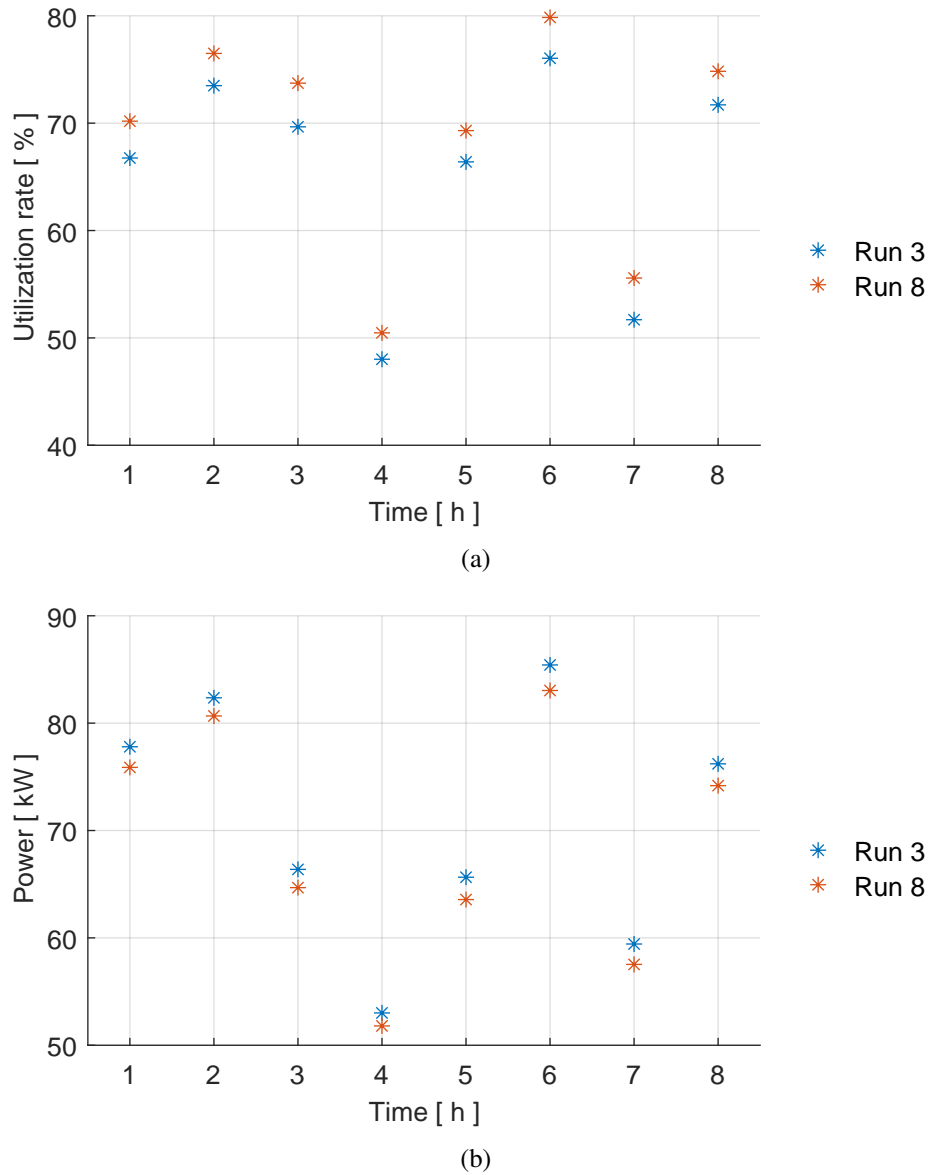
Figure 6.10: Influence of the control strategy to the final values of the main performance indicators.
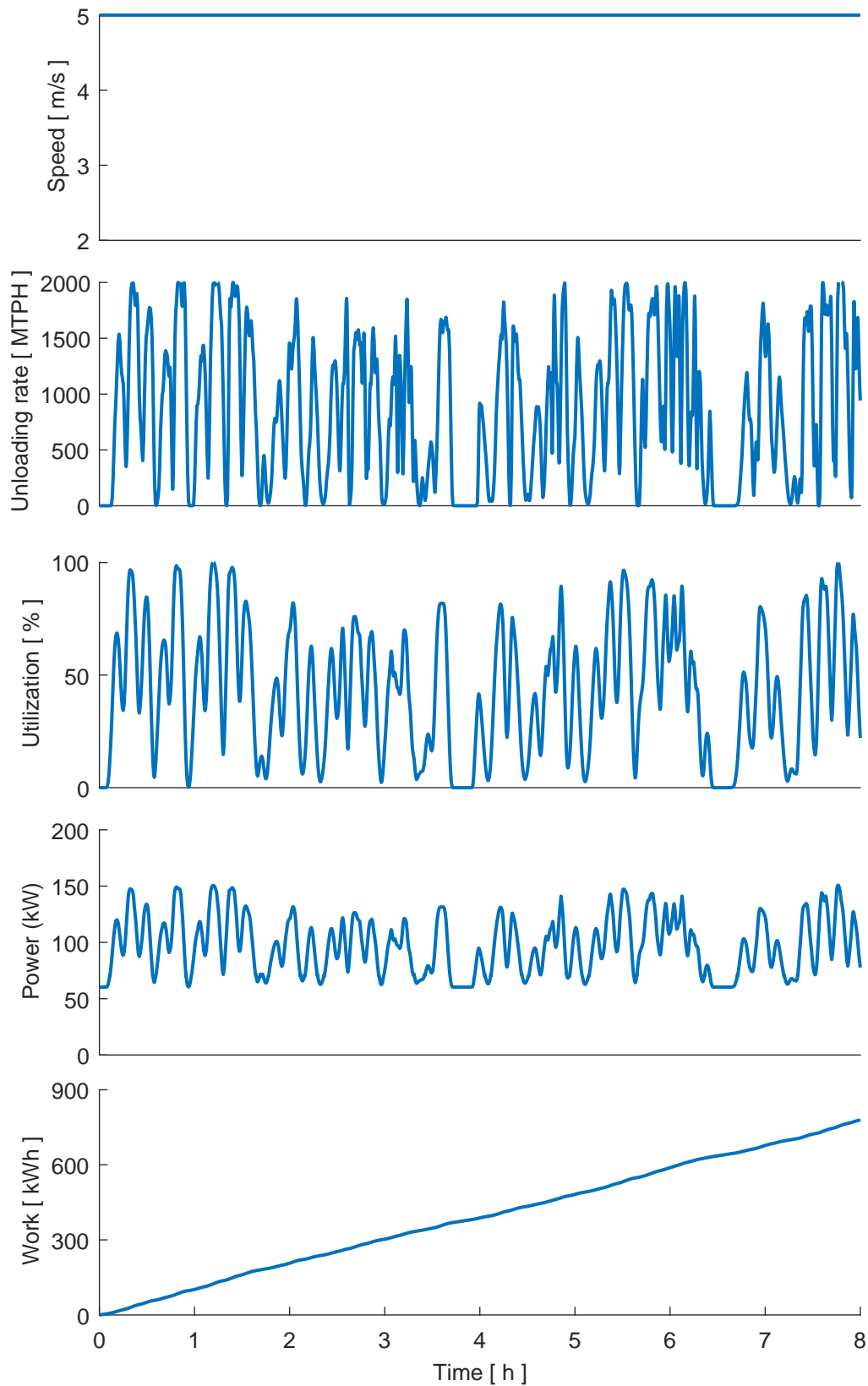
Figure 6.11: Experimental results of Run 1 where the conveyor is running at nominal speed. Averagely, the conveyor utilization is 43.4% and the power consumption is 97 kW. After eight hours' operation, the total energy consumption is around 780 kWh.
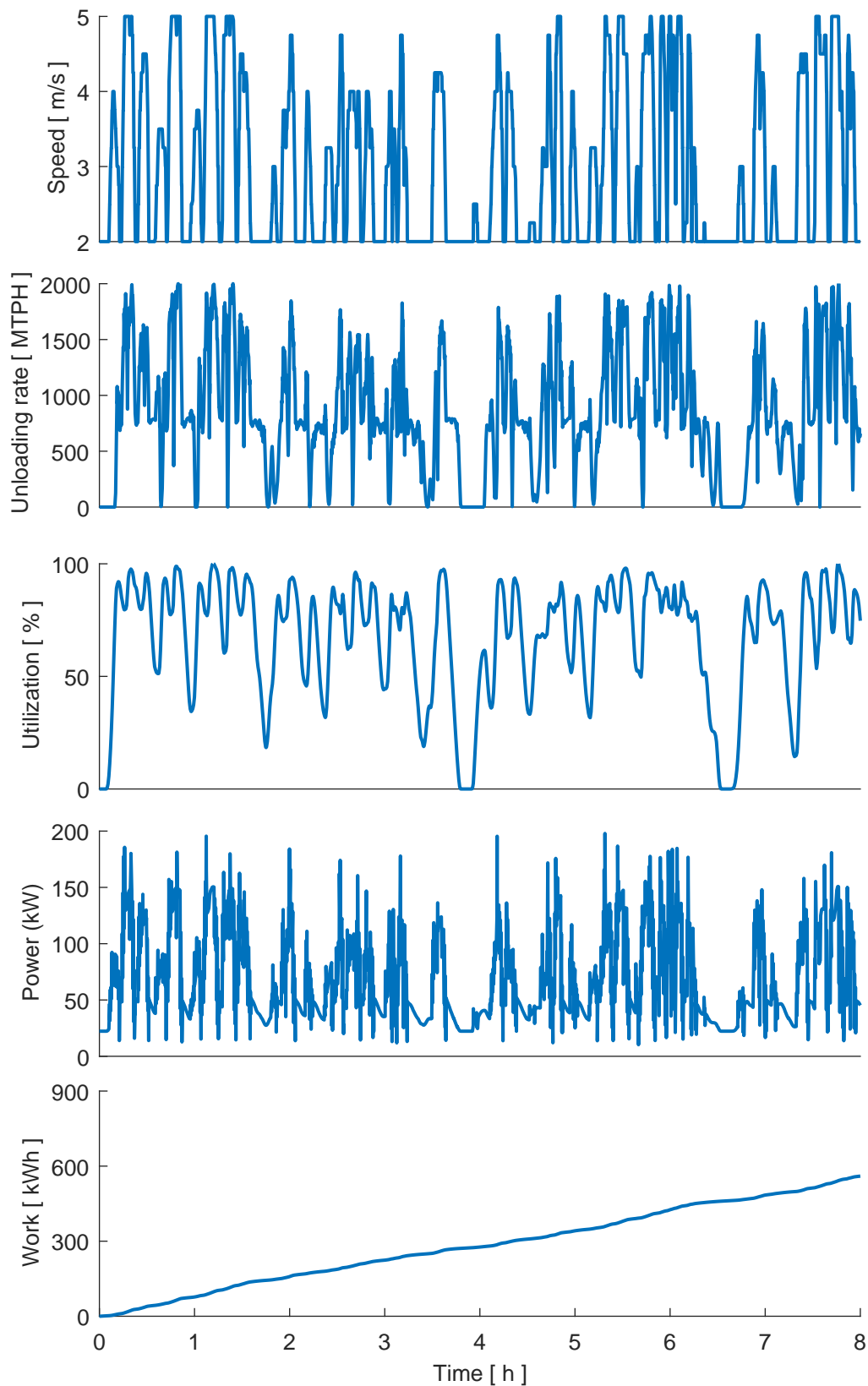
Figure 6.12: Experimental results of Run 2 where the conveyor speed is actively controlled with the fixed time interval strategy. The time interval is 30 seconds. The speed set is {2,2.25,2.5,..,4.5,4.75,5} in m/s. Averagely, the conveyor speed is 3.02 m/s and the conveyor utilization is 67.0%. The power consumption is 70 kW in an average. After eight hours' operation, the total energy consumption is 560 kWh.
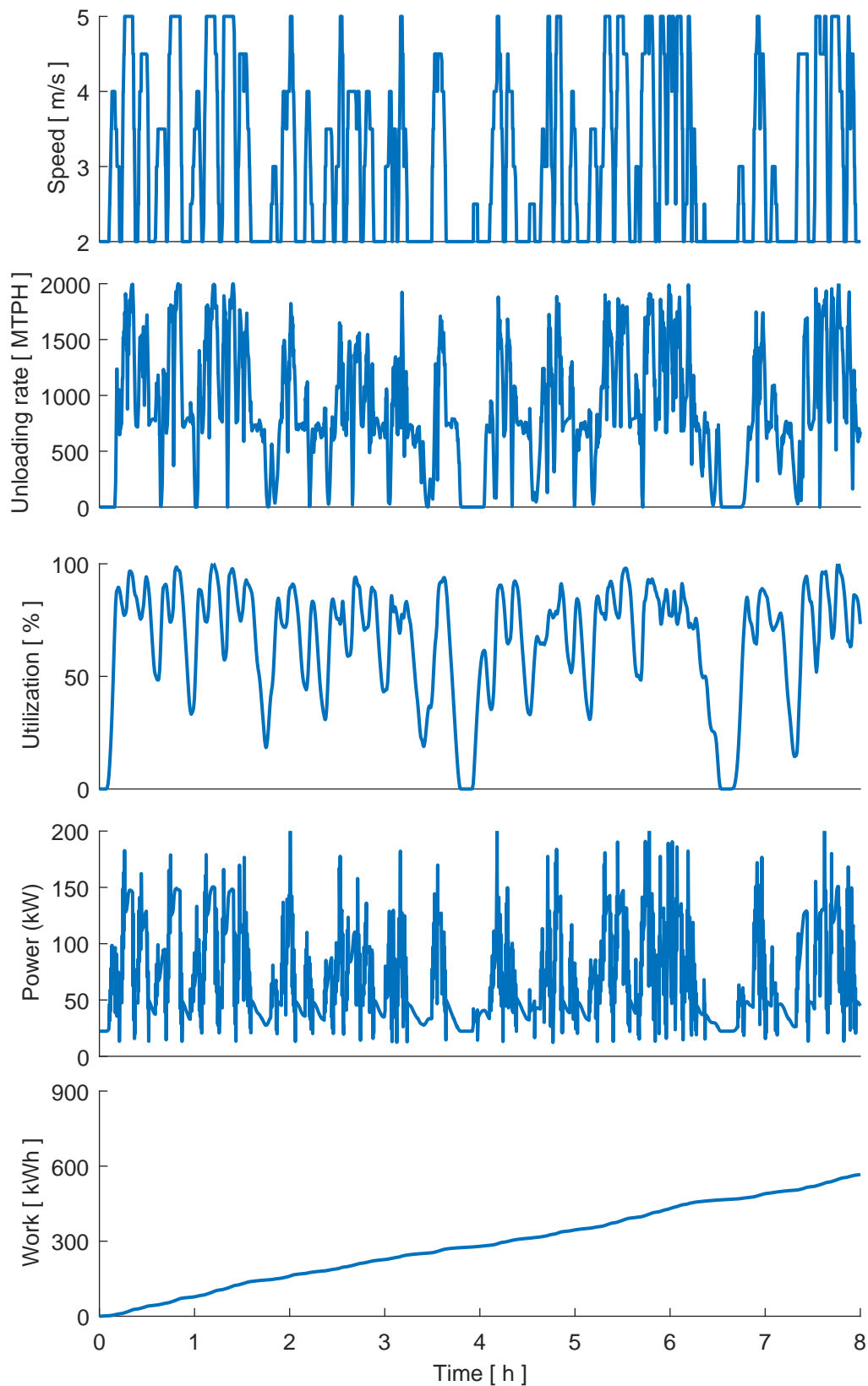
Figure 6.13: Experimental results of Run 3 where the conveyor speed is actively controlled with the fixed time interval strategy. The time interval is 30 seconds. The speed set is {2,2.5,3,..,4,4.5,5} in m/s. Averagely, the conveyor speed is 3.09 m/s and the conveyor utilization is 65.5%. The power consumption is 71 kW in an average. After eight hours' operation, the total energy consumption is 566 kWh.
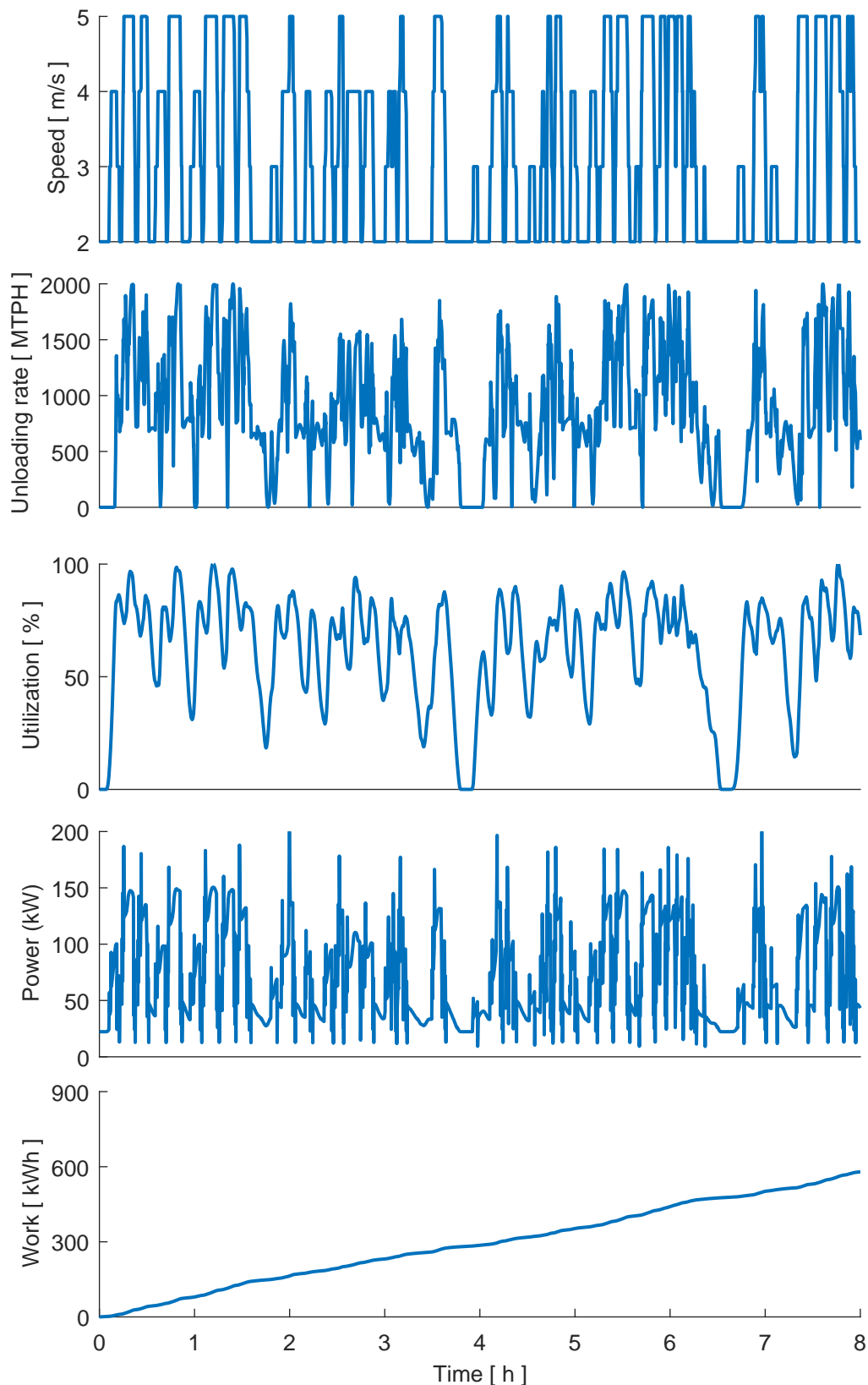
Figure 6.14: Experimental results of Run 4 where the conveyor speed is actively controlled with the fixed time interval strategy. The time interval is 30 seconds. The speed set is {2,3,4,5} in m/s. Averagely, the conveyor speed is 3.23 m/s and the conveyor utilization is 62.2%. The power consumption is 72.5 kW in an average. After eight hours' operation, the total energy consumption is 580 kWh.
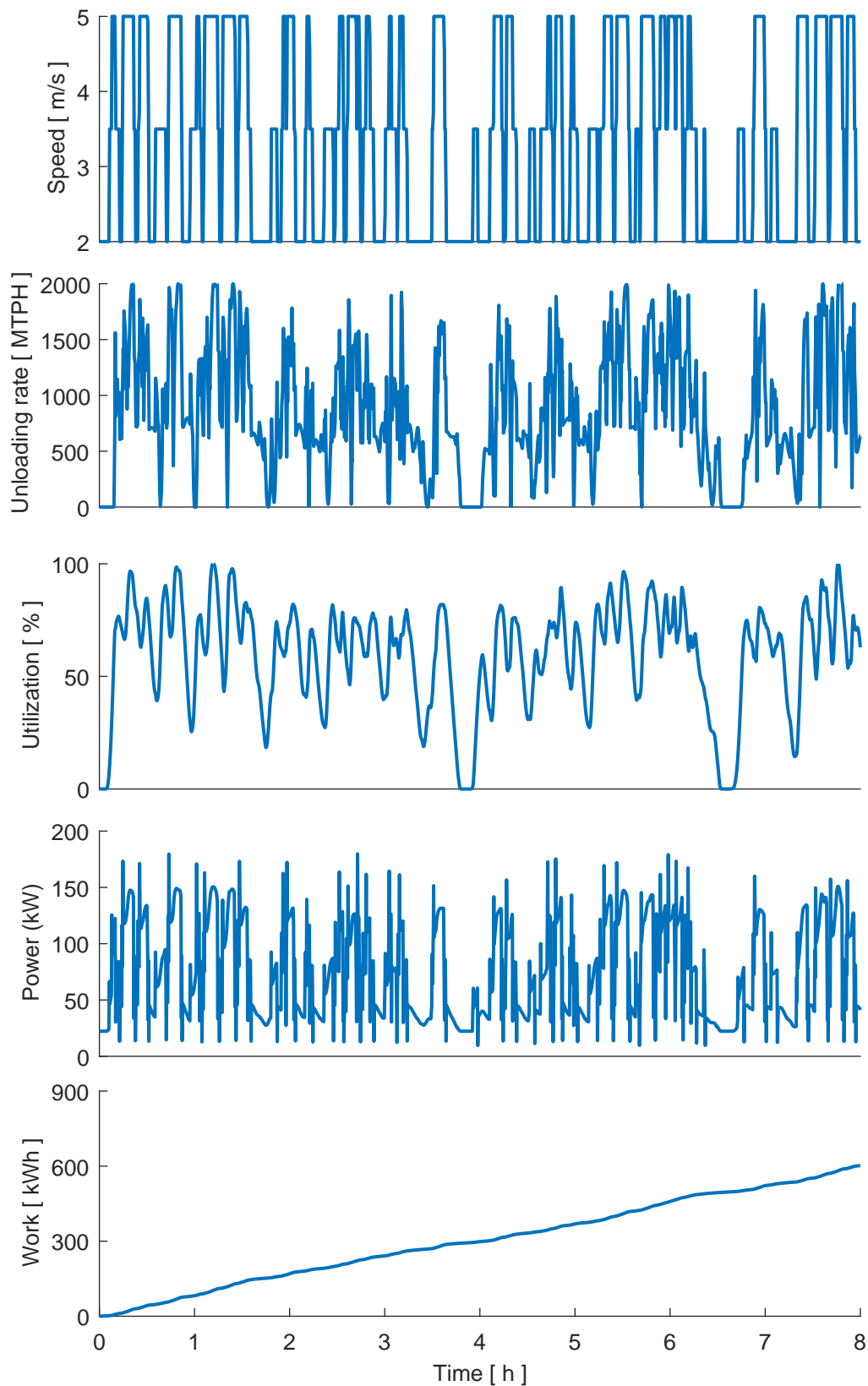
Figure 6.15: Experimental results of Run 5 where the conveyor speed is actively controlled with the fixed time interval strategy. The time interval is 30 seconds. The speed set is {2,3.5,5} in m/s. Averagely, the conveyor speed is 3.39 m/s and the conveyor utilization is 59.2%. The power consumption is 75.3 kW in an average. After eight hours' operation, the total energy consumption is 602 kWh.
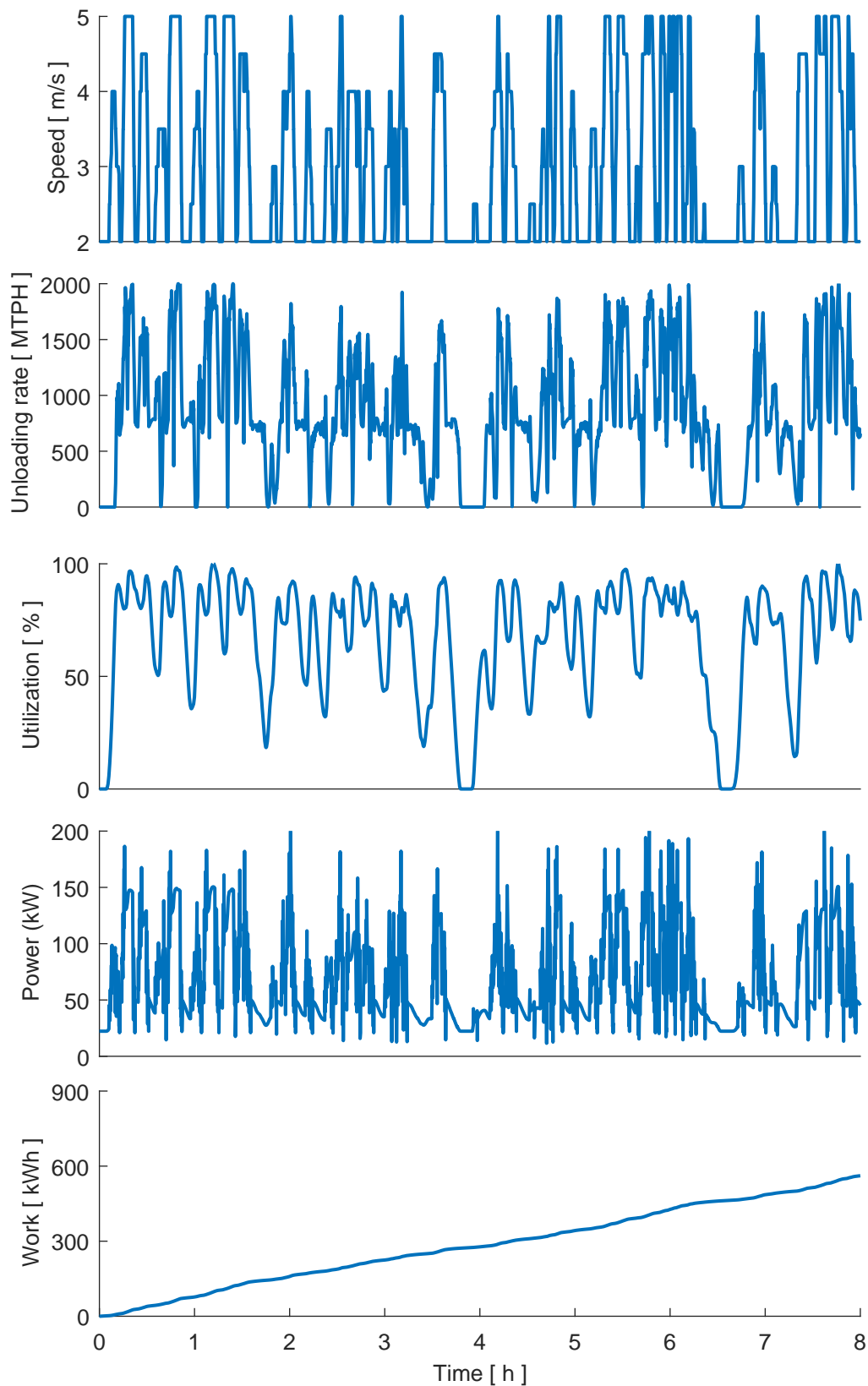
Figure 6.16: Experimental results of Run 6 where the conveyor speed is actively controlled with the fixed time interval strategy. The time interval is 20 seconds. The speed set is {2,2.5,3,..,4,4.5,5} in m/s. Averagely, the conveyor speed is 3.04 m/s and the conveyor utilization is 66.5%. The power consumption is 70.2 kW in an average. After eight hours' operation, the total energy consumption is 562 kWh.
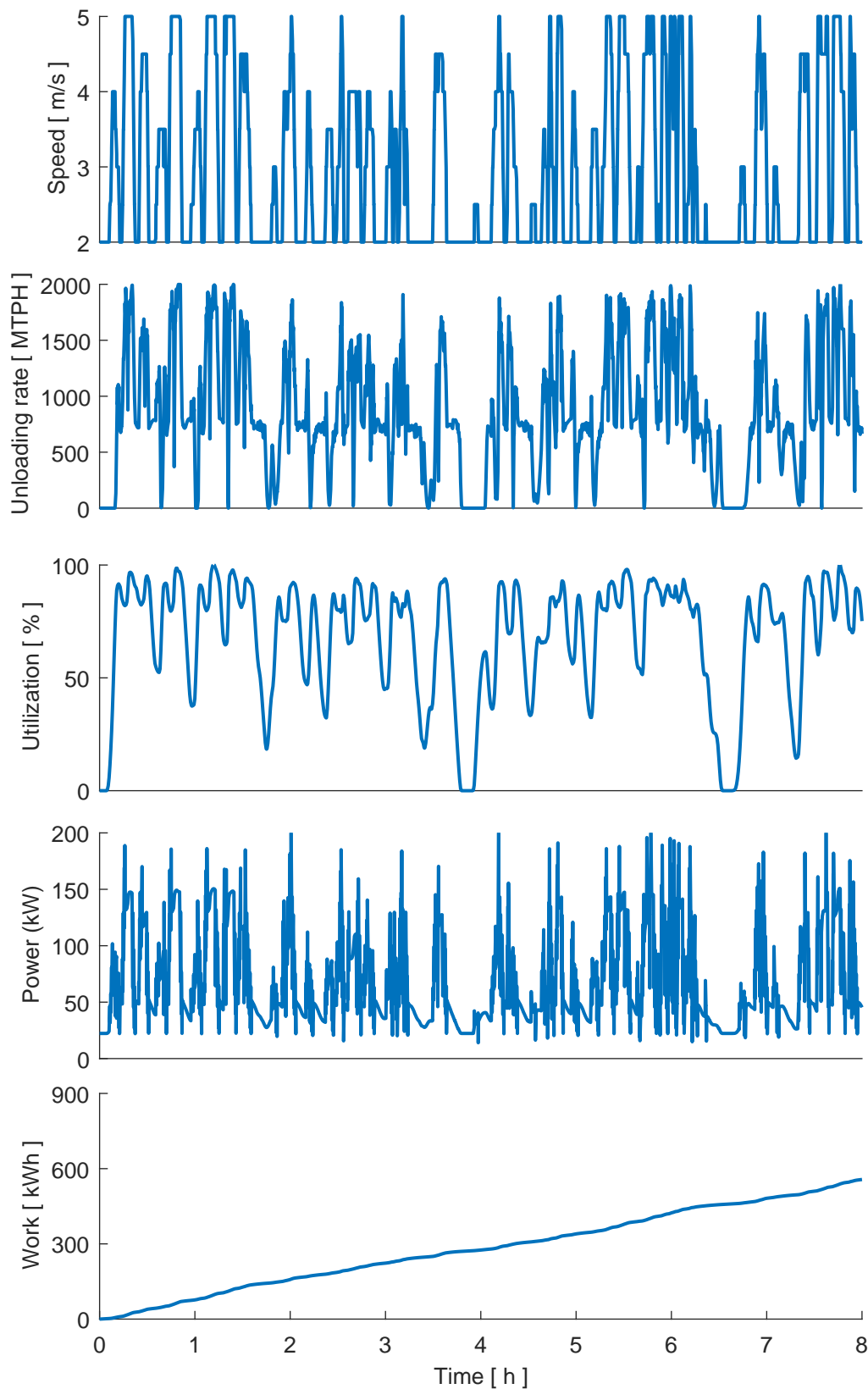
Figure 6.17: Experimental results of Run 7 where the conveyor speed is actively controlled with the fixed time interval strategy. The time interval is 10 seconds. The speed set is $\{2,2.5,3,..,4,4.5,5\}$ in m/s. Averagely, the conveyor speed is 2.99 m/s and the conveyor utilization is 67.8%. The power consumption is 69.6 kW in an average. After eight hours' operation, the total energy consumption is 557 kWh.
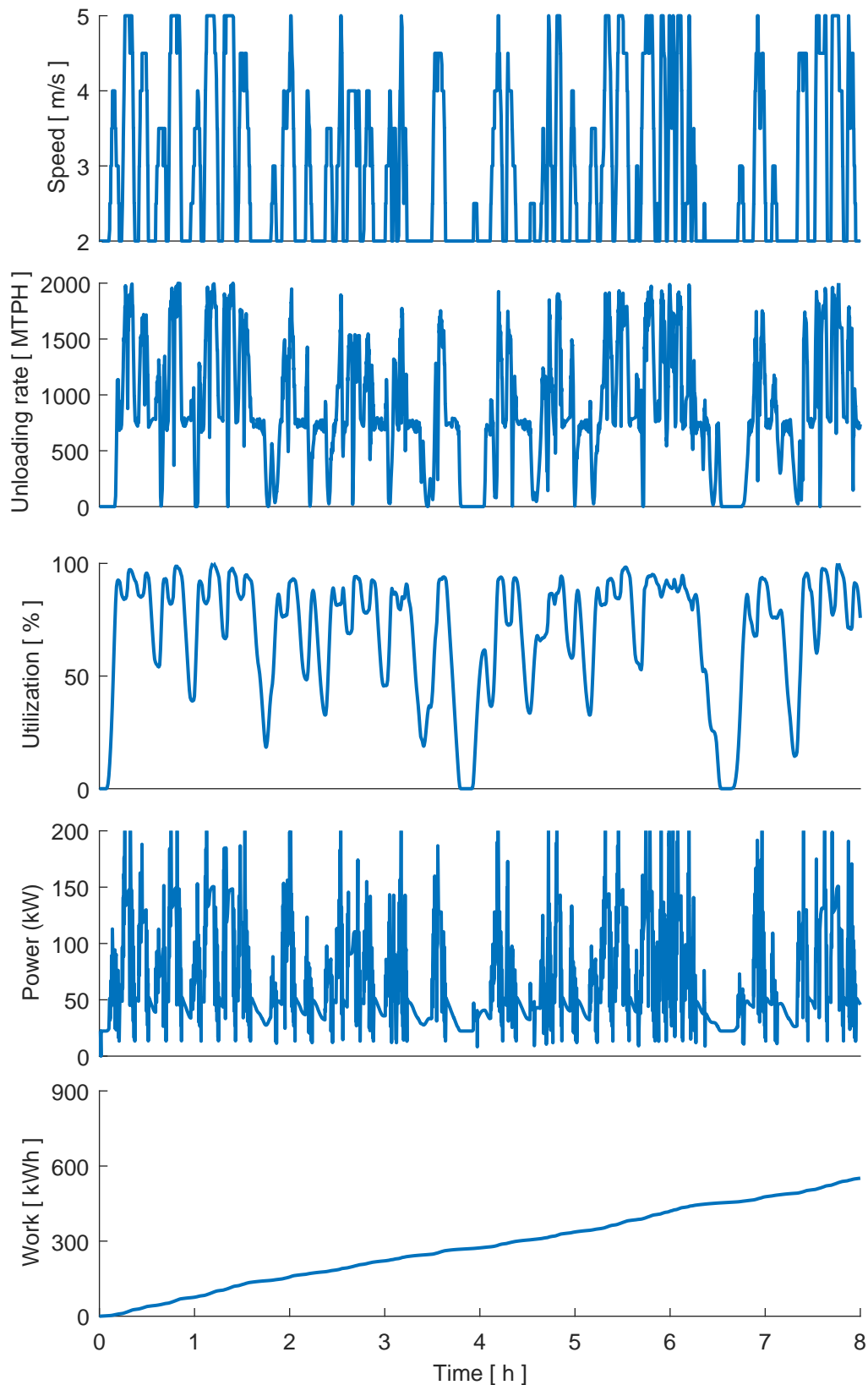
Figure 6.18: Experimental results of Run 8 where the conveyor speed is actively controlled with the variable time interval strategy. The speed set is {2,2.5,3,..,4,4.5,5} in m/s. Averagely, the conveyor speed is 2.95 m/s and the conveyor utilization is 68.8%. The power consumption is 68.9 kW in an average. After eight hours' operation, the total energy consumption is 551 kWh.

6.4   Conclusion

This chapter analyzed and compared the conveyor performance under difference control manners. Based on the experimental results, a general conclusion can be given that the power consumption can be reduced if the conveyor speed is running at a lower speed. According to the experimental results, the f factor value has a considerable variation between different loads and speeds. In the case of non-nominal loading rate, if the conveyor speed is reduced then the conveyor utilization is increased as a consequence, and the DIN f factor value has an increase as compared to the operation running at nominal speed. Nevertheless, the experimental results show a positive power reduction if the conveyor is running at non-nominal speeds. In addition, it can be concluded from the experimental results that for the defined belt conveyor, the optimum conveyor speed generally is that enables 100% conveyor utilization rate. Moreover, the experimental results suggests that if the DIN f factor value is treated as a constant, the final power saving rate may be over-estimated as compared to the variable DIN f value.

In terms of the active speed control with the fixed time interval strategy, the simulation results show that the conveyor utilization improvement and the power reduction vary with different speed sets. In addition, the results indicate that the definition of the time interval also has an impact to the final result of power savings. Moreover, the experimental results further suggests that the variable time interval strategy generally is more efficient than the fixed time interval strategy.

Chapter 7

Conclusions and recommendations

The goal of the thesis is to investigate the application of speed control to belt conveyors for reducing energy consumption. The main body of the thesis is composed of five chapters, each of them answering one of the key research questions presented in Chapter 1. To reflect the research in previous chapters, this chapter firstly provides conclusions in Section 7.1. Recommendations for further researches are discussed in Section 7.2.

7.1   Conclusions

In the thesis, the following main research question was addressed: *How well can belt conveyors perform under speed control, taking both the dynamic belt performance and the energy savings into account?* To answer this question, five sub research questions were formulated in Chapter 1. The answers to these questions are as follows:

- **What is the research status of the belt conveyor speed control?**

  Chapter 2 reviewed the academic researches and the industrial applications of speed control. Through the literature review, it can be concluded that speed control is a promising approach for reducing power consumption of belt conveyors. The research on speed control has been carried out for decades. However, these researches fail to cover some issues like the dynamic performance and the potential risks on belt conveyors in transient operations. The literature review further shows that, rare implementations of speed control can be found in practice to reduce energy consumption. Moreover, the literature survey suggests that, the current research on investigating the application of belt conveyor speed control faces two major challenges: providing a method to determine the requested minimum speed adjustment time to ensure healthy dynamics of a belt conveyor during transient operations, and seeking an accurate energy model to assess the effectiveness of the belt conveyor speed control.

- **How to determine the permitted maximum acceleration and the demanded minimum acceleration time in transient operations, taking both potential risks and dynamic performances of belt conveyors during speed control into account?**

  Unhealthy conveyor dynamics can result in risks like belt over-tension and belt slippage around the drive pulley during transient operations. To improve the applicability of speed control, Chapter 3 proposed the Estimation-Calculation-Optimization (ECO) method to calculate the minimum speed adjustment time. The ECO method is derived from the method provided by Lodewijks (1997). It takes both the potential risks and the conveyor dynamics in transient operations into account. From the experimental results, it can be observed that the finite element method has been successfully used to examine the conveyor dynamic performance in transient operations. The experimental data also indicates that the transient operations with the initialized acceleration time may result in risks like belt slippage. In addition, it also shows that these risks can successfully be prevented if the optimized speed adjustment time is used. Above all, the conclusion can be drawn that the ECO method has successfully determined the required minimum speed adjustment time.

- **How to accurately estimate the energy consumption of belt conveyors?**

  Chapter 4 introduced the energy model based on the standard DIN 22101 (German Institute for Standardization, 2015), and proposed the analytical method to calculate the DIN f factor value. The calculation result shows that, when the concerned belt conveyor is running at nominal speed with fully loaded, the DIN f factor equals 0.0187. The value is in the range from 0.01 to 0.02, which is suggested by DIN 22101. From the experimental data, it can be further observed that the variations of loads and of speeds have a considerable impact on the f factor value. In addition, it can also be found that the f factor value has a slight change over different material flow distribution profiles. Moreover, the calculation results show that when the loading rate is at a certain level, a lower speed of a belt conveyor results in a larger DIN f coefficient due to the increase of load. Overall, it is highly suggested to use the variable f factor values to improve the estimation accuracy.

- **How should the belt conveyor speed control system be modeled to assess the conveyor performance under speed control?**

  Chapter 5 modeled the belt conveyor speed control system which was built up by two sub-systems: the operational system and the control system. The comparison between the simulation result and the calculation result shows that the operational system was successfully modeled by the discrete tool. In addition, the experimental result shows that the conflicts between neighboring transient operations were also successfully prevented by the improved control algorithm.

  To evaluate the conveyor performance under speed control, Chapter 5 also defined several key performance indicators (KPIs). The belt utilization rate and the power consumption were grouped into the primary indicators. Derived from the power consumption, some

other indicators were defined as secondary evaluation indicators, such as the total energy consumption, the relevant carbon dioxide (CO_2) emissions and the social cost of carbon.

- **To what extent can the energy consumption be reduced by using speed control in different manners?**

  Chapter 6 carries out the assessment of the speed control performance. Two belt conveyor systems are studied. One system uses the passive speed control. From the steady-state calculation and the dynamic simulation, it clearly shows that the passive speed control allows a certain number of power savings. In addition, the static calculation results show for the concerned belt conveyor, the savings are in the rang from 5% to 27% in terms of different bulk materials. In the dynamic simulation, the average conveyor utilization rate is improved to 79.3% from 47.8%. In addition, the power consumption is reduced by 29.4% on average.

  Another belt conveyor system uses the active speed control. The experimental results show that due to the active speed control, the average conveyor utilization is significantly improved, and that a considerable power reduction is achieved. Due to different control strategies, the average power reduction varies from 23% to 29%. In terms of the fixed time interval strategy, the experimental results further show that both the speed set and the time interval have an impact to the final power savings. In addition, the experimental results indicates that the variable time interval strategy enables more power reduction, compared to the fixed time interval strategy.

7.2 Recommendations

Recommendations for further investigations in the sub topics are formulated as follows:

- **Belt conveyor energy model**

  In the analytical calculation of the DIN f factor value, it is assumed that the conveyor is running at a steady state. The influence of the conveyor dynamics on the f factor value is still unknown. Therefore, it is recommended for the future research to analyze the impact of transient operations to the f factor, taking the conveyor dynamics into account, especially in the cases where the conveyor speed is frequently and/or continuously adjusted.

  Another recommendation is to investigate the influence of the operating condition to the f factor value. In the current analytical calculation, it is assumed that the conveyor is operating in favorable conditions. However, the performance of rollers is affected for instance by lack of lubrication after a long term operation. That will highly increase the frictional resistances of a belt conveyor. Therefore, it is recommended to calibrate the current energy model by using an index determined by the service time of the conveyor.

- **Negative impact of belt conveyor speed control**

  Due to speed control, the conveyor utilization rate can be improved. On the one hand, the increased belt load can have a negative impact on the belt life due to the large frictional

resistances. However, on the other hand, the lower belt speed causes the belt to travel over a smaller distance, which can result in a positive effect on the belt life. Therefore, numerical analyses or experimental measurements are needed to evaluate the exact impact of speed control to the belt life. Similar researches are also recommended on other conveyor components, such as the idler bearings.

- **Economic feasibility of speed control**

  As suggested in Chapter 2, the application of speed control on a belt conveyor at least requires a speed controller, a variable speed drive and a material flow sensor. For an existing belt conveyor system which does not have these devices, it may require a large capital investment to realize speed control. If a belt conveyor is equipped with multiple drive units, more investment is needed. Therefore, it is recommended to evaluate the economic feasibility of speed control by comparing the extra capital investment for speed control and the cost savings in certain years by means of speed control. In addition, the extra costs caused by like maintenance also should be taken into account.

Bibliography

Aarniovuori, L., Laurila, L., Niemelä, M., Pyrhönen, J., Oct. 2007. Loss calculation of a frequency converter with a fixed-step circuit simulator. Aalborg, pp. 1–9.

ABB, 2000. Variable-speed drives for belt-conveyor systems. Project report IN/BF 0901 EN, ABB Process Industries GmbH, Germany.

Al-Sharif, L., 2007. Intelligent braking systems for public service escalators. Elevator World 55 (1), p. 122.

Alles, R., 1994. Conveyor belt service manual- Conveyor belt system design. ContiTech Tranporband systeme GmbH, Hannover, Germanny.

Alspaugh, M., 2004. Latest developments in belt conveyor technology. In: MINExp200, LasVegas, NV, USA. LasVegas, United States.
URL `http://www.overlandconveyor.com/pdf/Latest%20Developments%20in%20Belt%20Conveyor%20Technology.pdf`

Anonymity, 2016. Speed control of DC motor.
URL `http://www.electrical4u.com/speed-control-of-dc-motor/`

A.P. Wiid, F. Sithole, M. Bagus, T.H. Khosa, 2009. Constant speed versus variable speed operation for belt conveyor systems. South Africa.
URL `http://www.beltcon.org.za/docs/b1502.pdf`

Attaway, S. W., 1999. The mechanics of friction in rope rescue. pp. 1–16.

Barnes, M., 2003. Practical variable speed drives and power electronics. Newnes.

Belzona, 2016. Belzona gets grip on conveyor slippage.
URL `http://khia.belzona.com/EN/view.aspx?id=1256`

BMG, 2016. BMG conveyor services- inspection and training.
URL `http://www.bmgtampa.com/Inspection-and-Training.html`

Boglietli, A., Cavagnino, A., Lazzari, M., Pastorelli, A., 2003. Induction motor efficiency measurements in accordance to IEEE 112-B, IEC 34-2 and JEC 37 international standards. Vol. 3. IEEE, pp. 1599–1605.

Brander, M., Sood, A., Wylie, C., Haughton, A., Lovell, J., 2011. Electricity-specific emission factors for grid electricity. White paper.

Conveyor Equipment Manufacturers Association, Apr. 2005. Belt conveyors for bulk materials, 6th Edition. CEMA.

ConveyorBeltGuide, 2016. Conveyor components.
URL http://www.conveyorbeltguide.com/Engineering.html

Dalgleish, A., Grobler, L., 2003. Measurement and verification of a motor sequencing controller on a conveyor belt. Energy 28 (9), pp. 913–927.

Daniel Clénet, Jan. 2010. Optimising energy efficiency of conveyors.
URL http://www2.schneider-electric.com/documents/original-equipment-manufacturers/pdf/Energy-efficiency-of-conveyors.pdf

Daus, W., Koerber, S., Becker, N., 1998. Raw coal loading and belt conveyor system at Nochten Opencast Mine- A new conveying and loading system based on drives controlled and adjusted by frequency converter. BRAUNKOHLE 50 (2), pp. 117–130.

Dilefeld, M., Jul. 2014. Gearless belt conveyor drives-The new technology for high capacity systems.
URL http://www.bulk-solids-handling.com/?q=topics/conveying-transportation/mechanical-belt-conveyor-systems/gearless-belt-conveyor-drives

Dilshad, M., Ashok, S., Vijayan, V., Pathiyil, P., 2016. An energy loss model based temperature estimation for permanent magnet synchronous motor (PMSM). IEEE, Chennai, pp. 172–176.

EagleTechnologies, Jun. 2010. Conveyor systems: a brief history.
URL http://eagletechnologies.com/conveyer-systems-a-brief-history/

Edenhofer, O., Pichs-Madruga, R., Sokona, Y., Seyboth, K., Kadner, S., Zwickel, T., Eicke-meier, P., Hansen, G., Schlömer, S., von Stechow, C., 2011. Renewable energy sources and climate change mitigation: Special report of the intergovernmental panel on climate change. Cambridge University Press.

Emadi, A., 2004. Energy-efficient electric motors, 3rd Edition. CRC Press, Chicago.

Encyclopedia, 2010. Fluid coupling: automobiles.
URL http://kids.britannica.com/comptons/art-167124/Oil-permits-the-fluid-coupling-to-slip-at-low-speeds

Entelwein, F., 1832. Handbuch der statik Fester korper... G. Reimer.

Euler, M. L., 1762. Remarques sur l'effect du frottement dans l'equilibre. Mem. Acad. Sci 18, pp. 265–278.

Eurostat, Apr. 2016. Electricity prices for industrial consumers-bi-annual data.
URL http://ec.europa.eu/eurostat/statistics-explained/index.php

Falkenberg, S., Wennekamp, T., 2008. Doping of conveyor belt materials with nanostructured fillers to adapt innovative performance characteristics. IEEE, pp. 1526–1533.

Fernandes, C. M., Marques, P. M., Martins, R. C., Seabra, J. H., 2015. Gearbox power loss. Part II: friction losses in gears. Tribology International 88, pp. 309–316.

FLSmidth Pfister Limited, 2017. Steel belt weighers.
URL http://www.transweigh-india.com/steel_belt_weighers.html

Fluke Corporation, 2016. 5 steps to measuring output voltage from a VFD to a motor.
URL http://en-us.fluke.com/industries/manufacturing/5-steps-to-measuring-output-voltage-from-a-vfd-to-a-motor.html

Funke, H., 1973. Zum dynamischen verhalten von Förderanlagen beim anfahren und stillsetzen unter berücksichtigung der Bewegungswiderstände. Doctoral Thesis, Hannover University of Technology.

Gerard van den Hondel, 2010. Aramids for low weight and low rolling resistance of conveyor belts. Scotland.

German Institute for Standardization, 2015. Continuous conveyors-Belt conveyors for loose bulk materials-Basis for calculation and dimensioning. Standard DIN 22101, German Institute for Standardization, Germany.

Goto, K., Yogo, K., Higashii, T., Nov. 2013. A review of efficiency penalty in a coal-fired power plant with post-combustion CO_2 capture. Applied Energy 111, pp. 710–720.
URL http://www.sciencedirect.com/science/article/pii/S0306261913004212

Graaf, M. d., Jan. 2013. Viability study of an energy-recovery system for belt conveyors. Research assignment 2013.TEL.7747, Delft University of Technology, Delft.

Harrison, A., 1983. Criteria for minimising transient stress in conveyor belts. Mechanical Engineering Transactions 8 (3), pp. 129–134.

He, D., Pang, Y., Lodewijks, G., 2016a. Belt conveyor dynamics in transient operation for speed control. International Journal of Civil, Environmental, Structural, Construction and Architectural Engineering 10 (7), pp. 828–833.

He, D., Pang, Y., Lodewijks, G., 2016b. Determination of acceleration for belt conveyor speed control in transient operation. International Journal of Engineering and Technology 8 (3), pp. 206–211.

He, D., Pang, Y., Lodewijks, G., 2016c. Speed control of belt conveyors during transient operation. Powder Technology 301, pp. 622–631.

Hetzel, F. V., 1922. Belt conveyors and belt elevators. J. Wiley and Sons.

Hiltermann, J., Jul. 2008. Reducing the electrical power consumption of troughed belt conveyor by speed control. Masters Thesis, Delft University of Technology, Delft, the Netherlands.

Hiltermann, J., Lodewijks, G., Schott, D. L., Rijsenbrij, J. C., Dekkers, J. A. J. M., Pang, Y., 2011. A methodology to predict power savings of troughed belt conveyors by speed control. Particulate science and technology 29 (1), pp. 14–27.

Hunter, S. C., Dec. 1961. The rolling contact of a rigid cylinder with a viscoelastic half space. Journal of Applied Mechanics 28 (4), pp. 611–617.
    URL http://dx.doi.org/10.1115/1.3641792

International Energy Agency, 2015. CO2 emissions from fuel combustion highlight. France.
    URL   https://www.iea.org/publications/freepublications/publication/
    CO2EmissionsFromFuelCombustionHighlights2015.pdf

International Organization for Standardization, 1989. Continuous mechanical handling equipment- Belt conveyors with carrying idlers- calculation of operating power and tensile forces. standard ISO 5048:1989 (E), International Organization for Standardization, Switzerland.

Jeftenic, B., Ristic, L., Bebic, M., Statkic, S., Mihailovic, I., Jevtic, D., 2010. Optimal utilization of the bulk material transportation system based on speed controlled drives. IEEE, pp. 1–6.

JLV Industries Pty Ltd, Oct. 2009. Glideseal idler roller technical analysis. Technical Report, Australia.

Kärkkäinen, H., 2015. Converter-fed induction motor losses: Determination with IEC methods. Ph.D. thesis, Lappeenranta University of Technology.

KDHI, 2016. Belt conveyors in Shanghai Port, Luojing Phase II ore terminal.
    URL http://en.kdhi.net/products_detail/&productId=25.html

Kolonja, B., Jeftenić, B., Ignjatović, D., 2003. The application of frequency converters for the regulation of belt conveyor drives in surface mining. Transport i logistika (5), pp. 11–26.

Krause, F., Hettler, W., 1974. Die belastung der tragrollen von gurtbandforderern mit dreiteiligen tragrollenstationen infolge fordergut unter beachtung des fordervorganges und der schuttguteigenschaften. Wissenschaftliche Zeitschrift der Technischen Hochschule Otto von Guericke, Magdeburg, Germany 18 (6/7), pp. 667–674.

Kropf-Eilers, A., Overmeyer, L., Wennekamp, T., 2009. Belt conveying-energy-optimized conveyor Belts–development, test methods and field measurements. bulk solids handling 29 (1), p. 24.

Levi, E., May 2008. Multiphase electric machines for variable-speed applications. Ieee Transactions on Industrial Electronics 55 (5), pp. 1893–1909.
URL ://WOS:000255677200002

Limberg, H., 1988. Untersuchung der raumbezogenen bewegungswiderstände von gurtfördern. Thesis, Hannover University.

Lodewijks, G., 1995. The rolling resistance of conveyor belts. Bulk Solids Handling 15 (1), pp. 15–24.

Lodewijks, G., 1996. Dynamics of belt systems. Doctoral thesis, TU Delft, Delft University of Technology, Delft, the Netherlands.

Lodewijks, G., 1997. Non-linear dynamics of belt conveyor systems. bulk solids handling 17 (1), pp. 57–68.

Lodewijks, G., 2002. Two decades dynamics of belt conveyor systems. Bulk Solids Handling 22 (2), pp. 124–132.

Lodewijks, G., 2011. The next generation low loss conveyor belts. Bulk Solids Handling 32, pp. 52–56.

Lodewijks, G., Kruse, D., 1998. The power of field measurements-part I. Bulk Solids Handling 18, pp. 415–428.

Lodewijks, G., Pang, Y., 2013a. The application of flywheels on belt conveyors. Beltcon 17, pp. 1–10.

Lodewijks, G., Pang, Y., 2013b. Belt de-tensioning in dips. pp. 1–17.

Lodewijks, G., Pang, Y., 2013c. Energy saving options for continuous transport systems, an explorationpp. 214–217.

Lodewijks, G., Schott, D., Pang, Y., 2011. Energy saving at belt conveyors by speed control. pp. 1–10.

Luo, J., Huang, W., Zhang, S., 2014. Energy cost optimal operation of belt conveyors using model predictive control methodology. Journal of Cleaner Production.

Marais, J., 2007. Analysing DSM opportunities on mine conveyor systems. Ph.D. thesis.

May, W. D., Morris, E. L., Atack, D., 1959. Rolling friction of a hard cylinder over a viscoelastic material. Journal of Applied Physics 30 (11), pp. 1713–1724.

Michael Prenner, Franz Kessler, Oct. 2012. Energy recovery system for continuous conveyors. Berlin, pp. 1–16.

Michaelis, K., Höhn, B.-R., Hinterstoißer, M., 2011. Influence factors on gearbox power loss. Industrial lubrication and tribology 63 (1), pp. 46–55.

Mukhopadhyay, A., Chattopadhyay, A., Soni, R., Bhattnagar, M., 2009. Energy efficient idler for belt conveyor systems. Bulk Solids Handling 29 (4), p. 214.

Munzenberger, P., Wheeler, C., Dec. 2016. Laboratory measurement of the indentation rolling resistance of conveyor belts. Measurement 94, pp. 909–918.
URL http://www.sciencedirect.com/science/article/pii/S0263224116304912

Nave, M., 1996. A comparison of soft start mechanisms for mining belt conveyors. Tech. rep., Intertec Presentations, Inc., Englewood, CO (United States).

Nel, P., Shortt, G., 1999. Controlling belt slip. Bulk Solids Handling 19 (4), pp. 481–486.

Nordell, L., 1987. The theory and practice of belt conveyor dynamic analysis. South Africa: Johannesburg.

Nordell, L., 1998. Improving belt conveyor efficiencies: power, strength and life.
URL http://www.ckit.co.za/secure/conveyor/papers/troughed/improving/improving.htm

Nuttall, A., Lodewijks, G., 2007. Dynamics of multiple drive belt conveyor systems. Particle & Particle Systems Characterization 24 (4-5), pp. 365–369.

Nuttall, A. J. G., 2007. Design aspects of multiple driven belt conveyors. Ph.D. thesis, TU Delft, Delft University of Technology.

Pal, S., 2009. Numerical methods: principles, analyses, and algorithms. Oxford University Press.

Pang, Y., 2010. Intelligent belt conveyor monitoring and control. Netherlands TRAIL Research School, Delft, the Netherlands.

Pang, Y., He, D., Lodewijks, G., 2016. Transient acceleration in belt conveyor speed control. Engineers Australia, p. 305.

Pang, Y., Lodewijks, G., 2011. Improving energy efficiency in material transport systems by fuzzy speed control. IEEE, pp. 159–164.

Phillips, G. M., Taylor, P. J., 1996. Theory and applications of numerical analysis. Academic press.

Phoenix Conveyor Belt Systems GMBH, 2004. Phoenix conveyor belts design fundamentals. Brochure 513-102-0804, Hamburg, Germany.

Press, W. H., Flannery, B. P., Teukolsky, S. A., Vetterling, W. T., Kramer, P. B., 1987. Numerical recipes: the art of scientific computing, 2nd Edition. Press Syndicate of the University of Cambridge.

Reznik Leonid, 1997. Fuzzy controllers. Vol. 1. Newnes, Melbourne, Australia.

Ricardo, May 2010. Ricardo launches race-proven GT transmission.
    URL `http://tinyurl.com/z3gd9u2`

Ristic, L., Bebic, M., Jevtic, D., Mihailovic, I., Statkic, S., Rasic, N., Jeftenic, B., 2012. Fuzzy
    speed control of belt conveyor system to improve energy efficiency. IEEE, pp. DS2a. 9–1–
    DS2a. 9–7.

Ristic, L. B., Jeftenic, B. I., Sep. 2011. Implementation of fuzzy control to improve energy
    efficiency of variable speed bulk material transportation. Industrial Electronics, IEEE Trans-
    actions on 59 (7), pp. 2959–2969.
    URL `http://ieeexplore.ieee.org/stamp/stamp.jsp?tp=&arnumber=6029333`

Rodriguez, J., Pontt, J., Becker, N., Weinstein, A., Jan. 2002. Regenerative drives in the
    megawatt range for high-performance downhill belt conveyors. IEEE Transactions on In-
    dustry Applications 38 (1), pp. 203–210.

SICK B.V., 2017. SICK Netherlands.
    URL `https://www.sick.com/nl/en/`

Singh, M., 1994. The role of drive system technology in maximizing the performance and
    economics of long belt conveyors. Bulk Solids Handling 14 (4), pp. 695–704.

SKF, 2016. The SKF model for calculating the frictional moment.
    URL   `http://www.skf.com/group/products/bearings-units-housings/`
    `ball-bearings/principles/friction/skf-model/index.html`

Song, W., Zhao, C., 2001. Research on the rule of conveying belt resistance coefficient varied
    with the velocity. Coal Mine Machinery (3), pp. 16–18.

Spaans, C., 1991. The calculation of the main resistance of belt conveyors. Bulk Solids Handling
    11 (4), pp. 1–16.

Stephens Adamson, Feb. 2014. Super ESIdler - Advanced super energy saving troughing idler
    technology.
    URL `http://www.stephens-adamson.com/esidlers.htm`

Tapp, A., 2000. Conveying technology-energy saving troughing idler technology. Bulk Solids
    Handling 20 (4), pp. 437–450.

Tsoumas, I., Tischmacher, H., Köllensperger, P., 2014. The European Standard EN 50598-2:
    Efficiency classes of converters and drive systems. IEEE, pp. 929–935.

Umair Mirza, 2013. Determining causes for electric motor failure.
    URL `http://www.brighthubengineering.com/commercial-electrical-applications/`
    `78579-determining-causes-for-electric-motor-failure/`

United States Environmental Protection Agency, Dec. 2015. EPA fact sheet-Social cost of car-
    bon.

van den Bijgaart, I., Gerlagh, R., Liski, M., 2016. A simple formula for the social cost of carbon. Journal of Environmental Economics and Management 77, pp. 75–94.

Veeke, H. P., Ottjes, J. A., Lodewijks, G., 2008. The Delft systems approach: Analysis and design of industrial systems. Springer Science & Business Media.

Wheeler, C., 2003. Analysis of the main resistances of belt conveyors. University of Newcastle.

Wheeler, C. A., 2016. Rotating resistance of belt conveyor idler rolls. Journal of Manufacturing Science and Engineering 138 (4), pp. 041009–041009–8.

Wiedenbrug, E. J., 2003. Overheating electric motors: a major cause of failure.
URL `http://www.maintenancetechnology.com/2003/04/overheating-electric-motors-a-major-cause-of-failure/`

Yester, M., 1997. The basics and cost savings of utilizing vertical conveyor technology. Bulk Solids Handling 17 (3), pp. 357–368.

Zhang, S., 2010. Model predictive control of operation efficiency of belt conveyor. IEEE, pp. 1854–1858.

Zhang, S., Xia, X., 2009. A new energy calculation model of belt conveyor. IEEE, pp. 1–6.

Zhang, S., Xia, X., Jun. 2010. Optimal control of operation efficiency of belt conveyor systems. Applied Energy 87 (6), pp. 1929–1937.
URL `http://www.sciencedirect.com/science/article/pii/S0306261910000085`

Zhang, S., Xia, X., 2011. Modeling and energy efficiency optimization of belt conveyors. Applied Energy 88 (9), pp. 3061–3071.

Nomenclature

Non capitals

a	Front part of contact length between belt and idler	m
a	The value of acceleration	m/s^2
$a_{ac,max}$	Maximum acceleration	m/s^2
$a_{de,max}$	Maximum deceleration	m/s^2
b	Rear part of contact length between belt and idler	m
b_c	Contact length of bulk material	m
b_i	Fuzzy boundary	$-$
b_{Sch}	Internal diameter between chute walls	m
c_1	Propagation speed of longitudinal stress waves	m/s
$c_{Schb}c_{Rank}$	Coefficient for calculating the resistance F_{Schb}	$-$
d_{1s}	Contact diameter of lip seal	m
d_{1s}	Contact diameter of lip seal	m
d_b	Thickness of belt	m
d_{be}	Average bearing diameter	m
d_s	Thickness of solid material layer	m
$\bar{f}$	Function	$-$
f	Artificial frition coefficient	$-$
f_0	Factor for calculaitng the lubricant frictional monent, depending on the bearying type and lubricantion	$-$
f_1	Load dependent friction factor	$-$
f_b	Fuzzy membership function	$-$

f_{ih}^*	Indentation resistance factor derived from Hunter	–
f_{im}^*	Indentation resistance factor derived from May	–
f_s	Correction factor of indentation resistance defined by Gabriel	–
$f(t)$	Function with respect to the risk of belt slippage	–
g	Acceleration due to gravity	m/s^2
$g(t)$	Function with respect to the risk of pushing a motor into the regenerative operation	–
h	Thickness of belt cover	m
h_{rel}	Belt sag ratio	–
$h(t)$	Function respect to the risk of material spiilage caused by the excessive lower belt speed	–
i_{rf}	Reduction factor of a gearbox	–
i_{sf}	Motor service factor	–
k	Deborah number and $k = \frac{V\tau}{a} = \frac{V\eta}{aE_2}$	–
k_N	Belt tension rating	kN
l	Distance between neighbouring idler stations	m
l_1	Width of the covered belt section on the wing roll	m
l_b	Belt conveyor acceleration length	m
l_m	Length of shell of the central idler in a three piece carrying idler arrangement	m
m	Total mass of a belt conveyor, including the total mass of the rollers, of the belt and of the bulk material	kg
m'_{belt}	Mass of belt per length unit	kg/m
$m_{block,n}$	The material mass of the nth block	kg
$m_{block,n,dis}$	The discharged material mass from the nth block	kg
m'_{bulk}	Mass of bulk solid per length unit	kg/m
m'_{roll}	Mass of idler rolls per length unit	kg/m
n	Roller rotation speed	s^{-1}
x_n	Traveling distance of the nth block	m

p	Cycle time of the fluctuating material flow	s
p_{Gr}	pressure between belt cleaner and belt	N/m^2
q	Homogeneous load distribution with respect to the total of the belt and the bulk material	N/m
r_0	A basic reduction which takes the dynamic fatigue strength of the belt splice into account	$-$
r_1	The reduction factor taking the belt elongation into account	$-$
r_2	A reduction taking the peak belt loading in transient operations into account	$-$
r_i	Peak of the material loading rate in percentage	$-$
t_f^*	Function root with respect to the risk of belt slippage	$-$
t_g^*	Function root with respect to the risk of pushing a motor into the regenerative operation	$-$
t_h^*	Function root with respect to the risk of material spiilage caused by the excessive lower belt speed	s
t_a	Acceleration time	s
$t_{ac,min}$	Minimum acceleration time	s
t_{delay}	Traveling time from the sensor location to the head of a belt conveyor	s
$t_{de,min}$	Minimum deceleration time	s
t_l	Traveling time from the tail to the head of a belt conveyor	s
$\ddot{\mathbf{v}}$	Vector of nodal acceleration	$-$
$\dot{\mathbf{v}}$	Vector of nodal velocity	$-$
$\mathbf{v}$	Vector of nodal displacement	$-$
v	The speed of a belt conveor	m/s
v_0	horizontal speed of solid material	N
v_1	Speed of the upstream conveyor	m/s
v_2	Speed of the downstream conveyor	m/s
v_{act}	Actual belt conveyor speed	m/s
v_b	Desired speed of an acceleration operation	m/s

v_{nom}	Nominal speed of a belt conveyor	m/s
v_{th}	Theoretical speed of the downstream conveyor	m/s
x	Distance to belt edge	m
x_r	Distance from the support to the radius of curvature	m

Capitals

A_1	Cross section of a material block at the upstream belt conveyor	m^2
A_2	Cross section of a material block at the downstream belt conveyor	m^2
A_{act}	Actual cross section of material on the belt	m^2
A_{Gr}	Effective contact area between belt cleaner and belt	m^2
A_{nom}	Nominal cross section of material on the belt	m^2
B	Belt width	m
$B_{A1,A5}$	Uncovered width of a belt section on a wing roll	m
$B_{A2,A4}$	Covered width of a belt section on a wing roll	m
B_{A3}	Covered width of a belt section on a center roll	m
B_n	Distance to belt edge (n=1,2,...,5)	m
$\mathbf{C}$	Matrix of damping factors	$-$
C	Coefficient for the all-inclusive consideration of the secondary resistances	$-$
D_P	Pulley diameter	m
DW_{ref}	Speed error	m/s
E_1	Young's modulus	N/m^2
E_2	Young's modulus	N/m^2
E_I	Flexure rigidityo of beltl	Nm^2
$\mathbf{F}$	Vector of force	$-$
F	Kinetic resistances, equal to the total motional resistances in the steady state operation	N
F_1	Decisive load for frictional torque	N
F_a	Axial force on bearing	N

F_{ac}	Extra driving forces caused by the acceleration opertion	kN
F_{Auf}	Inertia resistance and frictional resistance between the material conveyed and the belt in the zone of a feeder point	N
F_d	Driving forces	kN
$F_{d,max}$	Maximum driving forces	kN
$F_{d,max,heat}$	Maximum driving forces with respect to the risk of motor over-heating	kN
$F_{d,max,slip}$	Maximum driving forces with respect to the belt slippage risk	kN
$F_{d,max,tension}$	Maximum driving forces with respect to the belt over-tension risk	kN
F_f	Frictional resistances	N
F_{fb}	Flexure resistance of belt	N
$F_{f,bd}$	Maximm available friction between the belt and the drive pulley	kN
F_{fb}^k	Flexeral resistances of the kth element	N
$F_{f,max}$	Maximum value of the available frictional forces between a belt and a drive pulley	kN
F_{fs}	Flexure resistance of solid material	N
$F_{fs,l}$	Flexure resistance of bulk material due to longitudinal deformation	N
$F_{fs,t}$	Flexure resistance of bulk material due to transverse deformation	N
F_{Ga}	Scraper resistances	N
F_{Gb}	Wrap resistance between belt and pulleys	N
F_{Gr}	Frictional resistance caused by belt cleaner	N
F_H	Main resistances	kN
F_i	Belt indentation resistance	N
F_i^k	Indentation resistances of the kth element	N
F_{im}'	Belt indentation resistance per width unit according to May	N/m
F_k	Frictional resistances of the kth element	N
F_N	Normal force	kN
F_N	Secondary resistances	kN
F_{Nc}	Normal force on the center roll	N

F_{Nw}	Normal force on the wing roll	N
F_r	Radial force on bearing	N
F_r	Rotating resistance of idler rolls	N
F_r^k	Rotating resistances of the kth element	N
F_{Rst}	Tilting resistances of idlers	N
F_S	Special resistance	kN
F_{Schb}	Frictional resistance between the material conveyed and the lateral chutes within the acceleration zone of a feeder point	N
F_{St}	Gradient resistance	N
F_T	Vectorial sum of the two belt tensions acting on the pulley and of the forces due to the mass of the resolving parts of the pulley	N
F_{Tr}	pulley bearing resistance	N
F_v	Vertical force between neighboring roll stations due to the weight of belt and the bulk solid	N
F_v'	Vertical force per width unit	N/m
Fvs	Vertical force due to the weight of solid material	N
F_x	The forces in the x direction	kN
F_y	The forces in the y direction	kN
H	The change in elevation between head and tail pulleys	m
I_m	Mass flow	kg/s
$\mathbf{K}$	Matrix of sping factors	$-$
K_a	Coefficient in active stress state	$-$
K_p	Coefficient in passive stress state	$-$
L	Conveyor length	m
$\mathbf{M}$	Mass matrix	$-$
M	Moment	Nm
M_0	Bearing friction moment due to the viscous drag of the lubricant	Nm
M_1	Bearing friction moment due to the rolling elements of the bearing	Nm

M_1 Bending moments occurring within the belt at the point directly above the idler roll Nm

M_2 Bending moments occurring within the belt at the point of maximum sag Nm

M_s Roller friction moment due to the contact lip seal Nm

M_T Mass of a gravity take-up device kg

$N(DW_{ref})$ Ramp rate of the belt speed m/s^2

P_0 Equivalent static bearing load N

P_1 Decisive load for frictional torque N

P_e Electric power kW

P_{elec} Input electric power of a drive motor kW

P_{in} Input power of a frequency converter kW

P_m Mechanical power kW

P_{mech} Output mechanical power of a drive motor kW

$P_{mech,in}$ Input power of a gearbox kW

$P_{mech,out}$ Output power of a gearbox kW

P_{out} Output power of a frequency converter kW

Q_{act} Actual loading rate $MTPH$

Q_{in} Input of a belt conveyor, equalling the material loading rate $MTPH$

Q_{nom} Nominal conveying capacity $MTPH$

Q_{out} Output of a belt conveyor, equalling the material discharging rate $MTPH$

R Rollerl redius m

R_1 Radium of a curvate over the idler m

R_2 Radium of a curvate at the point of maximum sag m

R_d Radium of a drive pulley m

R_T Proportion of motors' monimal torque $-$

R_v Proportion of motors' monimal speed $-$

$S_{A,min}$ Minimum safety factor in the steady operating condition $-$

$S_{B,min}$ Minimum safety factor in the non-steady operating condition $-$

F_{Sch}	Extra chute frictional resistances	N
F_{St}	Gradient resistance	kN
T	Belt tension	N
T_1	Belt tension before the drive pulley	kN
$T_{1,a}$	Belt tension before the drive pulley in an acceleration operation	kN
$T_{1,max}$	Maximum belt tension before the drive pulley without slippage	kN
T_2	Belt tension after the drive pulley	kN
T_e	Drive torque	Nm
$T_{max,A}$	Maximum safe working tension in the steady operating condition	kN
$T_{max,B}$	Maximum safe working tension in the non-steady operating condition	kN
T_{min}	Minimum belt tension through the whole belt conveyor	kN
$T_{motor,max}$	Maximum drive torque exerted on the motor shaft	Nm
$T_{motor,nom}$	Nominal drive torque exerted on the motor shaft	Nm
$T_{shaft,k}$	Driving toruqe of the kth driving pulley	kN
U	Belt utilization rate	m/s
W	Total power consumption	kWh
X_0	Radial factor depending on the bearing design	$-$

Greek non capitals

α	Wrap angle of a belt around the drive pulley	$^{\circ}$
β	Repose angle of solid material	$^{\circ}$
δ	Angle of inclination of the installation	$^{\circ}$
η	Damping efficient	$-$
η_{freq}	Efficiency of a frequency converter	$-$
η_{gear}	Efficiency of a gearbox	$-$
η_{motor}	Efficiency of a drive motor	$-$
η_{sys}	Drive system efficiency	$-$
λ	Trough angle	$^{\circ}$

μ	Friction coefficient between a belt and a drive pulley	−
μ_2	Friction coefficient between materiel conveyed and lateral chutes	−
μ_4	Friction coefficient between belt and belt cleaner	−
ν	Viscosity of lubrication oil	$m^2 s$
ω	Factor defined by $\omega = \sqrt{T/E_I}$	m
$\omega_{shaft,k}$	Angular speed of the kth driving pulley	rad/s
ϕ_i	Internal friction angle of bulk solid material	°
ϕ_w	Wall friction angle between belt and bulk materiall	°
ρ_s	Density of bulk solid material	kg/m^3
ρ_b	Desity of conveyor belt	kg/m^3
σ	Stress	N/m^2
τ	Relaxation time	s
φ_i	Angle of the internal friction of the bulk material	°
φ_T	Torque ratio of a drive motor, equal to the actual torque divided by nominal torque	−
φ_v	Speed ratio of a belt conveyor, equal to the actual speed divided by nominal speed	−

Greek capitals

| Ψ_b | Belt damping factor of energy loss due to bending | − |
| Ψ_i | Belt damping factor of energy loss due to indentation | − |

Acronyms

ECO	Estimation-Calculation-Optimization
FEM	Finite-Element-Model
KPIs	Key performance indicators
SCC	Social Cost of Carbon

Other Symbols

$Cost_{ele}$	Electricity cost	€
$Cost_{tot}$	Total cost	€
EF_{CO2}	Emission factor of carbon with respect to the electricity generation	g/kWh

$Emission_{CO2}$ Carbon dioxide (CO2) emission kg

$Saving_{tot}$ Total saving by means of speed control   €

$\sum loss_{freq}$ Power loss of a frequency converter kW

$\sum loss_{motor}$ Power loss of a drive motor kW

$\sum loss_{gear}$ Power loss of a gearbox kW

Summary

Belt conveyors are widely used in bulk solids handling and conveying systems. Considering the extensive use of belt conveyors, their operations involve a large amount of energy. Taking the relevant economic and social challenges into account, there is a strong demand for lowering the energy consumption of belt conveyors, and for reducing the carbon footprint. Speed control is one of the promising approaches for reducing the power consumption of belt conveyors.

This thesis focuses on the application of speed control to belt conveyors for reducing their energy consumption. Research on belt conveyor speed control has already been carried out for more than twenty years. However, rare implementations of speed control to reduce energy consumption can be found in practice. One major reason is that the current research does not cover issues like the potential risks (such as the risk of belt over-tension, the risk of belt slippage around the drive pulley and the risk of motor over-heating) and the dynamic analyses of belt conveyors in transient operations. Therefore, speed control of belt conveyors is not often successfully applied in practice.

With the aid of a dynamic belt model, the belt conveyor's dynamic behavior is investigated during the transient operations. In addition, a three-step method is proposed to determine the minimum speed adjustment time. The method can be briefly summarized as the Estimation-Calculation-Optimization (ECO) method. The ECO method takes both the potential risks and the conveyor dynamics into account. With this method, the minimum speed adjustment time for different speed ranges can be calculated. The transient operation with an acceleration time no less than the minimum results in healthy dynamics, and the potential risks can be avoided. Accordingly, the ECO method improves the applicability of speed control.

To assess the applicability of belt conveyor speed control, a belt conveyor energy model is required to calculate the power consumption and to estimate the power savings via speed control. This thesis uses an energy model based on the standard DIN 22101. The DIN-based model uses the artificial frictional coefficient f to calculate the main resistances. The value of the f factor can be calculated either by physical experiments or by analytical calculations. The physical experiments are expensive and they may have a negative impact on the operational plan of belt conveyor systems. Therefore, this thesis uses an analytical method to calculate the DIN f factor. The analytical method uses the calibrated sub-resistances models from literature to calculate the main resistances. Derived from the main resistances, the f factor value can be achieved. With the analytical approach, the f factor of a long horizontal belt conveyor is calculated. From the calculation results, it can be observed that the f factor varies with different loads and speeds. Therefore, it is suggested to use a variable f factor value to calculate power

consumption and to estimate the final power reduction via speed control.

Using the ECO method and the DIN-based energy model, the simulation models of belt conveyor speed control systems are developed to assess the performance of speed control. The simulation model is built up by the operational system and the control system. In the modeling of the operational system, a discrete tool is used to represent the continuous material flow. The modeling of the control system accounts for different speed control manners. According to different loading scenarios, two types of controllers are built: passive and active speed controllers. In terms of the passive speed control, the "high-medium-low" strategy is highly suggested. In terms of the active speed control, both the fixed time interval strategy and the variable time interval strategy are discussed. Importantly, the conflicts between adjacent transient operations should be accounted for in the active speed control.

An experimental study is conducted to evaluate the speed control performance. Two belt conveyors are studied. One conveyor uses the passive speed control. Both the static calculation and the dynamic simulations are performed. All experimental results show that the passive speed control achieves power reductions for the concerned belt conveyor. The data of the static calculation further shows that the variable f factor has a considerable impact on the final results of the power savings. Another belt conveyor uses the active speed control. The experimental result shows that the control strategy has a large impact on the power reduction. According to the data, it can be observed that the operation with the variable time interval strategy gains more energy savings than that with the fixed time interval strategy. In addition, it also can be found that in terms of the fixed time interval, the value of power savings varies with different speed sets and with different time interval lengths.

Overall, speed control is a promising method of reducing power consumption of belt conveyors.

Samenvatting

Bandtransporteurs worden veel gebruikt in systemen voor de handling en het transport van bulkgoed. Door de uitgebreide toepassing van bandtransporteurs is het elektriciteitsgebruik ervan hoog. Door relevante economische en sociale vragen is er een dringende behoefte om het energic gebruik ervan te verminderen en de CO2-footprint te verkleinen. Een van de mogelijkheden om het energiegebruik van bandtransporteurs te verminderen is snelheidsregeling.

In dit proefschrift ligt het accent op snelheidsregeling van bandtransporteurs voor de verlaging van het energic gebruik. Al meer dan 20 jaar wordt onderzoek gedaan aan snelheidsregeling van bandtransporteurs, maar er zijn in de praktijk nagenoeg geen toepassingen van ervan voor de vermindering van energiegebruik. Een belangrijke reden daarvoor is dat in het huidige onderzoek geen aandacht wordt besteed aan onderwerpen als de mogelijke risico's (breken of slippen van de band, overbelasting of oververhitting van een motor) en aan de analyse van het dynamisch gedrag van bandtransporteurs in niet-stationaire toestand.

Met behulp van een dynamisch model van de band is het dynamisch gedrag van de band in de niet-stationaire toestand onderzocht. Daarnaast is een driestappenmethode opgesteld voor het bepalen van de kortste tijd voor het aanpassen van de snelheid. Deze methode kan worden samengevat als Schatten-Berekenen-Optimaliseren (English: Estimation-Calculation-Optimization, ECO). In de ECO-methode wordt rekening gehouden met potentiële risico's en met de dynamica van het systeem. Met deze methode kan de minimale omschakeltijd voor verschillende snelheidsintervallen worden berekend. Bij een snelheidsverandering met een versnellingstijd niet korter dan de minimale omschakeltijd kunnen risico's worden vermeden. Hierdoor verbetert de ECO-methode de bruikbaarheid van snelheidsregeling.

Om de effecten van snelheidsregeling op het energiegebruik van bandtransporteur te kunnen bestuderen is een model van het energiegebruik nodig. In dit proefschrift wordt een energiemodel gebruikt dat is gebaseerd op de norm DIN 22101. In dit model wordt een fictieve wrijvingscoëfficiënt f gebruikt voor de berekening van de belangrijkste weerstandskrachten. Omdat fysieke experimenten duur zijn en een nadelige invloed kunnen hebben op de beschikbaarheid van een transportsysteem voor het operationele gebruik, wordt in dit proefschrift een analytische methode gebruikt voor het berekenen van de coëfficiënt f. In deze methode wordt erkende deelmodellen uit de literatuur gebruikt om de grootste weerstanden te berekenen. Uit deze weerstandskrachten kan de factor f worden bepaald. Met de analytische benadering is de factor f van een lange horizontale bandtransporteur berekend. Uit de berekende resultaten blijkt dat de wrijvingscoëfficiënt f verandert bij verandering van belasting en snelheid. Er wordt daarom voorgesteld om een variabele factor f te gebruiken voor de berekening van het en-

ergiegebruik en voor de schatting van de uiteindelijke energiebesparing door snelheidsregeling.

Om het gedrag van snelheidsregeling te kunnen bestuderen zijn simulatiemodellen van de snelheidsregelingen van bandtransporteurs ontwikkeld, gebruikmakend van de ECO-methode en het op DIN 22101 gebaseerde model van het energiegebruik. Het simulatiemodel bestaat uit een model van het operationele systeem en een model van het regelsysteem. In het model van het operationele systeem wordt de continue stroom materiaal discreet afgebeeld. In het model van het regelsysteem is rekening gehouden met verschillende snelheidsregelingen. Er zijn twee types snelheidsregelingen gemaakt voor verschillende beladingscenario's: actieve en passieve regelingen. Als passieve regeling wordt de strategie "hoog-gemiddeld-laag" voorgesteld. Als actieve regelingen worden zowel de strategie met een vast interval als de strategie met variabele intervallen besproken. Het is belangrijk om aandacht te besteden aan actieve snelheidsregeling in verband met conflicten door elkaar opvolgende overgangsoperaties.

Er is experimenteel onderzoek gedaan om de effecten van snelheidsregeling te evalueren. Daarvoor zijn twee bandtransporteurs bestudeerd. Eén transporteur gebruikt een passieve snelheidsregeling. Er is een statische berekening gedaan en dynamische simulaties. Uit alle experimentele resultaten blijkt verlaging van het energiegebruik van de betreffende transporteur bij toepassing van de passieve regeling. Verder blijkt uit de statische berekening dat de factor f een behoorlijke invloed heeft op de vermindering van het energiegebruik. Voor de andere transporteur wordt actieve snelheidsregeling gebruikt. De gebruikte regelstrategie blijkt een grote invloed te hebben op de vermindering van het energiegebruik. Uit de resultaten blijkt dat met een strategie met variabele intervallen een grotere energiebesparing kan worden bereikt dat met een strategie met een vast interval. Bovendien is gevonden dat bij een regeling met een vast interval de besparing afhankelijk is van de snelheid en van de gekozen lengte van het interval.

Samenvattend: snelheidsregeling is een veelbelovende methode voor verlaging van het energiegebruik van bandtransporteurs.

Curriculum Vitae

Daijie He was born on January 24, 1988 in Jiangyou, P.R. China. In 2011 he received his BSc degree in Agricultural Mechanization and its Automation at Southwest University, Chongqing, P.R. China. In the same year, he started his master study at the same college and joined the research group of Prof. Peixiang He.

In 2013, he received his MSc degree in Agricultural Mechanization Engineering. In 2013 Daijie started his Ph.D. at Section of Transport Engineering & Logistics at Delft University of Technology, the Netherlands. His research was sponsored by the Chinese Scholarship Council. His research project is about improving the energy efficiency of industrial applications, especially the bulk material handling and conveying systems. In his research, he focused on belt conveyor systems and their automation. His research interest includes belt conveyor technology, finite element analysis, and modelling & simulation. He is a reviewer for the journal Applied Energy.

List of Publications

1. **He, D**., Pang, Y., Lodewijks, G., Yan, G., Can speed control still enable green operations of belt conveyors by accounting for variable frictional coefficient?. *Applied Energy* (submitted)

2. **He, D**., Pang, Y., Lodewijks, G., 2017. Green operations of belt conveyors by means of speed control. *Applied Energy* 188, pp.330–341.

3. **He, D**., Pang, Y., Lodewijks, G., 2016. Speed control of belt conveyors during transient operation. *Powder Technology* 301, pp.622–631.

4. **He, D**., Pang, Y., Lodewijks, G., 2016. Determination of acceleration for belt conveyor speed control in transient operation. *International Journal of Engineering and Technology* 8, 206.

5. **He, D**., Pang, Y., Lodewijks, G., 2016. Belt conveyor dynamics in transient operation for speed control. *International Journal of Civil, Environmental, Structural, Construction and Architectural Engineering* 10, 7 (2016), pp.828--833.

6. Pang, Y., **He, D**., Lodewijks, G., 2016. Transient acceleration in belt conveyor speed control. Presented at the *12th International Conference on Bulk Materials Storage, Handling and Transportation (ICBMH 2016)*, The Engineers Australia, p. 305.

TRAIL Thesis Series

The following list contains the most recent dissertations in the TRAIL Thesis Series. For a complete overview of more than 150 titles see the TRAIL website: www.rsTRAIL.nl.

The TRAIL Thesis Series is a series of the Netherlands TRAIL Research School on transport, infrastructure and logistics.

He, D., *Energy Savinsg for Belt Conveyors by Speed Control*, T2017/10, July 2017, TRAIL Thesis Series, the Netherlands

Bešinović, N., *Integrated Capacity Assessment and Timetabling Models for Dense Railway Networks*, T2017/9, July 2017, TRAIL Thesis Series, the Netherlands

Chen, G., *Surface Wear Reduction of Bulk Solids Handling Equipment Using Bionic Design*, T2017/8, June 2017, TRAIL Thesis Series, the Netherlands

Kurapati, S., *Situation Awareness for Socio Technical Systems: A simulation gaming study in intermodal transport operations*, T2017/7, June 2017, TRAIL Thesis Series, the Netherlands

Jamshidnejad, A., *Efficient Predictive Model-Based and Fuzzy Control for Green Urban Mobility*, T2017/6, June 2017, TRAIL Thesis Series, the Netherlands

Araghi, Y., *Consumer Heterogeneity, Transport and the Environment*, T2017/5, May 2017, TRAIL Thesis Series, the Netherlands

Kasraian Moghaddam, D., *Transport Networks, Land Use and Travel Behaviour: A long term investigation*, T2017/4, May 2017, TRAIL Thesis Series, the Netherlands

Smits, E.-S., *Strategic Network Modelling for Passenger Transport Pricing*, T2017/3, May 2017, TRAIL Thesis Series, the Netherlands

Tasseron, G., *Bottom-Up Information Provision in Urban Parking: An in-depth analysis of impacts on parking dynamics*, T2017/2, March 2017, TRAIL Thesis Series, the Netherlands

Halim, R.A., *Strategic Modeling of Global Container Transport Networks: Exploring the future of port-hinterland and maritime container transport networks*, T2017/1, March 2017, TRAIL Thesis Series, the Netherlands

Olde Keizer, M.C.A., *Condition-Based Maintenance for Complex Systems: Coordinating maintenance and logistics planning for the process industries*, T2016/26, December 2016, TRAIL Thesis Series, the Netherlands

Zheng, H., *Coordination of Waterborn AGVs*, T2016/25, December 2016, TRAIL Thesis Series, the Netherlands

Yuan, K., *Capacity Drop on Freeways: Traffic dynamics, theory and Modeling*, T2016/24, December 2016, TRAIL Thesis Series, the Netherlands

Li, S., *Coordinated Planning of Inland Vessels for Large Seaports*, T2016/23, December 2016, TRAIL Thesis Series, the Netherlands

Berg, M. van den, *The Influence of Herding on Departure Choice in Case of Evacuation*: Design and analysis of a serious gaming experimental set-up, T2016/22, December 2016, TRAIL Thesis Series, the Netherlands

Luo, R., *Multi-Agent Control of urban Transportation Networks and of Hybrid Systems with Limited Information Sharing*, T2016/21, November 2016, TRAIL Thesis Series, the Netherlands

Campanella, M., *Microscopic Modelling of Walking Behavior*, T2016/20, November 2016, TRAIL Thesis Series, the Netherlands

Horst, M. van der, *Coordination in Hinterland Chains: An institutional analysis of port-related transport*, T2016/19, November 2016, TRAIL Thesis Series, the Netherlands

Beukenkamp, W., Securing Safety: *Resilience time as a hidden critical factor*, T2016/18, October 2016, TRAIL Thesis Series, the Netherlands

Mingardo, G., *Articles on Parking Policy*, T2016/17, October 2016, TRAIL Thesis Series, the Netherlands

Duives, D.C., *Analysis and Modelling of Pedestrian Movement Dynamics at Large-scale Events*, T2016/16, October 2016, TRAIL Thesis Series, the Netherlands

Wan Ahmad, W.N.K., *Contextual Factors of Sustainable Supply Chain Management Practices in the Oil and Gas Industry*, T2016/15, September 2016, TRAIL Thesis Series, the Netherlands

Liu, X., *Prediction of Belt Conveyor Idler Performance*, T2016/14, September 2016, TRAIL Thesis Series, the Netherlands

Gaast, J.P. van der, *Stochastic Models for Order Picking Systems*, T2016/13, September 2016, TRAIL Thesis Series, the Netherlands

Wagenaar, J.C., *Practice Oriented Algorithmic Disruption Management in Passenger Railways*, T2016/12, September 2016, TRAIL Thesis Series, the Netherlands

Psarra, I., *A Bounded Rationality Model of Short and Long-Term Dynamics of Activity-Travel Behavior*, T2016/11, June 2016, TRAIL Thesis Series, the Netherlands

Ma, Y., *The Use of Advanced Transportation Monitoring Data for Official Statistics*, T2016/10, June 2016, TRAIL Thesis Series, the Netherlands

Li, L., *Coordinated Model Predictive Control of Synchromodal Freight Transport Systems*, T2016/9, June 2016, TRAIL Thesis Series, the Netherlands

Vonk Noordegraaf, D.M., *Road Pricing Policy Implementation*, T2016/8, June 2016, TRAIL Thesis Series, the Netherlands